Investigating process stresses on *Saccharomyces cerevisiae* using isothermal microcalorimetry

Matthew Myers

Supervisors: Prof STL Harrison; Dr S Tai, Dr R Huddy; Dr M Fagan-Endres

Department of Chemical Engineering
Faculty of Engineering and the Built Environment
University of Cape Town

04 June 2017

Abstract

Maximising performance of microbial processes, including yeast-based processes, in an industrial setting requires understanding of the impact of process stresses. These may be the result of process configuration, dilution, temperature changes, hydrodynamic conditions or process perturbations. Methods to determine the microbial metabolic response to such stresses have long been sought, but are typically limited, often requiring the use of a suite of methods to assess the physiological status and state. The recent technical advances in microcalorimetry suggest potential for the use of isothermal microcalorimetry (IMC) to determine yeast viability and vitality and is investigated here. IMC is a laboratory method whereby the real-time heat produced by a chemical, biological or physical process is measured in the micro to nano watt range. It is proposed that this heat production may be correlated to the physiological state of the microbial catalyst and can be used to measure the impact of different stresses. In this study, the potential of IMC as a method for exploring process stress is investigated using *Saccharomyces cerevisiae* and its application in the beer brewing industry as a case study. Here, it is well known that yeast viability and vitality have commercial significance.

IMC is sufficiently sensitive to detect the heat given off by 1000 yeast cells. However, IMC cannot distinguish between different heat flows within a system i.e. it is non-specific. The literature demonstrates how IMC has been used in the study of numerous microbiological fields, including the growth and metabolism of yeast. Previous studies have successfully derived the specific growth rate and cell numbers of a growing yeast population from analysing power and heat curves. The specific growth activity and specific growth retardation of yeast and how these parameters relate to bactericidal and bacteriostatic effects has also been examined by a number of authors.

The key objectives of this study were to determine the viability and vitality of *Saccharomyces cerevisiae* using IMC and to assess the impact of stresses on yeast viability and vitality. This was achieved by measuring the thermal power produced by a growing yeast suspension as a function of its overall growth and metabolism. Two industrially relevant stresses were examined: cold shock and ethanol shock. The effect of these stresses has yet to be studied using microcalorimetry. The growth of *Saccharomyces cerevisiae* under ethanol stress was used as an inhibition study to isolate its effects on the growth thermogram.

Following the generation of thermograms under control and stress conditions using IMC, a method for their quantitative analysis was developed. Curves were fitted to the heat data using an exponential growth equation and the time for the heat flow curve to peak was determined. From the exponential curve, the specific growth rate of the yeast was determined with a high degree of repeatability. The coefficient of the exponential term in the growth equation gave highly reproducible and distinguishable results relating to the viability and vitality of the initial yeast population. The time of peak heat flow was also affected by the initial viability and vitality of the yeast and was used to estimate the initial active cell population size.

The slow cold shock (0.13 °C/minute) had no impact on cell viability but did cause a slight decrease in cell vitality. As expected, the rapid cold shock (18 °C/minute) had no impact on cell viability but a significant negative effect on cell vitality. Ethanol shock – the sudden suspension of yeast cultures in ethanol and subsequent removal of the ethanol in the range 4% to 8% (v/v) – had no observable impact on cell viability or cell vitality and the growth thermogram. The growth of cells in the presence of ethanol, known for product inhibition, had a significant effect on the growth thermograms, which is in line with previous literature findings. The combination of a rapid cold shock and growth in ethanol had no significant cumulative effect on the growth thermogram.

The results show that yeast is more susceptible to a rapid cold shock than a gradual cooling and that yeast is largely resistant to rapid ethanol exposure however, continual ethanol exposure severely retards growth. The method developed has been shown to be repeatable and accurate for assessing yeast viability and vitality. Further, it is sufficiently sensitive to determine both stress response and inhibition trends.

Acknowledgements

I would like to thank the entire CeBER cohort, not to mention the CeBER academic staff, lab staff and administrative staff for their support and guidance. A special thank you to my supervisors; Siew Tai, Rob, Marijke Fagan-Endres and Sue Harrison for their invaluable input.

I also would like to thank my siblings, grandparents and especially my three parents, Peter, Michelle and Candace who have supported and encouraged me through all my endeavours.

Contents

List of Figures

List of Tables

Glossary

Aerobic	Metabolic process that makes use of oxygen in order to release energy
Agar	A gelatinous solid growth media
Ampoule	Small glass vessel, cylindrically shaped that can hold ca. 4 ml, that can be sealed using metal caps (via crimping)
Anabolism	Biological process that entails the synthesis of substances – the constructive metabolism
Anaerobic	Metabolic processes that take place in the absence of oxygen (air)
Bactericidal	Action which exclusively kills cells
Bacteriostatic	Action which exclusively inhibits cellular growth activity
Batch microcalorimetry	Type of microcalorimetry which involves the study of static samples
Bijoux bottle	Small glass vessel, cylindrically shaped that can hold ca. 4 ml, that can be sealed using screw-on metal caps
Bud/budding	The division of cells asymmetrically, asexually via mitosis
Calorimetric baseline	The power signal produced by a calorimeter with no sample present in the measuring position. This signal is subject to drift and shift, but should ideally be constant at zero (or near zero).
Calorimetry	The science of measuring the heat evolved or consumed (heat transfer) by a given system – performed using a calorimeter
Catabolism	Biological process that entails the breaking down of molecules to release energy – the destructive metabolism
Cropping/Cropped	The removal of yeast from a fermentation vessel upon completion of the fermentation process
Diploid	A cell that contains two complete sets of chromosomes inherited from two distinct parent cells
Eppendorf tube	Small plastic micro-centrifuge tubes (conical bottom) that can hold ca. 2 ml.
Flow microcalorimetry	Type of microcalorimetry where the sample continuously moves through the measurement positon via flow lines
Glycerol stock	The preservation of the microbial culture as a stock culture in the presence of glycerol (a simple polypol – organic sugar alcohol) to preserve the cells when frozen at low temperatures (e.g. – 80 °C)

Haploid	A cell that contains a single set of unpaired chromosomes
Haze	The degree of opacity of a yeast slurry – formed due to either a reduction in yeast viability or vitality
McCartney bottle	Glass vessel, cylindrically shaped that can hold ca. 25 ml, that can be sealed using screw-on metal caps
Microcalorimetry	Heat flow measurements (often carried out isothermally) that are accurate in the micro- and nano-watt range
Peltier element	A device that operates based on the Peltier effect and produces a current proportional to a temperature differential or vice versa
Pitched	The transfer of yeast (usually in slurry form) into a fermentation vessel
Physiological state	The health of yeast in terms of its overall viability and vitality
Pseudohyphal growth	Type of growth whereby yeast cells become invasive by changing shape to become elongated, remaining attached to each other and budding in a unipolar fashion
P value	The result of a statistical hypothesis test that yields the probability of obtaining a result greater than or equal to the average observation for a population, assuming that the null hypothesis is true
Specific growth activity	The ratio of the specific growth rate of a stressed population relative to that of a healthy population
Specific growth retardation	The ratio of the time taken for a healthy population of cells to reach a given power output, α, and dividing by the time taken for a stressed population of cells to reach the same power output
Thermogram	The calorimetric signal (in either watts of Joules) produced by a calorimeter
Thermopile	A device that converts thermal energy into electrical energy
Viability	The number of living yeast cells in a given population, related to ability to reproduce
Vitality	The physiological capabilities of the living cells in a given yeast population, related to metabolic activity
Wort	A nutrient rich aqueous solution that contains malted barley and hops

Nomenclature

Symbols

A	Grouping of constants: $A = N_0 \frac{q_1}{\mu \cdot exp(\mu \cdot \tau)}$
α	A given level of power output (W)
B	Grouping of constants: $B = N_0\left(\int_0^\tau N_0 dt - {}^{q_1}/_{\mu}\right)$
$f(t)$	Heat (cumulative power) evolved by a sample as a function of time (J)
$f'(t)$	Power (heat flow) evolved by a sample as a function of time (W or µW)
$f(\infty)$	The final heat value – the maximum heat evolved by a sample (J)
$g(t)$	Complex heat flow processes arising due to factors other than the cells (W or µW)
K_s	Monod substrate constant (g/L)
$N(t)$	Number of cells at time t (cells)
P	Cell dry weight (g)
P_{max}	Maximum cell dry weight (g)
pH_{20}	The value of the pH in the APT after 20 minutes
Φ_t	= $N(t) * q$ where q is constant (W)
Φ_0	= $N(t) * q_0$ where q_0 is constant (W)
q	Power output of each cell (W/cell)
q_0	Initial power output of each cell (W/cell)
q_1	Power output per cell in the exponential phase (W/cell)
$\dot{q}_0$	Heat flow produced due to the basic cell metabolism (W/cell)
r	Transition coefficient – heat flow per gram of cellular material (W/g)
σ	Heat flow per unit substrate (W/g)
t	Time (seconds or hours)
t_{max}	Time taken for the heat flow (power) of a sample to reach its maximum (peak) heat flow value (seconds or hours)
t_{50}	Time taken for the heat flow (power) of a sample to reach 50% of the maximum (peak) heat flow value (seconds or hours)
τ	Lag time (seconds or hours)
μ	Specific growth rate (h^{-1})
μ_{max}	Maximum specific growth rate (h^{-1})
v/v	Liquid concentration as a volume/volume percent

Abbreviations

APT	Acidification Power Test
ATP	Adenosine triphosphate
Ca.	Circa (approximately)
CAP	Cumulative Acidification Power
CBS	Centraalbureau voor Schimmelcultures
CFU	Colony Forming Unit
df	Degrees of Freedom
E. coli	*Escherichia coli*
EtOH	Ethanol
GPT	General Performance Test
HSP	Heat Stress Protein
HPLC	High Performance Liquid Chromatography
IDU	Imidazolidinyl urea,
IMC	Isothermal Microcalorimetry
ITC	Isothermal Titration Calorimetry
MIC	Minimum Inhibitory Concentration
MS	Microsoft
MV	Methylene Violet (viability stain)
OD	Optical Density
Rcf	Relative Centrifugal Force
rpm	Revolutions Per Minute
S. cerevisiae	*Saccharomyces cerevisiae*
SCI	Bacteriostatic/Bactericidal index
STDEV	Standard Deviation
VBA	Visual Basic for Applications
TAM	Thermal Activity Monitor
TAP	Total Acidification Power
YPD	Yeast Peptone Dextrose

1 Introduction

1.1 Background and context

The microbial category of yeast have been studied extensively because of its ubiquity, robust nature and usefulness (Bergman, 2001). Yeast are classified as unicellular eukaryotes and fall under the kingdom of fungi. They are widely used in medical research (Sherman, 2002) and has numerous commercial uses in the brewing, winemaking, bread making and bioethanol industries. *Saccharomyces cerevisiae* has been used for baking, winemaking and brewing since ancient times (Madigan et al., 2010). *S. cerevisiae* holds great economic importance because of the range of industries that depend on it as a biological catalyst. The health of yeast cells is consequently critical to these industries. The number of living yeast cells capable of reproduction (cell viability) and their physiological capabilities and metabolic activity (cell vitality) are affected differently by stresses encountered in commercial processes, with this having implications for the final product as well as yeast management within industries (Heggart et al., 2000). This is especially relevant in the brewing industry where yeast cells are used for multiple brews and are exposed to various stresses, through the process and subsequent storage, that effect their viability and vitality (Gibson et al., 2007). Determining cell viability and vitality independently is therefore of interest for the optimisation of certain commercial processes as well as producing a consistent product (White et al., 2003).

Calorimetry is used to determine the heat flow associated with a body or process by measuring the change in particular state variables. A device used to measure this heat flow is termed a calorimeter. Calorimetry has been formally used in the study of the biological sciences since 1783, when Lavoisier and La Place used calorimetry to measure the heat emitted by a guinea pig (Morris, 1972). Calorimetry has developed steadily over the last century with the gradual advent of different calorimetric techniques. Modern day calorimetric assays are often carried out isothermally and can measure minute heat flows, with the latest instruments being accurate in the micro- and nano-watt range (Braissant et al., 2015), giving rise to the term isothermal microcalorimetry (IMC). Isothermal microcalorimetry can be used to measure the heat evolved from as few as 1000 cells, allowing for the detection of cell populations traditionally below the detection limit of other techniques (Braissant et al., 2010). Since the heat evolved from microorganisms is proportional to their overall metabolic activity (Anderson et al., 2002), IMC has become a useful tool in the study of microorganisms. Batch isothermal microcalorimetry has the advantage of being unobtrusive. However, it is non-specific as the heat flow measured is the sum of all processes releasing and taking up heat in the system of interest (Schaarschmidt and Lamprecht, 1978).

IMC has been used to investigate the effects of stress on yeast metabolism and thus heat output (Antoce et al., 1996b). No work has been published to date in which isothermal microcalorimetric measurements are used to derive a quantification of yeast viability and vitality to describe the physiological state and status of the cells. Given the recent technical advances in microcalorimetry, there is opportunity to investigate the use of IMC in determining

the viability and vitality of yeast, which has significant commercial importance. This forms the focus of the current study

1.2 Scope

The primary focus of this study was the development of a method to determine cell viability and vitality using isothermal microcalorimetry. This was done using a single lab strain of the yeast, *S. cerevisiae* as the model micro-organism.

The beer brewing industry was used as a case study and a potential sphere of application of the work presented, therefore stresses commonly associated with the brewing industry were of primary interest. Two brewing stresses were investigated, namely: temperature shock as cold shock and exposure to high ethanol concentrations. These were considered individually and in combination. Furthermore, given that commercial brewing typically occurs batch wise, only batch systems were investigated.

1.3 Objectives

The overall objectives of this project were:

1. Determine the viability and vitality of a lab strain of *S. cerevisiae* based on the heat generation measured using isothermal microcalorimetry;
2. Subject the yeast to different process stresses and assess the impact on cell viability and vitality based on the calorimetric output; and
3. Establish an acceptable degree of repeatability for the methods developed.

1.4 Structure of dissertation

The above introduction is followed by a review of the relevant literature. The literature review established the basics of yeast metabolism as well exploring the various aspects of yeast viability and vitality. This is followed by a review of microcalorimetry and its application in the microbiological sciences. Thereafter, the status quo regarding the use of microcalorimetry to investigate various aspects of yeast health is presented. The literature review is concluded by providing a summary of the findings and identifying areas requiring further study. The detailed project objectives are developed from the review, and key questions and overall hypothesis presented. Chapter 3, focussed on material and methods, describes the procedures employed to propagate yeast and analyse its viability and vitality. These include microcalorimetry as well as other traditional viability and vitality assays. The programme formulation for each experiment is presented. Chapter 4 provides insight into the use of the microcalorimetry and the development of the method used to determine yeast health, using repeatability and heat killing experiments. In Chapter 5, the results and discussion of subjecting the yeast to various cold stresses and ethanol stresses then follows. Lastly, in Chapter 6, overarching conclusions stemming from both the method development and stress testing are drawn and recommendations made.

2 Literature Review

In Section 2.1 yeast metabolism and growth are described, followed by a review of yeast viability and vitality. Common stresses yeast encounter in the brewing process are also examined. Section 2.2 reviews the technical aspects relating to calorimetry, focusing on isothermal microcalorimetry (IMC). The application of IMC in the microbiological sciences is reviewed in Section 2.3. Common problems encountered with IMC in a biological context are reported. Section 2.4 covers the application of IMC in relation to yeast, focusing on yeast growth and metabolism as well as how the response of yeast to different stresses is analysed using IMC. Sections 2.5 to 2.8 provide a summary of key findings, the detailed project objectives, key questions arising from the literature and the project hypothesis, respectively.

2.1 *Saccharomyces cerevisiae* as a model organism

The yeast *Saccharomyces cerevisiae* has had industrial importance since ancient times and is one of the most intensively studied eukaryotic organisms. It is a key component to the alcoholic beverage industry including wine, beer and cider fermentations as well as the food industry (e.g. bread baking), fine chemical production and more recently the bioethanol industry (Lodolo et al., 2008). In this investigation, the applications of *S. cerevisiae* in the beer brewing industry is considered.

2.1.1 Yeast metabolism and growth

Yeast growth in batch cultures occurs typically in four main stages, namely; the lag phase, exponential phase, stationary phase and finally the death phase (Madigan et al., 2010) (Figure 2-1).

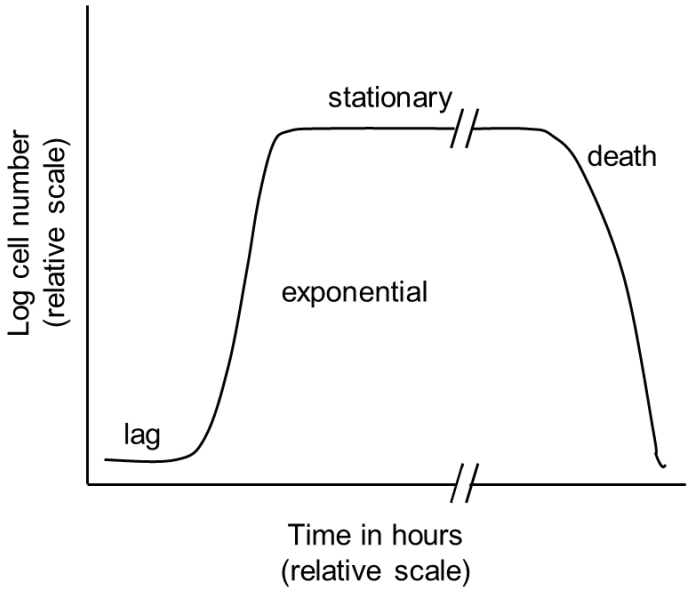

Figure 2-1: Simplified sketch of a microbial growth curve, with the four major phases indicated and labelled as shown.
Figure adapted from Braissant et al. (2013).

Yeast are chemoorganotrophic and require an organic carbon source in order to grow. In nutrient rich aerated media *S. cerevisiae* has a doubling time of approximately 90 minutes (Bergman, 2001). However, yeast can also grow anaerobically. The simplistic stoichiometric equations for aerobic and anaerobic growth of industrial *S. cerevisiae* growth are shown in Equation 2-1 and Equation 2-2, respectively (Villadsen et al., 2011).

$$C_6H_{12}O_6 + 2.37\ O_2 + 0.69\ NH_3 \rightarrow 3.46\ CH_{1.8}0_{0.5}N_{0.2} + 2.54\ CO_2 + 3.90\ H_2O \qquad \textit{Equation 2-1}$$

$$C_6H_{12}O_6 + 0.0519\ NH_3 \rightarrow 0.431\ CH_{1.74}0_{0.6}N_{0.12} + 1.64\ C_2H_6O + 0.196\ C_3H_8O_3 + 1.76\ CO_2 \qquad \textit{Equation 2-2}$$

In a typical commercial lager brewing process, yeast is propagated aerobically (yeast biomass is generated) in a nutrient rich aqueous solution that contains malted barley and hops, known as wort. The yeast is then pitched into aerated wort mixture in a closed vessel. The yeast experiences a short lag phase and grows aerobically until the oxygen in the media is depleted, creating an anaerobic environment under which the yeast shifts to an anaerobic metabolism and the fermentable sugars present in the wort are metabolized to produce ethanol (Gibson et al., 2007). At the end of the fermentation the yeast sediments at the bottom of the fermentation vessel, where it is cropped (removed) and stored before subsequent re-pitching. The serial re-pitching of yeast has significant effects on the yeast quality. The overall quality and health of a yeast population is of great industrial importance and is assessed based on yeast viability and vitality (Kwolek-Mirek and Zadrag-Tecza, 2014). Similarly, top-fermenting ale yeast are also re-pitched.

2.1.2 Yeast viability

Yeast viability generally refers to the percentage of living cells in a given population (Heggart et al., 2000; Kwolek-Mirek and Zadrag-Tecza, 2014; van Zandycke et al., 2010a). Bendiak (2000) defines living cells as those that can reproduce by budding, no matter how slowly. Kaprelyants & Kell (1992) define viability from a bacteriological perspective as the ability of a cell to grow and produce macroscopically observable colonies, which also requires reproduction.

In general, obtaining a measure of viability is subjective, depending on the method and definition of viability used (Heggart et al., 1999). Table 2-1 provides a brief summary of the methods most commonly used to measure cell viability. Two of the methods, cell replication and staining are discussed in more detail below.

Table 2-1: Summary of methods used to measure yeast cell viability

Method category	Method	Examples of assays	References
Cell replication	Plate counts	Colony forming units, spotting test, growth in media, growth inhibition zone	(Basson, 1996; Heggart et al., 2000; Kwolek-Mirek and Zadrag-Tecza, 2014)
	Slide counts	Micro-colony counting	(Basson, 1996; Heggart et al., 2000; Kwolek-Mirek and Zadrag-Tecza, 2014)
Staining	Brightfiled stains	Methylene blue, methylene violet, erythrosine	(Kwolek-Mirek and Zadrag-Tecza, 2014; van Zandycke et al., 2010a)
	Fluorescent stains	Aniline Blue, Acridine Orange, Bromocresol Purple, FUN-1, Rhodamine 123, Oxonol, Primuline	(Heggart et al., 2000; Kaprelyants and Kell, 1992; Kwolek-Mirek and Zadrag-Tecza, 2014; van Zandycke et al., 2010b)
Measurement of cellular components	Adenosine Triphosphate	Firefly bioluminescence	(Stannard and Gibbs, 1986)
	NADH content	Fluorescence at 460nm	(Heggart et al., 2000; Zabriskie and Humphrey, 1978)
Other methods	Electrokinetic measurement	Use of zeta potential	(Heggart et al., 2000; Thonart et al., 1982)
	Capacitance	Application of a 0.3MHz radio signal to a yeast suspension	(Austin et al., 1994; Heggart et al., 2000)

Cell replication

Cell replication methods such as observing the number of colony forming units are a popular way to measure viability as they are inexpensive and easy to perform (Kwolek-Mirek and Zadrag-Tecza, 2014). The number of colonies formed on the surface of solid media is counted after a set incubation time with the assumption that each colony originates from a single cell. The standard plating method is accurate and detects cell viabilities over a wide dynamic range, however, it has a low throughput rate, requiring long incubation times, and can be time consuming (Welch and Koshland, 2013). Slide counts have the advantage of reduced incubation times and providing information on the rate of replication. In addition to cell replication taking long periods of time before results are produced, they further fail to take into account viable but non-reproducing cells (Kwolek-Mirek and Zadrag-Tecza, 2014; Mirisola et al., 2013).

Methylene Blue and Methylene Violet stains

Cell staining identifies both replicating and non-replicating viable cells. There are two main categories of cell stains to determine cell viability (Kwolek-Mirek and Zadrag-Tecza, 2014):

1. Dyes that penetrate the cell membrane and are then metabolised or actively 'pumped out' of the cytoplasm by living cells leaving such cells colourless when observed under a standard light microscope (e.g. methylene blue and methylene violet).
2. Dyes that cannot penetrate a functioning cell membrane, leaving living cells appearing colourless under a light microscope (e.g. propidium iodide, ethidium bromide and trypan blue).

The brewing industry standard for measuring viability is the use of vital dyes (White et al., 2003) such as either the methylene blue assay or the methylene violet assay, despite their lack of reproducibility for viabilities below 90% (Heggart et al., 2000; Lodolo et al., 2008). According to Smart et al. (1999), the methylene violet stain is the preferred vital dye as it exhibits greater resistance to oxidative demethylation and produces less colour variation yielding clearer differentiation between living and dead cells. However, methylene blue has been the industry standard for measuring cell viability as it is easy to perform and is relatively inexpensive (Kgari, 2008). However, the reliability and accuracy of the methylene blue assay has come into question (White et al., 2003). The lack of reproducibility and inaccuracies is thought to be related to the impurities present in the methylene blue dye (Kgari, 2008).

2.1.3 Yeast vitality

The traditional brewing definition of cell vitality is the ability of a cell to metabolise rapidly after moving from a nutrient poor to a nutrient rich environment (Kaprelyants and Kell, 1992). Axcell & O'Connor-Cox (1996) refer to vitality as the ability of a cell to endure a period of stress and still perform. Vitality is also often referred to as the physiological state of the cells that are viable (van Zandycke et al., 2010b). Moonsamy et al. (1995) simply term yeast vitality as its 'fitness for use'. Heggart et al. (2000, 1999) state that there is no strict definition of cell vitality and that in broad terms vitality is a measure of how active the living cells in a given population are.Table 2-2 provides a summary of methods used to measure vitality.

Table 2-2: Summary of methods used to measure yeast cell vitality

Method category	Method	Examples of assays	References
Metabolic activity	Vital stains (can use flow cytometry)	Rhodamine B, rhodamine 123, FUN-1	(Deere et al., 1998; Heggart et al., 2000; Kwolek-Mirek and Zadrag-Tecza, 2014)
	Vicinal Diketone (VDK) reduction	VDK colourimetric assay @540nm	(González and Canales, 1979; Heggart et al., 2000)
	Yeast enzymatic activity	Often carried out using stains	(Kwolek-Mirek and Zadrag-Tecza, 2014)
	Magnesium ion release test	Magnesium release test	(Mochaba et al., 1997)
	Specific oxygen uptake rate	BRF yeast vitality test	(Peddie et al., 1991)
	Acidification power test	AP, CAP, TAP	(Opekarová and Sigler, 1982a; Sigler, 2013a)

Method category	Method	Examples of assays	References
	Intracellular pH	H^+ extrusion activity	(Sigler and Hofer, 1991)
Measurement of cellular components	Adenosine Triphosphate	Firefly bioluminescence	(Siro et al., 1982)
	Adenylate Energy charge	HPLC, GC-MS	(Heggart et al., 2000)
	NADH	NADH probes, UV fluorescence	(Xie, 2008)
	Glycogen, Trehalose, HSP-12	Near infra-red reflectance spectrometry, iodine staining	(Heggart et al., 2000; Sahara et al., 2002)
	Sterols & Unsaturated Fatty Acids	GC-MS	(Rencken et al., 1995)
Fermentative capacity	Glycolytic flux rates	Glycolysis Stress Test, Seahorse XF	(Larsson et al., 1997)
	CO_2 measurements	CO_2 probe	(Heggart et al., 2000)
	Short fermentation test	(ethanol production) HPLC	(Heggart et al., 2000)

The disadvantage of most methods used to measure microbial vitality is that they tend to be complex to execute, requiring advanced equipment. The acidification power test (APT) is an exception to this and is thus an assay of particular interest due to its simplicity. The APT is discussed in further detail in the following section.

The degree of opacity of a dilute yeast slurry, referred to as ‘haze’ formation, is commonly used in the brewing industry as a way to measure yeast quality. The exposure of yeast to shear stress (Stafford, 2003) or high alcohol and/or low pH’s (Siebert, 2006) can result in the formation of haze. The haze is generated by the release of certain cellular compounds such as betaglucans, arabinoxylans, glycoproteins and proteins into the surrounding media (Douglas et al., 2006). The degree of haze formation can vary considerably and depends on the nature of the stress the yeast is exposed to. The haze of a yeast suspension cannot be used to directly measure yeast viability or vitality due to the formation of haze not being directly linked to either the number of living cells or their overall physiological state. The occurrence of haze can either come from dead cells breaking up or living cells releasing certain cellular compounds. Therefore the occurrence of haze is linked to a loss in yeast quality or cell damage (Basson, 1996). Therefore haze formation is not an appropriate measure of cell vitality, while remaining important for assessment of beer quality.

Acidification power test (APT)

Sigler (2013) describes the APT to be an attractive measure of yeast vitality as it is easy to perform, is fast, requires basic equipment and yields results that have satisfactory reproducibility. The APT was originally developed by Opekarová & Sigler (1982b) as a measure of brewing yeast fermentation performance. The APT has since been modified for use in the baking and milk processing (cheese making) industries (Sigler, 2013b). The test is based on the principle that yeast cells actively balance the concentration of intracellular and extracellular hydrogen ions (H^+) in the presence of an un-buffered medium or after the addition

of a suitable substrate (Kara et al., 1988; Sigler et al., 1981). The method developed by Opekarová & Sigler (1982b) measures the pH change (proton efflux) of a yeast sample in response to being suspended in de-ionised water (spontaneous acidification power) and the pH change in response to the addition of glucose (substrate-induced acidification power). The magnitude of this pH shift gives an indication of the ability of the yeast to perform a successful fermentation. This provides insight to the physiological state or 'metabolic vigour' of the yeast (Gabriel et al., 2008; Kara et al., 1988; Opekarová and Sigler, 1982b; Sigler, 2013b). The APT has been shown to differentiate between different physiological states of yeast with great sensitivity (Riis et al., 1995). The APT gives an indication of cell growth rate, oxygen consumption rate, cellular ATP reserves, cellular glycogen profiles, intracellular and extracellular buffering capacity as well as the ability of the cells to establish a proton balance by the fermentation of glucose (Basson, 1996; Kara et al., 1988; Opekarová and Sigler, 1982b).

The biochemical mechanisms involved in the underlying principle of the APT are powered by a number glycolytic substrates, as well as endogenous and exogenous substrates (Basson, 1996). The acidification process occurs in both anaerobic and aerobic cultures. Basson (1996) lists the factors that determine the accuracy and reproducibility of the APT to be: the concentration of the yeast in the final yeast suspension, washing the yeast pellet, calibration of the pH probe, temperature control, the pH of the suspending medium, fermentable substrate added, sample handling, duration of the test and the interpretation of the results.

The most recent modification of the acidification power was by Gabriel et al. (2008) who developed the "Optimised Acidification Power Test of Yeast Vitality and its Use in Brewing Practice". The authors investigated the effect of various parameters on the APT and concluded that the APT be determined at 25 °C in a 15 ml sample containing ≥ 5% glucose and ≥ 1.5 g yeast wet weight. The final APT value is given as:

$$APT = 6.3 - pH_{20} \qquad \textit{Equation 2-3}$$

where pH_{20} is the pH of the yeast slurry after 20 minutes – with the addition of the glucose solution occurring after 10 minutes. The '6.3' in Equation 2-3 is the pH of the de-ionised water used to conduct the test. Gabriel et al. (2008) uses a constant value of 6.3 as the initial pH is difficult to measure accurately and, given the logarithmic nature of the pH scale, the initial pH value has much less importance than the final APT value.

2.1.4 Stresses associated with commercial yeast applications

A yeast crop is exposed to various stresses in commercial brewing, including fluctuations in: dissolved oxygen concentration, pH, ethanol concentrations, nutrient availability, osmotic potential, temperatures, pressures and carbon dioxide concentrations. A schematic representation depicting the nature of these stresses at different stages in the commercial brewing process is illustrated in Figure 2-2.

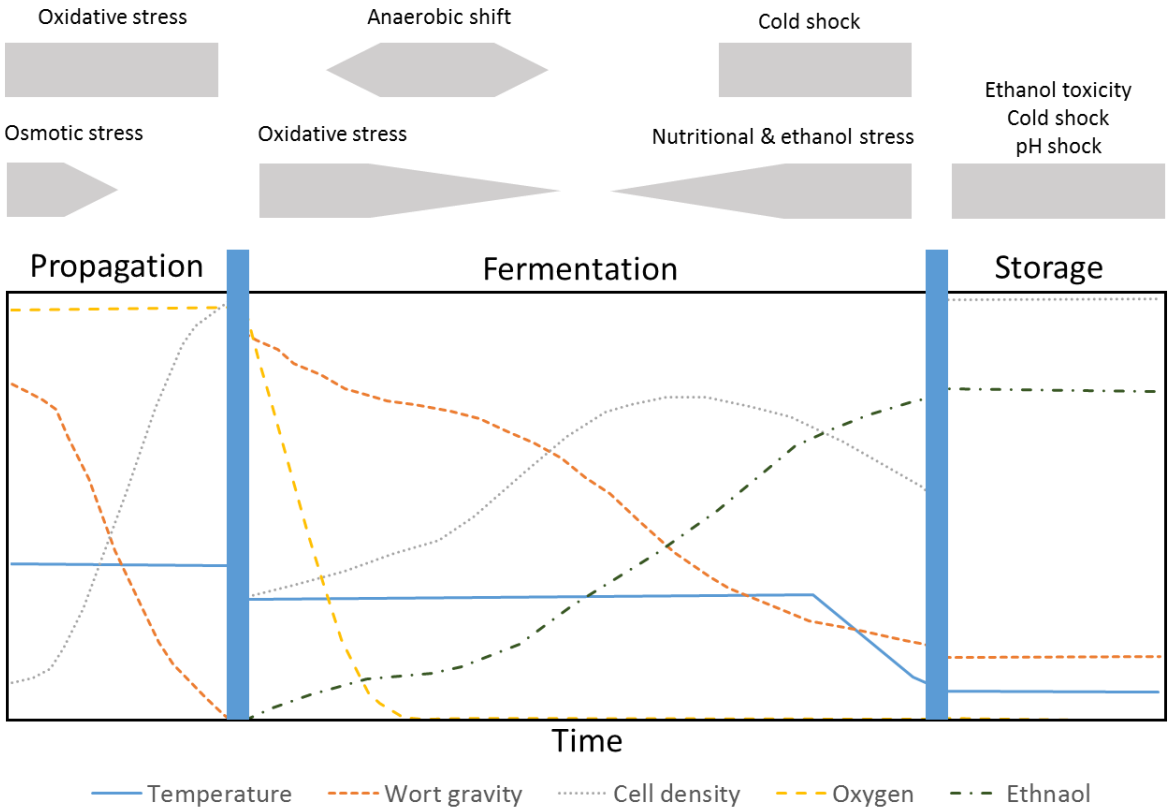

Figure 2-2: Schematic representation of the stresses encountered by yeast during a typical commercial brewing cycle – propagation, fermentation and storage.
Adapted from Gibson et al. (2007).

The stresses shown in Figure 2-2, to which the yeast may be exposed multiple times owing to the practice of re-pitching, reduce the overall yeast quality by lowering the yeast viability and vitality. The overall fermentation performance of a batch of yeast is characterised by its ability to endure such stresses. Fermentation performance of yeast is especially important in the commercial batch brewing process where a single yeast slurry (culture) is recycled (re-pitched) for use in numerous fermentations (Gibson et al., 2007). If the cropped yeast is determined to have too low a viability or vitality, it is discarded and replaced with a freshly propagated yeast culture (Lodolo et al., 2008). Ethanol toxicity and decrease in temperature are used as representative stresses in this study, owing to the potential to mediate these stresses through process operation, hence only these are reviewed in detail.

Cold stress

Within a commercial brewery yeast are exposed to cold stresses, including cold shock and extended storage at low temperature. A cold shock for *S. cerevisiae* is characterised by a drop in temperature to approximately 10 °C or less (Abramova et al., 2001; Kondo et al., 1992; Schade et al., 2004). Ale fermentations usually take place at temperatures between 18 – 25 °C and lager fermentations between 6 – 15 °C (Briggs et al., 2004). The most significant cold shock experienced by brewing yeast is when it is cropped and stored at 4 °C after being brewed at comparatively warmer temperatures, often by passing the yeast slurry through a heat exchanger. This is done in order to minimise contamination and physiological changes of a yeast crop (Gibson et al., 2007).

Low positive temperatures have a number of negative effects on yeast cells, including (as reviewed by Walker, 1998):

- Cell membrane fatty acids may undergo a phase transition, compromising cell membrane integrity;
- Sterol synthesis is reduced, weakening membranes;
- Yeast cells shrink, inhibiting budding; and
- Vaculour membrane damage may occur leading to changes in metabolic activity.

When yeast is cold stressed it produces 'heat shock' proteins (HSPs) that aid in the protection of the cell (Schade et al., 2004). Yeast also produce HSPs as part of the general (or global) stress response when exposed to other stresses, such as oxidative stress, pH stress, nitrogen starvation and osmotic stress (Gibson et al., 2007). One of the primary HSPs produced when yeast is exposed to cold shock is HSP-12. This protein belongs to a small family of HSPs that protect the cell membrane against desiccation by helping to stabilise the membrane (Sales et al., 2000).

Kgari (2008) concluded that the cooling of yeast to 4 °C (at a rate of 0.1 - 1 °C/second) weakens the cell membrane and cell wall, with yeast stored at 4 °C having a lower overall growth rate compared to control yeast stored under ambient temperature conditions. In terms of the effect of the rate of cooling on yeast quality, Fargher & Smith (1995) subjected ale yeast (grown at 25 °C) to a cold shock (8 °C/min) and noticed a prolonged lag phase when cultured thereafter. Nkosi (2001) found that rapidly chilled yeast (3.09 °C/second), by the addition of a beer-based diluent, had 28 - 37% more HSP-12 expression than slow cooled (2 °C/hr) yeast when cooled to a final temperature of 4 °C. It was also observed that rapidly cooled yeast had a 200% increase in protease absorbance, lower CO_2 evolution in small-scale fermentation and increased cell wall damage, which are all considered indications that the yeast suffered a decline in both vitality and viability. Furthermore, Fernández et al (1991) demonstrated by way of an APT coupled with methylene blue stain that cold storage of yeast has a more significant impact on cell vitality than cell viability. The above studies confirm that slow cooling and rapid cooling have an impact on cell viability.

Ethanol stress

During the fermentation process yeast is exposed to increasingly toxic ethanol concentrations. Under normal fermentation conditions, the final ethanol concentration reaches approximately 3 - 6% (v/v). However, in high gravity wort fermentations, which are now the industry standard, the final ethanol concentration can be greater than 10% (Briggs et al., 2004; Gibson et al., 2007). High ethanol concentrations can affect factors relating to both cell viability and vitality. Ethanol can inhibit cell growth (Mager and Varela, 1993; Walker, 1998) by damaging the cell membrane, causing it to leak (Šajbidor and Grego, 1992) resulting in an overall loss in yeast viability (Pina et al., 2004; Sales et al., 2000). Therefore, increasing ethanol concentrations causes the yeast's specific growth rate and fermentation rate to drop (Van Uden, 1983). Yeast viability is especially susceptible to high ethanol concentrations at elevated temperatures (Gibson et al., 2007; Stewart, 2001).

The manner in which yeast responds to ethanol stress is in most cases similar to that of heat stress, with both stresses resulting in the expression of HSPs (Birch and Walker, 2000; Kandror et al., 2004; Palhano et al., 2004). Maximum expression of HSPs, which is yeast's primary response to ethanol, occurs roughly 40 minutes after first exposure (Piper et al., 1994). The threshold response of appreciable HSP production occurs at approximately 4% ethanol by volume and full induction of HSPs occurs from 6 - 10% (Piper et al., 1994). Chandler et al. (2004) termed the gene expression after 1 hour of exposure to ethanol to be the 'early gene response', and after 3 hours of exposure to be the 'late genetic response', with a different suite of genes being expressed in each case.

Yeast adapts to the ethanol stress by increasing the catabolism of ethanol, synthesising stress proteins, including HSPs, and increasing membrane unsaturated fatty acids which alters the membrane fluidity (Walker 1998). Sales et al. (2000) showed, through the use of wild type yeast and a mutant yeast strain with a HSP-12 knock-out, that HSP-12 plays a significant role in protecting the yeast from ethanol stress. Pina et al. (2004) investigated cell inactivation due to progressive ethanol exposure in *S. cerevisiae* (PYCC 3507). They found that there was no impact on cell viability following a 4 minute exposure to 20% (v/v) ethanol. In terms of constant ethanol exposure, Chandler et al. (2004) found that a haploid lab strain yeast displayed no appreciable growth in the presence of 10% (v/v) ethanol.

Therefore, depending on the ethanol concentration, exposure of yeast to ethanol can have a significant effect on growth. Exposure to ethanol causes yeast to express HSPs, in particular HSP-12, which helps protect the cell from ethanol stress. Short exposure of yeast to ethanol appears not to affect yeast growth as significantly as long-term exposure.

2.2 Microcalorimetry

There are many types of calorimetry: direct calorimetry, bomb calorimetry, dynamical calorimetry and indirect calorimetry. The focus of this review is on isothermal microcalorimetry (IMC) – a type of direct calorimetry. The focus on IMC is due to its potential use in biotic systems and application in yeast quality research.

2.2.1 Isothermal microcalorimetry

Microcalorimetry is a sub-branch of calorimetry and deals with heat fluxes measured in the nano- and micro-watt range, hence microcalorimetry. In isothermal microcalorimetry (IMC), the system of interest is kept in an isothermal state while the heat flux is measured. The heat evolved or taken up by the system has to flow from the surroundings into the system, or vice versa, in order to keep the system in an isothermal state (Wadsö, 1997). Therefore isothermal microcalorimeters are also referred to as heat conduction calorimeters, as the heat produced in the calorimetric vessel (the system) flows to or from a heat sink (Braissant et al., 2010). Figure 2-3 gives a simple diagrammatic representation of an exothermic reaction taking place inside an ampoule (vial) placed inside an isothermal microcalorimeter.

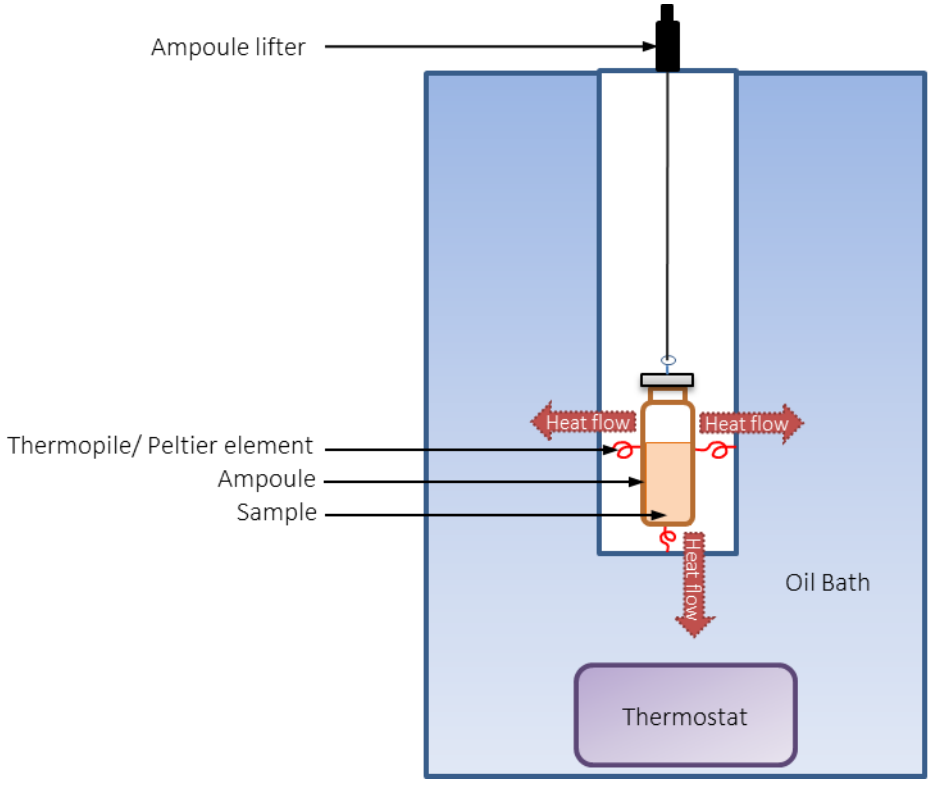

Figure 2-3: Simple diagrammatic representation of a one channel isothermal microcalorimeter.
Note since heat is flowing from the sample into the surrounding bath, the sum of the net reaction taking place in the sample is exothermic.

In practice IMC is not perfectly isothermal, as small variations in sample and system temperature are observed (Braissant et al., 2010). However, modern isothermal microcalorimeters are considered essentially isothermal as the negligible temperature deviation in the calorimetric vessel yields results effectively the same as if the system were perfectly isothermal (Wadsö, 2010). The heat sink itself is often placed in a thermostat to further maintain temperature stability (Braissant et al., 2010). The calorimeter is kept essentially isothermal using electric heaters and/or Peltier elements (Wadsö and Goldberg, 2001). Most modern calorimeters are designed as 'twin instruments' whereby the heat flow data from the sample is measured relative to an inert reference. This is a design feature that reduces noise and increases sensitivity (Wadsö and Goldberg, 2001). The reference sample should ideally be situated in the same heat sink and have the same heat capacity as the system of interest (Braissant et al., 2010).

Microcalorimeters typically produce a continuous, real-time electric signal related to the current being induced in the Peltier element or thermopile. The signal is proportional to the heat flow between the calorimetric vessel and the surroundings, known as the Seebeck effect (Wadsö, 1997). Using constants unique to each calorimeter (determined via a calibration process) the electric signal can be converted into a measure of heat flow in Watts (W). The heat flow signal can then be integrated to produce a heat curve in Joules (J). The calorimetric signal (in either Watts of Joules) is often referred to as a thermogram.

Two important factors regarding the calorimetric signal are signal baseline and noise. The baseline of a calorimeter is defined as the "value recorded for the calorimetric signal when no thermal power is evolved in the reaction vessel, except for a constant or predictable power from stirring, etc." (Wadsö and Goldberg, 2001). The noise of a calorimetric signal is defined as "short time (normally <1 min) random fluctuation of the baseline value", given as "± (twice) the standard deviation of the fit" (Wadsö and Goldberg, 2001). Noise usually occurs due to thermal disturbances relating to the surroundings or due to the electronic system (Wadsö and Wadsö, 2005).

IMC typically makes use of small static sealed ampules ranging from 4 – 20 ml that are made from clear glass or various metals (Braissant et al., 2013). These are the simplest type of systems and are often the most unambiguous, allowing the subsequent analysis of the undisturbed samples after they have been extracted from the calorimeter (Braissant et al., 2010). IMC is appealing due to samples requiring little to no prior preparation. Samples can be tested in any phase, do not require a transport phase, can be label free and samples do not need to have any other specific properties such as opacity (Braissant et al., 2015).

Another type of calorimetry that falls under the branch of IMC is Isothermal Titration Calorimetry (ITC). ITC is used in the characterisation of fast reactions and is routinely used to compute ligand binding energies (Braissant et al., 2010). ITC is primarily a tool for molecular studies, although it has been used to study biological systems as well (Atri et al., 2015; Ladbury, 2004; Theerarattananoon et al., 2008). The main difference between batch IMC and ITC is that with ITC chemicals can be precisely injected into the reaction vessel.

2.2.2 Errors associated with isothermal microcalorimetric measurements

In some studies, authors have modified microcalorimeters to measure other useful parameters such as pH and turbidity simultaneously (Bäckman et al., 1995; Johansson and Wadsö, 1999). However, due to the sensitivity of the isothermal calorimeters, combining calorimeters with additional devices that can be used to measure other properties can result in technical errors, lower throughputs and higher costs (Braissant et al., 2013).

Due to the non-specific nature of IMC, IMC is susceptible to systematic errors arising due to evaporation, condensation, corrosion, adsorption and friction (Wadsö and Goldberg, 2001). As expected, the smaller the heat quantities being measured the more susceptible the measurement is to such systematic errors. Out of the many systematic errors that can occur, water evaporation is a significant issue due to its high heat of vaporisation combined with its small molecular size (Wadsö and Wadsö, 2005). The evaporation of water is endothermic, causing a significant flow of heat from the surroundings into the system. The evaporation of water can cause major error in the measured heat flow (Wadsö, 2010). Evaporation usually appears as a drop in the heat flow, in most cases resulting in a negative heat flow. The major source of evaporation is a poorly sealed vessel or system (Wadsö and Wadsö, 2005).

Isothermal microcalorimeters require routine calibration; this calibration is usually carried out by the release of electrical heat by an electric heating device located inside the calorimetric vessel (Wadsö and Goldberg, 2001). Electrical calibration errors can result in errors on the

order of 5% (Wadsö and Wadsö, 2005). Ideally, the calibration of an IMC should be checked using a test reaction, with many standard test reactions being described by Wadsö & Goldberg (2001). Once determined, calibration constants usually remain constant over a number of years (Wadsö, 2010). However, Wadsö (2010) states that the intervals between calibrations should be based on the amount of data one is prepared to loose in the event that the calorimeter's properties change or the machine breaks down.

2.3 Application of isothermal microcalorimetry in the microbiological sciences

Almost all metabolic processes involve the generation of heat. This heat is associated with underlying biological behaviour, which although unspecific in nature, offers a more intuitive and quicker reflection of biological processes than other more sophisticated sensor types (Theerarattananoon et al., 2008). The heat flow curve produced by a calorimeter (e.g. Figure 2-4) is directly proportional to the rate at which a reaction is taking place. The heat flow curve is thus a good proxy for metabolic activity and as such correlates well with the growth curve (Braissant et al., 2015).

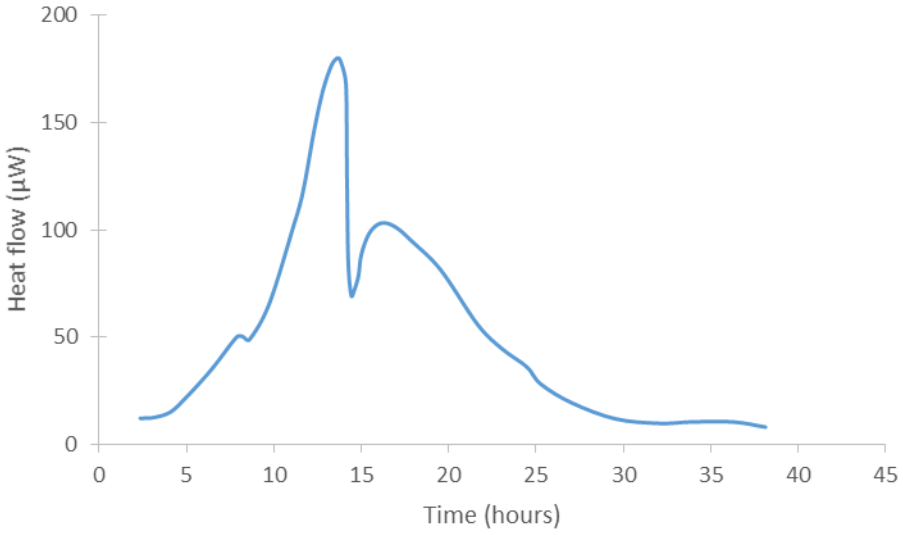

Figure 2-4: Simplified sketch of a typical microcalorimetric measurement of an *Enterococcus faecalis* 3 ml culture.
Raw data from Braissant et al. (2013).

Given the sensitivity of IMC, as few as 1 000 -10 000 active cells can be monitored non-destructively, with samples requiring little to no preparation (Braissant et al., 2010). Cell numbers per millilitre as low as these are not possible to measure using traditional techniques such as direct counting or turbidity (using a spectrophotometer). Conventional petri-dish counts, considered the universal standard for measuring cell growth, are time consuming, usually only delivering results in 24 - 48 hours and in some cases even longer (Braissant et al., 2015). This is in contrast to IMC, which can provide real time heat data relating to the activity of otherwise macroscopically unobservable microbial communities.

IMC is primarily used to monitor bacterial activity and growth of various systems, with an increasing use in the field of biotechnology as a monitor of process yield, growth rate or stoichiometry (Braissant et al., 2013). The use of calorimetry in biotechnology can be a useful quantitate analytical tool especially when combined with dissolved oxygen concentration, pH, substrate utilization and biomass production data. The online measurement of heat evolution of biological processes can be used on a production scale to aid in advanced control strategies and predict fermentations via the indirect determination of product formation and biomass concentration (Maskow and Harms, 2006; Yonsel et al., 2007).

The heat flow curve generated by a microcalorimetric measurement relates closely to assays such as turbidity or optical density and measures of metabolite production (Alklint et al., 2005; Braissant et al., 2015, 2013). However, many papers presenting isothermal microcalorimetry data do not have supporting data from other microbiological measurements, such as cell counts, optical density or other metabolic assays (Braissant et al., 2013).

Given the broad range of applications relating to IMC, Braissant et al. (2010) remark that it is surprising that IMC has not become more widely adopted in the microbiological sciences. Braissant et al. (2015, 2010) attribute the slow uptake of the technology to the cost associated with modern calorimeters, a lack of education and the fact that many biologists are unaware of the potential applications of IMC in their fields.

2.3.1 Application of calorimetry in the environmental sciences, medicine and the food industry

As outlined in the review by Braissant et al. (2010), IMC has been used in the field of environmental microbiology to study mixed microbial communities. Soil science is a field that microcalorimetry has been used extensively in for the past few decades, with soil systems still presently being analysed using IMC (e.g. Qian et al., in press; Chen et al., 2014; Zhang et al., 2014). The caveat in such complex systems is the non-specific nature of IMC – that is distinguishing between the heat released due to microbial activity and the heat produced due to other chemical reactions.

An extensive review by Rong et al. (2007) into the applications of IMC in the soil sciences identified the following major areas of application: investigation and quantification of microbial activity; monitoring of soil organic pollutant toxicity and decomposition; risk assessment of heavy metal contamination; heat effect of adsorption and ion exchange. Using the effective growth rates of mixed microbial communities in soil, determined using power and heat curves, it is further possible to determine the substrate utilization efficiency (Barros et al., 1999; Braissant et al., 2015). The use of IMC in the soil sciences is promising as such complex systems are difficult to analyse using conventional methods (Braissant et al., 2015).

IMC is increasingly being employed in medicine as a tool for the rapid detection of infections and the rapid identification of pathogens (Baldoni et al., 2009; Bonkat et al., 2012; Trampuz et al., 2007a, 2007b). Furthermore, the inhibitory effects of drugs/antimicrobials can also be

determined passively yielding more accurate and reproducible results in the same amount of time as compared to traditional methods (von Ah et al., 2009; Yang et al., 2010).

IMC has been successfully used to gain further understanding and insight into certain aspects of commercial food production/processing. IMC is advantageous as many food products are opaque liquids or solids and do not lend themselves easily to other forms of microbial assays (Braissant et al., 2015). IMC has primarily been investigated as a tool to predict the shelf-life of perishable food stuffs such as juices and vegetables (Alklint et al., 2005; Gómez et al., 2004; Wadsö and Gómez Galindo, 2009). There is also scope to make use of IMC to help select strains of microorganisms used in food manufacturing.

2.3.2 Problems with the different types of microcalorimeters in the context of biological systems

Two of the main problems associated with batch isothermal microcalorimetry are the long equilibration times (~1 hour), during which data cannot be collected but metabolic changes may occur, and the ever changing environment in the sample vessel, which accumulates metabolic waste products (Braissant et al., 2010). Furthermore, there are challenges associated with aeration (oxygen depletion in sealed vessels) and stirring (Brettel et al., 1980; Maskow and Harms, 2006). In unstirred vessels the sedimentation of cells can occur creating unfavourable diffusion gradients (Wadsö and Wadsö, 2005).

Much of the older microcalorimetric work on biological systems was performed using flow microcalorimeters (Braissant et al., 2015). Flow microcalorimetry, while allowing high throughput, has many associated problems. The main associated problem is linked to the low volumetric flow constrained by the time required for the system temperature to equilibrate. Given this significant ‘lag time’, the exact environment to which the cells are exposed is difficult to control. The long residence time in the system may result in the dissolved oxygen and/or nutrients being significantly depleted in the flow line before heat output is measured (Lamprecht, 1980). The Teflon flow lines of the flow calorimeter used by Hoogerheide (1975) in his anaerobic investigations allowed the diffusion of small amounts of oxygen into solution causing conditions to not be entirely anaerobic. Further, flow isothermal microcalorimetry requires precise control of the flow rate and is time consuming to set up and sterilise (Braissant et al., 2010). There is possibility of adhesion or settling of microorganisms onto the internal surfaces of the flow lines which can lead to large systematic errors in the calorimetric measurement (Lamprecht, 1980; Wadsö and Wadsö, 2005).

Sterilised growth medium can produce significant quantities of heat due to non-biological reactions (Wadsö, 2009). The subtraction of the signal produced by a suitable sterile control sample from the signal from the system of interest has been deemed acceptable to counteract this phenomenon (Braissant et al., 2015).

Lastly, special note should be made concerning the non-specificity of the heat flow signal produced. The heat flow/calorimetric signal at any point in time represents the sum of the catabolic and anabolic processes occurring in a biological system (Schaarschmidt and

Lamprecht, 1978). Thus, careful planning is required in order to ensure that the observed heat flows are due to the process being studied – the system of interest.

2.4 Application of isothermal microcalorimetry relating to yeast

IMC has been used to study a number of yeast systems. There are three main categories of studies in the literature: those that investigate yeast growth; those that investigate various aspects of yeast metabolism (including issues regarding substrate usage); and studies that investigate the effect of a stress or drug on the functioning of yeast.

2.4.1 Yeast growth

IMC thermograms have been used to accurately measure yeast growth. It is important to note that not all parts of a thermogram (calorimetric signal) relate to cell numbers, as is sometimes misconstrued by certain authors (Braissant et al., 2013). This is to say a decline in power output does not necessarily correlate to a decrease in cell numbers. Often the use of power data as a proxy for cell numbers only remains true during the early exponential phase of growth (Braissant et al., 2013). More often the heat curve (integrated power curve) has been recognised as a direct proxy for population growth.

The model most commonly used to relate cell numbers to power output, due to its simplicity, is one that assumes a constant heat output per cell (Braissant et al., 2013). The model was developed by Chang-Li et al. (1988), and is given by Equation 2-4:

$$N_t \cdot q = N_0 \cdot q \cdot exp[\mu(t-\tau)] \qquad \textit{Equation 2-4a}$$

$$\Phi_t = \Phi_0 \cdot exp[\mu(t-\tau)] \qquad \textit{Equation 2-4b}$$

where N_t is the number of cells at time t, N_0 is the initial number of cells, q is the power output of each cell, τ the lag time and μ the specific growth rate. In the early exponential phase of growth when there are no growth limiting factors μ is equal to the maximum specific growth rate, μ_m. If the power output per cell is assumed constant, then Φ represents the heat flow at time t (Φ_t) and the initial heat flow (Φ_0). Equation 2-4 can easily be linearized and additional terms can be added to take into account artefacts arising due to the calorimetric signal baseline drift and shift. An analogous equation can be related to fit heat data rather than heat flow data. The downfall of such simple equations is that they can only be applied to the exponential phase.

Other more complex sigmoid models that fit the entire cumulative heat curve (integral of the power curve) are available. Such models improve the reproducibility of the parameters determined, as they fit the entire heat curve, not just a portion thereof (Braissant et al., 2013). Examples of such models include the modified Gompertz and the modified Richards equations, which allow for the determination of lag time, the maximum specific growth rate and a ‘maximum growth’ parameter. Another more complex sigmoid model, commonly used to model bacterial contamination of food is the Baranyi equation (Baranyi, 2010; Grijspeerdt and Vanrolleghem, 1999).

Hashimoto & Takahashi (1982) used the power output of baker's yeast to determine quantitatively a link between inoculum size and growth thermograms. They used a mixed yeast culture in a twin conduction calorimeter with a single 200 cm^3 sample chamber with a stirrer operating at 450 rpm. The initial inoculum size was determined by weight. They observed that using different inoculum sizes primarily shifted the growth curves, yielding differing lag times, as shown in Figure 2-5 (A). Furthermore, they confirmed a direct link between the heat signal and turbidity of a growing yeast culture.

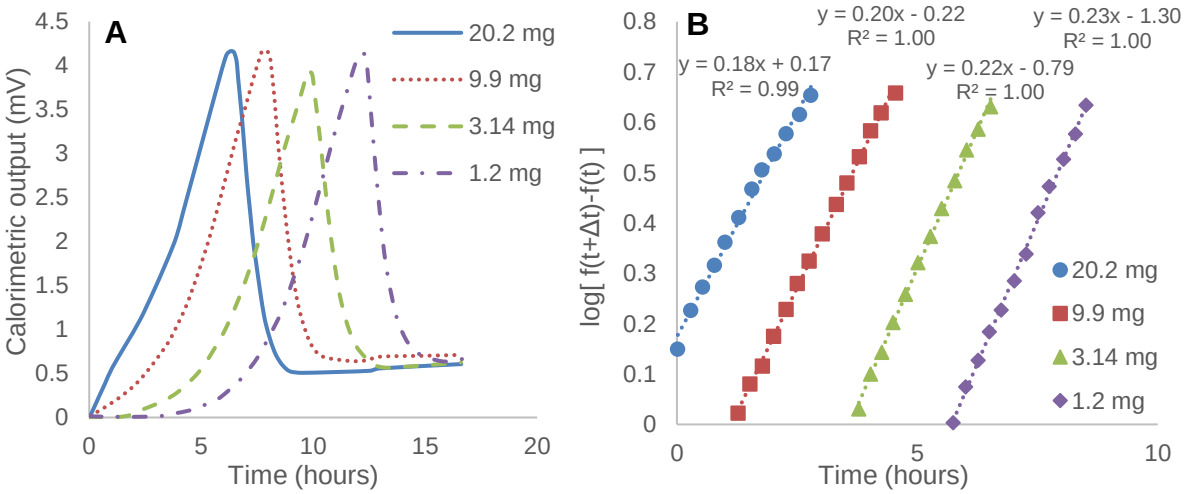

Figure 2-5: A) Growth thermograms and B) Guggenheim plots; observed for batch cultures of baker's yeast of varying inoculum sizes.
Raw data from Hashimoto & Takahashi (1982). The units of graph A are given as mV (as opposed to milli- or nano-watts) as the authors presented their heat flow data as unconverted electric signal data.

Hashimoto & Takahashi (1982) start their derivation to link cell numbers to the thermograms by assuming simple exponential growth, with the inclusion of a lag time, τ. It is then assumed that the initial cell population on inoculation, N_0, has a given power value per cell, q_0, and that exponential phase cells have a different power output, q_1. Given that the heat released, termed $f(t)$, is simply the integral of the power time curve, the total heat release at any given time, after performing the necessary integration and collecting constants, is equal to;

$$f(t) = N_0 \cdot a \cdot exp(\mu \cdot t) + N_0 \cdot b \qquad \textit{Equation 2-5}$$

where $a = {q_1}/{(\mu \cdot exp(\mu \cdot \tau))}$ and $b = \int_0^\tau N_0 dt - {q_1}/{\mu}$

Hashimoto & Takahashi (1982) isolated the specific growth rate μ by linearizing Equation 2-5 using the Guggenheim method:

$$log[f(t + \Delta t) - f(t)] = log\, N_0 \cdot a \cdot [exp(\mu \cdot \Delta t) - 1] + {\mu}/{2.303} \cdot t \qquad \textit{Equation 2-6}$$

By plotting $\log[f(t + \Delta t) - f(t)]$ versus t, a straight line with slope $\mu/2.303$ is obtained, as shown in Figure 2-5 (B). Given the assumption above, Equation 2-6 only applies to the exponential growth phase, where μ is equal to the maximum specific growth rate, μ_m.

Ultimately Hashimoto & Takahashi (1982) demonstrated that the cumulative heat curves [$f(t)$] correlated well to cell numbers, with the different inoculum sizes having a negligible effect on μ_m. This finding was confirmed in the group's later works (Antoce et al., 1997b, 1996a). This property has been confirmed for a number of microbial systems and is stated in the review by Braissant et al. (2013) to be true in the general case during the early exponential phase of growth.

Following on from the work done by Hashimoto & Takahashi (1982), Itoh & Takahashi (1984) analysed the effect of temperature on the growth kinetics of the same baker's yeast strain. The growth thermograms from their work are shown in Figure 2-6 (A).

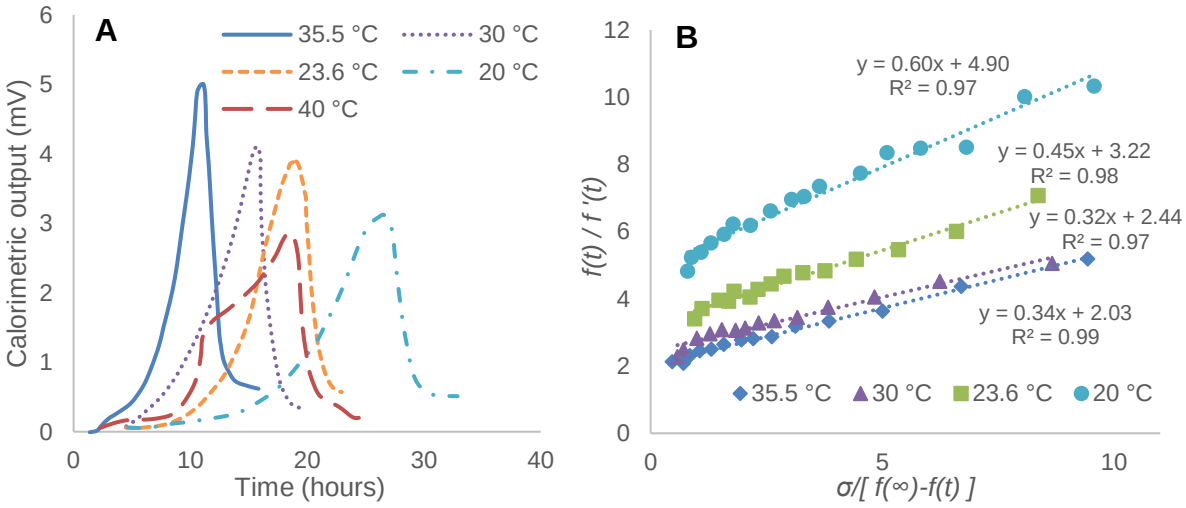

Figure 2-6: A) Growth thermograms and B) Lineweaver-Burk plots; observed for cultures of baker's yeast growing at different temperatures.
Raw data from Itoh & Takahashi (1984).

Although Itoh & Takahashi (1984) acknowledge the study to be a continuation of their previous work, they make use of a different method to determine the specific growth rate; no reason is given for this. They start their derivation by defining the theoretical heat curve and assuming that the heat released per cell is constant. This differs from Hashimoto & Takahashi (1982) in which two specific heat outputs were defined, one for stationary phase cells and one for exponential phase cells. Using Monod growth kinetics and the definition of specific growth rate, they derived Equation 2-7, after simplifying:

$$f'(t)\Big/_{f(t)} = \mu_m[f(\infty) - (t)]\Big/_{\{\sigma K_s + [f(\infty) - f(t)]\}} \qquad \textit{Equation 2-7}$$

where $f'(t)$ is the heat flow curve, $f(\infty)$ the final heat value, σ the heat flow per unit substrate, K_s the substrate constant. A plot of $f(t)/f'(t)$ versus $\sigma/_{[f(\infty) - f(t)]}$ should theoretically yield a straight line with a gradient equal to K_s/μ_m, with an intercept of 1/ μ_m, as seen in Figure 2-6 (B). Itoh & Takahashi (1984) claim this type of plot to be a Lineweaver-Burk plot (Lineweaver and Burk, 1934), also known as a double reciprocal plot. This is the same type of plot employed by Belaich in his microcalorimetric studies of yeast and *E. Coli* growth

kinetics (Belaich and Belaich, 1976; Belaich et al., 1968; Murgier and Belaich, 1971). As with Equation 2-6, Equation 2-7 only applies to the early exponential phase of growth.

Itoh & Takahashi (1984) found the specific growth rate to have an Arrhenius type dependence on temperature, with the optimum growth temperature occurring at approximately 33 °C. This Arrhenius dependence is commonly accepted. The change in K_S with temperature was best expressed as a van't Hoff plot, inferring that there was no significant change of K_S with temperature.

Roy & Samson (1988) investigated the heat evolution associated with stirred and unstirred batch cultures of aerobic and anaerobic baker's yeast growing in a glucose medium using flow microcalorimetry. They found a linear relationship between total heat output and biomass concentration and a linear relationship between the total heat output and the initial glucose concentration. They further found a linear relationship between the log of the viable cell numbers (determined using petri-dish counts) and the log of the heat output, as did Tsukamoto et al. (2004). Furthermore, Roy & Samson (1988) proposed a logistic equation to predict biomass concentration as a function of heat output of anaerobically growing cultures. A direct link between heat output and ATP concentration (an indicator of microbial biomass), determined using bioluminometry, was also shown.

Using the theory of irreversible thermodynamics applied to living organisms, Schaarschmidt et al (1977) derived an equation to relate dry weight to the heat production rate of an organism. Schaarschmidt et al (1977) found their equation to fit their thermal data from batch experiments on *S. cerevisiae* at varying temperatures well (R^2 = 0.98). The transition coefficients (heat released per dry gram biomass) of diploid and haploid *S. cerevisiae* grown at 30 °C were calculated to be 53 mW/g and 41 mW/g, respectively.

2.4.2 Yeast metabolism

Theerarattananoon et al. (2008) investigated the effect of temperature variation on yeast metabolic heat release in very-high-gravity (wort with a very high sugar content) fermentations. They further investigated the effect of urea on a fermentation. Adding urea aided in high-gravity wort fermentations and prolonged the logarithmic phase of growth. Theererarttananoon et al. (2008) used an isothermal titration calorimetric setup whereby wort of varying concentrations was injected into a reaction vessel containing stationary phase yeast. The reaction chamber was stirred at a rate of 200 rpm and kept anaerobic.

Schaarschmidt & Lamprecht (1978, 1977) used a flow calorimeter to investigate the growth of wild strain diploid yeast on different carbohydrates. The focus of the study was mainly the occurrence of diauxic growth in different media. Growth thermograms from the study are shown in Figure 2-7.

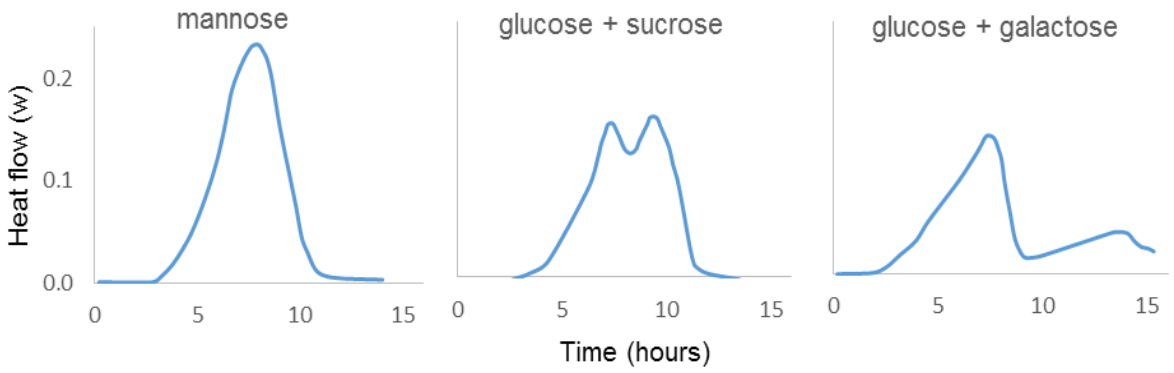

Figure 2-7: Thermograms illustrating the growth of wild type yeast cultures on different carbohydrate substrates. Raw data from Schaarschmidt & Lamprecht (1978).

The occurrence of diauxic growth is clearly distinguishable in growth thermograms by the double peak, with each peak corresponding to a specific sugar being metabolised. Glucose is metabolised first owing to catabolite repression. This is followed by simple monosaccharide sugars as they tend to only differ by one glycosidic bond with only a single intermediate step occurring before such simple sugars join the glycolytic pathway. The processing of comparatively more complex disaccharides requires the synthesis of new transport enzymes and proteins and the hydrolysis into monosaccharides, therefore a considerable lag time occurs before such sugars are metabolised (Schaarschmidt and Lamprecht, 1977). Schaarschmidt & Lamprecht (1978, 1977) further illustrated that this type of diauxic growth can be successfully modelled using Michaelis-Menten kinetics.

Through HPLC analysis, Roy & Samson (1988) showed the significance of the different peaks that occur in a power-time curve due to aerobic and anaerobic *S. cerevisiae* cultivation. In aerobic cultures, the first peak represents the conversion of glucose to ethanol, the second peak represents the conversion of the produced ethanol to acetate and CO_2, the third and last peak that can be observed represents the conversion of acetate to CO_2. This type of calorimetrically observed triphasic growth of aerobic cultures of *S. cerevisiae* is corroborated by the findings of Brettel et al (1980) who performed energy balances over batch and continuous *S. cerevisiae* cultures using flow IMC. For anaerobic *S. cerevisiae* cultures, only a single peak is observed – the conversion of glucose to ethanol and CO_2.

The same bi-modal thermogram curves, similar to that observed for diauxic growth (Figure 2-7), was observed by von Stockar & Birou (1989) when the yeast cultures transitioned from an aerobic to an anaerobic metabolism. The anaerobic heat output was however found to be significantly less than the aerobic heat output – as is consistent with yeast metabolic stoichiometry (presented in Section 2.1.1)

Using flow IMC, the anaerobic fermentation of glucose by Baker's yeast was investigated by Hoogerheide (1975). Rather than basing the metabolic heat output on glucose consumption, the heat output was based on CO_2 production. This was to account for the glucose not completely converted by the anaerobic (ethanol producing) metabolism of the yeast. The study made use of resting cells that were not actively growing. It was found that approximately 80%

of the glucose was fermented anaerobically. It was further found that in the absence of any substrates (yeast was suspended in a phosphate buffer), a significant heat release due to the endogenous metabolism was observed with the no detectable CO_2 evolution.

In order to better understand the metabolism of *S. cerevisiae* in the absence of growth, Fujita & Nunomura (1977) studied aerobic and anaerobic batch cultures of *S. cerevisiae* under non-growing conditions. This was achieved by growing cultures of *S. cerevisiae* in media lacking an exogenous energy source, such as solutions of deionized water, phosphate buffer or 0.2 *M* NaCl. Fujita & Nunomura (1977) found that initially a large spike in heat production was observed, being attributed to the stressed cells using up endogenous energy sources. This is in agreement with the finding of Hoogerheide (1975) (detailed in the previous paragraph).

Given that prior to 1976 most work with yeast and microcalorimetry was done with haploid strains, Lamprecht et al (1976) looked at the effect of ploidy on yeast growth and metabolism using batch microcalorimetry. The authors employed a parallel approach of testing the ploidy of yeast; they used both liquid media and solid agar media (coated to the inside of the calorimetric vessel) in their investigations. The media was glucose rich allowing the metabolism of maintenance to be investigated as well. They found little difference between the two growth media.

2.4.3 The response of yeast to differing stress types

This project explores the potential to use IMC to determine the effect of different stresses, to which yeast is exposed in the industrial brewing industry, on yeast viability and vitality. The focus of this sub-section is to review the techniques used in previous studies to analyse and quantify the effects of stress on yeast.

Beezer et al. (1977) developed a qualitative bioassay using flow isothermal microcalorimetry to determine the effect that nystatin (an antifungal agent produced by certain bacteria) has on yeast. The method is based on taking a relative ratio of the performance of stressed to healthy yeast cells. The method compared well to the agar petri-dish diffusion method. The flow microcalorimetric method used by Beezer et al. (1997) is no longer a widely used calorimetric technique (as discussed in Section 2.3.2).

Much of the work involving batch IMC and stressed yeast originates from the early nineties (e.g. Antoce et al., 1996; Antoce, Takahashi & Nămoloşanu, 1996; Wirkner et al., 2002; Tsukamoto et al., 2004; Arao et al., 2005). A limited number of research groups have investigated the effects of stresses on yeast using IMC. As a result, the body of literature on the topic is small and contains self-citation and use of similar methodologies. The majority of studies involving stressed yeast populations and batch IMC have been authored by Antoce et al. (Antoce et al., 1997b, 1996a, 1996b; Antoce and Nămoloşanu, 2011). The study by Antoce (1996) formed the foundation for a number of microcalorimetric research papers published primarily by Antoce and Takahashi as well as other authors' work in the field. The microcalorimetric work by Antoce and Takahashi has been published in a number of peer-reviewed journals, in both Japanese and English, helping lend credibility to the methodologies employed.

The primary aim of the study by Antoce et al. (1996a) was to determine the inhibitory action of ethanol on the growth at 30 ˚C of ten different strains of yeast using batch IMC. The study develops a quantitative method as a tool to predict yeast performance in the presence of high ethanol concentrations. The authors define a parameter termed the 'specific growth activity', which is calculated by taking the ratio of the specific growth rate of a stressed population to that of a healthy population. The specific growth rate was calculated by fitting the growth equation (Equation 2-5) to the early exponential part of the heat curve. The early exponential part of the growth curve has been confirmed to correlate well to cell numbers in both this study and others (see Section 2.4.1). The procedure is illustrated in Figure 2-8.

Using the heat flow/power curve, Antoce et al. (1996) defined a new parameter called the specific growth retardation. The specific growth retardation is calculated by taking the ratio of the time taken for a healthy population of cells and a stressed population of cells to reach a given power output, α, and dividing by the time taken for a stressed population of cells to reach the same power output. The procedure is illustrated in Figure 2-9. While Antoce et al. (1996a) did not clearly define how the value of α is chosen, Takahashi (2000) (the corresponding author of the study) later describes that the exact value of α is not important so long as the value of α occurs in the exponential phase of growth for all thermograms being analysed.

Antoce et al. (1996a) found that while the absolute values of $t_\alpha(0)$ and $t_\alpha(i)$ were found to vary with inoculum size, the ratio of the two parameters was found to be independent of inoculum size. The specific growth activity and specific growth retardation were then plotted separately for different ethanol concentrations, shown in Figure 2-10.

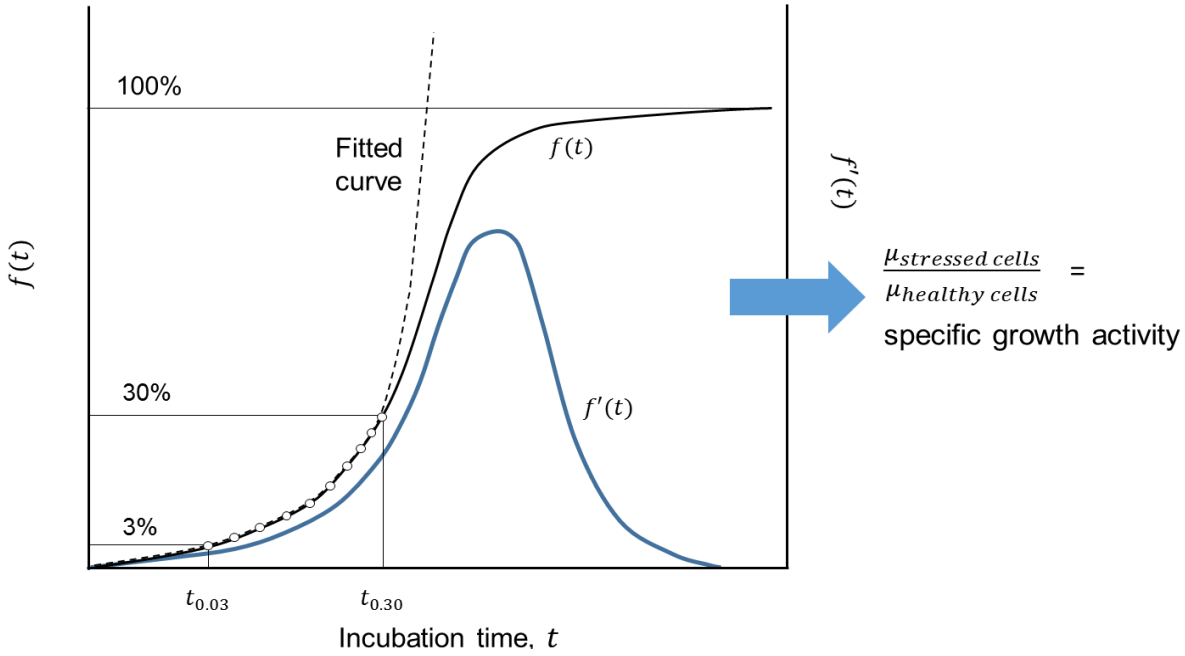

Figure 2-8: Schematic representation of the procedure employed to determine the specific growth rate.
Using the power curve, $f'(t)$, the corresponding heat evolution curve, $f(t)$, is determined via the integration of $f'(t)$. The initial portion of the $f(t)$ curve between 3% and 30% of the final heat output is fitted with the exponential growth equation, Equation 2-5. The equation allows the determination of μ, the specific growth rate. Figure adapted from Antoce et al. (1996).

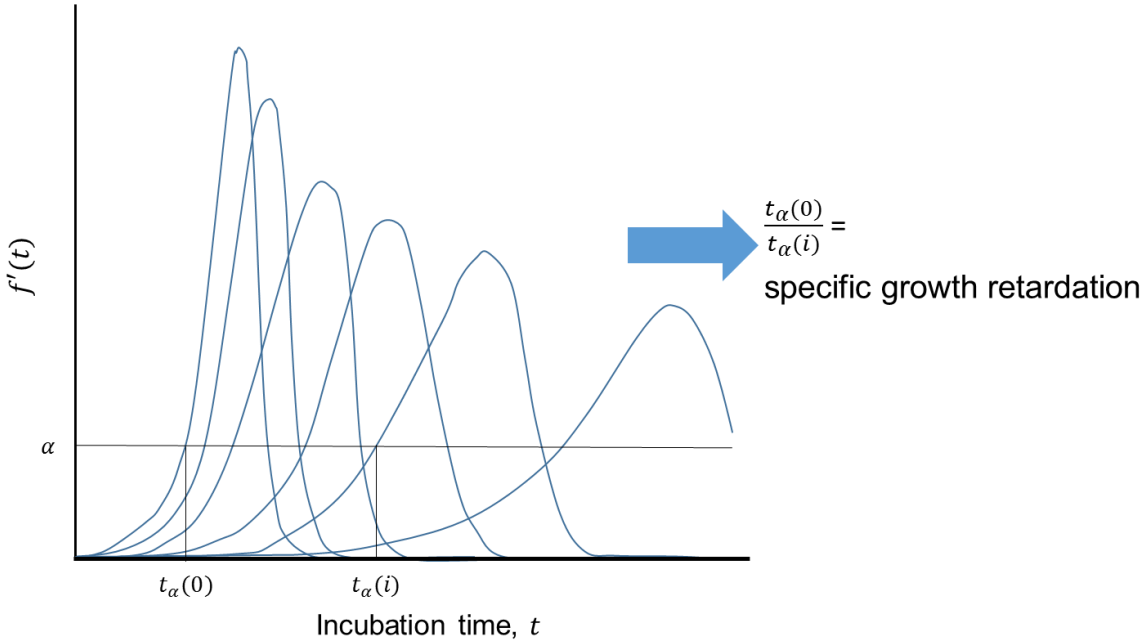

Figure 2-9: Schematic illustration of the procedure employed for the determination of tα(i) , the time necessary for a culture in the presence of an inhibitor with a concentration/ magnitude of i to reach the level α.
Adapted from Antoce et al. (1996).

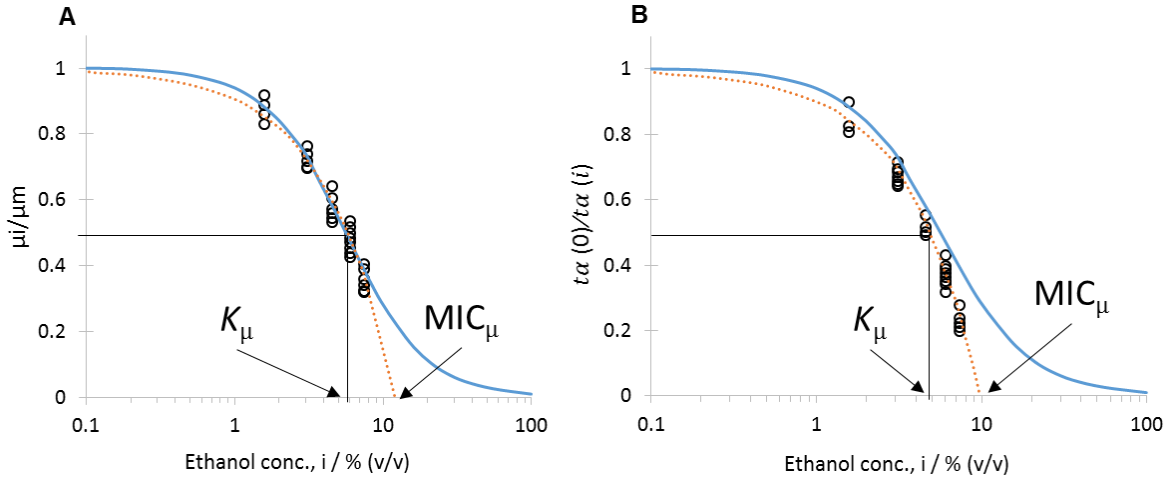

Figure 2-10: Ethanol potency curves (solid lines) and minimum inhibitory concentration (MIC) curves (dotted line) calculated on the basis of A) specific growth rate and B) specific growth retardation.
Raw data from Antoce et al. (1996).

The specific growth activity and specific growth retardation values plotted in Figure 2-10 were then fitted using a sigmoid equation to determine the minimum inhibitory ethanol concentration (MIC – the minimum ethanol concentration that stops any sign of growth) and the concentration at which the cell activity was inhibited by 50%, K_{50}. The curves are referred to as ethanol potency curves and can be used to predict the effect of ethanol concentration on the yeast species investigated.

The topics of papers published by Takahashi's research group using the same method as developed by Antoce et al. (1996) include: yeast growth in the presence of added ethanol and methanol (Antoce et al., 1997b), the inhibitory effects of C1-C4 hydrocarbons on yeast growth (Antoce et al., 1977), the inhibitory effect of ethanol at various pHs and temperatures (Antoce et al., 1997a), the antifungal and antibacterial actions of different drugs (Okuda et al., 1996) and testing the resistance of winery yeast to different concentrations of ethanol (Antoce and Nămoloşanu, 2011). The topics of papers published by corresponding author Katsuhiro Tamura using the method developed by Antoce et al. (1996) (i.e. a different research group to that of Takahashi) include: the effects of different pesticides on yeast (Arao et al., 2004), the effect of high pressure gas on yeast growth (Arao et al., 2005) and the effects of compressed hydrocarbon gasses on yeast growth (S Kawachi et al., 2010; Satoshi Kawachi et al., 2010). Tsukamoto et al. (2004), not affiliated with any of the aforementioned authors, investigated the effects of sonication and chlorination on *S. cerevisiae* also using the method developed by Antoce et al. (1996).

The studies by Antoce et al. (1996), Arao et al. (2005) and Tsukamoto et al. (2004) are essentially variations of a theme. The work by Arao et al. (2005) and Tsukamoto et al. (2004) are confirmatory of the work performed by Antoce et al. (1996). The studies by Antoce et al. (1996) and Tsukamoto (2004), although written by different research groups, have authors that originate from the same university (Osaka Prefecture University). Tsukamoto et al. (2004) took the work by Antoce et al. (1996) and expanded upon it from a more qualitative approach. Arao et al. (2005) expanded the predictive aspect of Antoce's work. It is interesting to note that Antoce et al. (1996) makes reference to Beezer et al. (1977), which is possibly where Antoce developed the idea to define qualitative parameters to analyse yeast thermograms.

Antoce et al. (1996) made brief mention of a possible link between bacteriostatic and bactericidal effects and the specific growth rate and specific growth retardation respectively. The definition of bactericidal and bacteriostatic effects state that bactericidal action kills microbial cells and bacteriostatic action inhibits growth activity (Pankey and Sabath, 2004; Takahashi, 2000). The idea was expanded by Okada et al. (1999), with reference to the bacteriostatic and bactericidal actions of antimicrobial drugs. However, the idea was not fully and clearly expanded until Takahashi (2000), the corresponding author in both the papers by Antoce (1996) and Okada et al. (1999). Takahashi (2000) aimed to develop a bactericidal/bacteriostatic index for different drugs.

Takahashi (2000) shows the effect of two drugs, imidazolidinyl urea (IDU) and p-hydroxybenzoic acid propyl ester (propylparaben), on the effect of yeast growth. IDU is known to have bactericidal effects (Cahill and Nixon, 2005) and causes the thermograms of yeast cultures to shift towards having longer lag times. Propylparaben is known to not necessarily kill cells but weaken them, causing slower growth – having a bacteriostatic effect (Nagel et al., 1977). The effect of the two drugs on heat generation at varying concentrations are shown in Figure 2-11.

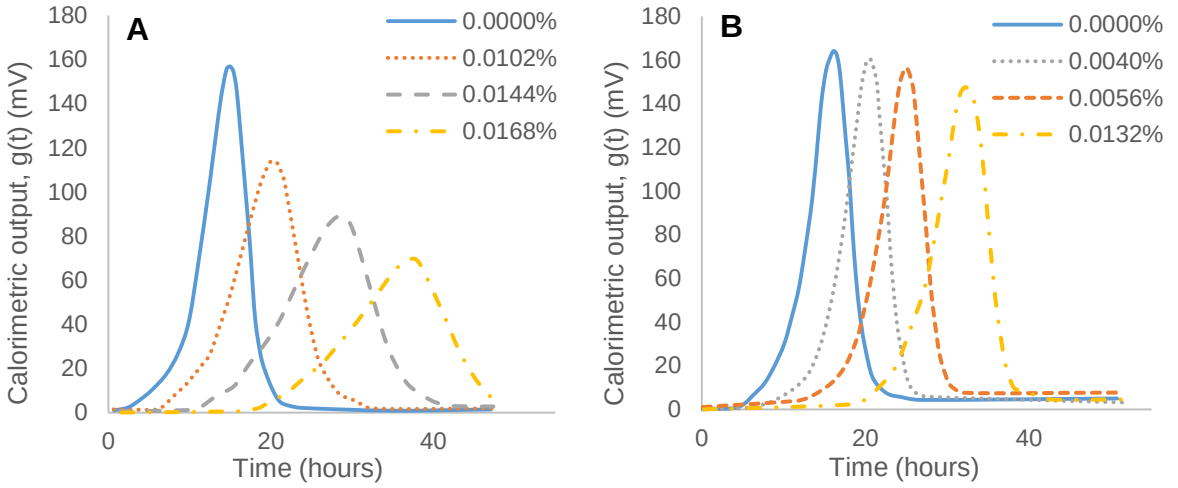

Figure 2-11: Growth thermogram of S. cerevisiae at 30 °C in brain-heart infusion media containing varying concentrations of A) propylparaben and B) IDU. Concentrations are given as % (w/v).
Raw data from Takahashi (2000).

Curves for the early exponential phase of growth, similar to the ones shown in Figure 2-11 (A), can be obtained by changing μ while keeping the lag time constant, representing bacteriostatic effects (c.f. Equation 2-4). Curves similar to the ones shown in Figure 2-11 (B) can be obtained by varying the lag time, τ, while keeping μ constant – representing bactericidal effects. Based on the work by Antoce et al. (1996), changing the lag time while keeping the growth rate constant amounts to only affecting the specific growth retardation [$t_\alpha(0)/t_\alpha(i)$, as defined in Figure 2-9]. However, changing the specific growth rate while keeping the lag time constant affects both the specific growth retardation and specific growth activity (μ_i/μ_m as defined in Figure 2-8). This effect of bacteriostatic drugs on both the specific growth retardation and the specific growth activity can be seen in Figure 2-11 (A).

It is clear that growth curves with the same growth rate but different lag times only yield changes in the specific growth retardation. However, the link between changing the specific growth rate and its effect on both the specific growth retardation and specific growth activity is not as clear. If the exponential growth of an unstressed population growing with a specific growth rate of μ_m is compared to a stressed population growing with a specific growth rate of μ_i, both with the same lag times (τ) and initial cell populations (N_0), this can be represented by Equation 2-8 and Equation 2-9, respectively Takahashi (2000).

$$N_{unstressed} = N_0 exp[\mu_m(t-\tau)] \qquad \textit{Equation 2-8}$$

$$N_{stressed} = N_0 exp[\mu_i(t-\tau)] \qquad \textit{Equation 2-9}$$

The ratio of the time for the stressed population, $t_\alpha(i)$ to reach the same heat output/cell numbers, α ($\alpha = \alpha_m = \alpha_i$) as that of the unstressed population $t_\alpha(0)$, can be represented as Takahashi (2000);

$$1 = {}^{\alpha_m}/_{\alpha_i} = \frac{N_0 exp[\mu_i(t_\alpha(i))]}{N_0 exp[\mu_m(t_\alpha(0))]} \qquad \textit{Equation 2-10}$$

By taking the natural logarithm and simplifying it can be shown that,

$$\frac{t_\alpha(0)}{t_\alpha(i)} = \frac{\mu_i}{\mu_m} \qquad \textit{Equation 2-11}$$

Takahashi (2000) then plot specific growth activity versus specific growth retardation to show the above relation, for theoretically pure bactericidal and pure bacteriostatic effects, as shown in Figure 2-12 (A).

Takahashi (2000) defined the slope of the plot between the specific growth activity and the specific growth retardation as the bacteriostatic/bactericidal index or SCI. Takashi showed that for drugs known to have primarily bacteriostatic effects, the SCI is close to unity. Examples of a plot to determine the SCI for different drugs is shown in Figure 2-12 (B). For propylparaben, a known bacteriostatic, the SCI was equal to 1 and for IDU, a known bactericide, the SCI was equal to 0.17.

Wirkner & Takahashi (2000) further expanded the work of Takahashi (2000) by introducing a new parameter called the bactericidality. Previously the SCI was assumed independent of drug concentration, i.e. the ratio of the bactericidal/bacteriostatic effects of a drug are independent of drug concentration, as implied by Figure 2-12 (B). In the work by Wirkner & Takahashi (2000), the bactericidality parameter takes into account that for some drugs this ratio is not fixed i.e. the SCI is not constant across all drug concentrations as indicated by a upward curve when μ_i/μ_m is plotted against $t_\alpha(0)/t_\alpha(i)$. Using the updated method including bactericidality, Wirkner et al. (2002, 2001) investigated the effects of ^{60}Co gamma rays on yeast as well as other microorganisms.

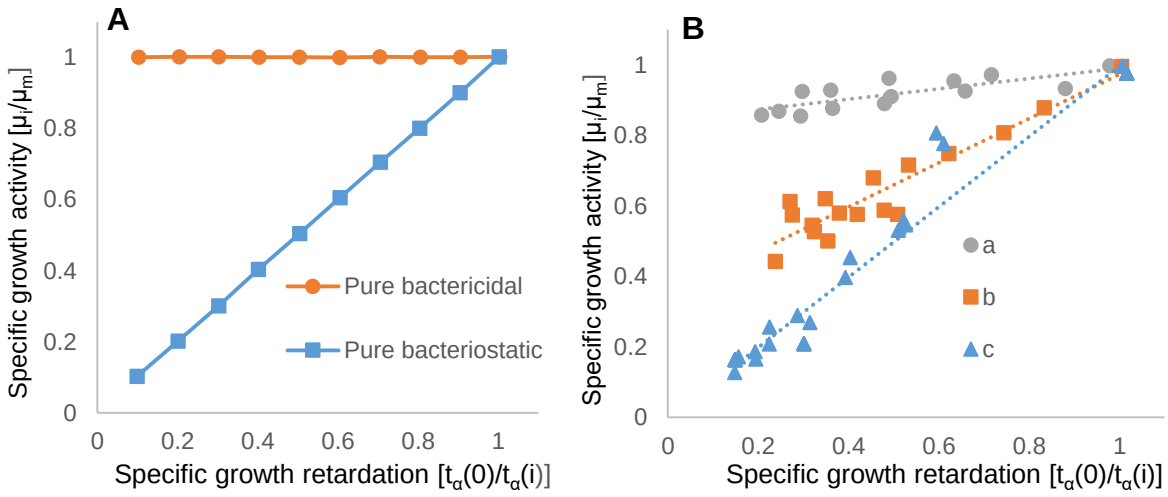

Figure 2-12: Relationship between specific growth activity and specific growth retardation. A) purely bactericidal effects (obtained by varying the lag time while keeping the specific growth rate constant) and purely bacteriostatic effects (obtained by varying the specific growth rate while keeping the lag time constant). B) a plot of μ_i/μ_m versus $t_\alpha(0)/t_\alpha(i)$ for (a) IDU on *K. pneumoniae*, (b) sodium benzoate on *A. oryzae* and (c) propylparaben on *K. pneumonia* at 30 °C.
Raw data from Takahashi (2000).

2.5 Summary of key findings

Yeast growth occurs in four main stages: a lag phase, exponential phase, stationary phase and death phase. It can grow either aerobically or anaerobically. There is consensus that viability is linked to the proportion of living cells in a population and that vitality is linked to the health of the living cells – the definitions adopted in this work. In a commercial brewing process, yeast is exposed to numerous stresses that affect yeast viability and vitality. Two primary stresses with potential to be manipulated by operating practice include: cold stress and ethanol stress. In both cases, the yeast primarily responds by the production of heat shock proteins. Knowledge of stress response is key in the optimising of process performance.

Most isothermal microcalorimeters are of the conduction type and operate using the Peltier/Seebeck effect. Isothermal calorimeters are most commonly arranged in a 'twin' manner with one vessel serving as the inert reference to which the measured signal is compared. Given the non-specific nature of the IMC heat signal, significant systematic errors can arise due to factors such as friction and evaporation/condensation. It is important that microcalorimeters are calibrated to ensure accurate measurements.

IMC is very sensitive and has a detection limit below most other commonly used biological assays. The power and heat curves generated correlate well to cell numbers in the early exponential phase. Other sigmoid models that fit the entire heat curve using biologically based parameters are also available. IMC has been used extensively in the soil and environmental sciences. Furthermore, there are novel applications of IMC in medicine and the food industry. IMC also has potential in bioprocess control applications. The main problems with batch IMC are stirring and aeration. While flow IMC was used extensively in the past, it has many associated issues that have driven a decline in its popularity.

IMC has been used to study the growth and metabolism of yeast. The notion of using normalised, relative measures of yeast performance (i.e. μ_i/μ_mversus μ_i) has been used when comparing the performance of stressed yeast (e.g. specific growth activity). The use of these normalised values is advantageous, allowing certain trends to be determined independently of population size (or the other factors being held constant) and more accurately from one experiment to another. The specific growth rate and cell numbers of a growing yeast population can be successfully derived from analysing power and heat curves. Substrate usage of yeast and heat release under non-growing conditions have also been studied. In the literature examined, no studies were found that link yeast viability and vitality directly to power and heat curves. However, numerous authors have examined the specific growth activity and specific growth retardation of yeast and its relation to bactericidal and bacteriostatic effects. Bacteriostatic effects have been linked to effects on yeast specific growth rate and bactericidal effects have been linked to the number of living cells in a population. This approach may provide a useful platform to analyse effects of various stresses on yeast and aid in the independent evaluation of yeast viability and vitality.

2.6 Detailed project objectives

The detailed project objectives, developed based on the findings above, are outlined below.

1. Demonstrate the repeatability of the method developed in this work using lab strain yeast, by demonstrating the same results for biological repeats (within experimental error).
2. Determine the specific growth rate and lag time of the yeast population using growth thermograms with an acceptable degree of repeatability.
3. Relate yeast viability and vitality to the specific growth rate and/or lag time calculated from the growth thermograms.
4. Investigate the response and recovery of yeast viability and vitality to two commonly encountered stresses in the commercial brewing industry: temperature shock, exposure to high ethanol concentration and a combination thereof.
5. Assess the consistency of these results with those presented in the literature to date.

2.7 Key questions

- Can the analysis of the calorimetric thermograms produce the required parameters to determine cell viability and vitality from heat flow data?
- Can the thermometric data from the microcalorimetry be used to differentiate yeast viability and vitality?
- Do the stresses imposed on the yeast cells cause distinguishable differences in cell viability and vitality?

2.8 Hypothesis

Yeast quality in terms of its viability and vitality, can be determined by examining the calorimetric growth curve of a yeast population. Changes in the calorimetrically observed specific growth rate and lag time reflect different forms of physiological stress.

The combination of stresses on a yeast population is non-commutative as long as the stresses applied are countered by the production of the same stress response proteins, preventing any additional stresses from leading to further calorimetrically observable stress responses.

3 Materials and Methods

The aim of this chapter is to detail the materials, equipment and methods employed in this study. First, the experimental materials used are presented thereafter the method used is detailed. This chapter also describes the overall research approach. In Chapter 4, the development of methodologies specific to the microcalorimetric work is presented. Unless otherwise stated; sterile growth media and reagents were prepared by autoclaving at 121°C for 20 min and all media and chemicals were obtained from Sigma-Aldrich or Merck.

3.1 Growth media and cultivation conditions

The yeast strain used was *Saccharomyces cerevisiae* CBS8803 (S288C), Taxom name: *Saccharomyces cerevisiae* Meyen ex E.C. Hansen, Medd. Carlsberg Lab.: 29 (1883) [MB#163963]. This strain of yeast has been studied extensively as it was the first strain of yeast to have its genome completely sequenced (CBS Databse, 2014; Sherman, 2002). CBS8803 (S288C) is haploid and therefore does not reproduce sexually, only via replication- as long as the culture remains pure. This helps minimise the possibility of genetic changes occurring. CBS8803 is considered a non-harmful lab strain yeast as it is non-invasive and does not express pseudohyphal growth (Klingberg et al., 2008; Schneiter, 2004). Furthermore, its cultivation gives rise to well dispersed cells (Sherman, 2002). For the aforementioned reasons CBS8803 is commonly used in yeast research (Schneiter, 2004). As with most haploid yeast strains, the optimum growth temperature of CBS8803 is 30 °C (Schneiter, 2004).

The strain was sourced from Centraalbureau voor Schimmelcultures (CBS), Utrecht, The Netherlands. The culture was reconstituted and revived, according to the supplier's instructions, and plated onto Yeast Peptone Dextrose (YPD) agar (20 g/L D-glucose, 20 g/L peptone, 10 g/L yeast extract and 15 g/L Bacteriological agar). Following incubation at 30 °C for approximately 48 hours, a single colony was aseptically inoculated into 10 mL of YPD broth (20 g/L D-glucose, 20 g/L peptone and 10 g/L yeast extract) and incubated at 30 °C with shaking for approximately 16 hours. A series of cryostocks were prepared by combining the overnight culture with a 50% (v/v) glycerol solution (in deionized water) in 2 ml Cryo® vials, in the ratio of one part 50% glycerol to two parts culture. The glycerol-culture solution was then stored at -60 °C (Bergman, 2001).

3.2 Yeast propagation

In this investigation a plate-based inoculum preparation approach was employed, for which the reproducibility is demonstrated in Chapter 4.1.1. Briefly, *S. cerevisiae* CBS8803 (S288C) was streaked onto a series of fresh YPD agar plates from a frozen cryostock vial (section 3.1). The agar plates were incubated for 72 hours at 30 °C, until yeast colonies were clearly visible on the agar surface. These single yeast colonies were then used to aseptically inoculate fresh YPD agar plates. The harvesting process was performed inside a laminar flow cabinet to reduce the potential for microbial contamination. The same lineage of yeast was used for a

maximum of three sub-cultures before a fresh inoculum was prepared from the stored glycerol stock yeast. The procedure employed is illustrated in Figure 3-1.

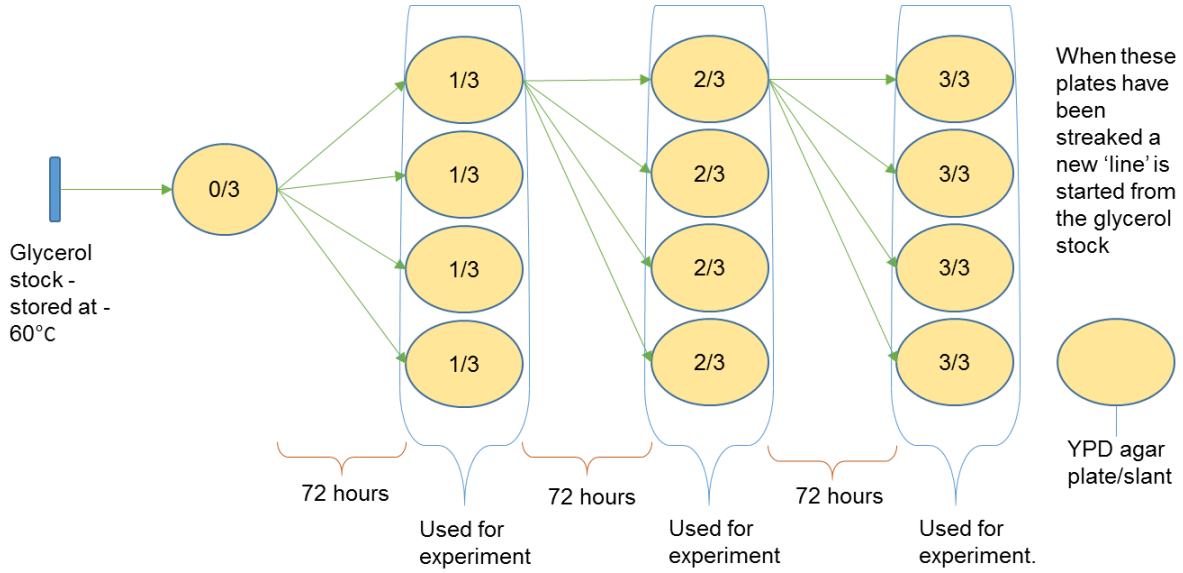

Figure 3-1: Schematic of the procedure used to grow up yeast on YPD agar (solid media) for each experiment.
Appendix A.4 describes the yeast streaking procedure in further detail.

3.2.1 Sample preparation

The yeast used for the calorimetric testing was taken from yeast colonies growing on agar slants. The inoculum was either taken directly from yeast colonies growing on an agar slant (grown at 30 °C for 72 hours), or from a yeast slurry produced by scraping all the yeast off an agar slant into a Bijoux bottle, using a sterile surgical blade. In all cases the yeast was first suspended in YPD. For the initial repeatability tests, ca. 4 yeast colonies growing on an agar slant were used to inoculate 5 ml YPD. A streaking loop was used to deposit the cells in the YPD creating an initial cell concentration of between 10^7 – 10^8 cells/ml. In the case of the yeast slurry inoculum in the Bijoux bottle, the yeast slurry was made up to a 20% consistency (20% yeast by mass in YPD) by first weighing the amount of yeast removed from the slant into the bottle and adding the appropriate amount of YPD. Ten microliters of this 20% yeast slurry was added to 2 ml of YPD in order to get a cell suspension in the range of 10^7 – 10^8 cells/ml. The rest of the yeast slurry was used for the acidification power test. The simpler method of inoculating 5 ml of YPD using a few yeast colonies from a single YPD agar petri-dish was used when no acidification power test was performed.

A 20% consistency yeast slurry was chosen to mimic brewery yeast handling conditions where yeast is exposed to various stresses in slurry form. Furthermore the use of a ca. 20% yeast slurry provides consistency with the work done in the CeBER laboratories by Basson (1996), Nkosi (2001) and Kgari (2008).

3.3 Assays used for analysing yeast viability and vitality

Direct microscopy cell counts, plating viability tests (based on the number of colony forming units), cell staining and visualisation and the acidification power tests were used to determine yeast viability and vitality during the course of this investigation.

3.3.1 Direct cell counts

Yeast cell numbers were routinely determined by direct microscopy cell counts, as outlined in Appendix A.3, following the preparation of an appropriate dilution in sterile deionised water. In the present work, cell counts were performed using a Helber (Hawksley) counting chamber (depth of 0.02mm and area per counting block of 1/400 mm^2) and an Olympus BX40 phase contrast Microscope fitted with a 100x magnification objective oil immersion lens. This assay works most effectively when the cell suspension is roughly 10^7 – 10^8 cells/ml, below 10^6 cells/ml it is difficult to detect the presence of any cells.

3.3.2 Viability staining and cell counting

Direct cell counting of a given culture does not distinguish viable from non-viable cells. Therefore, direct cell counting was combined with methylene violet cell staining, to allow for the simultaneous determination of both the overall cell number and proportion of viable cells within a given yeast sample.

The methylene violet viability test used was adapted from the original alkaline methylene violet procedure developed by Smart et al. (1999). The method developed by Smart et al. (1999) is considered more reproducible than the older methylene blue stain historically used in the brewing industry. The major change to the methylene violet staining protocol, as developed by Smart et al. (1999), was the exclusion of the suggested cell washing stages. While Smart et al. (1999) prescribe three sequential cell washing steps, a number of studies (Kwolek-Mirek and Zadrag-Tecza, 2014; Maskell et al., 2003; White and Zainasheff, 2010; White Labs, 2014) have omitted these and as a result increased the assay consistency. It is well-known that yeast quality can be affected by centrifugation and filtration associated with the washes. The modified methylene violet staining procedure was performed as described in Appendix A.1. The cells were counted under a microscope (Olympus BX40 phase contrast Microscope fitted with a 100x magnification objective oil immersion lens), as described in Section 3.3.1. Cells that appeared stained (violet in colour) were presumed dead and those that remained unstained (colorless) were presumed viable. Methylene violet is considered reproducible across a wide range of cell viabilities, but is most reproducible when the overall population viability is >90%.

3.3.3 The Acidification Power Test

Cell vitality was assessed using the acidification power test (APT) as described by Gabriel et al. (2008) with minor modifications. The changes to the published methodology used in this investigation included a decrease in the quantity of yeast used, from >1.5 to >0.3 g per test, and a reduction in the centrifugation regime in order to make the re-suspension of the yeast pellet easier.

The final APT value, the measure of yeast vitality, is given as 6.3 minus the pH after 20 minutes (Equation 2-3). Further details of the procedure are given in Appendix A.2. The APT is considered effective and reproducible over a wide range of cell vitalities.

3.3.4 Colony forming unit counts

The standard plating was carried out by spreading 100 µl of an appropriately diluted liquid yeast culture (diluted using liquid YPD to the order of 10^3 cells/ml) onto solid YPD agar media. The number of colonies formed on the surface of the media was counted after a 48 hour incubation period at 30°C, with the assumption that each colony originates from a single cell. When performed using a culture that has been serially diluted (dispensing each different dilution onto a separate plate) this assay is effective in detecting a nearly limitless range of cell concentrations. This assay is considered fairly reproducible.

3.4 The TAMIII isothermal microcalorimeter

The metabolic heat produced by the yeast was measured using a Thermal Activity Monitor III (TAMIII) isothermal microcalorimeter (TA instruments, Thermometric AB, Sweden). The TAMIII instrument employed in this investigation is equipped with two modules, namely an isothermal titration calorimeter (ITC) module and a multicalorimeter module. The two modules share the same heat sink/thermostat but operate independently. The shared thermostat has an accuracy of < ± 0.1 °C and a long-term stability of < ± 100 µK/24-hour (TA Instruments, 2012). In the present work, the TAMIII thermostat was set to 30 °C as this is the optimum growth temperature of *S. cerevisiae* CBS8803 (S288C). The TAMIII multicalorimeter module was used in this project. It has six identical channels arranged in a circular pattern. Each channel can be loaded with 4 ml glass ampoules sealed with aluminium caps containing sealing discs of butyl rubber and Teflon. The multicalorimeter measures heat output with: a short term noise of < ± 100 nW, a baseline drift of < 200 nW/24h, an accuracy of < 5% and a precision of ± 200 nW (TA Instruments, 2012). The TAMIII microcalorimeter was subject to routine calibration, according to the manufacturer's instructions (see Appendix B.4 for further information regarding calibration). Over the duration of a 12 hour experiment the TAMIII stores approximately 6000 data points (ca. 30 second sampling intervals) for each of the six channels. An image of the TAMIII microcalorimeter and multicalorimeter module is shown in Figure 3-2.

The TAMIII was operated according to the manufacturer's instructions. The default baseline recording settings were used (30 minute baseline and 'moderate' signal stability criteria). Following the generation of a stable baseline, the ampoules were inserted into the respective channels' equilibration position and held there for 15 minutes. In the equilibration position, the ampoules reach thermal equilibrium with the thermostat-controlled oil bath within the microcalorimeter. After the equilibration period, the ampoules were lowered into the measuring position. The TAMIII software waits a further 45 minutes, to allow for any thermal disturbances within the system due to the ampoules being lowered into the measuring position, before the heat flow signal is considered 'correct' and the software starts integrating the heat flow data to form the heat curve (cumulative power time curve) of each respective ampoule. In most

cases the end of this waiting period was manually adjusted back to the point where the average minimum heat flow across all the channels was observed. This manual adjustment has a minor effect on the heat data, as the heat flows in this initial region are very small. After the waiting period, when the signal is considered 'correct', or the point where the signal is 'correct' has manually been set, the TAMIII software begins integrating the heat flow curve (usually in μW) to form the heat curve (measured in Joules).

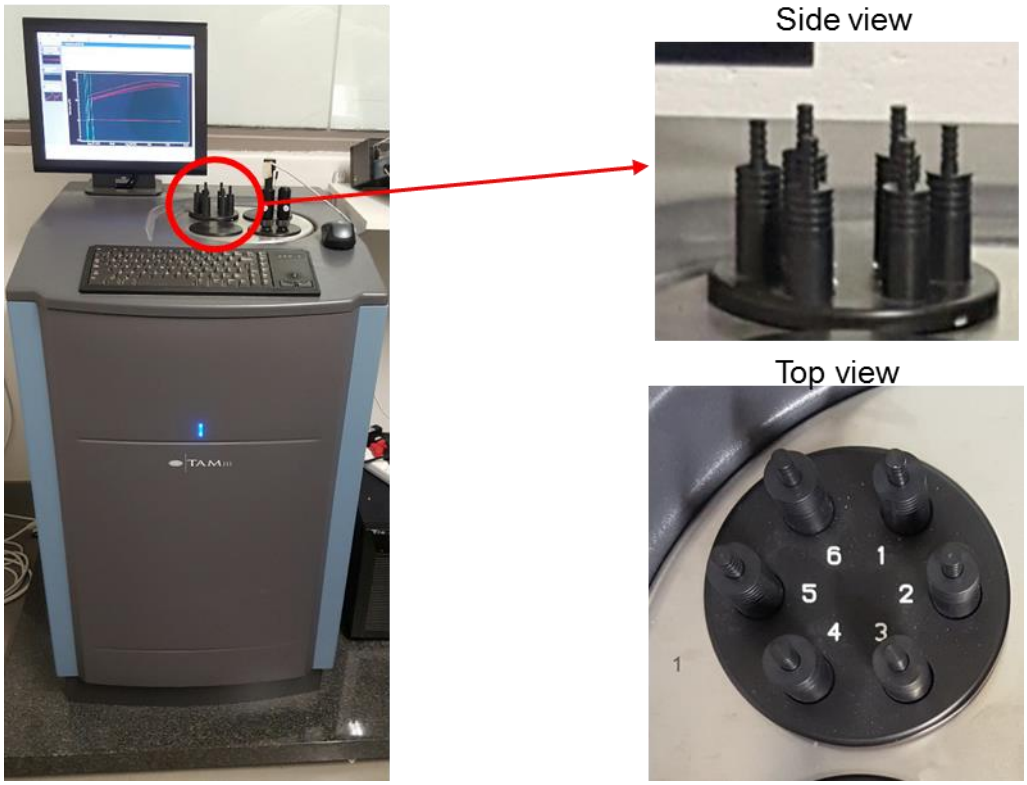

Figure 3-2: The Thermal Activity Monitor III (TAMIII) microcalorimeter located in the Department of Chemical Engineering at the University of Cape Town. The image to the right shows an enlarged image of the six channel multicalorimeter.

To terminate a run, the ampoules are removed and, once the heat flow stabilises to the prescribed signal stability conditions, a final baseline is recorded. The TAMIII software automatically subtracts the average baseline, including the baseline data taken before the ampoules were inserted, from the heat flow signal recorded for each channel. This baseline subtraction takes into account any signal offset or drift that may have occurred over the duration of the experiments, associated with the machine's heat flow sensors.

3.4.1 Preparation of samples for the microcalorimeter ampoule

In the case of all biotic tests, a 1 ml cell suspension containing approximately 10^4 cells/ml was pipetted into each ampoule. The justification for the use of 1 ml and a 10^4 cells/ml cell concentration is discussed in the Appendix B.3 and in Section 4.1. In all cases, the ampoules and ampoule caps used were sterilised by autoclaving at 121 °C for 15 minutes and dried overnight in an 80 °C drying oven before use. In all experiments, one ampoule was prepared as an abiotic control. It contained 1 ml sterile YPD media, the same YPD used to perform the

necessary dilutions of the yeast slurry samples to 10^4 cells/ml. After the cell suspension or control medium was aseptically dispensed into the ampoules, the aluminium caps were crimped onto the glass ampoules to form an airtight seal. Improperly sealed ampoules led to a significant error in the measured heat flow (discussed further in Appendix B.2). The ampoules were kept upright at all times before being loaded into the TAMIII. Furthermore, all work was carried out in a sterile manner in a laminar flow hood to minimise any chance of contamination.

3.5 Programme formulation

The experimental programme contains five main parts:

1. reproducibility experiments,
2. heat killing experiments,
3. temperature shock experiments,
4. ethanol shock/toxicity experiments and
5. a combined temperature shock and ethanol exposure experiment.

In all experiments an abiotic negative control ampoule containing sterile YPD media was included in one of the channels. In the case of the stress tests, an ampoule containing a healthy yeast suspension (un-stressed) was included in one of the channels as a positive control. The different experimental programmes are outlined below.

3.5.1 Repeatability experiments

The repeatability experiments form a part of the method development in relation to the acceptable use of the microcalorimeter and the analysis of the calorimetric data. These experiments helped form the basis of the experiments to follow.

Repeatability refers to the ability of the same operator, over a relatively short timeframe, using the same laboratory and apparatus to obtain results that are statistically valid (Lau, 2009). Reproducibility refers to the ability of different operators, over an unspecified timeframe, using different laboratories and experimental equipment to obtain results that are statistically the same. It is thus important to note that, in the case, only the repeatability of the results obtained can be analysed statistically. However, the method developed was formulated such that it is likely to have a high degree of reproducibility (i.e. by employing simpler rather than more complex methods).

The repeatability experiments were carried out while investigating the effects of different inoculum sizes, in order to establish a consistent experimental method as well as providing a measure of healthy cell performance.

In the baseline experimental plan used for all experiments, approximately 5 yeast colonies were harvested from the surface of a YPD agar plate, inoculated and incubated as described in Section 3.2.1, re-suspended in 5 ml of YPD broth and prepared for microcalorimetric analysis as well as the viability and vitality assays. As the repeatability experiments focused

primarily on the use and analysis of the microcalorimeter, not all experimental runs included methylene violet cell staining or the APT or both to assess vitality or viability, respectively. An experimental block flow diagram of the repeatability experiments is shown in Figure 3-3.

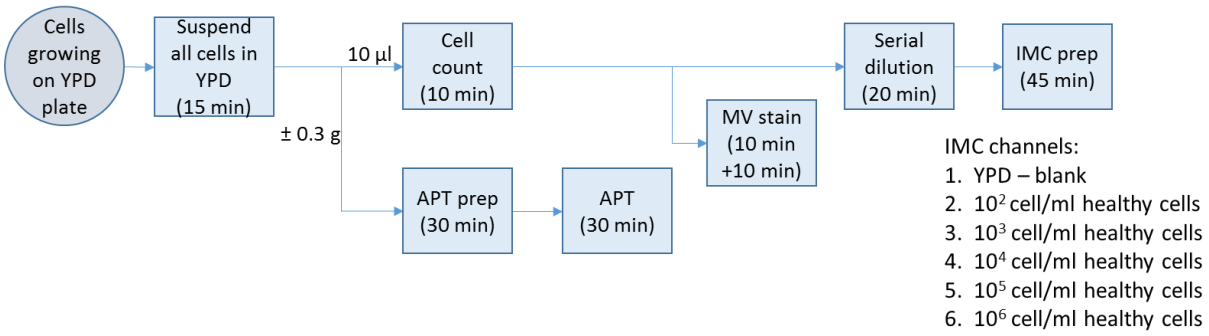

Figure 3-3: Repeatability experiments experimental block flow diagram.
The approximate time taken to complete each step is given in brackets. Yeast colonies growing on an agar slant at 30 °C for 72 hours were suspended in YPD. A small sample was removed for cell counts, viability staining and microcalorimetric analysis. The majority of the suspended yeast slurry was used for the APT. Cell counts were performed in conjunction with the methylene violet (MV) stain. The yeast slurries were diluted using YPD to the necessary concentration(s) based on the cell counts performed. A total of six samples containing: a YPD blank (negative control), 10^2 cells/ml, 10^3 cells/ml, 10^4 cells/ml, 10^5 cells/ml and 10^6 cells/ml of healthy cells were loaded into the TAMIII microcalorimeter.

3.5.2 Heat killing experiments

Yeast cells were inactivated by exposure to heat in order to provide varying levels of yeast viability to allow validation of the microcalorimetric technique. In these validation experiments, healthy viable cells were combined with inactivated cells in known proportions to provide a range over which to confirm the metabolic heat output from vital and viable cells when placed into the TAMIII.

Heat killed yeast cells were prepared according to Deere et al (1998) and Molecular Probes™ (2005). Briefly, freshly harvested yeast cells suspended in YPD (ca. half the total yeast slurry, ~1.5 ml) were heat killed by exposing them to approximately 80 °C for 10 minutes in a Labnet AccuBlock™ digital dry bath. The experimental block flow diagram for the heat kill experiments is given in Figure 3-4. The timeframe given in Figure 3-4 includes the time taken to prepare the samples and execute a procedure in its entirety. Microscopic assessment and APT tests were conducted, as described in Sections 3.3.1 to 3.3.3, following the heat kill procedure to ensure the resultant cells were intact and non-vital.

3.5.3 Cold shock experiments

The cold shock experiments were conducted to test the response of yeast to a rapid drop in temperature; from room temperature (~22 °C) to 4 °C. This corresponds to the temperature yeast is stored at under brewery conditions. The two types of cold shocks chosen were a rapid (18 °C/minute) and a slow cold shock (0.13 °C/minute).

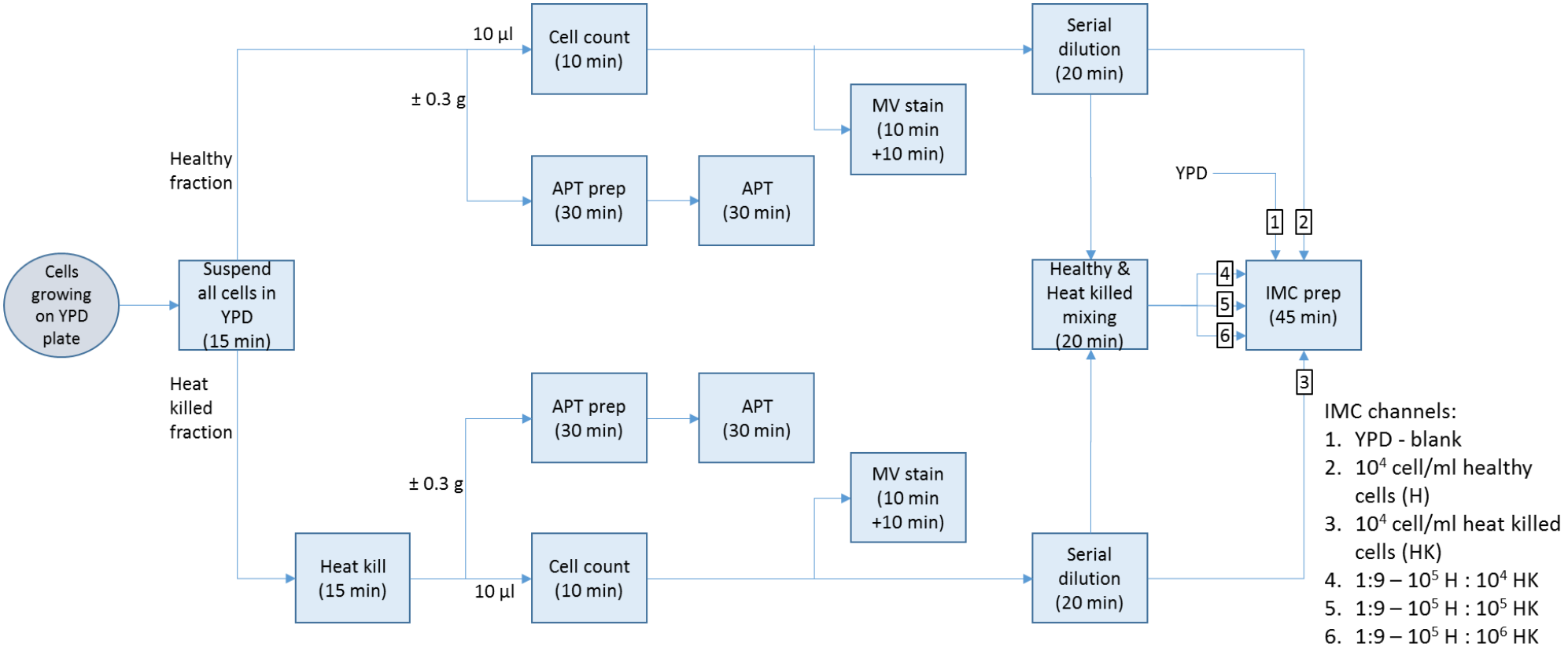

Figure 3-4: Heat killing experimental programme block flow diagram.
Approximate time taken to complete each step given in brackets. Yeast colonies grown on YPD agar at 30 °C for 72 hours were suspended in YPD. The yeast slurry was split into two equal fractions. One fraction was heat killed by exposure to 80 °C for 10 minutes. A sample of both the heat killed fraction and the healthy faction was used to perform cell counts, for viability testing and microcalorimetric analysis. The majority of the suspended yeast slurry was used for the APT. The heat killed cells and healthy cells were mixed to provide varying concentrations of healthy and heat killed yeast. These were analysed by microcalorimetry against a YPD blank (negative control), a population of purely heat killed cells (negative control) and a population containing only healthy cells (positive control).

Yeast was harvested and suspended before being cooled as a 20% consistency (by mass) slurry. Briefly, this was achieved by scraping roughly equal portions of yeast from the surface of YPD agar plates into sterile bottles and adding the required amount of YPD to achieve a 20% consistency. For the rapid cold shock experiment, the YPD was maintained at 4 °C prior to adding it to the yeast slurry. After the addition of the YPD, the bottles were aseptically sealed and gently shaken to suspend all the yeast and form the desired slurry. The bottles were then placed into a cold bath vessel, where the yeast was continuously stirred at approximately 60 rpm to ensure homogeneity. The cold bath vessel was formed by circulating poly ethylene glycol from a refrigerated bath (MRC BL-20) through the jacket of a 2 L glass reactor (Figure 3-5 and Figure 3-6). The reactor was filled with ~250 mL of pre-chilled deionised water and the system allowed to equilibrate for approximately 1.5 hours prior to commencing the rapid cold shock experiment. In the case of the slow cold shock, the flow-rate of the ethylene glycol through the reactor jacket was controlled (using the Masterflex console drive peristaltic pump) in order to achieve the desired rate of cooling (Figure 3-5 and Figure 3-6). The temperature of a duplicate reference yeast slurry, placed into the same cold bath vessel, was logged using a Metrohm 913 pH meter data logger in order to determine the cooling rate. The control, namely the healthy yeast fraction, was incubated for the duration of the experiment at room temperature with constant agitation at 60 rpm. A profile (side) view depicting the cooling apparatus experimental set-up is shown in Figure 3-5 and an aerial (top) view is shown in Figure 3-6.

The rate of the rapid cold shock was approximately 18 °C/minute as yeast at room temperature (~22 °C) was diluted using pre-chilled YPD and then placed in a cold bath at 4 °C, with the whole process taking less than one minute. The slow cold shock rate varied - was hyperbolic in nature as the rate of cooling slowed as the cold bath approached its set point of 4 °C. The initial rate of cooling was close to 0.3 °C /min and this slowed to 0.05 °C/min toward the end of the two hour period – yielding an average rate of 0.13 °C/minute. The overall cold shock experimental procedure is shown in Figure 3-7. After the yeast had been exposed to the cold shock, the yeast were removed from the cold bath and allowed to return to room temperature. Cell counts were performed and the cell viability tested in the same manner as before (Sections 3.5.1 and 3.5.2).

In order to increase the accuracy and repeatability of the results, technical repeats were performed for each experiment. An APT was completed, as previously described, to assess cell vitality at least once in each experimental run for both the healthy and cold shocked cells. An abiotic control was included in all IMC experimental runs, with a further two channels being used as untreated control references for the healthy cells and the three remaining channels were used for the cold shocked yeast.

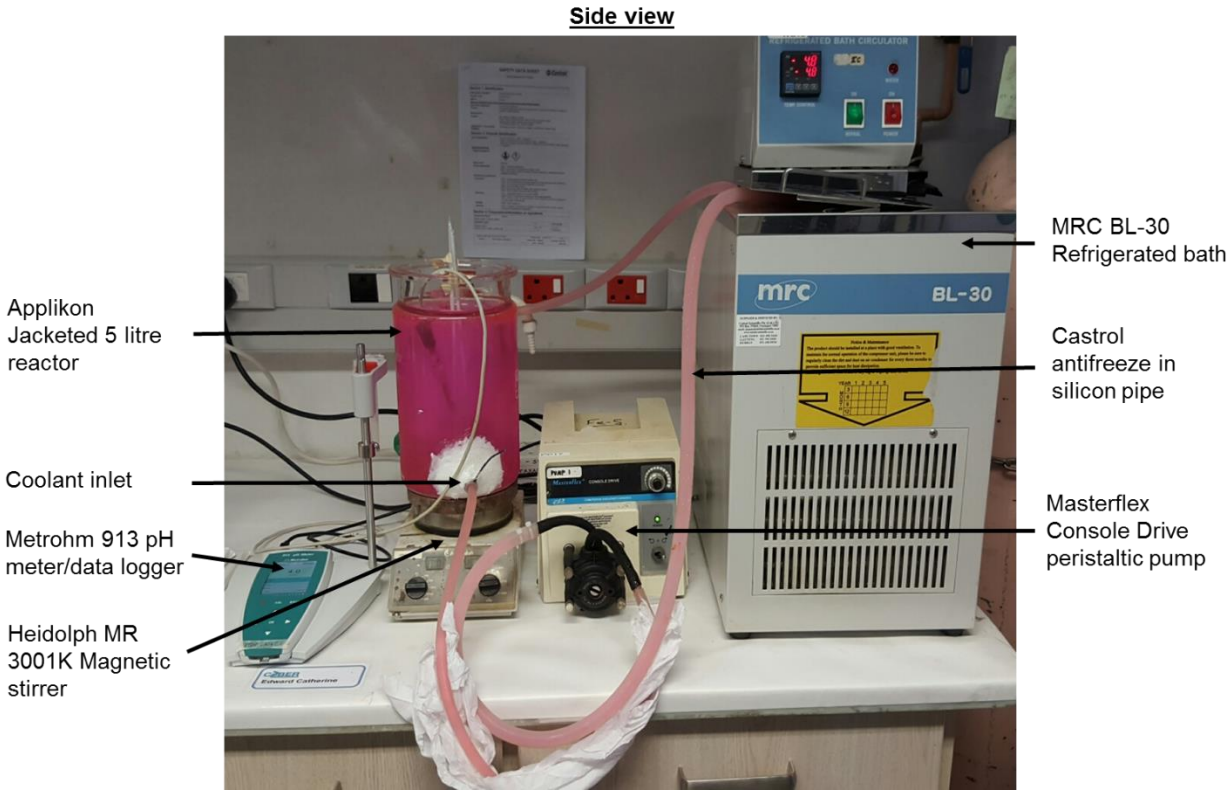

Figure 3-5: Side view of the cold shock experimental set-up.

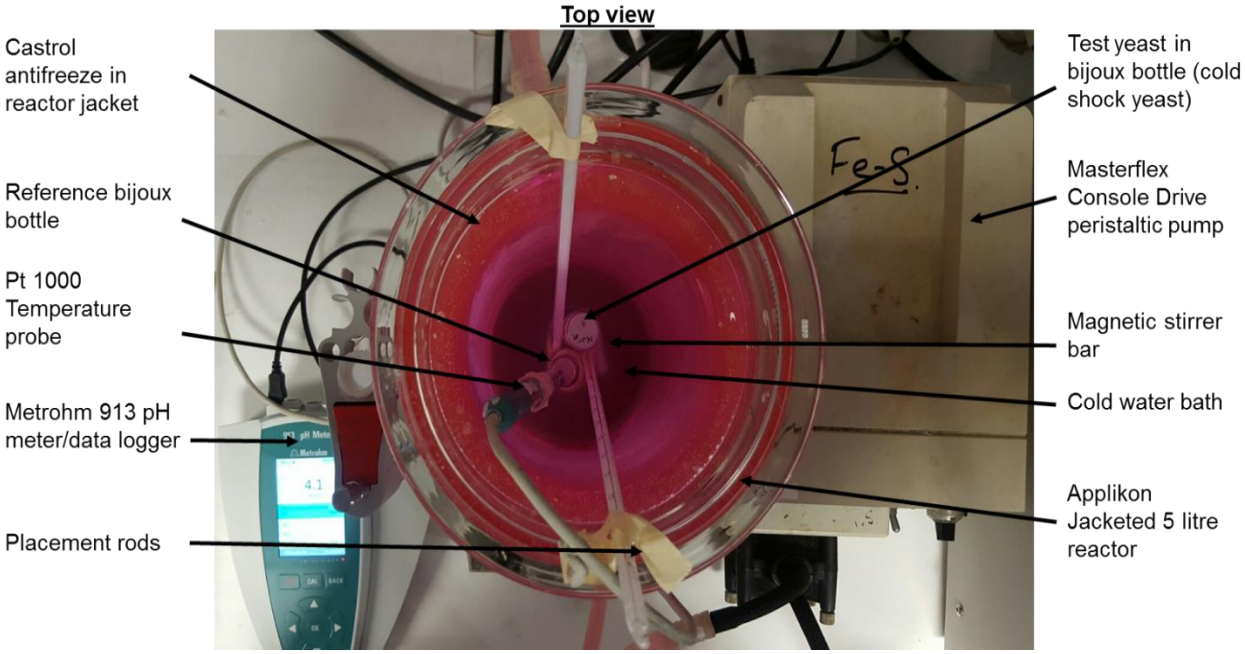

Figure 3-6: Top view of the cold shock experimental set-up.

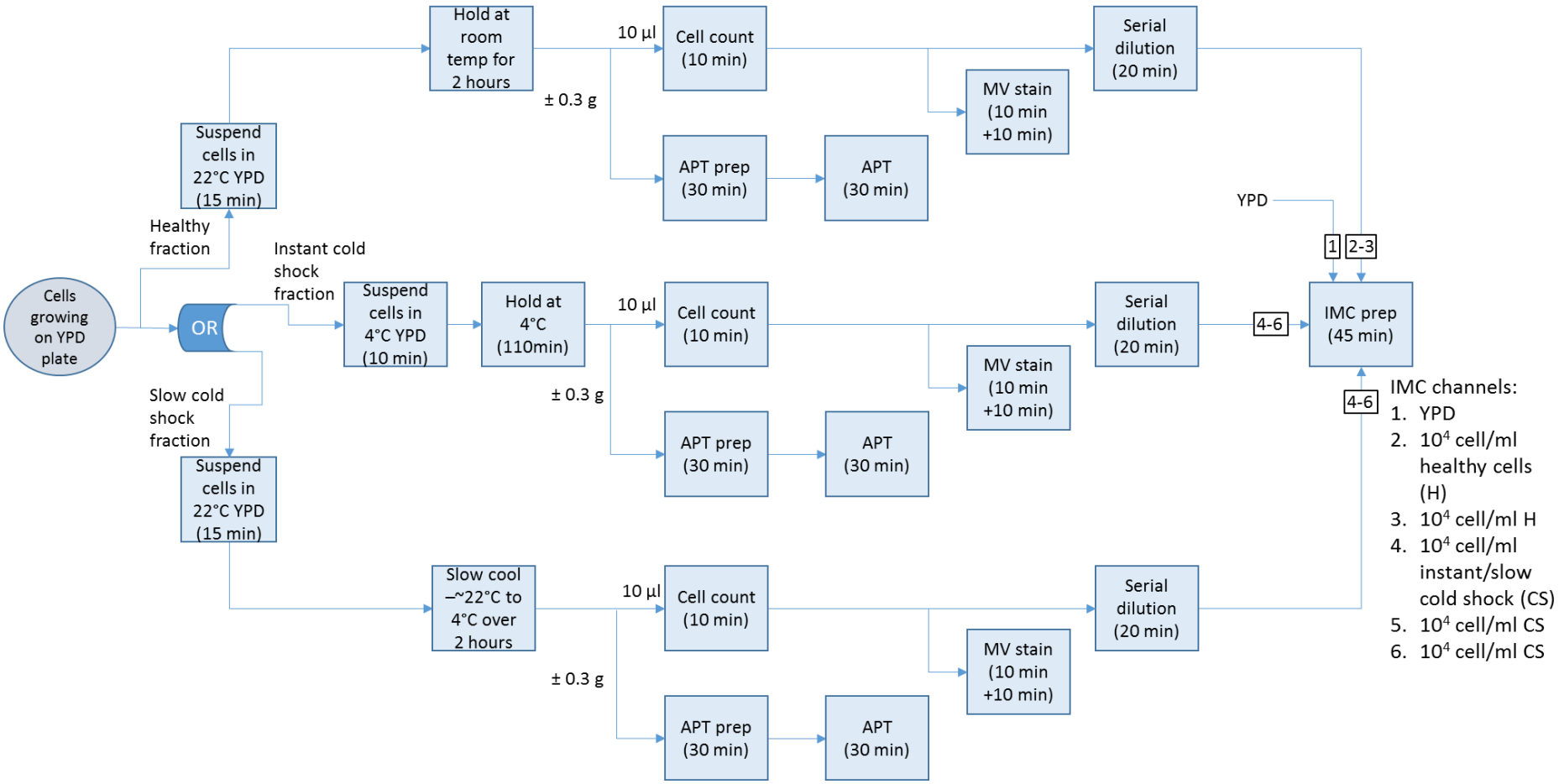

Figure 3-7: Cold shock experimental programme block flow diagram.
Approximate time taken to complete each step is given in brackets. The 'OR' block indicates that the 'instant' and 'slow' cold shocks were executed as separate experimental runs. Yeast colonies grown on YPD agar at 30 °C for 72 hours were split into two equal fractions. One fraction was cold shocked, either by rapid dilution in 4 °C YPD or by slow cooling to 4 °C over 2 hours (initially suspended in 22 °C YPD). After the 2 hour holding period, both the cold shocked fraction and the healthy faction was sampled for cell counts with MV, viability testing and microcalorimetric analysis. The majority of the suspended yeast slurry was used for the APT. The cold shocked cells and healthy cells were analysed by microcalorimetry along with a YPD blank (negative control). At least two technical repeats of both the healthy cells and the cold shocked cells were included.

3.5.4 Ethanol shock experiments

The ethanol shock experiments were designed to test the response of yeast to transient ethanol stress. The yeast was exposed to a moderate and extreme ethanol concentration for a 60 minute period, after which the ethanol was 'removed' by serial dilution. A 4% ethanol shock was chosen as the minimum concentration as this is considered to be a threshold value for full gene expression (Piper et al., 1994). Exposure of the yeast to 8% (v/v) was chosen as the higher ethanol shock as it is reported to be an upper bound, without being lethal, of what yeast can tolerate. The exposure time to the ethanol was chosen to be 1 hour as this correlates with the expression of most heat shock proteins (discussed in Section 2.1.4 – ethanol stress). In addition to the ethanol shock, the growth of yeast in the presence of ethanol was also tested.

The yeast was ethanol shocked by diluting freshly harvested yeast with YPD containing either 4% or 8% (v/v) ethanol, to form a 20% (w/v) yeast slurry in a sterile 4 ml Bijoux bottle containing a stirrer bar. In addition to the experimental samples exposed to the ethanol stress, an untreated healthy yeast control was prepared by diluting the equivalent concentration of yeast with YPD, also in a sterile Bijoux bottle containing a stirrer bar. After the addition of the YPD, the yeast slurries were stirred at approximately 60 rpm using a magnetic stirrer for 60 minutes. Thereafter, the ethanol was removed by serial dilution. Briefly, an aliquot of the ethanol stressed yeast slurry was removed and diluted by 1:200 in fresh YPD. Cell counts and the methylene violet stain was performed using this yeast slurry. Thereafter, the yeast suspension was further diluted roughly 1000 fold again (yielding a total dilution ratio of 1:200,000 to form the final yeast sample in the case of the 8% ethanol shock) before being loaded into the glass microcalorimetry ampoules.

The growth of yeast in the presence of ethanol was also assessed. The initial ethanol concentrations used were 4% and 8%, in parallel to the ethanol shocks. In addition, 1% and 2% ethanol was used in subsequent experiments. The yeast for the constant ethanol exposure testing came from the healthy cells that had not been subjected to prior ethanol exposure. Yeast cells were harvested, as previously described and added to YPD containing 1%, 2%, 4% or 8% (v/v) ethanol in the final step prior to being loaded into the microcalorimetr. This negates the interference of any metabolic product release in the acclimatization period and allows these results to be compared to those of Antoce (1997b, 1996b). An experimental block flow diagram of the ethanol shock experiments is shown in Figure 3-8.

3.5.5 Combined ethanol and cold shock experiments

The purpose of this set of experiments was to test the compound effect of two stresses, namely a cold shock in conjunction with ethanol exposure. This was achieved by rapidly cold shocking the yeast, as per the cold shock experiments (Section 3.5.3), prior to exposing the yeast to 1% and 2% (v/v) ethanol, respectively, as per the ethanol shock experiments (Section 3.5.4). A block flow diagram of the experimental procedure followed is shown in Figure 3-9.

As a part of the combined ethanol and cold shock experiments (Section 5.3), a number of constant ethanol exposure experiments were also run for repeatability purposes (see Figure 3-9). While the individual quantitative data from each channel are included in Section 5.3.2,

the results from these channels have been aggregated into the average constant ethanol exposure results presented in this section.

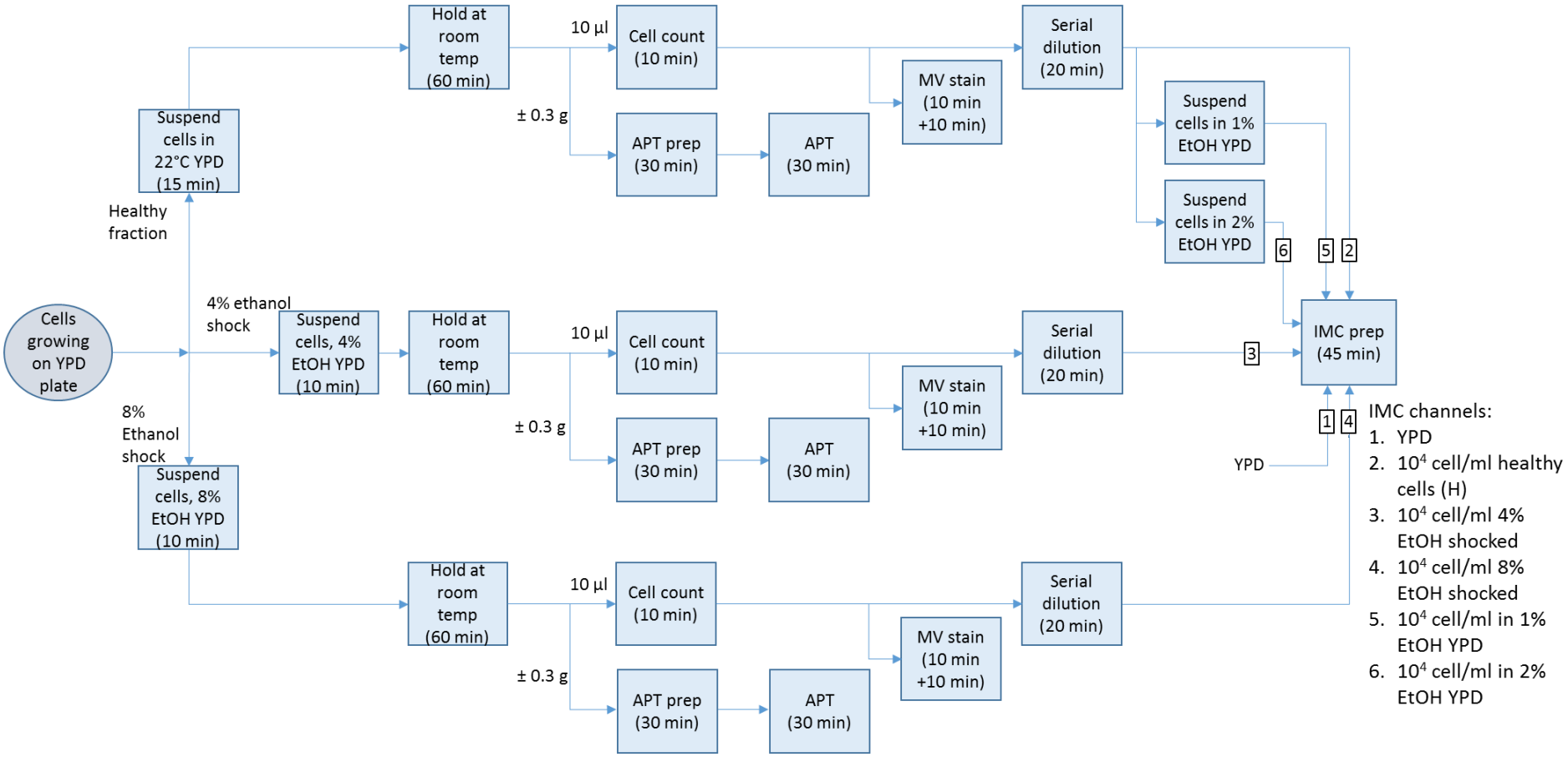

Figure 3-8: Ethanol shock experimental programme block flow diagram.
Approximate time taken to complete each step is shown in brackets. Yeast colonies grown on YPD agar at 30 °C for 72 hours were suspended in YPD. The yeast slurry was split into three equal fractions. Two fractions were exposed to 4% and 8% ethanol in YPD for 1 hour, respectively. The other fraction was suspended in YPD for an hour. After the 1 hour holding period, the yeast slurry from all the fractions were subject to cell counts, viability testing and microcalorimetric analysis. The majority of the suspended yeast slurry was used for the APT. The ethanol exposed cells were appropriately diluted and analysed by microcalorimeter along with a YPD blank (negative control). Using cells from the original healthy (non-ethanol exposed) cell suspension, two further samples were made to contain cell suspensions exposed to 1% and 2% ethanol in YPD (constant ethanol exposure).

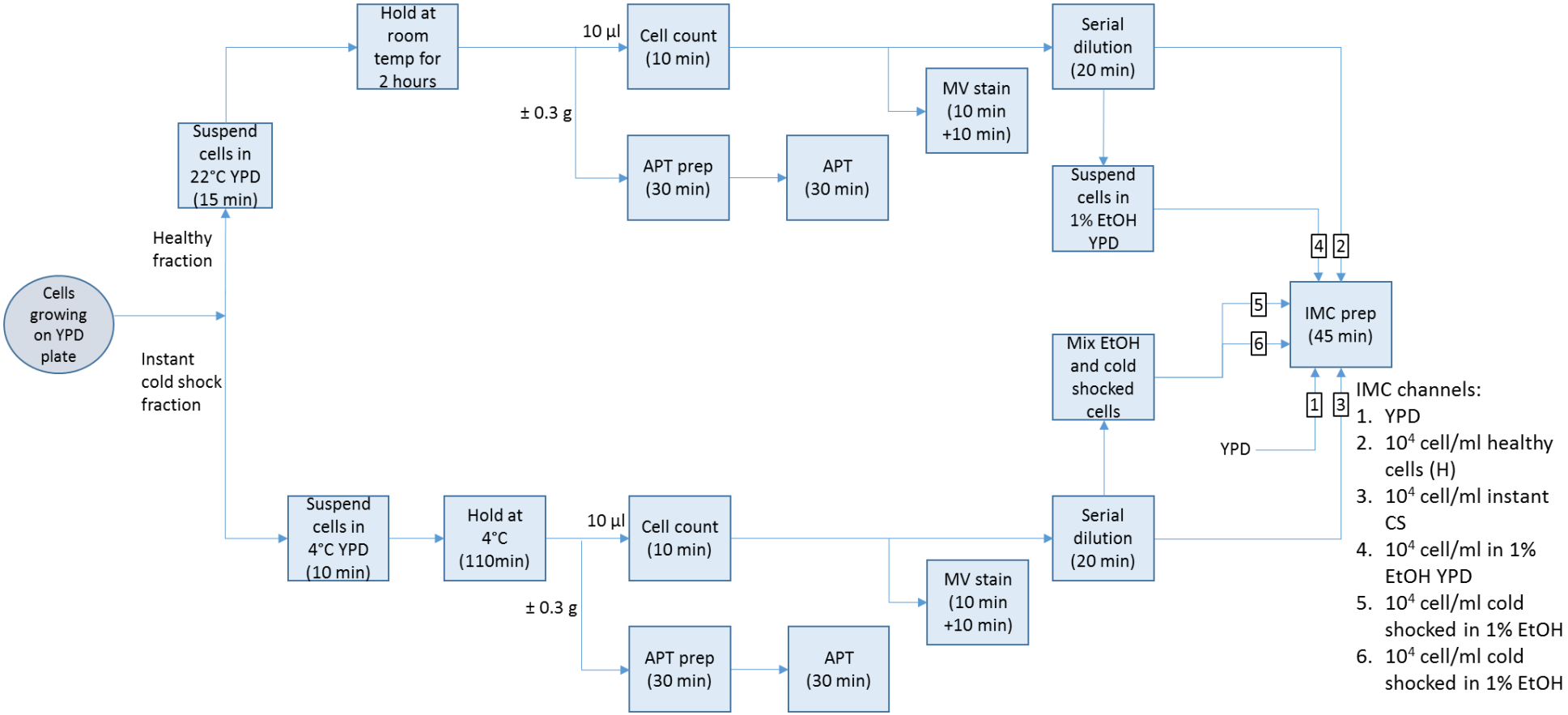

Figure 3-9: Combined cold shock and ethanol exposure experimental programme block flow diagram (approximate time taken to complete each step in brackets).
Yeast colonies grown on YPD agar at 30 °C for 72 hours were split into two equal fractions. One fraction was cold shocked by rapid dilution in 4 °C YPD and the other fraction held at room temperature (suspend in YPD) for the same length of time. After the 2 hour holding period, a small portion of the slurry from both the cold shocked fraction and the healthy faction was removed to perform cell counts and be used for viability testing and microcalorimetric analysis. The majority of the suspended yeast slurry was used for the APT. A portion of the healthy cells and the cold shocked cells were then suspended in ethanol. All cell populations were then appropriately diluted to the correct concentration using YPD and loaded into the TAMIII microcalorimeter along with a YPD blank (negative control).

4 Development of the Microcalorimetric Method

There is progressive development, as this chapter builds, of the microcalorimetric method used to analyse the data produced. This section starts by analysing the repeatability experimental results. The results of tests in which different healthy cell concentrations and mixed proportions of healthy and heat-killed cells are used to demonstrate the overall repeatability, in order to provide a means of further validation of the experimental methods used.

Each experiment is referred to by the date it was initiated so that all the results, graphs and raw data can easily be cross-referenced. In some cases, certain data sets within experimental runs have been discarded – details of the discarded data along with the reason for discarding the data can be found in Appendix B.1.

4.1 Repeatability experiments

4.1.1 Introduction of the experimental data - a visual comparison of thermograms data

Before any stressing of the yeast was undertaken, the repeatability of the experimental methods was verified. The repeatability experiments commenced with demonstrating the repeatability of yeast growth in the microcalorimeter. Following this, the repeatability of the APT was determined. The repeatability associated with the viability assays was determined as part of the heat killing results (Section 4.2).

The graphical representation of the heat flow and heat curves from each of the repeatability experiments are shown in Figure 4-1 to Figure 4-5. Each Figure is comprised of two 'sub-figures', the one on the left, sub-figure A, showing the heat flow curve and the curve on the right, sub-figure B, showing the heat curve (the integrated heat flow curve).

The heat flow curves (sub-figure A) have a bell curve shape, similar to that of a Gaussian distribution. The same curve shapes are found in other microcalorimetric studies of yeast (Section 2.4), and are therefore expected. The first portion of the curve, before a decline in heat flow is observed, represents unrestrained exponential growth – the early to mid-exponential phase. After the heat flow curve peaks and the heat flow begins to decline, the system has entered the late exponential/early stationary phase.

Figure 4-1 to Figure 4-3 illustrate the effect of inoculum size on the growth thermogram. It is important to note that zero heat flow does not equate to zero cells. Similarly, a decline in heat flow also does not correlate with cell death. In terms of the calorimetric signal produced, the highest cell numbers are observed when the heat flow returns to the baseline (at the end of an experiment), where the highest heat is observed. This is proved in numerous experiments in the literature where cell numbers and the heat flow and resultant heat generated are continuously monitored, of which Lamprecht (1980) provides an extensive review.

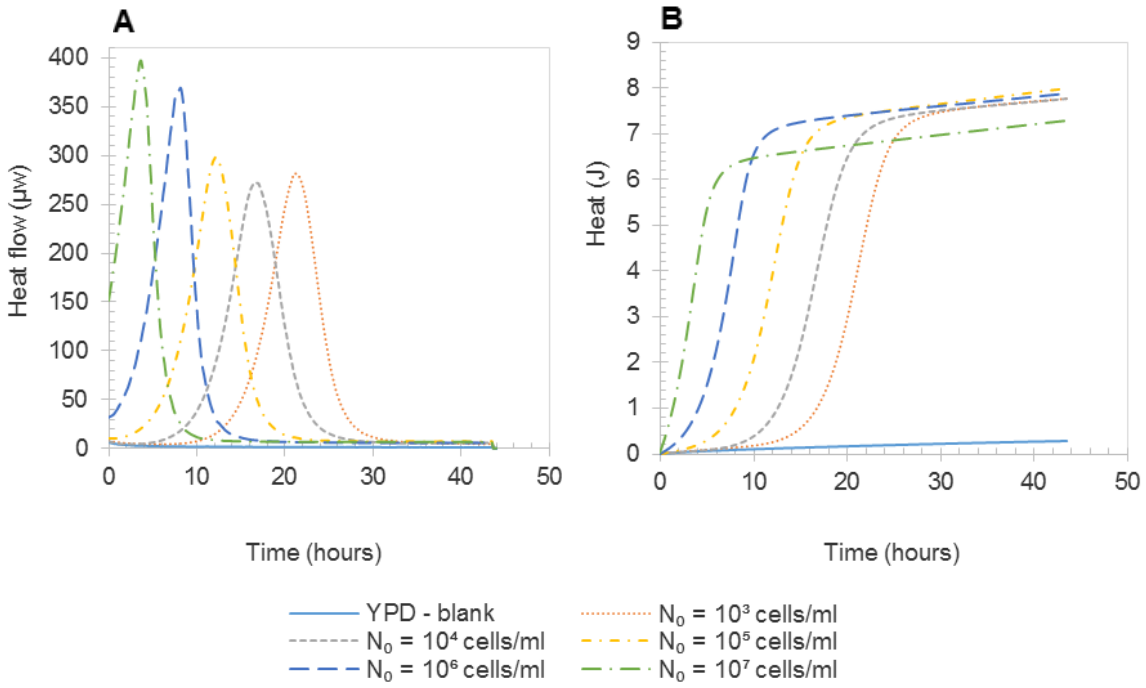

Figure 4-1: Heat flow (A) and heat curves (B) for different inoculum sizes, where N_0 is the initial concentration (experiment 15/05/2015).

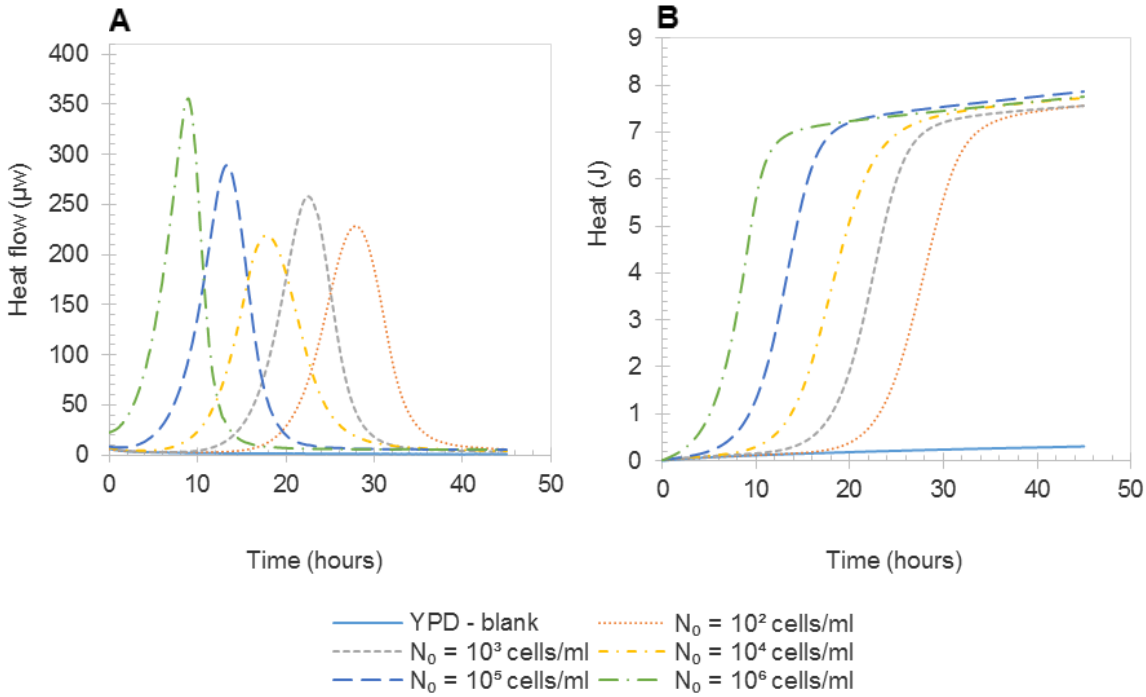

Figure 4-2: Heat flow (A) and heat curves (B) for different inoculum sizes, where N_0 is the initial concentration (experiment 19/05/2015).

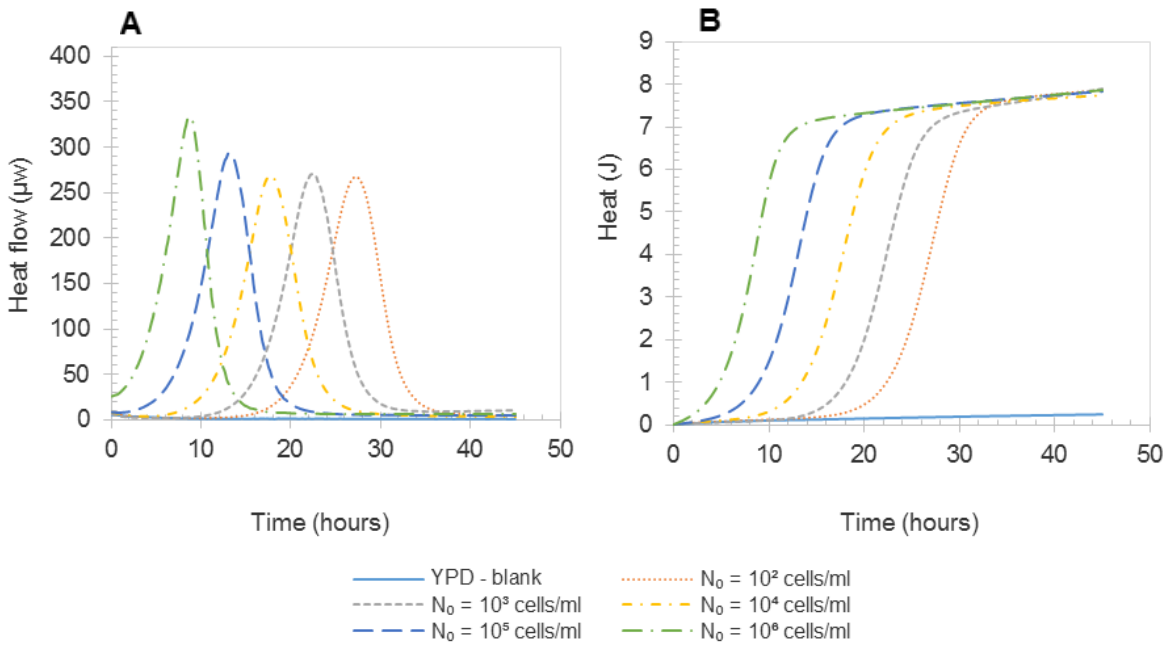

Figure 4-3: Heat flow (A) and heat curves (B) for different inoculum sizes, where N_0 is the initial concentration (experiment 22/05/2015).

The heat flows from inocula with 10^6 cells/ml or more all start at non-negligible heat flows (approximately >10% of the maximum net output achieved). This non-negligible initial heat flow illustrates that the heat generated due to lowering the ampoules into position can become convoluted with the heat flow due to the cells. It is thus difficult to discern when the calorimetric signal can be considered 'correct', which has a direct impact on the heat signal calculated (refer to Section 3.4 for information regarding signal conditions). The same issue exists, though to a lesser degree, when an inoculum size of 10^5 cells/ml is used, especially if there is a delay in inserting the ampoules into the calorimeter.

The lag phase (before any significant heat is produced by the cells) associated with an initial inoculum of 10^4 cells/ml ensured the observation of the full heat flow curve and allowed for some leeway in time to prepare the ampoules. It also allows the effect of stresses on the lag phase to be observed. While starting inoculum sizes of less than 10^4 cells/ml are suitable for the same reasons, a smaller inoculum size results in a prolonged duration of the measurement – due to the time required for the cells to divide and generate enough heat to be detected by the TAMIII. The shorter the duration of an experiment the higher the potential throughput for industrial application. Therefore, the initial inoculum size was chosen to be 10^4 cells/ml to standardize the method, as a lead time (before the signal moves into exponential growth) occurs for accurate calculation of the heat signal, and the lag phase does not negatively impact the potential throughput of the method.

Figure 4-4 and Figure 4-5 illustrate the repeatability, both within single experiments (technical repeats) and across different experiments (biological repeats) of using an inoculum size of 10^4 cells/ml.The curves in Figure 4-4 and Figure 4-5 indicate a high degree of technical repeatability within each experiment. By simple visual analysis it is observed that the shape of the two sets of curves between experiments (Figure 4-4 compared to Figure 4-5) look much

the same. This comparison extends to the curves shown for an inoculum size of 10^4 cells/ml in Figure 4-1, Figure 4-2 and Figure 4-3. The curves are shown to be statistically repeatable in Section 4.1.2.

Any deviation in the curves' agreement occurs only after the peak heat flow. Slight differences in sample handling or preparation could cause the deviations. In the case of green curve (– · –) of Figure 4-4, a significant deviation occurs due to the ampoule being knocked over - see Appendix B.2 for further supporting information.

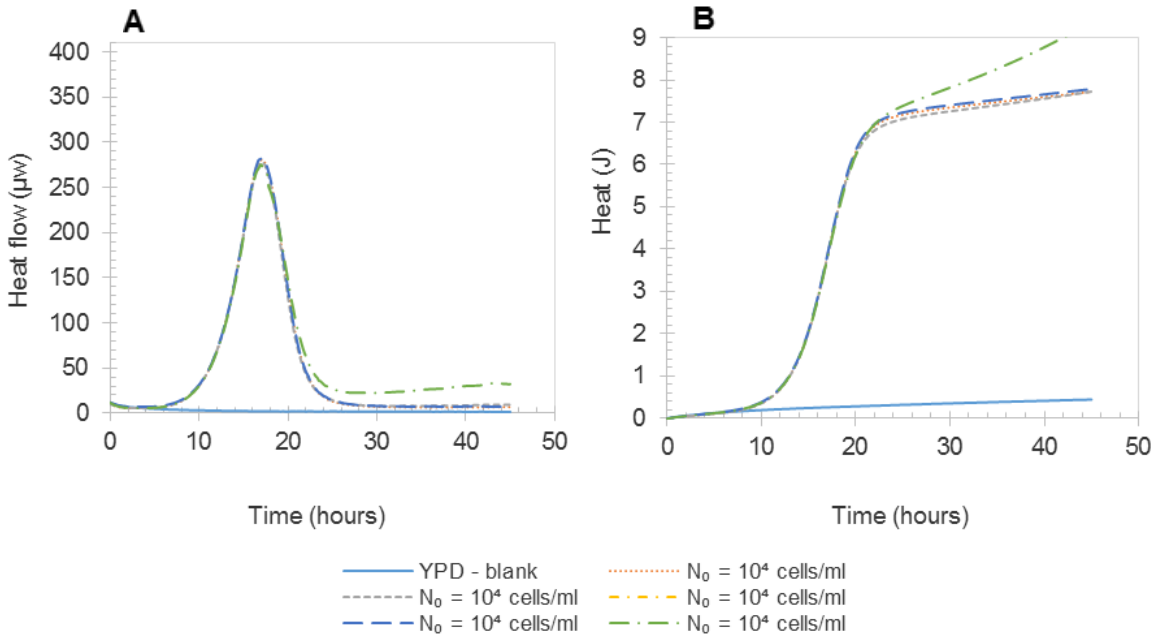

Figure 4-4: Heat flow (A) and heat curves (B) for the same inoculum size, investigating repeatability, where N_0 is the initial concentration (experiment 15/04/2015).

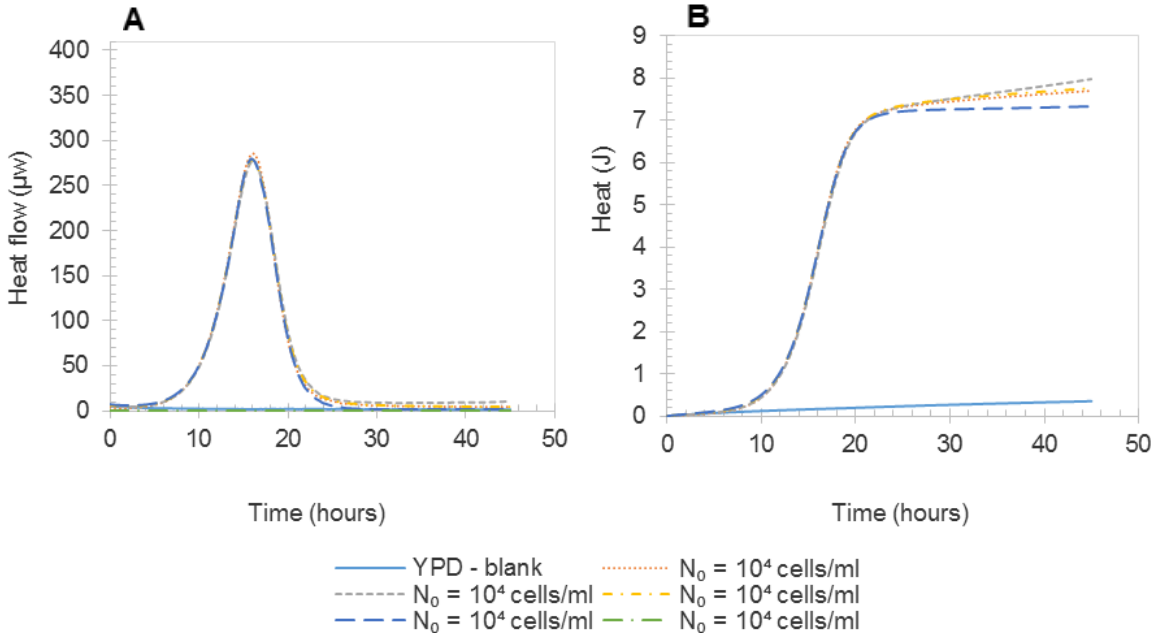

Figure 4-5: Heat flow (A) and heat curves (B) for the same inoculum size, investigating repeatability, where N_0 is the initial concentration (experiment 21/04/2015).

4.1.2 Development of microcalorimetric data analysis techniques

Following confirmation of the technical repeatability, the microcalorimetric data was analysed to extract meaningful quantitative parameters.

Baseline correction using the YPD blank

The TAMIII automatically takes a baseline reading from each channel (when empty) and subtracts it from the overall heat flow. This baseline correction handles the heat flow bias of each channel – an artefact of the TAMIII hardware.

In order to correct for baseline disturbances due to other artefacts, a further baseline correction was instituted. Here the heat flow of the YPD blank (included in every experiment) was subtracted from the heat flow recorded for the other channels. This procedure takes into account any non-linear exothermic or endothermic decay processes occurring in the media, as indicated by Wasdö (2009). It also takes into account any residual heat created by frictional forces when inserting the ampoules. The subtraction of the YPD baseline reduces the significance in choosing when the signal is 'correct' (see Section 3.4.1 and paragraph above) because any residual heat still being dissipated is roughly the same for each channel and thus is essentially negated.

An example of a single channel's heat flow from which the heat flow of the YPD blank has been subtracted is shown in Figure 4-6.

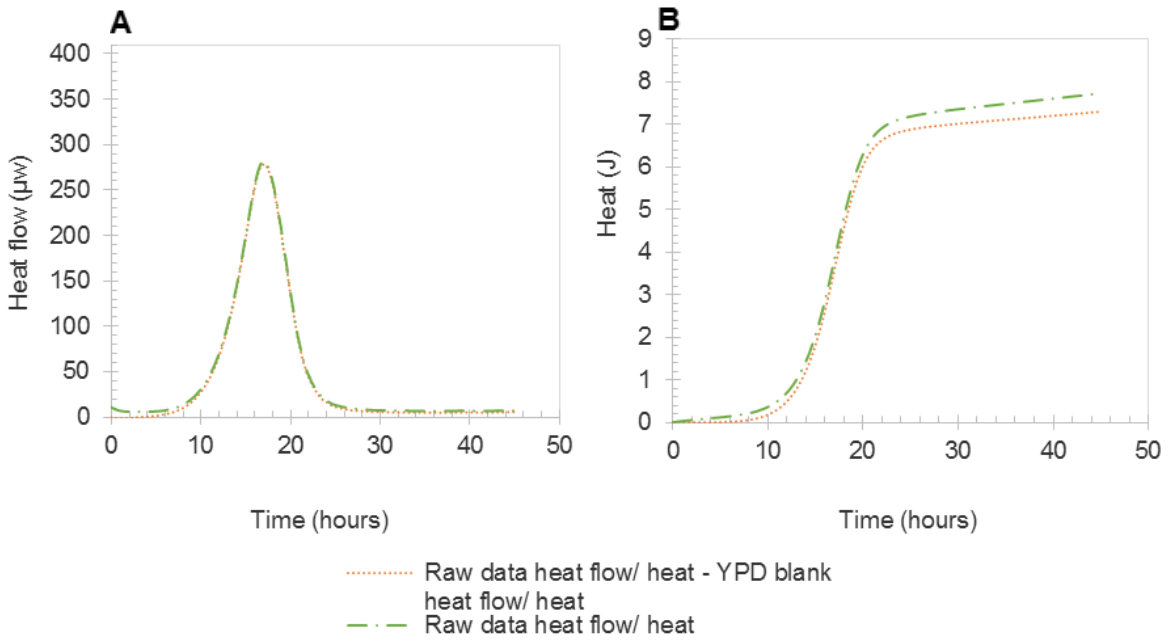

Figure 4-6: Comparison of a heat flow (A) and heat curve (B) for which the heat flow from the YPD blank has and has not been subtracted from the calorimetric signal.
The curve shown is for a single channel from the 15/04/2015 experiment, investigating the repeatability of using the same inoculum size – 10^4 cells/ml.

In terms of the heat flow signal, there is no readily apparent difference between the corrected and uncorrected curves other than a slight deviation in the first five hours where the heat flow

generated due to lowering the sample into the calorimeter has been corrected. However, a more significant difference appears between the corrected and uncorrected heat signals. Even slight differences in the heat flow signal can significantly affect the heat signal due to the integral function from which the heat curve is formed. The integral magnifies any slight signal offset due to the long period over which the signal is integrated. This confirms the importance of making this adjustment.

Determining the specific growth rate – equation fitting

Given the shape of the thermograms seen above and the results found in the literature (Section 2.4), the initial heat flow from a sample is anticipated to be in the form:

$$heat\ flow = a_1 * exp(\mu * t) + g(t) + b_1 \qquad \textit{Equation 4-1}$$

where a_1 is a constant, $g(t)$ is some complex heat flow process due to factors other than microbial metabolism (e.g. friction or decay of media) and b_1 is the channel baseline offset. The b_1 value is corrected for by the TAMIII software when it performs a baseline correction (see Section 3.4). Any complex heat flow processes occurring due to factors other than the microbial system of interest, $g(t)$, are accounted for by subtracting the heat flow of the YPD blank (Section 4.1.2 – baseline correction). Therefore applying the aforementioned corrections allows Equation 4-1 to be simplified to:

$$heat\ flow = a_1 * exp(\mu * t) \qquad \textit{Equation 4-2}$$

Equation 4-2 could be used to determine the specific growth rate by means of linearization, but, in practice, this is rarely done for two main reasons. Firstly, the heat flow signal tends to be noisy which can introduce errors into any parameters determined using the heat flow signal. Secondly, it is known that the heat curve corresponds better to cell numbers than the heat flow curve which corresponds to metabolic activity at that point i.e the product of cell number and specific metabolic activity (Braissant et al., 2013). The most intuitive confirmation of this is the peak and subsequent decline in heat flow, whereas in fact the highest cell numbers occur at the end of the experiment. In order to derive the heat curve, Equation 4-2 is integrated, yielding:

$$heat = \int heat\ flow\ dt = \int a_1 * exp(\mu * t)\ dt = A * exp(\mu * t) + B \qquad \textit{Equation 4-3}$$

where A is a new constant ($A = a_1/\mu$) and B is a constant of integration. The heat flow data extracted from the TAMIII can be numerically integrated to generate the heat curve. The TAMIII assistant software package performs the integration for the user.

Equation 4-3 is of exactly the same form as Equation 2-5. Hashimoto & Takahashi (1982) and Itoh & Takahashi (1984) use two different exponential equation linearization approximation techniques to linearize the fundamentally derived Equation 2-5, linking heat to cell growth to determine the value of the specific growth rate. The linearization was performed to determine the specific growth rate using a linear plot rather than using the data in its exponential form. Both linearization methods make certain approximations and assumptions.

It is not clearly stated by the authors why Equation 2-5 was not fitted directly to the data using a curve fitting method such as non-linear least squares minimisation. It may have been due to a lack of the required computing power at the time these studies took place. It is now common practice to fit data in its most basic form, not to reduce data quality through estimations and approximations.

Before direct fitting of an equation, the region over which the data is to be fitted has to be determined. In the case of fitting an exponential equation, such as Equation 4-3, this is usually performed in the region where a plot of the natural logarithm of the curve is linear. However, in the case of heat data, Antoce et al. (1996a) and Takahashi's subsequent work (see Section 2.4.3) fit the data between 3% and 30% of the total heat output (see Figure 2-8). The authors do not justify use of this region, only stating that this region is where exponential growth occurs. The problem with fitting data in a region based on a certain percentage of the total heat output is that the heat flow curve does not return to zero heat flow even well after a peak in heat flow has been observed. This heat flow curve offset causes the heat curve to rise continually, clearly observed in the preceding figures from >25 hours after a run was initiated. In most cases this continual rise in heat flow is non-negligible. Therefore depending on the duration of measurement of heat flow, the region over which an exponential is fit differs in terms of percentage of heat output.

A new method is proposed whereby the fit region is based on the value of the maximum heat flow which in all the repeatability experiments (n=5 biological repeats, with 25 technical repeats) was an average of 287 ± 22 μw. In order to determine the linear region, the natural logarithm of the heat flows were plotted, examples of which are shown in Figure 4-7 and Figure 4-8. By visual inspection the linear region occurred in the region of 10% to 70% of the maximum heat flow output. These regions were fitted with Equation 4-2, examples of the results represented as the bolded red region in the plots of the natural logarithm of the heat flow along with the heat flow curves in Figure 4-7 and Figure 4-8. The fit is only shown for a single 'different N_0 experiment' (Figure 4-7) and a single experiment where the initial population was the same ($N_0 = 10^4$ cells/ml) (Figure 4-8).

In terms of comparing the above defined fit region (between 10% and 70% of the peak heat flow) to that of Antoce et al. (1996a) (3% to 30% of the maximum heat value) – in most cases the fit region was similar, occurring within approximately 1.5 hours of one another. Therefore employing this new fitting region is not considerably different to what has been done before in the literature, but has the added benefit of seemingly being more reproducible. The similarity of employing the two different techniques is illustrated in Figure 4-9.

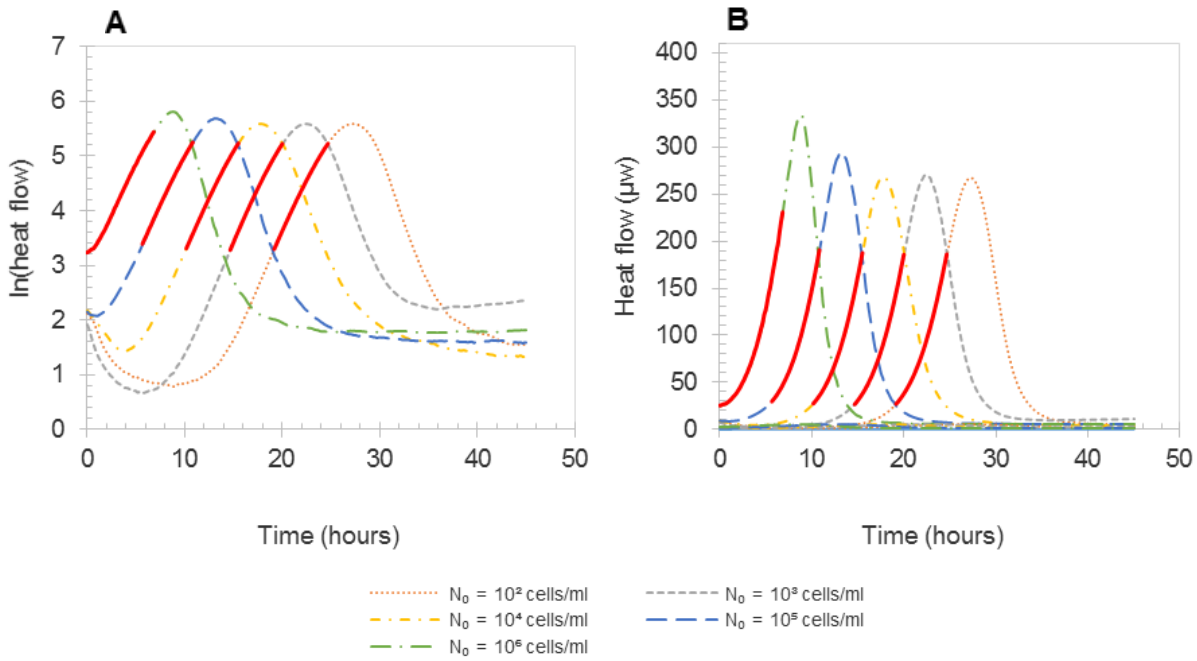

Figure 4-7: Natural logarithm of heat flow (A) alongside the heat flow curves (B) for experiment 22/05/2015 indicating the curve fitting region bolded in red for the different inoculum sizes.

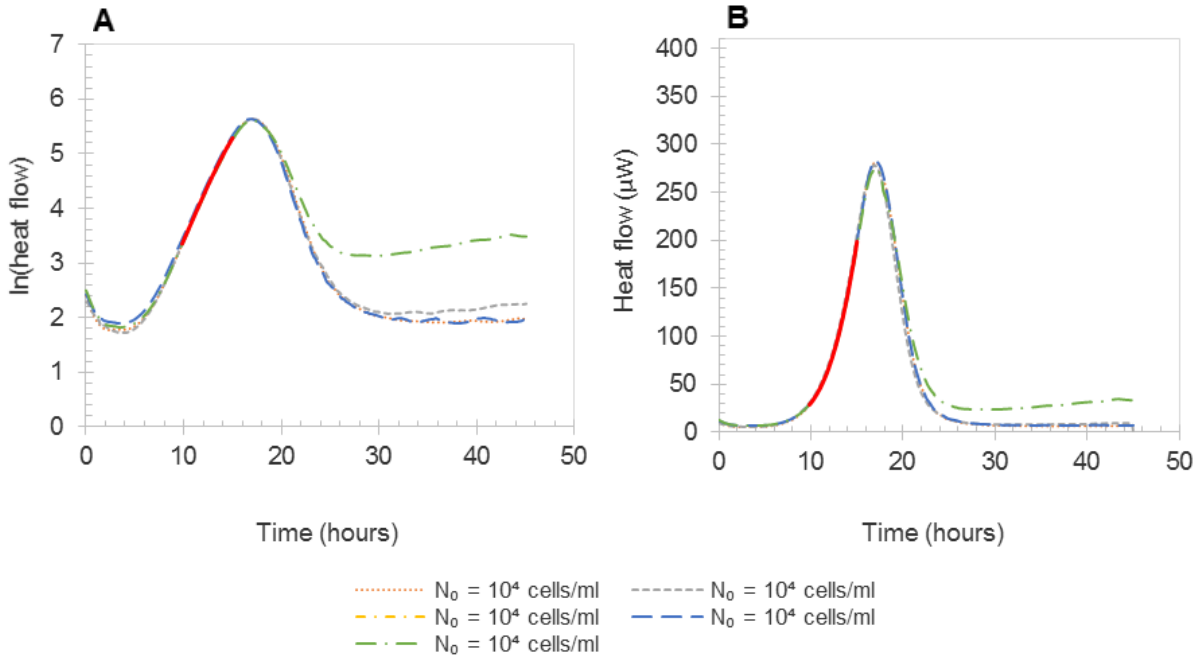

Figure 4-8: Natural logarithm of heat flow (A) alongside the heat flow (B) curves for experiment 15/04/2015 indicating the curve fitting region bolded in red.

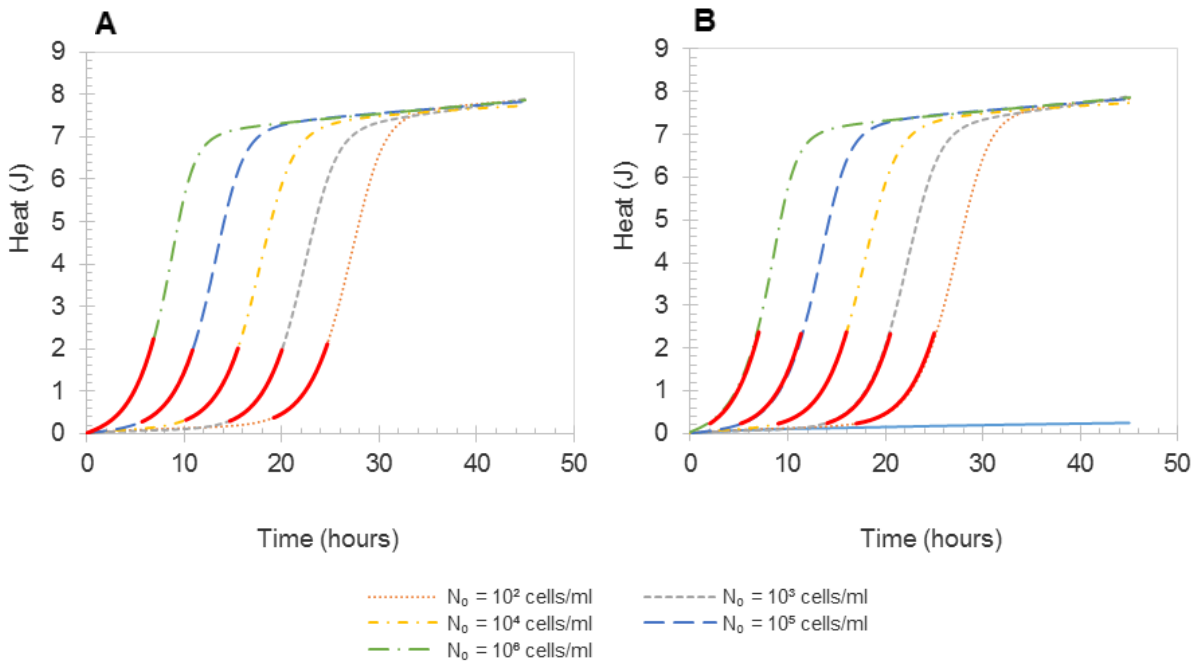

Figure 4-9: Comparisons of the fitting region used in this work (A) based on 10% - 70% of the peak heat flow (approx. 270 µW in each case) compared to the fit region of Antoce et al. (1996) method (B), based on 3-30% of the maximum heat (approx. 8 J).
In each case the raw data is the same and the fit region is shown in bold red. The above experimental data originates from the 22/05/2015 experiment – Figure 4-3.

Based on the relative similarity and added advantages of defining the region to fit the data as between 10% and 70% of the peak heat flow, the heat data was fitted with Equation 4-3. The heat data was fitted with MS Excel using a minimisation of the total sum of the error between the predicted values (Equation 4-3) and the experimental values (heat curve). In all cases the full set of data points were used. This yielded on average 6000 data points per data set for each channel and gave an average time between readings of 34 seconds.

In this analysis procedure, there is no reliance or importance assigned to the data collected after the peak in heat flow occurs. This implies that heat flow data only need be collected until the peak heat flow occurs for each channel, following which the experiment can be terminated. As much time is required for the heat flow curve to return to a stable baseline after peaking, in the experiments following the method development, data collection was routinely terminated after the peak in heat flow had been observed.

In addition to fitting an exponential equation to the data, the time taken for each sample to reach the maximum heat flow output and the time taken to reach 50% of the total heat flow output was recorded. These values were analysed in accordance with how Antoce et al. (1996a) examined specific growth retardation of yeast under stress (discussed in Section 2.4.3).

Table 4-1 presents the equation parameters for Equation 4-3 determined from the data as well as how closely the equation correlates to the data. The R^2 values, all close to unity, clearly show that Equation 4-3 fitted the data well. The time for the heat flow to peak (t_{max}) and the

time taken for the heat flow to reach 50% of the maximum heat flow value (t_{50}) are also shown in Table 4-1.

Table 4-1: Calculated parameters for all repeatability experiments

Date of experiment	N_0 (cells/ml)	R^2	μ (hr^{-1})	A (J)	B (J)	t_{max} (hr)	t_{50} (hr)
15/04/2015	10^4	0.99993	0.39	5.87E-03	-0.12	17.1	12.8
		0.99993	0.38	6.12E-03	-0.12	17.1	13.9
		0.99993	0.38	5.97E-03	-0.09	17.1	14.0
21/04/2015	10^4	0.99992	0.38	1.09E-02	-0.14	16.1	12.8
		0.99993	0.38	1.02E-02	-0.12	16.1	12.8
		0.99993	0.37	1.10E-02	-0.09	16.1	12.8
		0.99992	0.37	1.14E-02	-0.08	15.9	12.8
15/05/2015**	10^3	0.99993	0.36	1.95E-03	-0.05	21.3	18.0
	10^4	0.99993	0.37	8.97E-03	-0.09	16.7	13.5
	10^5	0.99993	0.36	5.23E-02	-0.10	12.2	9.1
	10^6	0.99992	0.38	2.51E-01	-0.27	8.2	5.2
19/05/2015	10^2	0.99990	0.35	2.42E-04	-0.11	28.0	23.9
	10^3	0.99992	0.36	1.30E-03	-0.08	22.6	19.1
	10^4	0.99992	0.37	5.49E-03	-0.06	18.0	14.2
	10^5	0.99993	0.37	2.98E-02	-0.10	13.5	10.3
	10^6	0.99992	0.38	1.58E-01	-0.19	9.0	6.2
22/05/2015	10^2	0.99992	0.35	3.62E-04	-0.08	27.4	23.6
	10^3	0.99992	0.36	1.46E-03	-0.13	22.5	19.1
	10^4	0.99993	0.36	7.08E-03	-0.08	17.8	14.5
	10^5	1.00000	0.36	3.80E-02	-0.11	13.4	10.1
	10^6	0.99991	0.37	1.76E-01	-0.19	8.9	5.9
Average *		0.99993	0.371	*7.68E-03**	*-0.09**	*17.14**	*13.72**
Standard deviation *		0.00001	0.009	*2.23E-03**	*0.02**	*0.79**	*0.67**

*the average values and associated standard deviations are only for the experiments where 10^4 cells/ml were used as the inoculum

**the parameters from the sample with 10^7 cell/ml as the starting inoculum were not included in the table due to the fit region falling outside the bounds of the data (see Figure 4-1)

Antoce (1996) used measures of yeast performance relative to a healthy, unstressed yeast population by normalising the growth parameters of a yeast population back to that of reference population included in each experiment. This is attractive as it takes into account any minor experimental differences occurring. Furthermore, if consecutive experiments are not set-up in the same manner, their results can be compared as long as each replicate in each experiment was prepared in the same manner. In this work, the healthy yeast population used for normalisation had not been exposed to any stress and had a starting inoculum of 10^4 cells/ml (denoted with a subscript 'm'). Employing this normalisation approach in each experimental run, the calculated growth parameters of each sample (denoted with a sub-script 'i') were normalised.

The value of using the normalised parameters becomes apparent when comparing experiments where the initial preparation time varied. In such cases, the absolute value of t_{max} and t_{50} can differ significantly making direct comparisons invalid. The results of the normalisation procedure are displayed in Table 4-2.

Table 4-2: Calculated normalized parameters for all repeatability experiments

Date of experiment	N_0 (cells/ml)	μ_i/μ_m	A_i/A_m	B_i/B_m	$t_{max,i}/t_{max,m}$	$t_{50,i}/t_{50,m}$
15/04/2015	10^4	1.003	0.98	1.07	1.00	0.94
		0.996	1.02	1.11	1.00	1.03
		1.000	1.00	0.82	1.00	1.03
21/04/2015	10^4	1.002	1.00	1.31	1.00	1.00
		1.008	0.94	1.09	1.00	1.00
		0.999	1.01	0.85	1.00	1.00
		0.991	1.05	0.74	0.99	1.00
15/05/2015	10^3	0.984	0.22	0.52	1.28	1.34
	10^4	1.000	1.00	1.00	1.00	1.00
	10^5	0.985	5.83	1.14	0.73	0.68
	10^6	1.016	27.94	2.91	0.49	0.39
19/05/2015	10^2	0.957	0.04	1.71	1.56	1.68
	10^3	0.976	0.24	1.29	1.26	1.34
	10^4	1.000	1.00	1.00	1.00	1.00
	10^5	1.010	5.43	1.53	0.75	0.72
	10^6	1.025	28.86	2.99	0.50	0.44
22/05/2015	10^2	0.966	0.05	1.02	1.54	1.63
	10^3	0.993	0.21	1.61	1.26	1.31
	10^4	1.000	1.00	1.00	1.00	1.00
	10^5	1.001	5.36	1.40	0.75	0.70
	10^6	1.033	24.92	2.41	0.50	0.41
Average		**0.998**				
Standard deviation		**0.003**				

Both Table 4-1 and Table 4-2 show the calculation of the specific growth rate using the heat curves, regardless of the starting concentration, to be highly reproducible. The standard deviation of the specific growth rate is less than 2.5% of the average absolute value.

To investigate the effect of inoculum size (N_0) on the above determined parameters, the logarithm of the inoculum size was plotted as a function of the logarithm of the determined normalised parameters. The specific growth rate was excluded from the analyses, as it is evident from Table 4-1 and Table 4-2 that the specific growth rate is not affected by the initial inoculum size, as expected. Figure 4-10 to Figure 4-13 show the results of these plots. Zero error was associated with the values determined at N_0 = 10^4 cells/ml, as each data set was normalised to these data.

There is a highly linear correlation between the starting inoculum size and the normalised value of 'A' determined from Equation 4-3 – a correlation coefficient of 0.9995, as seen in Figure 4-10. From rearranging Equation 4-3 and Equation 2-5, it can be seen that:

$$A = N_0 \frac{q_1}{\mu \cdot exp(\mu \cdot \tau)} \qquad \textit{Equation 4-4}$$

Given that A contains a term for both N_0 and lag time τ, it is unsurprising that a plot of A versus N_0 yields a linear trend (q_1 is power produced per cell in the exponential phase). Thus the value of A is a good indicator of initial inoculum size. Since the value of A and that of N_0 plotted in Figure 4-10 were determined using completely independent method, it suggests that the methods used are repeatable and accurate.

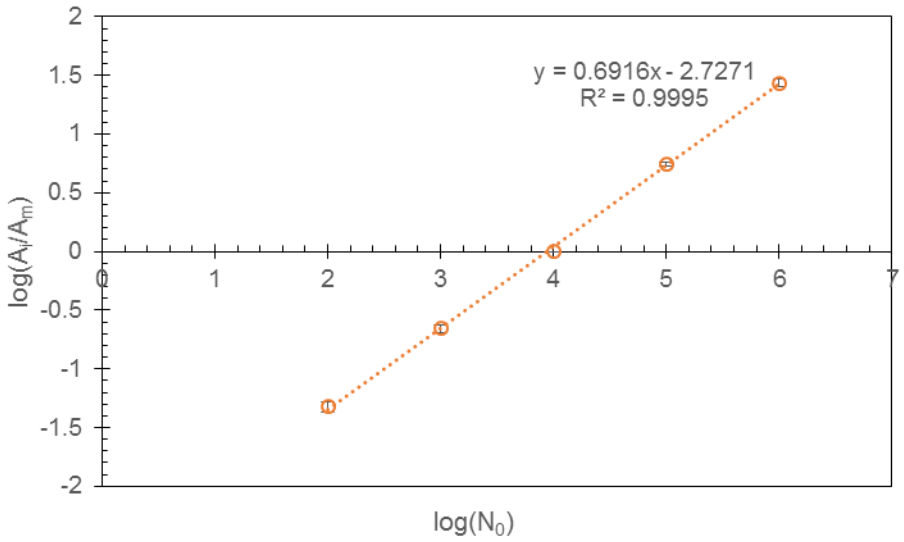

Figure 4-10: Plot of the logarithm of the normalised curve fitting value [log(A_i/A_m)] versus the logarithm of inoculum size.
Error bars represent one standard deviation from the mean.

A plot of normalised B values as a function of inoculum size indicates there to be no direct linear correlation between the value of B and the inoculum size, seen by the correlation coefficient of 0.4487 in Figure 4-11. From rearranging Equation 4-3 and Equation 2-5, it can be seen that:

$$B = N_0\left(\int_0^{\tau} N_0 dt - {}^{q_1}/_{\mu}\right) \qquad \textit{Equation 4-5}$$

Therefore, B is a much more complex function of the initial population than A. Furthermore, given the size of the error bars in Figure 4-11, it would seem that the value of B cannot be determined with a high degree of repeatability.

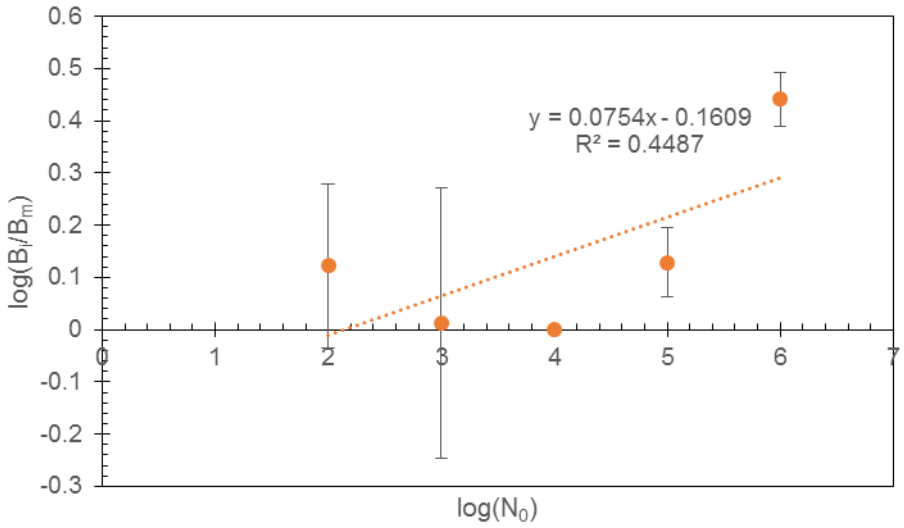

Figure 4-11: Plot of the logarithm of normalised 'B' [$\log(B_i/B_m)$] versus the logarithm of inoculum size.
Error bars represent one standard deviation from the mean.

There is a high degree of correlation ($R^2 = 0.9799$) between the normalised value of t_{max} and the starting inoculum size, as seen in Figure 4-12. This is unsurprising as a small inoculum results in an increased number of cell divisions required before any heat output is thus affecting the time for the culture to reach maximum heat output. Therefore, t_{max} is also a good predictor of initial inoculum size.

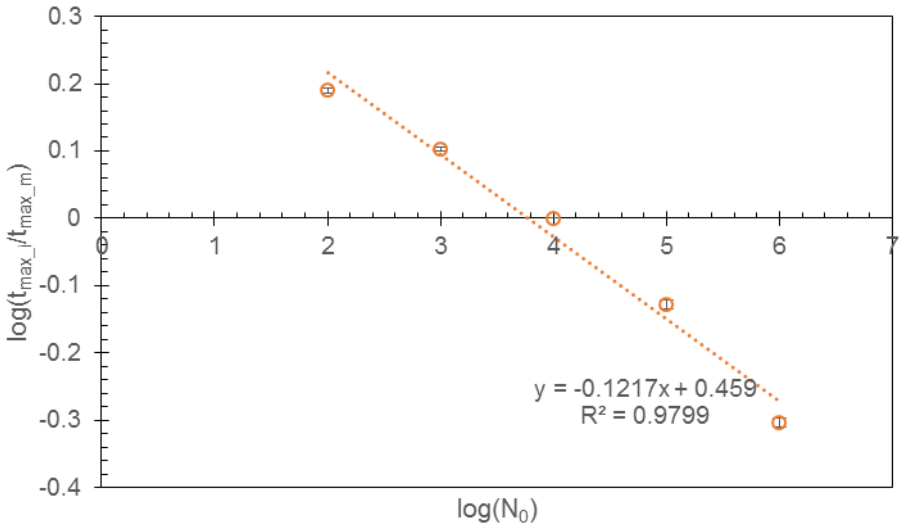

Figure 4-12: Plot of the logarithm of normalised t_{max} [$\log(t_{max\_i}/t_{max\_m})$] versus the logarithm of inoculum size.
Error bars represent one standard deviation from the mean.

There is also a high degree of correlation ($R^2 = 0.9698$) between the normalised value of t_{50} and the starting inoculum size. Due to the same reasoning above, this is unsurprising as a small inoculum results in an increased number of cells divisions before the heat evolution is detectable, thus affecting the time for the culture to reach 50% of the maximum heat output.

Therefore, t_{50} is also a good predictor of initial inoculum size. Comparing Figure 4-13 with Figure 4-12 it can be seen that there exists a slightly higher degree of correlation between the value of t_{max} and inoculum size than the value of t_{50}. The value of t_{50} is slightly less reproducible given the larger associated error bars. Due to the aforementioned reasons and for the sake of brevity, the results to follow only examine t_{max}.

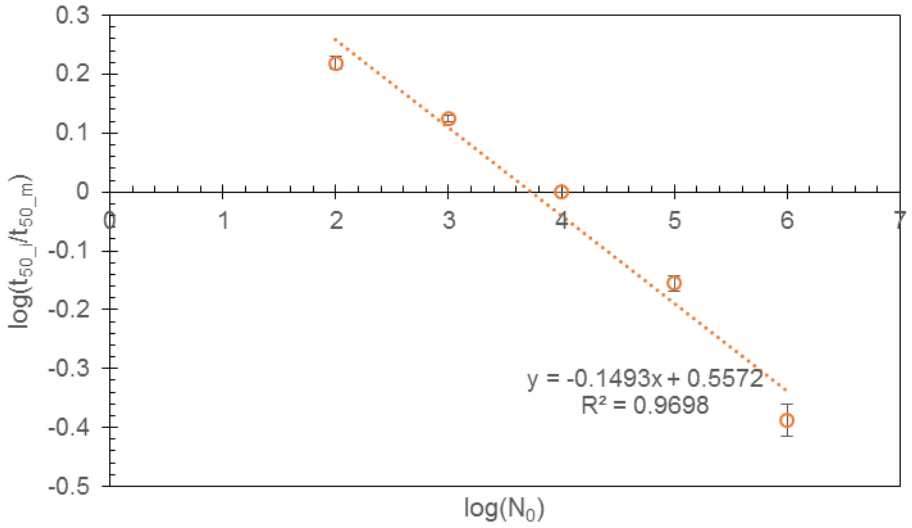

Figure 4-13: Plot of the logarithm of normalised t_{50} [$\log(t_{50\_i}/t_{50\_m})$] versus the logarithm of inoculum size.
Error bars represent one standard deviation from the mean.

Developing an automated analysis process

Using Excel macros, coded in MS Visual Basic for Applications (VBA), provided a platform to develop an algorithm to process the data more efficiently while reducing the chance of errors. The VBA code developed to process the data is given in Appendix A.5. A flow diagram of the logic the code executes to analyse the data is represented in Figure 4-14, and also serves as a summary of the overall data analysis process followed in all the experiments to follow.

4.1.3 Acidification power test

APT tests were performed to demonstrate the repeatability of the adapted method, described in Section 3.3.3. Figure 4-15 shows pH as a function of time for five different acidification power tests, all using 72-hour-old yeast grown on YPD agar petri-dishes. Variability was observed in the pH profiles (Figure 4-15), especially in the first 10 minutes. Similar variation was observed by Gabriel et al. (2008), the developers of the optimised APT. The general trend of the profiles seen in Figure 4-15 is similar to those of Gabriel et al. (2008). The APT value is reported as 6.3 minus pH_{20} (Equation 2-4).

The average APT value for the repeatability tests was calculated to be 2.89 ± 0.13. Brewing yeast with an APT value over 2.4 are considered ”highly active yeast with good fermentation performance” (Gabriel et al., 2008). Thus, these represent highly vital yeast cultures.

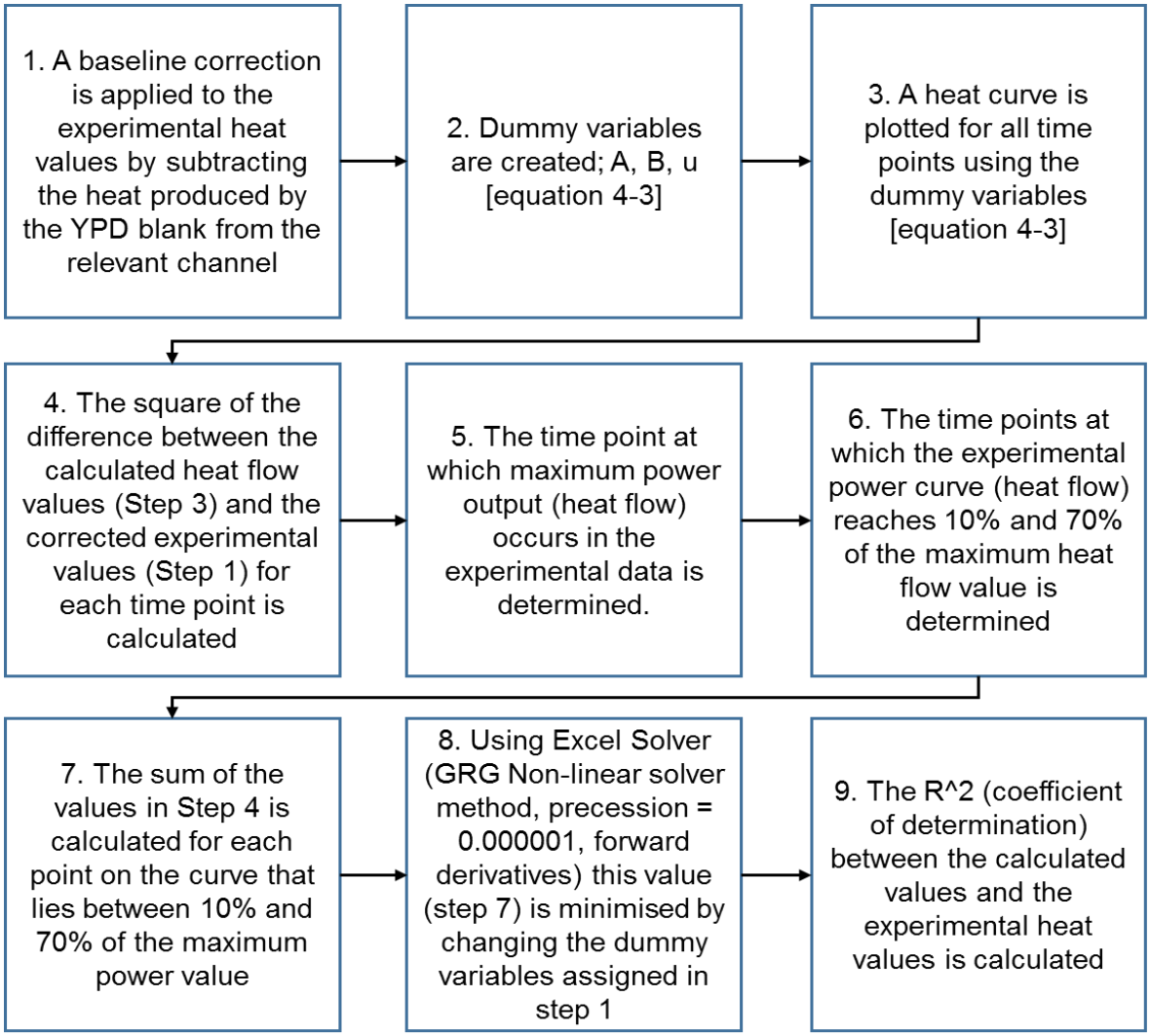

Figure 4-14: Flow diagram of the logic used to analyse the experimental data

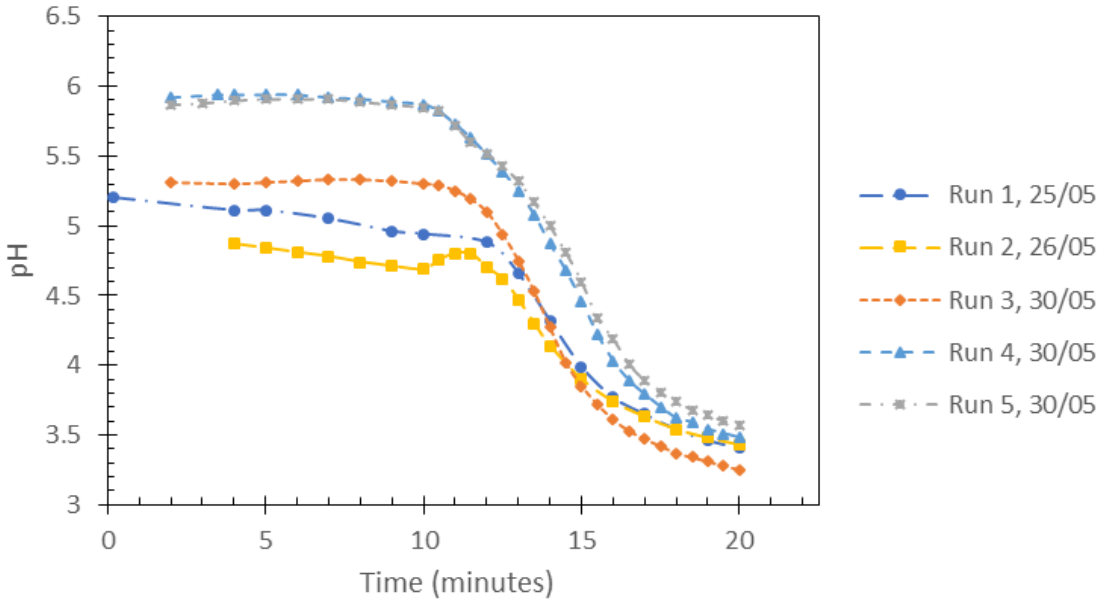

Figure 4-15: Acidification power test: pH versus time presented at 1 minute time intervals over 20 minutes for the repeatability experiments

4.1.4 Summary of key findings

The repeatability experiments show that the microcalorimeter is functioning correctly and that there is a negligible difference in the results yielded by the different channels of the TAMIII. Further, consistent yeast growth and metabolism was observed, with the expected dependence on inoculum size.

The method developed for preliminary data analysis, followed by analysis to determine the specific growth rate and associated parameters determined from fitting of Equation 4-3 to the data is highly reproducible. The procedure primarily involves a baseline correction, determining the region to fit the data and then minimising the sum of square errors between the data and the predicted values of Equation 4-3. The region of fit was chosen to be between 10% and 70% of the maximum heat flow value through correlation to the exponential region of growth for the control culture.

The normalisation of parameters to that of healthy yeast inoculated at 10^4 cells/ml was illustrated to be valuable when making comparisons. The normalised '*A'* and the t_{max} values were shown to be good predictors of initial cell population size, and thus were used in the examination of further results. The normalised '*B'* values were found to have no correlation to the initial cell population size thus they were not used in any further analyses. The t_{50} values did not predict the initial cell population size as well as t_{max}, therefore the t_{50} were also not used in any further analyses. The specific growth rate of healthy yeast across all inoculum concentrations was found to be very reproducible at 0.371 ± 0.009 h^{-1}.

The acidification power test, as adapted, was repeatable in terms of the determination of the respective cell vitalities.

4.2 Method validation across varied metabolic activity using heat killing experiments

The heat killing experiments serve to validate the response of the above developed method (Section 4.1) to both cell number and metabolic activity to ensure applicability to yeast stress experiments. Further, these test the repeatability of the APT and the cell staining. In the heat killing experiments, healthy cells were mixed with heat-killed cells in varying proportions. The expectation was that the dead cells would have little to no effect on the performance of the healthy cells.

4.2.1 Growth thermograms

Figure 4-16 to Figure 4-19 show the thermograms obtained from the heat killing experiments. The heat-killed cells were observed to have little to no effect on the calorimetric signal, as shown by the completely heat-killed populations giving off negligible heat when compared to that of the YPD blank. Figure 4-18 and Figure 4-19 confirm that diluting healthy cells with YPD or with heat-killed cells (suspended in YPD) makes a negligible difference to the overall heat flow.

Figure 4-16 to Figure 4-19 essentially show that only healthy living cells impact on the calorimetric signal. Dead cells do not generate any heat and are thus not detected by the microcalorimeter.

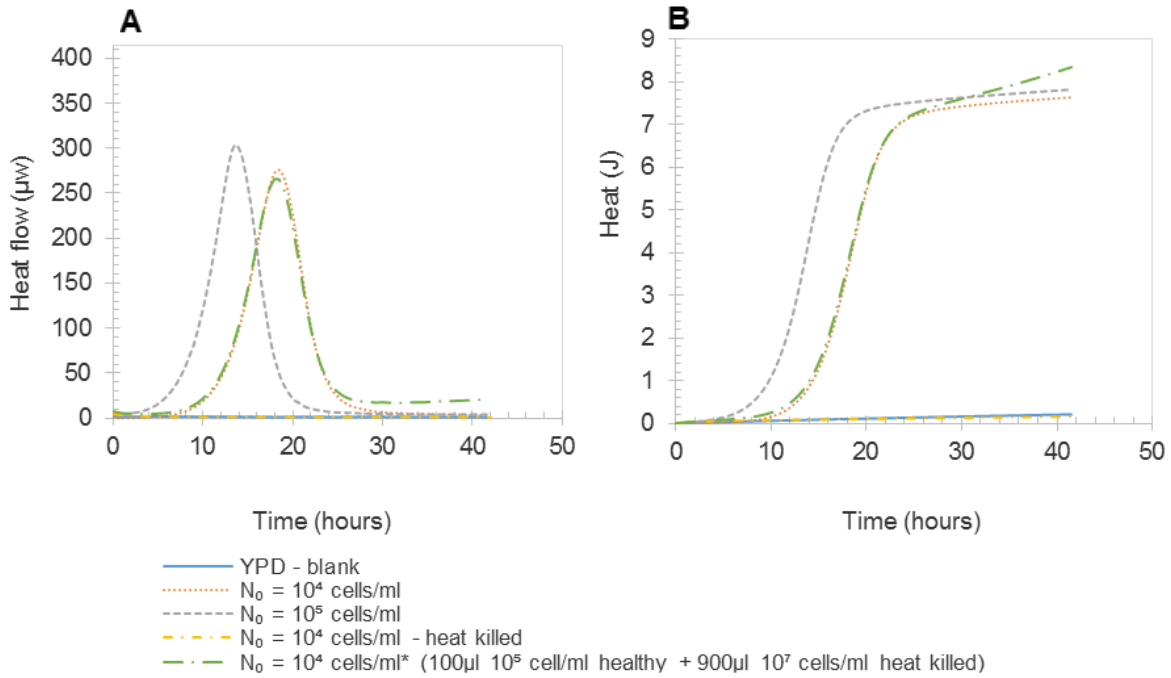

Figure 4-16: Heat flow (A) and heat curves (B) for experiment 02/06/2015, investigating the effects of using mixed populations of healthy cells and heat-killed cells. * indicates the effective inoculum size when only considering the healthy cell population.

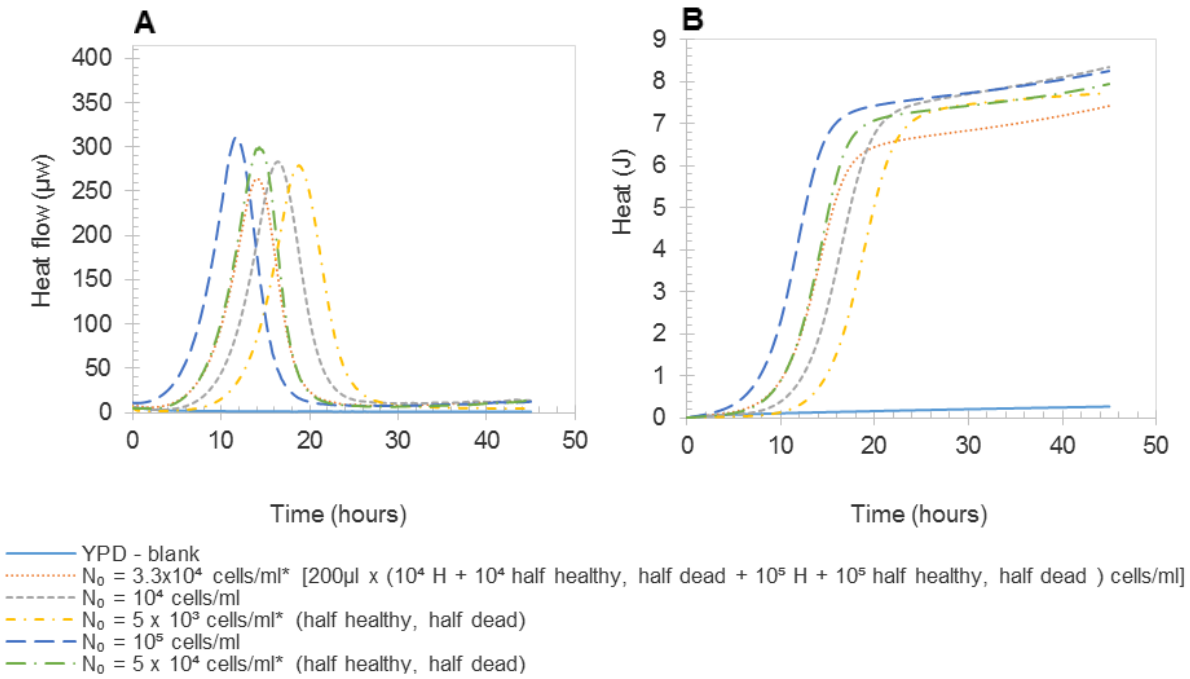

Figure 4-17: Heat flow (A) and heat curves (B) for experiment 04/06/2015, investigating the effects of using mixed populations of healthy cells and heat-killed cells. * indicates the effective inoculum size when only considering the healthy cell population

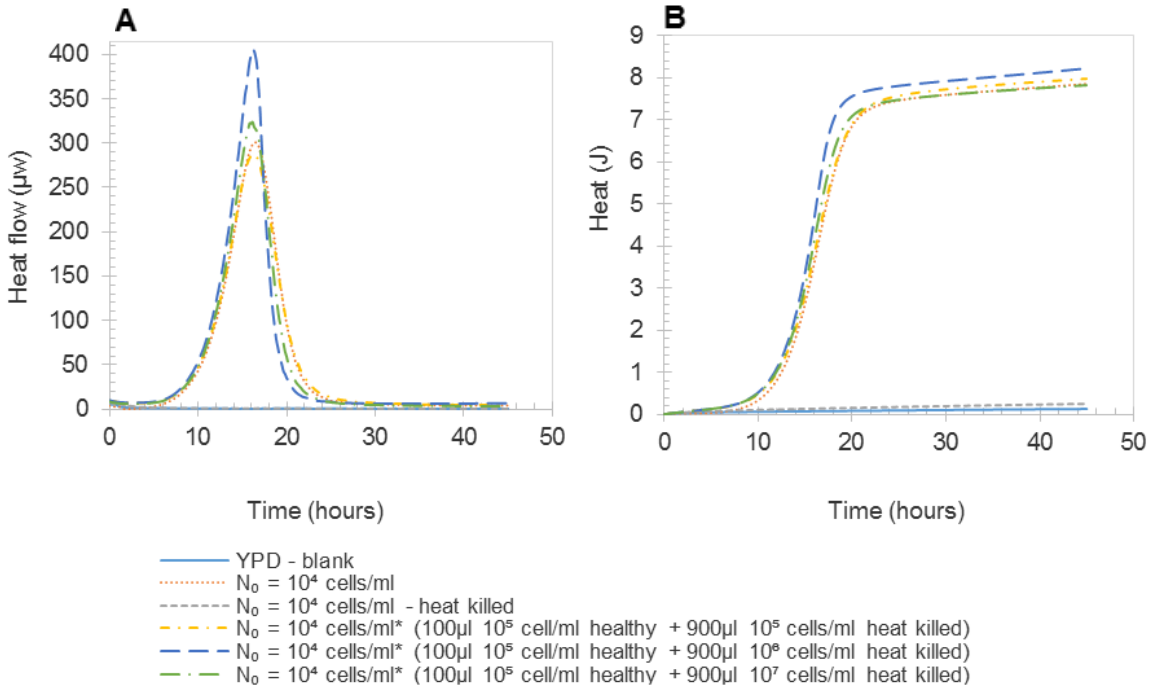

Figure 4-18: Heat flow (A) and heat curves (B) for experiment 07/06/2015, investigating the effects of using mixed populations of healthy cells and heat-killed cells. * indicates the effective inoculum size when only considering the healthy cell population

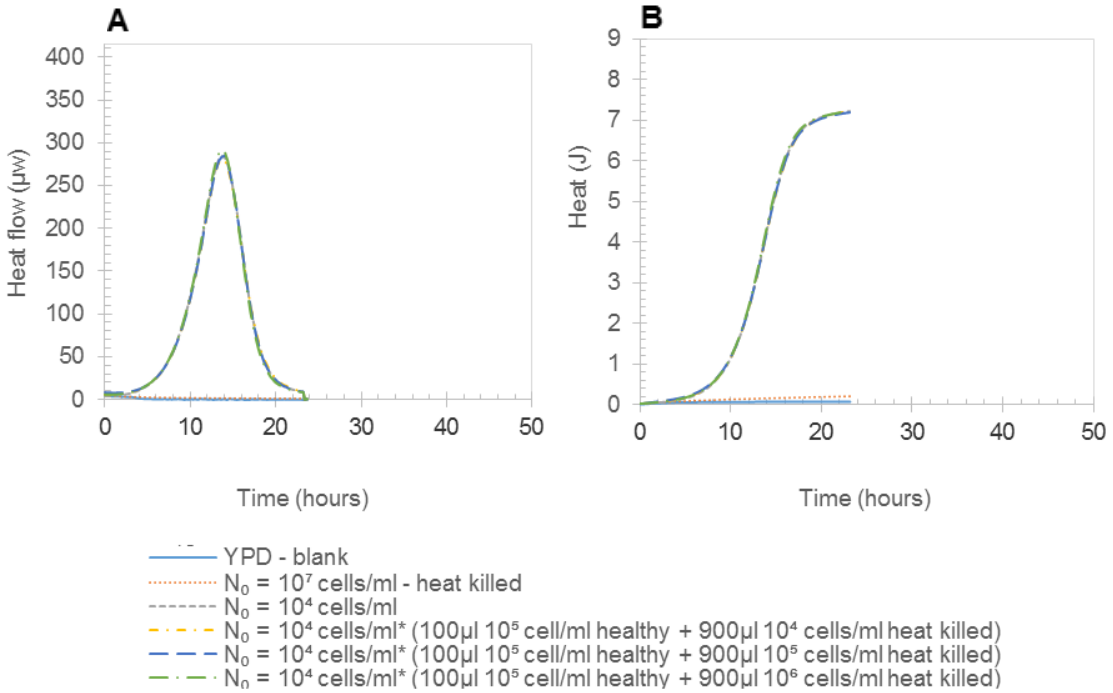

Figure 4-19: Heat flow (A) and heat curves (B) for experiment 23/06/2015, investigating the effects of using mixed populations of healthy cells and heat-killed cells. * indicates the effective inoculum size when only considering the healthy cell population

4.2.2 Quantitative analysis of thermograms

Analysing the results quantitatively (Equation 4-3), the values of the absolute value of the fitting parameters are given in Table 4-3 below and the normalised values are given in Table 4-4. The entirely heat-killed populations, where no growth was observed, do not appear in Table 4-3 and Table 4-4.

Table 4-3: Calculated parameters for all heat killing experiments

Date of experiment	$N_{0\_healthy}$ (cells/ml)	N_{0_total}	R^2	μ (hr^{-1})	A (J)	t_{max} (hr)
02/06/2015	10^4	10^4	0.99992	0.369	0.01	18.4
	10^5	10^5	0.99995	0.374	0.03	13.7
	* 10^4	$9x10^6$	0.99993	0.369	0.01	18.2
04/06/2015	* $3.3x10^4$	10^5	0.99994	0.375	0.02	14.3
	10^4	10^4	0.99992	0.373	0.01	16.6
	* $5x10^3$	10^4	0.99992	0.369	0.00	19.0
	10^5	10^5	0.99994	0.374	0.05	11.9
	* $5x10^4$	10^5	0.99992	0.374	0.02	14.4
07/06/2015	10^4	10^4	0.99993	0.374	0.01	16.6
	* 10^4	10^5	0.99994	0.369	0.01	16.4
	* 10^4	$9.1x10^5$	0.99995	0.376	0.01	16.3
	* 10^4	$9.01x10^6$	0.99994	0.377	0.01	16.3
23/06/2015	10^4	10^4	0.99994	0.364	0.03	13.7
	* 10^4	$1.9x10^4$	0.99994	0.365	0.03	13.8
	* 10^4	10^5	0.99994	0.363	0.03	14.1
	* 10^4	$9.1x10^5$	0.99995	0.368	0.03	13.8
Average			**0.99994**	**0.371**		
Standard deviation			**0.00001**	**0.004**		

*indicates the pseudo population size – the size of the inoculum if only the healthy cells are considered

Table 4-3 shows that the specific growth rate is unaffected by the presence of the heat-killed cells. As with the results from the repeatability experiments, the specific growth rate can be determined with a high degree of repeatability.

In order to test the relationship established between A_i/A_m and N_0 in Figure 4-10; the values of A_i/A_m in Table 4-4 were compared to those predicted by using the equation of the line appearing in Figure 4-10. It was found that the correlation coefficient of the actual N_{0_total} to the predicted value using the equation was -0.17, indicating that there is no correlation between the two values. However, the correlation coefficient of the N_0 predicted using the equation to the N_0 of only the healthy cells ($N_{0\_healthy}$) is 0.98 – indicating a very high degree of correlation. This further confirms that the value of 'A' is linked to the size of the inoculum (healthy cells) used. These results confirm that only the healthy cells, not heat-killed cells, contribute to the growth thermogram.

Table 4-4: Calculated normalized parameters for equation fits of all heat killing experiments

Date of experiment	$N_{0\_healthy}$ (cells/ml)	N_{0_total}	μ_i/μ_m	A_i/A_m	$t_{max,i}/t_{max,m}$
02/06/2015	10^4	10^4	1.000	1.00	1.00
	10^5	10^5	1.013	5.04	0.75
	* 10^4	$9x10^6$	1.001	1.01	0.99
04/06/2015	* $3.3x10^4$	10^5	1.006	2.03	0.86
	10^4	10^4	1.000	1.00	1.00
	* $5x10^3$	10^4	0.991	0.43	1.14
	* 10^5	10^5	1.003	5.43	0.72
	* $5x10^4$	10^5	1.004	2.16	0.87
07/06/2015	10^4	10^4	1.000	1.00	1.00
	* 10^4	10^5	0.985	1.13	0.99
	* 10^4	$9.1x10^5$	1.004	1.19	0.98
	* 10^4	$9.01x10^6$	1.008	1.06	0.98
23/06/2015	10^4	10^4	1.000	1.00	1.00
	* 10^4	$1.9x10^4$	1.000	0.98	1.01
	* 10^4	10^5	0.996	1.00	1.03
	* 10^4	$9.1x10^5$	1.008	0.97	1.01
Average			**1.002**		
Standard deviation			**0.002**		

*indicates the pseudo population size – the size of the inoculum if only the healthy cells are considered

4.2.3 Yeast quality indicators

Vitality results: APT

The APT was run at least twice for the healthy cells of each experiment. In some cases the APT was not completed for the heat-killed cells as there was not enough heat-killed yeast to run the test. An APT was also run once for a mixed population of heat-killed cells and healthy cells. The APT raw data can be found in Appendix D. Table 4-5 shows the APT of the healthy cells to have a standard deviation of less than 2% of the absolute value, indicating a good degree of repeatability. The results of the APT are shown in Table 4-5. The normalised APT was calculated for each experiment by dividing any given APT value by the average APT value of the healthy cells tested for that set of experiments.

Table 4-5: Average APT results of heat killing experiments

	Healthy cells		**Half heat-killed, half healthy (50:50 ratio)**		**Heat-killed**	
	Absolute	Normalised	Absolute	Normalised	Absolute	Normalised
Average APT	2.97	1.00	1.81	0.60	-0.78	-0.26
Standard deviation	0.05	0	-	-	0.06	0.02

According to Gabriel et al. (2008), an APT value above 2.4 indicates “highly active yeast with good fermentation potential”. The average APT value for the ‘healthy’ yeast of 2.96 confirms their active state. The APT of the mixed population of healthy and heat-killed cells, although only performed once, shows a much lower APT, 60% that of the healthy cells, most likely due to a non-linear relationship between healthy cell mass and the final APT value. The APT of the heat-killed cells was found to be negative, indicating that the dead yeast raised the pH of the supernatant. Heat killing of the cells caused cell lysis, with the basic intracellular fluids causing the pH to rise. According to Gabriel et al. (2008), an APT value of less than 1.8 denotes “low metabolic competence”.

The optimised APT method of Gabriel et al. (2008) had an average error of determination of 2%. In comparison to previous work and given the significant number of biological repeats and the low standard deviation, the modified APT procedure used in this work has a suitable repeatability.

Viability results

Both methylene violet staining and colony forming unit counts were used to measure viability. Figure 4-20 compares the viability results.

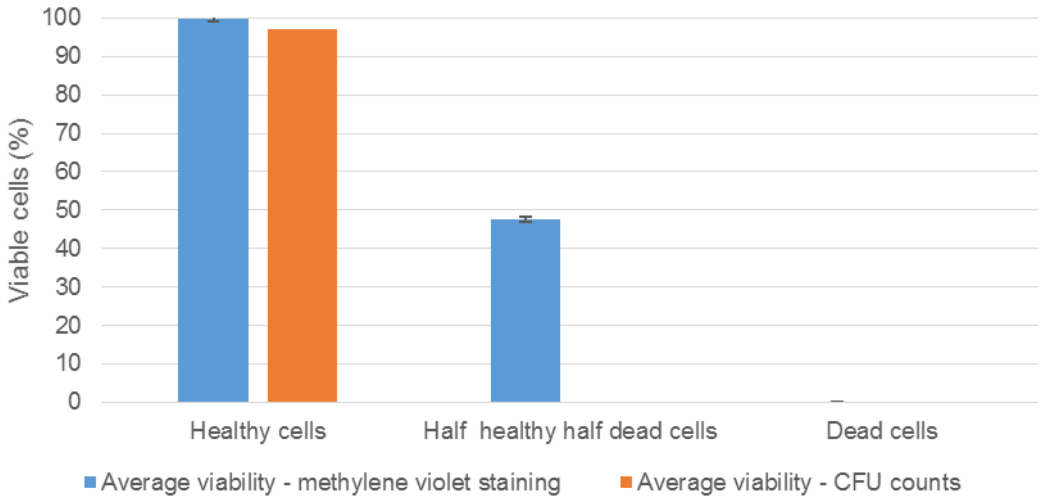

Figure 4-20: Viability test results in terms of methylene violet staining and CFU counts. Error bars represent one standard deviation from the mean.
Only a single CFU count was performed in this set of experiments - therefore no standard deviation could be calculated. The viability of the mixed population of healthy and heat-killed cells was also only determined using the methylene violet stain for a single experiment (with two technical repeats).

The viability of the healthy cells determined using the methylene violet stain can be seen to be very high (>99%), with essentially all the cells being classified as viable. This value was slightly lower at 98% in terms of CFUs. For a 50:50 ratio of healthy to heat-killed cells, the viability determined using the methylene violet stain decreased to roughly 50%, as expected. CFU counts were not performed for the 50:50 ratio of healthy to heat-killed cells.

The viability of the heat-killed cells in all cases, using both CFU counts and the methylene violet stain was zero. This verifies that the heat killing procedure worked effectively to kill all the cells present. The presence of no colony forming units is especially promising as this technique has a theoretical detection limit of a single cell.

4.2.4 Summary and discussion of key findings

The heat killing results confirmed the high repeatability associated with the determination of the specific growth rate. The heat killing experiments showed that it is not the total number of initial cells that affect the growth thermogram, only the number of metabolically active cells i.e. dead cells do not contribute.

The APT was highly reproducible for the healthy cells, validating the modifications made to the APT developed by Gabriel et al. (2008). The heat killing of the cells was effective; heat-killed cell populations produced essentially no heat. The absence of any viable cells in the heat-killed populations was further verified by the viability assays which both confirmed zero percent viability.

5 Stress test results and discussion

In this chapter, results are presented on the effect of subjecting the yeast to cold shock, ethanol shock and a combination of the two stresses. These are explored using microcalorimetry, the vitality assay APT and cell viability in terms of CFUs and methylene violet staining. While the results are analysed as they are presented, overarching conclusions and recommendations are presented in Chapter 6. The raw data for all the experiments can be found in the attached data file (Appendix – Data). In all cases, statistical comparisons made were done at the 95% confidence level – $P < 0.05$ to indicate a statistically significant difference.

As in Chapter 4, each experiment is referred to by the date it was initiated so that all the results, graphs and raw data can easily be cross-referenced. In some cases, certain data sets within experimental runs have been discarded; details of the discarded data along with the reason for discarding the data can be found in Appendix B.1.

5.1 Cold shock results

The cold shock experiments consisted of two types of cold shock; a slow cold shock (overall average of 0.13 ºC/min) and a rapid cold shock (18 ºC/minute). The colds shocks were performed in order to assess the response of yeast viability and vitality to the different rates of cooling due to their industrial relevance (Section 2.1.4).

5.1.1 Slow cold shock

As specified in specified in Section 3.5.3, in the slow cold shock experiments the temperature was gradually reduced from room temperature to 4 °C over a period of 2 hours.

Growth thermograms and temperature profiles

The temperature decline profile on placing the yeast into the cold bath until its removal is shown in Figure 5-1. The temperature declined with a hyperbolic trend. On average, there is approximately a 0.3 °C/min temperature decline for the first 40 minutes. In the last 80 minutes there is approximately a 0.05 °C/min temperature decline.

Apart from the experiment that took place on 02-07-2015, which showed a slightly more rapid temperature decline, there is no significant observable difference between the temperature profiles. This more rapid decline (0.34 °C/min temperature decline for the first 40 minutes) did not affect the thermogram (Figure 5-4) significantly.

In Figure 5-2 to Figure 5-5, the thermograms obtained in the slow cold shock experiments are presented. A visual inspection of the thermograms suggests that there is no difference in the performance between the healthy cells and those that were slowly cold shocked. Figure 5-2 is the only case where a slight difference is observable between the healthy cells and the cold shocked cells. Quantitative analysis is presented in Section 5.1.1 – Quantitative analysis of thermograms.

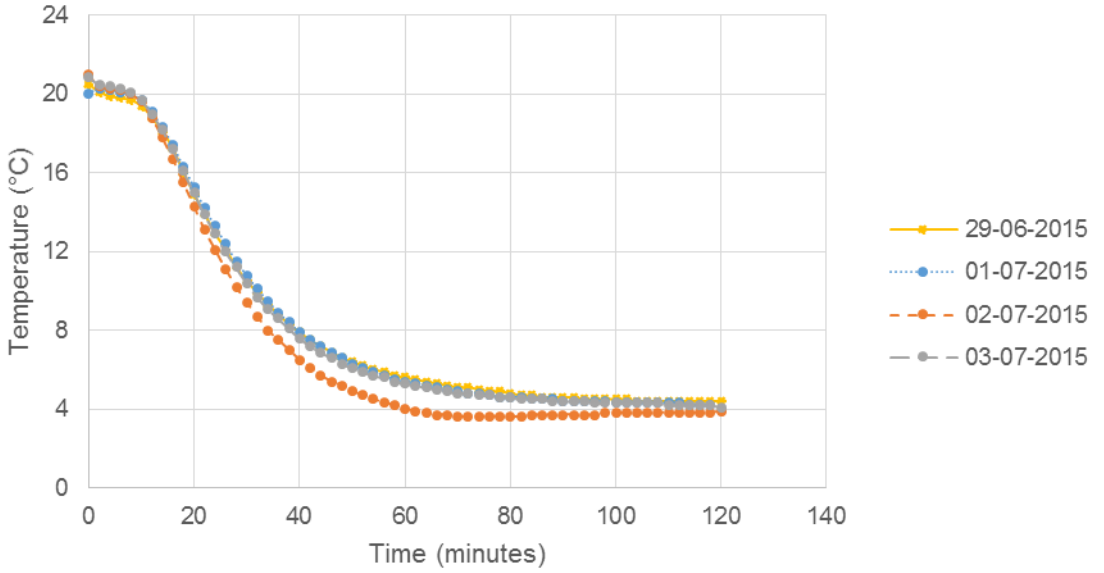

Figure 5-1: Temperature decline profile logged for each of the slow cold shock experiments

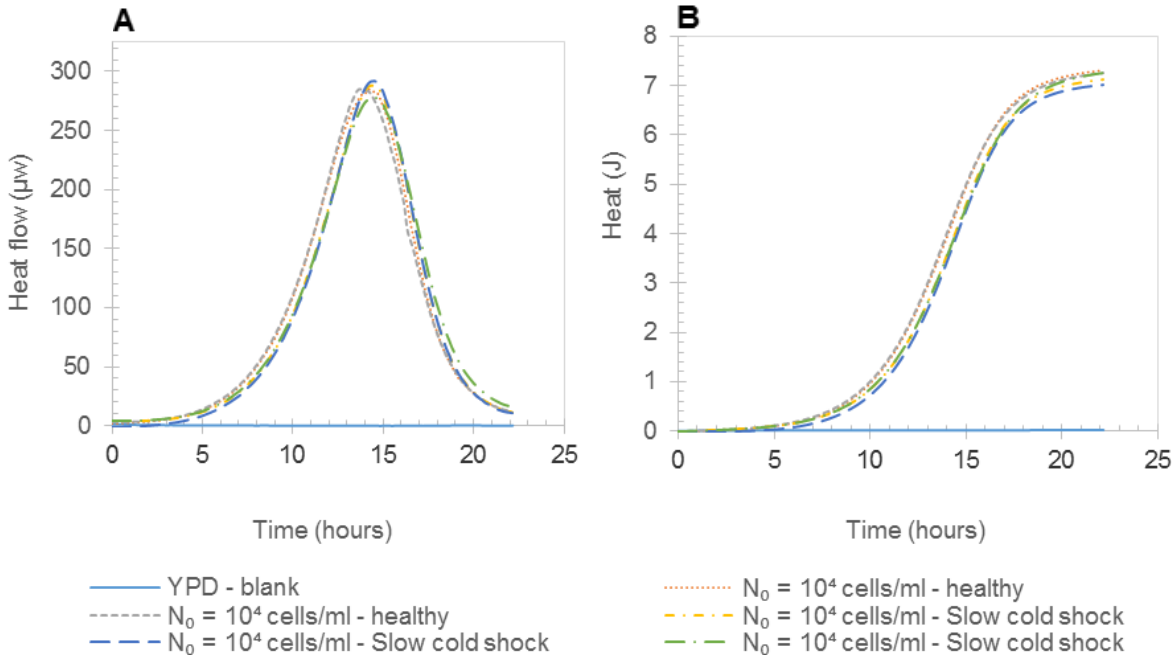

Figure 5-2: Heat flow (A) and heat curves (B) for experiment 29/06/2015, investigating the effects of a slow cold shock on a healthy cell population.

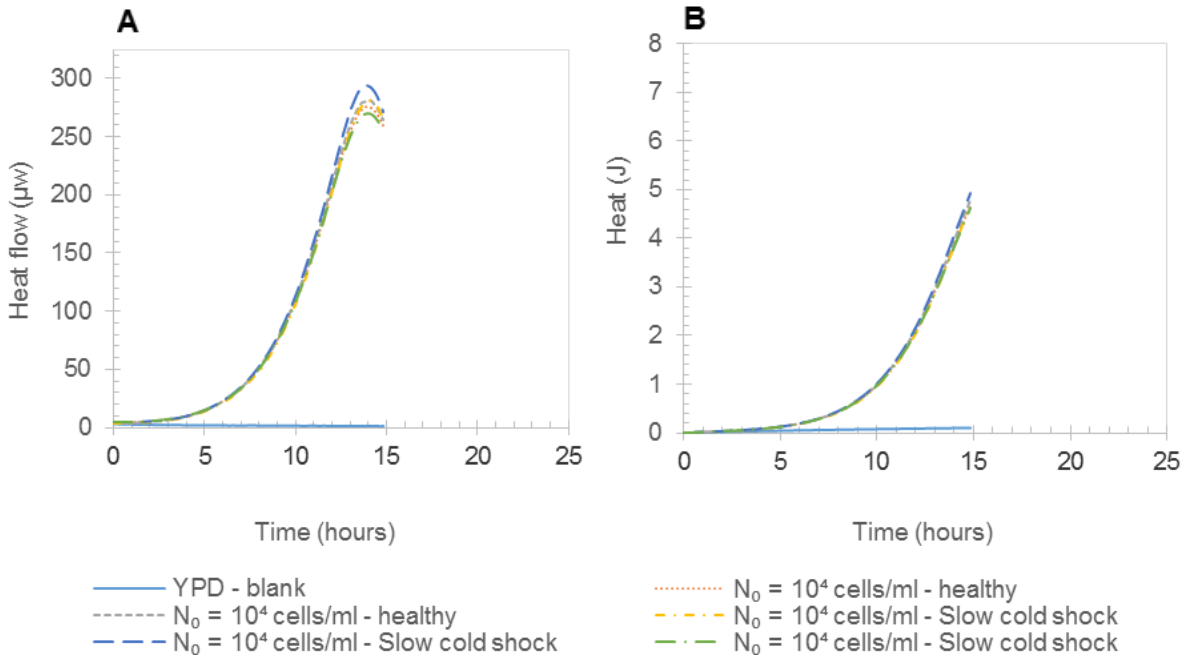

Figure 5-3: Heat flow (A) and heat curves (B) for experiment 01/07/2015, investigating the effects of a slow cold shock on a healthy cell population.

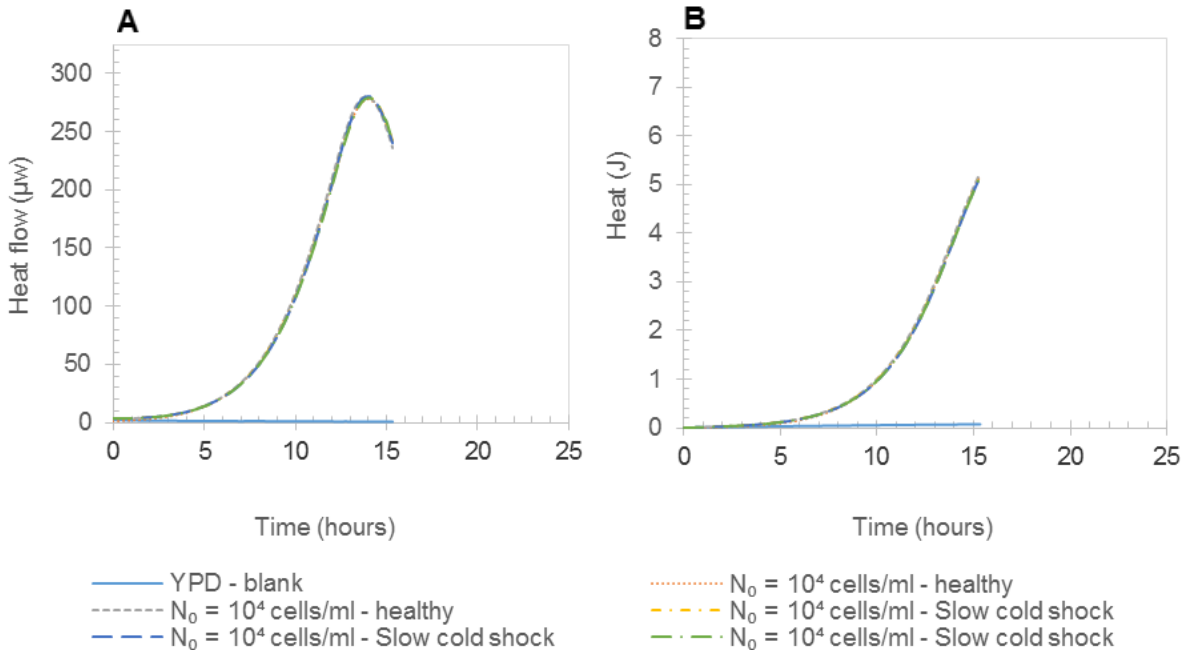

Figure 5-4: Heat flow (A) and heat curves (B) for experiment 02/07/2015, investigating the effects of a slow cold shock on a healthy cell population.

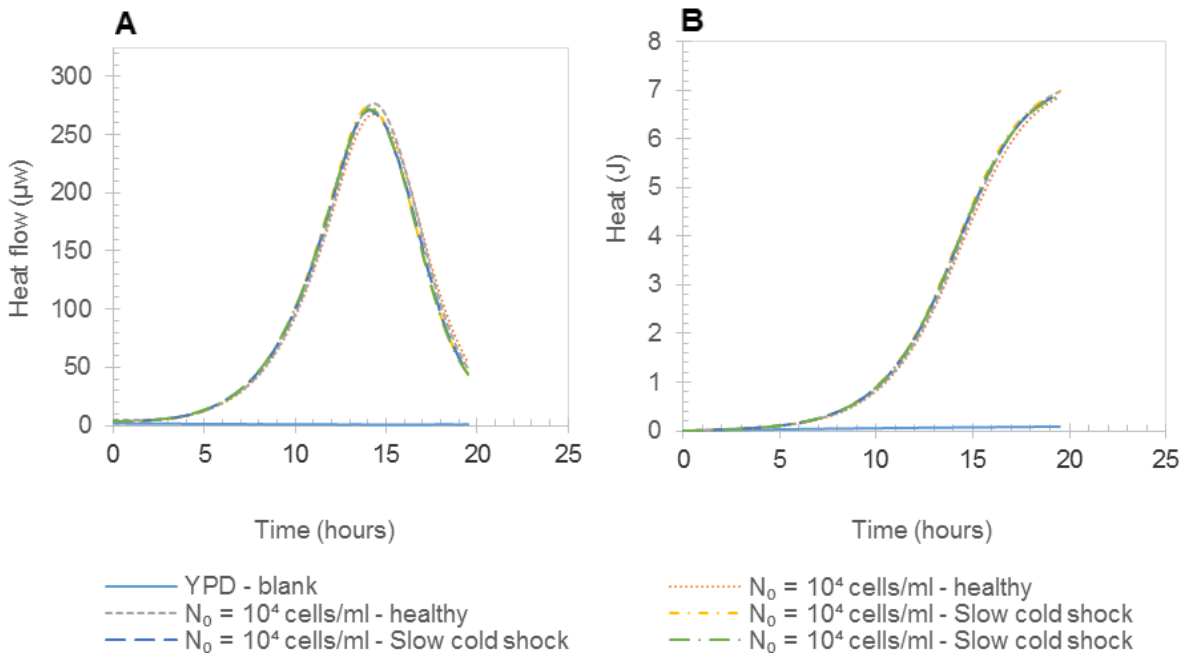

Figure 5-5: Heat flow (A) and heat curves (B) for experiment 03/07/2015, investigating the effects of a slow cold shock on a healthy cell population.

Quantitative analysis of thermograms

The quantitative analysis of the slow cold shock experiments in terms of absolute and normalised fitting parameters for Equation 4-3 are given in Appendix C.1. The equation fits to determine the specific growth rate and 'A' values, correlated well to the data (all R^2 >0.99992). Table 5-1 provides a comparison of the average normalised values determined for the slow cold-shocked cells and the healthy cells. The values of unity suggest no influence of cold shock. A statistical t-test was applied to the data. All p-values given in Table 5-1 are greater than 0.05, confirming no significant difference between the slow-cold shocked cells and the healthy cells. This supports the visual assessment of Figure 5-2 to Figure 5-5.

Table 5-1: Comparison between the average values of the normalized parameters determined for the healthy cells and slow cold shocked cells.

Parameter	Average for healthy cells		Average for slow cold shocked cells		P value: t-Test comparing healthy cells to slow cold shocked cells*
	Value	Standard deviation	Value	Standard deviation	
μ_i/μ_m	1.00	0.00	1.00	0.01	0.79
$t_{max,i}/t_{max,m}$	1.00	0.00	1.00	0.02	0.61
A_i/A_m	1.00	0.00	0.98	0.11	0.68

*Two-tailed test assuming unequal variances; df = 3 in all cases

Yeast quality indicators

Vitality results: APT

The results of the APT tests performed as well as a statistical comparison between the healthy cells and slow cold shocked cells appear in Table 5-2. The APT raw data can be found in Appendix D. The results in Table 5-2 show there to be a significant difference (P value < 0.05) between the APT of the healthy cells and the slow cold shocked cells. The lower APT values produced by the slow cold shocked cells indicates that they have a slightly lower vitality than the healthy cells.

Table 5-2: Acidification power test results comparing slow cold shocked to healthy cell performance

	Healthy cells		**Slow cold shocked cells**		**P value: t-Test comparing healthy cells to slow cold shocked cells***	
	Absolute	**Normalised**	**Absolute**	**Normalised**	**Absolute**	**Normalised**
Average APT	3.17	1	3.04	0.97	0.03	0.02
Standard deviation	0.03	0	0.09	0.01		

*Two-tailed test assuming unequal variances

Viability results

Table 5-3 presents methylene violet and plate count viability measures. The viability of the cells determined using methylene violet staining gave higher results than the CFU counts. This is due to the differing bias of viability measurement: intact cell membrane and transport systems versus the ability to reproduce. Large experimental error is typical of CFU counts, allowing only large differences to be seen.

Table 5-3: Viability test results from methylene violet and CFU counts for the slow cold shock experiments

		Healthy cells	**Slow cold shocked cells**	**P value: t-Test comparing healthy cells to slow cold shocked cells***
Methylene violet staining	Viability (%)	100.0	98.5	0.4
	Standard deviation	0.0	2.9	
CFU counts	Viability (%)	72	77	0.8
	Standard deviation	22	30	

*Two-tailed test assuming unequal variances

There is no significant difference between the viability of the slow cold-shocked cells and the healthy cells (P > 0.05 for both the methylene violet stain and the CFU counts). The large standard deviation of the CFU counts is representative of the lack of a high degree of repeatability of this assay. The lack of an effect of a slow cold shock on viability is confirmed by numerous other studies, e.g. Kgari (2008), Fargher & Smith (1995) and Fernández, González & Sierra (1991) (see Section 2.1.4 – Cold stress).

5.1.2 Rapid cold shock

As specified in Section 3.5.3, the rapid cold shock was achieved by rapid resuspension of yeast initially at room temperature in 4 °C YPD, followed by holding at this temperature for a further 2 hours. The rate of the rapid cold shock was approximately 18 °C/minute as yeast at room temperature (~22 °C) was diluted using pre-chilled YPD and then placed in a cold bath at 4 °C, with the whole process taking less than one minute. The cold bath was maintained at 4 °C for the duration of the two-hour holding period.

Growth thermograms

Figure 5-6 to Figure 5-9 show the thermograms obtained in the rapid cold shock experiments. In each, the healthy cell curves appear to enter the exponential phase sooner than the rapidly cold shocked cells. The healthy cells in all cases also reach the maximum heat flow 40 ± 12 minutes before the rapidly cold shocked cells.

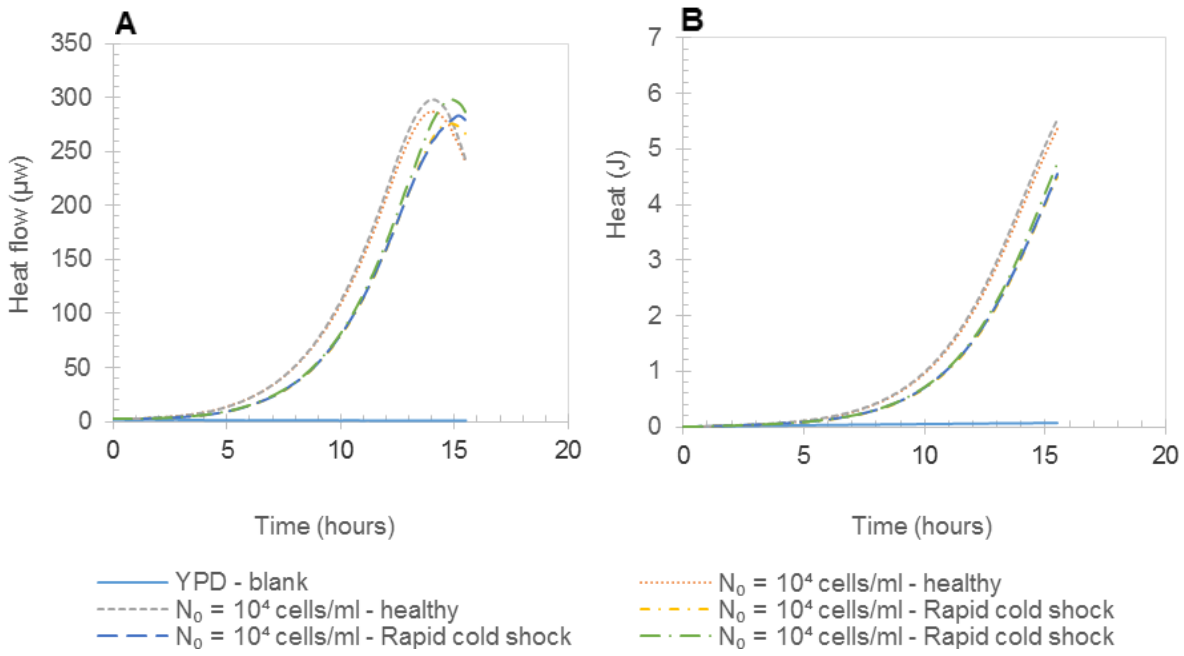

Figure 5-6: Heat flow (A) and heat curves (B) for experiment 05/07/2015, investigating the effects of a rapid cold shock on a healthy cell population.

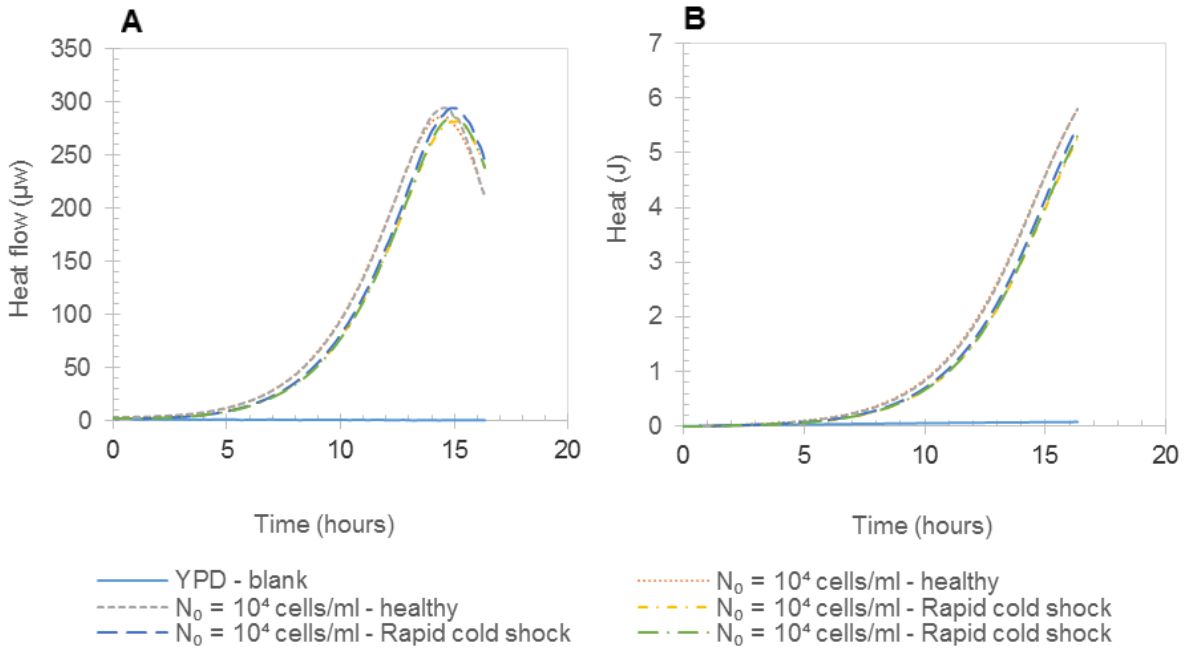

Figure 5-7: Heat flow (A) and heat curves (B) for experiment 07/07/2015, investigating the effects of a rapid cold shock on a healthy cell population.

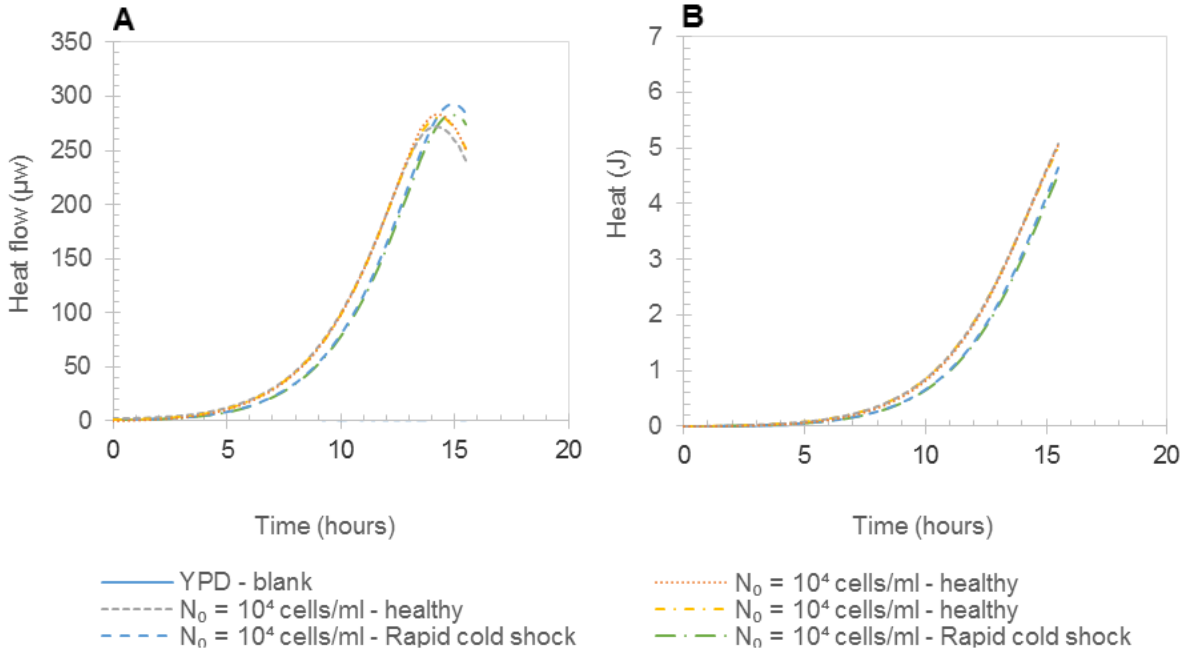

Figure 5-8: Heat flow (A) and heat curves (B) for experiment 08/07/2015, investigating the effects of a rapid cold shock on a healthy cell population.

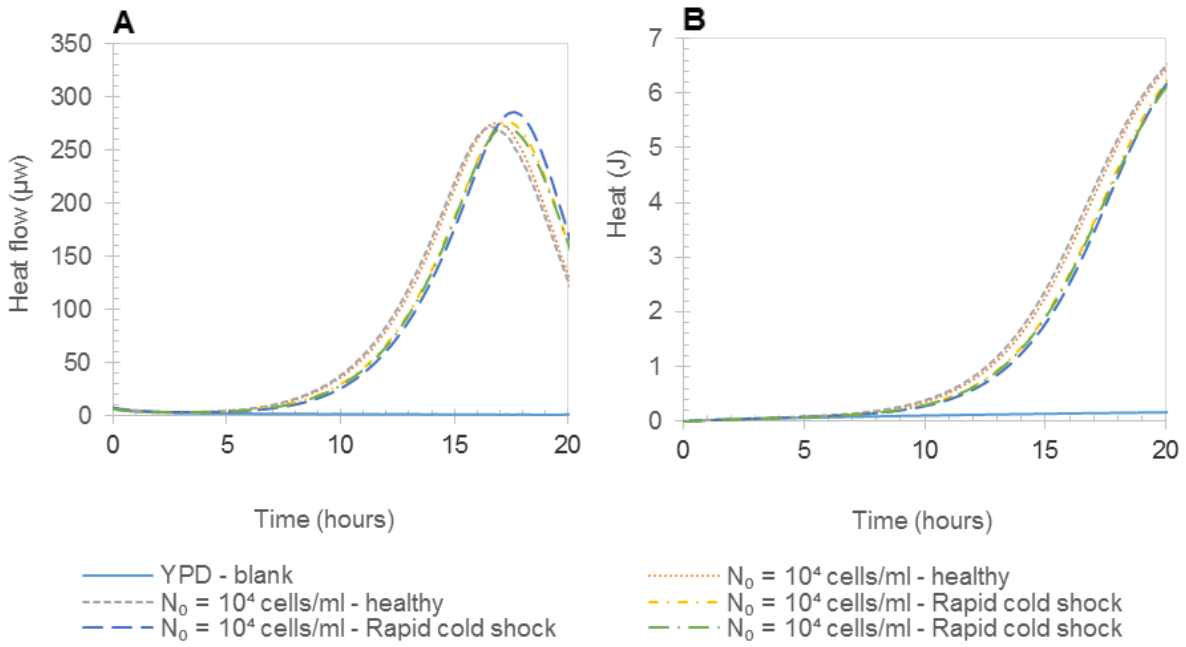

Figure 5-9: Heat flow (A) and heat curves (B) for experiment 09/07/2015, investigating the effects of a rapid cold shock on a healthy cell population.

Quantitative analysis of thermograms

Analysing the results quantitatively, the absolute and normalised values of the fitting parameters are given in Appendix C.1. The fitting parameters for Equation 4-3, to determine the specific growth rate and 'A' values, were highly correlated to the data – as seen by the R^2 values (R^2 >0.99992), in Appendix C.1. Table 5-4 provides a comparison of the average values determined for the rapid cold shocked cells and the healthy cells.

Table 5-4: Comparison between the average values of the normalized parameters determined for the healthy cells and rapid cold shocked cells.

Parameter	Average for healthy cells		Average for rapid cold shocked cells		P value: t-Test comparing healthy cells and rapid cold shocked cells*
	Value	Standard deviation	Value	Standard deviation	
μ_i/μ_m	1.00	0.00	1.00	0.002	0.100
$t_{max,i}/t_{max,m}$	1.00	0.00	1.04	0.02	0.005
A_i/A_m	1.00	0.00	0.83	0.070	0.001

* Two-tailed test assuming unequal variances

The data in Table 5-4 confirms that there is no significant difference (P > 0.05) between the specific growth rates of the healthy cells and the growth rates of cells exposed to rapid cold shock. There is however a significant difference (P < 0.05) between the t_{max} values and the *A* values of the healthy and rapid cold shock cells. This confirms the visual observation in Figure 5-6 to Figure 5-9. There is a more significant difference observed in the normalised *A* values (P = 0.001) as compared to the normalised t_{max} values (P = 0.005).

In Section 4.1 and Section 4.2, the *A* value was used to distinguish between different inoculum sizes. In this case, the inoculum sizes are the same. In this case, the difference in the *A* values for the healthy cells and rapid cold shocked cells suggests that *A* also contains a term relating to the population vitality. Examining Equation 4-4, the variables that make up the *A* value consist of the specific growth rate (μ), the inoculum size (N_0), the heat output per cell in the exponential phase (q_1) and the lag time (τ). From Table 5-5 and Table 5-6, it is known that the inoculum size and specific growth rate were constant for this experiment. The specific heat output of the cells in the exponential phase is also a constant, as indicated by the constant specific growth rate. Thus the only parameter that makes up the *A* value that could be effected is the lag time (τ). This implies that the rapid cold shock causes the cells to experience a longer lag time as compared to the healthy cells. It is expected that this lag time is required for adaptation to or recovery from the stress effect. However, it should be noted that without additional viability tests it is not possible to deduce from IMC data whether a change in A is due to a change in initial viable cell numbers, or lag time if specific growth rate (vitality) remains constant.

Yeast quality indicators

Vitality results: APT

The results of the APT tests performed as well as a statistical comparison between the healthy cells and rapid cold shocked cells appear in Table 5-5. These show there to be a significant difference ($P < 0.05$) between the APT of the healthy cells and the rapid cold shocked cells. The lower APT values produced by the rapid cold shocked cells indicate that they have a slightly lower vitality than the healthy cells. The APT raw data can be found in Appendix D.

Table 5-5: Acidification power test results comparing rapid shocked to healthy cell performance

	Healthy cells		**Rapid cold shocked cells**		**P value: t-Test comparing healthy cells and slow cold shocked cells***	
	Absolute	Normalised	Absolute	Normalised	Absolute	Normalised
Average APT	3.05	1.00	2.95	0.97	0.07	0.003
Standard deviation	0.12	0.00	0.10	0.02		

*Two-tailed test assuming unequal variances

Viability results

Table 5-6, like Table 5-3, shows that the methylene violet viabilities are close to 100% and the viabilities determined using CFU counts are less than 100%, but have a larger degree of uncertainty. In the case of the methylene violet stain, the initial viabilities are identical to one another. The CFU viabilities are also very similar. The similar viabilities rule out differences in initial population viability being the cause of any differences observed in the growth thermograms. The viable cell values show that the viabilities of the healthy cells and the rapid cold shock cells are in line with the viabilities determined in the other experiments.

There is no significant difference between the viability of the rapid cold shock cells and the healthy cells (P > 0.05 for both the methylene violet stain and the CFU counts). This lack of an effect of a cold shock on cell viability is consistent with numerous studies e.g. Kgari (2008), Fargher & Smith (1995) and Fernández, González & Sierra (1991) (see Section 2.1.4 - Cold stress).

Table 5-6: Viability test results from methylene violet and CFU counts for the rapid cold shock experiments

		Healthy cells	**Rapid cold shocked cells**	**P value: t-Test comparing healthy cells and rapid cold shocked cells***
Average viability - methylene violet staining	Viability (%)	99.1	99.0	0.7
	standard deviation	1.3	1.3	
Average viability - CFU counts	Viability (%)	61	69	0.3
	standard deviation	16	25	

*Two-tailed test assuming unequal variances

5.1.3 Summary and discussion of key findings of both the slow and rapid cold shocks

The slow cold shock showed a significant effect on the yeast vitality as determined by the APT. In contrast, there was no calculable or visual difference in the IMC data findings between the healthy cells and the slow cold shock cells. To understand this, the essence of each measurement must be considered. The APT detects a difference in cell vitality by measuring the ability of the yeast to maintain gradients across its membrane and thereby impact the cell environment. This is assessed directly following the stress exposure i.e. by measuring the vitality of the cells soon after they have been shocked (2.5 - 4 hours). In contrast, the IMC data is collected over a much longer timeframe (12-24 hours), thereby enabling time for dilution or reversal of the effects of a transient slow cold shock on the cells. Furthermore, the gradual cooling of the cell most likely allowed the cell to respond and prepare appropriately, resulting in faster recovery times. Therefore, by the time the cells were loaded into the TAMIII (>5 hours) they may have recovered to a degree There was no significant effect of the slow cold shock on yeast viability as measured using CFU counts and methylene violet staining. This is in accordance with prior reports of Nkosi (2001).

There was a significant calorimetrically observable effect of the rapid cold shock on the cells. The impact of the rapid cold shock was observed both through visual inspection of the growth thermograms and through quantitative analysis of the curve fitting parameters. The effect of the rapid cold shock manifests itself in the t_{max} value and the *A* value. Given the nature of the constants that make up the *A* value, and given that the methylene violet staining and CFU counts indicated no loss in viability, it is most probable that the rapid cold shock results in a longer lag time. This would account for the longer t_{max} values and the lower normalised *A* value, as compared to the healthy cells – indicating that the effects of the rapid cold shock are longer lasting than the slow cold shock and are therefore detectable using the IMC. The APT also confirmed a significantly lower average APT value of the rapid cold shock cells as compared to the healthy cells, indicating a decrease in vitality following the rapid cold shock.

Given the findings of Section 2.1.4 (Cold stress), it is expected that the rapid cold shock had an observable effect on yeast quality. The results are in agreement with Kgari (2008) who found that rapidly cooled yeast (by dilution) had higher HSP-12 expression, 200% increase in protease absorbance, lower CO_2 evolution in small scale fermentation and increased cell wall damage as compared to slow cooled yeast. Fernández et al. (1991) also found that cold shocking yeast has more significant impacts on cell vitality than cell viability.

5.2 Ethanol shock

The effect of ethanol stress was evaluated in two ways: through exposure to ethanol during the growth phase and through a sudden, short-term ethanol exposure. The ethanol shock experiments were primarily designed to test the response of yeast viability and vitality to a transient ethanol stress due to its industrial relevance (Section 2.1.4). In these experiments yeast was exposed to 4% and 8% ethanol concentrations (by volume) for a period of time after which the ethanol was 'removed' by serial dilution. The exposure time to the ethanol was one hour. The constant ethanol exposure experiments were executed by adding ethanol to healthy cells just prior to calorimetric testing, ensuring that the cells were exposed to ethanol throughout their growth phase.

5.2.1 Growth thermograms

Figure 5-10 to Figure 5-14 show the growth thermograms obtained from the ethanol shock experiments. An experiment (04/08/2015) containing two technical repeats, a 4% and an 8% ethanol shock, was performed to demonstrate the repeatability of the ethanol shocking procedure. The results of the technical repeats are shown in Figure 5-10. Visually, there is no significant observable difference between the heat and power profiles. This confirms the repeatability of the experiment but also suggests that the ethanol shock has a negligible effect on the yeast.

In a following experiment, the ethanol shock concentration was increased such that the cells were exposed to 8% and 12%. These results are shown in Figure 5-11. The results presented in Figure 5-11 tend to suggest that despite the higher ethanol concentration used to shock the yeast, these ethanol shocks also had a negligible effect.

Figure 5-12 shows in addition to further 4% and 8% ethanol shocks the results of yeast cultures grown in 4% and 8% ethanol in YPD (constant ethanol exposure). The cells grown in YPD with 8% ethanol showed negligible growth, illustrated by the negligible heat evolution by the sample – giving off much the same heat flow as that of the YPD blank to which no cells were added. The cell population growing in 4% ethanol also showed retarded growth, as indicated by the longer lag time and overall diminutive growth thermogram as compared to the healthy cells, as seen in Figure 5-12. In order to better examine the retarding effects of ethanol on yeast growth, the ethanol concentration was lowered four-fold in the subsequent constant ethanol exposure experiments.

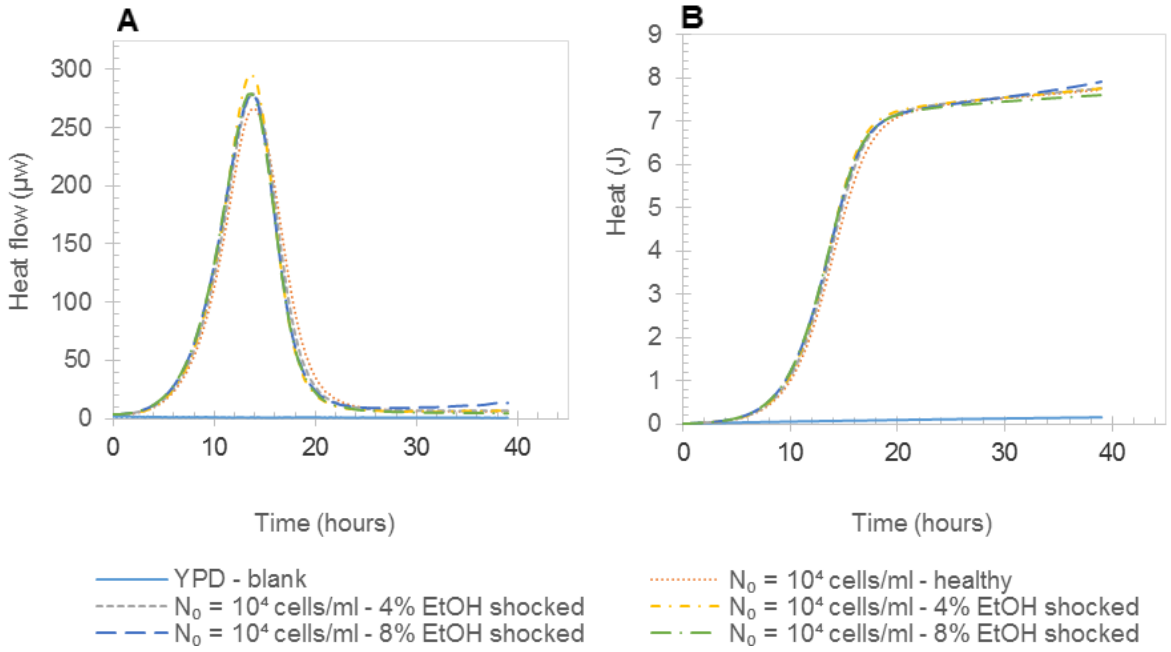

Figure 5-10: Heat flow (A) and heat curves (B) for experiment 04/08/2015, investigating the effects of an ethanol shock on yeast cells.

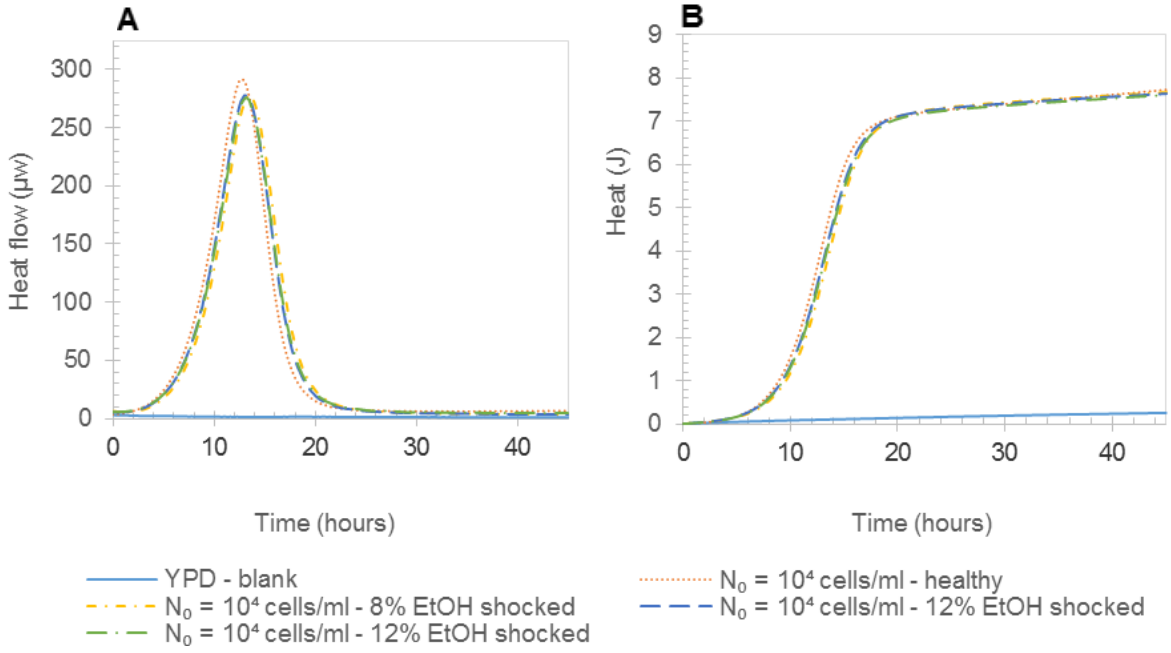

Figure 5-11: Heat flow (A) and heat curves (B) for experiment 06/08/2015, investigating the effects of an ethanol shock on yeast cells.

On considering all thermograms from ethanol shocked yeast (Figures 5-12, 5-13 and 5-15), it is clear that no significant or consistent effect of ethanol shock on heat generation resulted on exposure to 4 to 12% ethanol at 22 °C for 1 hour. . The lack of an ethanol shock causing any appreciable difference in long term cell growth is consistent with the findings of Pina et al. (2004). Pina et al. (2004) found using petri-dish counts that there was no ethanol inactivation after a 20% (v/v) ethanol shock (exposed for 1 hour).

On considering the tests on constant ethanol exposure during growth, a negative impact on growth was observed. Constant exposure to 8% ethanol (Figure 5-12) completely inhibited growth, with 4% exposure severely retarding growth. Constant exposure to 1% ethanol caused a noticeable lag in growth as compared to the ethanol shocked and healthy cells (Figure 5-13, Figure 5-14). The above results are consistent with that of Chandler et al. (2004), who found that exposure of yeast to an ethanol concentration of 10% ethanol completely inhibited growth.

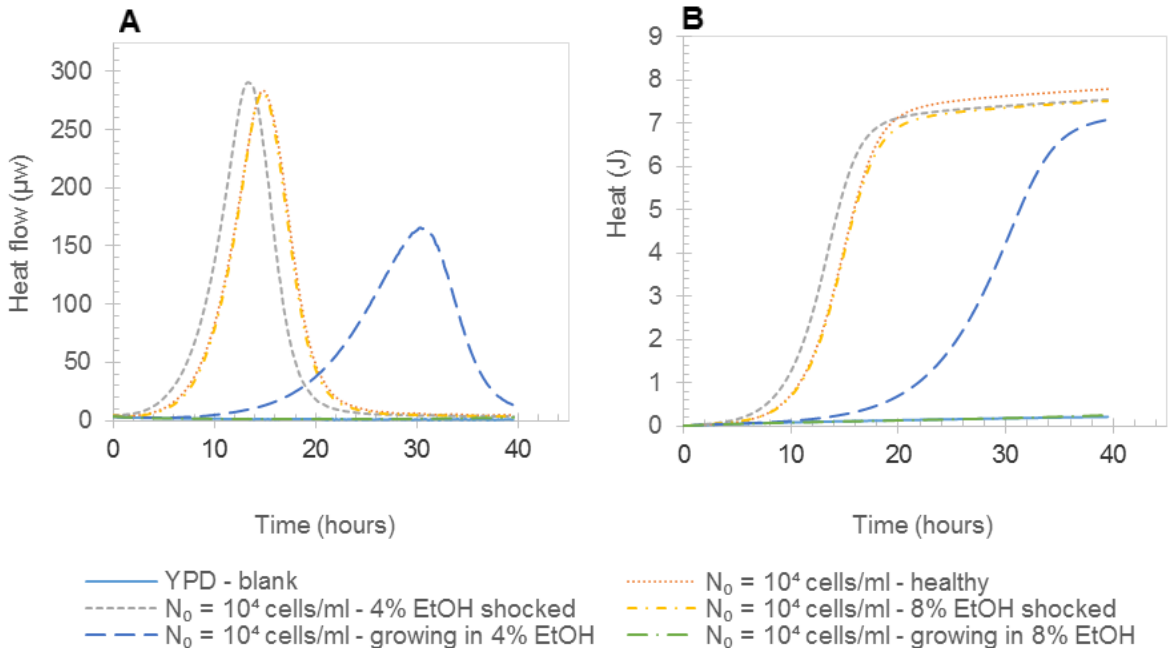

Figure 5-12: Heat flow (A) and heat curves (B) for experiment 28/07/2015, investigating the effects of an ethanol shock and growth in the presence of ethanol on yeast cells.

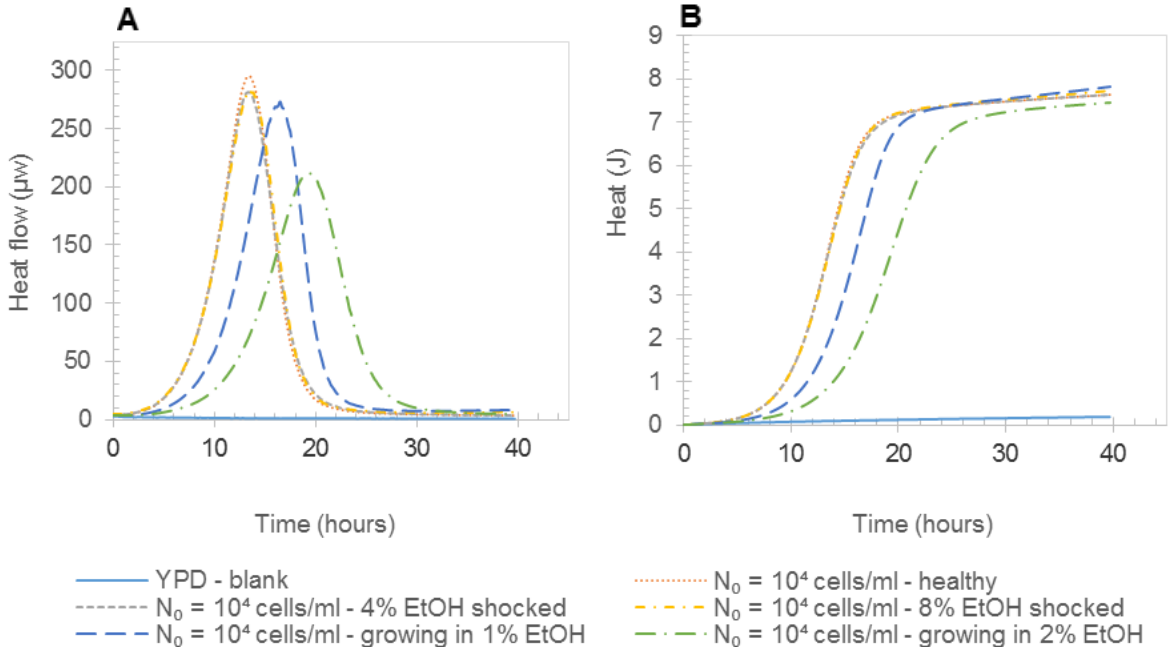

Figure 5-13: Heat flow (A) and heat curves (B) for experiment 30/07/2015, investigating the effects of an ethanol shock and growth in the presence of ethanol on yeast cells.

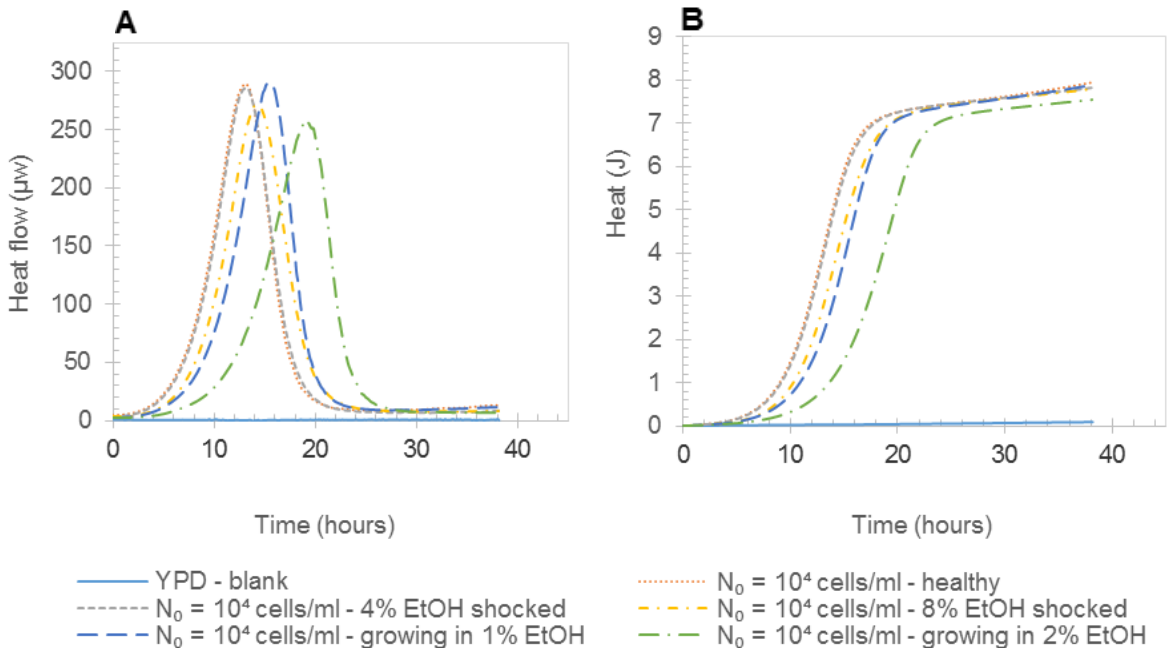

Figure 5-14: Heat flow (A) and heat curves (B) for experiment 02/08/2015, investigating the effects of an ethanol shock and growth in the presence of ethanol on yeast cells.

5.2.2 Quantitative analysis of the thermograms

Both the absolute and normalised equation fitting parameters determined through quantitative analysis of the data are given in Appendix C.2. As shown with the previous experiments, the data fitted the equation used to determine the specific growth rate and '*A*' values well, with high correlation seen by the R^2 values higher than 0.9999.

Table 5-7 provides a comparison of the average values determined for the 4% ethanol shocked cells and the healthy cells. Table 5-8 provides a comparison of the average values determined for the 8% ethanol shocked cells and the healthy cells. Table 5-7 and Table 5-8 show there to be no significant difference between the healthy cells and the ethanol shocked cells. In all cases the P values determined are much greater than 0.05. For the 12% ethanol shocked cells, only a single technical repeat was performed. This makes it invalid to compare statistically the performance of the 12% ethanol shocked cells to the healthy cells. However, in light of the fact that the 12% ethanol shocked cells performed much the same as the 8% ethanol shocked cells (by comparing the *A*, t_{max} and µ values given in Appendix C.2) in the 06/08/2015 experiment, this suggests that there is no significant difference between the 12% ethanol shocked cells and the healthy cells.

Table 5-9 gives the average normalised parameters determined for the cells exposed to 1% and 2% ethanol during the growth phase. The values of the normalised parameters for the healthy cells have been excluded for brevity – they are by definition all equal to unity and are shown in Table 5-7 and Table 5-8.

Table 5-7: Comparison between the average values of the normalized parameters determined for the healthy cells and 4% ethanol shocked cells

Parameter	Average for healthy cells		Average for 4% EtOH shock		P value: t-Test comparing healthy cells and 4%EtOH shocked cells*
	Value	Standard deviation	Value	Standard deviation	
μ_i/μ_m	1.00	0.00	0.99	0.01	0.2
$t_{max,i}/t_{max,m}$	1.0	0.00	0.97	0.04	0.3
A_i/A_m	1.0	0.00	1.20	0.40	0.3

*Two-tailed test assuming unequal variances

Table 5-8: Comparison between the average values of the normalized parameters determined for the healthy cells and 8% ethanol shocked cells

Parameter	Average for healthy cells		Average for 8% EtOH shock		P value: t-Test comparing healthy cells and 8%EtOH shocked cells*
	Value	Standard deviation	Value	Standard deviation	
μ_i/μ_m	1.00	0.00	0.99	0.01	0.3
$t_{max,i}/t_{max,m}$	1.00	0.00	1.02	0.04	0.3
A_i/A_m	1.00	0.00	0.90	0.30	0.6

*Two-tailed test assuming unequal variances

Table 5-9: Comparison between the average values of the normalized parameters determined for the cells suspended in 1% and 2% ethanol

Parameter	Average for cells growing in 1% EtOH		P value: t-Test comparing healthy cells and cells growing in 1% EtOH*	Average for cells growing in 2% EtOH		P value: t-Test comparing healthy cells and cells growing in 2% EtOH*
	Value	Standard deviation		Value	Standard deviation	
μ_i/μ_m	0.89	0.01	1E-06	0.77	0.01	0.02
$t_{max,i}/t_{max,m}$	1.21	0.03	2E-06	1.44	0.01	0.02
A_i/A_m	0.71	0.09	4E-04	0.6	0.05	0.06

*Two-tailed test assuming unequal variances

Table 5-9 shows that there is a significant difference between the specific growth rate, the t_{max} values and the *A* values when comparing the healthy cells to the cells growing in ethanol ($P << 0.05$). This is the first case where there is a significant difference observed between the specific growth rate of healthy cells and stressed cells in this work. In confirmation of the work by Antoce et al. (1996a), the magnitude of the effect on the specific growth and the lag time (measured by an increase in $t_{max,i}/t_{max,m}$ and decrease in A_i/A_m values) is proportional to the increase in ethanol concentration. The results from this experiment also confirm that increasing ethanol exposure has an increasing effect on the specific growth rate and lag time,

though noting that only single repeats for 4% and 8% ethanol exposure were performed (experiment 28/07/2015). A plot of $t_{max,m}/t_{max,i}$ versus A_i/A_m for different ethanol concentrations, shown in Figure 5-15, yields a straight line relationship (R^2 = 0.99), the same finding as Takahashi (2000). The straight-line trend with a gradient approximately equal to one shows the largely bacteriostatic nature (bacteriostatic action inhibits growth activity) of constant ethanol exposure to yeast (as discussed in Section 2.4.3).

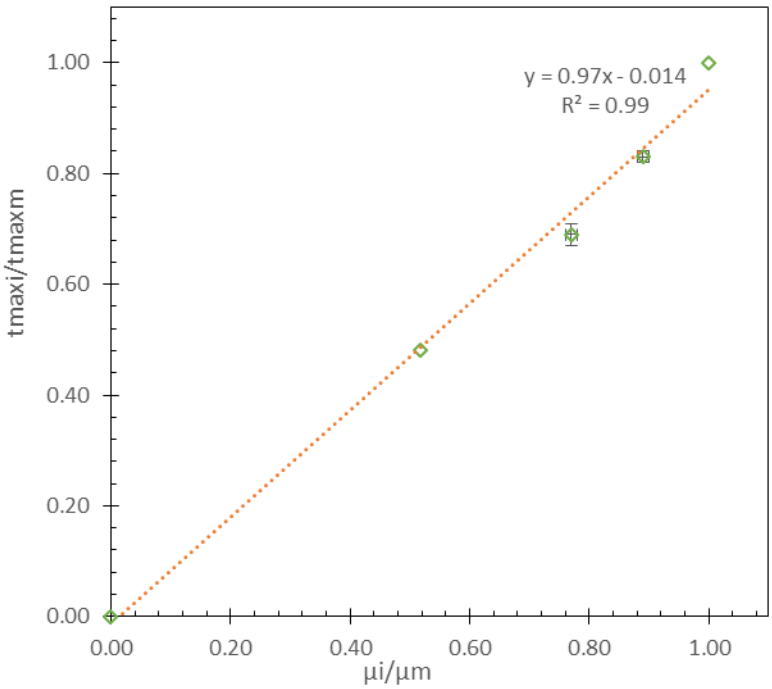

Figure 5-15: Plot of $t_{max,m}/t_{max,i}$ versus A_i/A_m for different ethanol concentrations.

5.2.3 Yeast quality indicators

Vitality results: APT

The results of the APT tests performed as well as a statistical comparison between the healthy cells and 4% and 8% ethanol shocked cells are shown in Table 5-10 and Table 5-11 respectively. There is no significant difference between the absolute values of the APT determined for the healthy cells and the 4% ethanol shocked cells, indicating that the ethanol shock has no significant effect on cell vitality - at the 95% confidence level. However, when comparing the normalised APT value there is a significant difference ($P < 0.05$) between the healthy cells and the 4% ethanol shocked cells, indicating that the ethanol shock may have an effect on cell vitality – significant at the 99% confidence level for this. The APT raw data can be found in Appendix D

Table 5-11 shows there to be no significant difference ($P > 0.05$) between both the absolute and normalised APT values of the healthy cells and the 8% ethanol shocked cells. This suggests that the confidence level of the APT may be lower than that applied as the norm in this work.

Table 5-10: Acidification power test results comparing 4% ethanol shocked to healthy cell performance

	Healthy cells		**4% EtOH shocked cells**		**P value: t-Test comparing healthy cells and 4% EtOH shocked cells***	
	Absolute	Normalised	Absolute	Normalised	Absolute	Normalised
Average APT	3.07	1.00	3.00	0.97	0.1	0.01
Standard deviation	0.07	0.00	0.05	0.01		

*Two-tailed test assuming unequal variances

Table 5-11: Acidification power test results comparing 8% ethanol shocked to healthy cell performance

	Healthy cells		**8% EtOH shocked cells**		**P value: t-Test comparing healthy cells and 8% EtOH shocked cells***	
	Absolute	Normalised	Absolute	Normalised	Absolute	Normalised
Average APT	3.07	1.00	3.03	0.99	0.3	0.2
Standard deviation	0.07	0.00	0.03	0.02		

*Two-tailed test assuming unequal variances

Viability results

The viability results for the ethanol shock experiments are presented in Table 5-12. As observed in previous viability tests, there is no significant difference ($P > 0.05$) between the viability determined by CFU counts or methylene violet staining between the ethanol shocked cells and the healthy cells. However, any such significant difference may be masked by the large variability (standard deviation) present in the viability results. In the case of the CFU counts, this lack of a significant difference appears to be due to the large variability in the viability of the healthy cells. As has also been observed in the other viability tests, the viability determined by the CFU counts is lower than that determined by the methylene violet stain.

Table 5-12: Viability test results from methylene violet and CFU counts for the ethanol shock experiments

		Healthy cells	4% EtOH shock	P value: t-Test comparing healthy cells to 4% EtOH shocked cells*	8% EtOH shock	P value: t-Test comparing healthy cells to 8% EtOH shocked cells*
Average viability - methylene violet staining	viability (%)	100.0	100.0	-	99.5	0.4
	standard deviation	0.0	0.0		1.2	
Average viability - CFU counts	viability (%)	73	103	0.3	59	0.5
	standard deviation	31	31		5	

*Two-tailed test assuming unequal variances

5.2.4 Summary and discussion of key findings

Effect of ethanol shock on yeast performance

The ethanol shock experiments showed there to be no consistently calorimetrically observable difference between the ethanol shocked (4%, 8% and 12% ethanol shock, at 22 °C for 1 hour) cells and the healthy cells. This lack of a visual difference in the thermograms was confirmed by the statistical analysis of the growth parameters. Furthermore, there was no difference observed in the methylene violet viabilities of the healthy cells and the ethanol shocked cells. While this was supported by plate counts, high standard deviations do not allow a conclusive outcome. On considering cell vitalities, there was no significant difference observed between the vitality of the 8% ethanol shocked cells and the healthy cells at a 95% confidence level. When comparing the normalised APT values of the 4% ethanol shocked cells, the lack of significant difference compared to the healthy cells was only observed at a 99% confidence level for the normalised APT but a confidence level of 95% for the absolute APT values, suggesting minimal difference in vitality as well.

The lack of any significant effect of the ethanol shock on cell growth is surprising given that the 4% and 8% ethanol shock were purposely chosen as it is known that shocks of this magnitude cause a significant genetic response by the cell (Chandler et al., 2004; Piper et al., 1994). Ethanol exposure is known to produce HSP-12, the same protein produced during cold shock. Thus in light of the findings of Section 5.1.2 (rapid cold shock), where it was shown that a rapid cold shock caused a significant effect on cell vitality, it is surprising that there is no major difference between the ethanol shocked cells and the healthy cells. This suggests that ethanol shocks are transient with the yeast cells being able to recover rapidly from the stress.

Effect of ethanol exposure during growth on yeast performance

When the cells were constantly exposed to ethanol during the growth cycle, 8% ethanol exposure was shown to inhibit cell growth completely, with 4% ethanol exposure severely retarding growth. Exposure to 1% and 2% ethanol also had a significant effect on the calorimetrically determined growth parameters. These findings are consistent with that of Antoce (1996) who showed that increasing ethanol concentrations has an increasing effect on the lag time and specific growth rate. It can be concluded yeast growth in the presence of ethanol has bactericidal (increases lag-time) and bacteriostatic (lower specific growth rate) effects.

5.3 Combined ethanol and cold shock

In the combined ethanol and cold shock experiments, the following treatments were compared: cell populations that were only cold shocked (rapid resuspension of yeast initially at room temperature in 4 °C YPD and holding at this temperature for 2 hours) before growth under standard conditions, unstressed (healthy) cell populations growing in 1% ethanol and cells that were first exposed to a rapid cold shock and then grown in 1% ethanol. The combined cold shock and ethanol exposure was performed in order to test the cumulative effect of the two stresses.

Due to the nature of the combined ethanol and cold shock experiments, APT and viability data for the cold shocked cells growing in ethanol was not compared. This was due to the effect of constant ethanol exposure only having an effect on the yeast in the IMC while APT and viability tests were performed before (refer to Section 3.5.5 for further clarification).

5.3.1 Growth thermograms

Figure 5-16 to Figure 5-19 compare the growth thermograms from replicate experiments following the combined ethanol and cold shock stress to healthy cells as well as cells exposed to cold shock or growth in the presence of ethanol only. Two sets of curves are observed in each case. The first set of curves (usually two curves that peak close together) show the healthy cells and rapid cold shock cells. The second set of curves show the healthy cells gown in 1% ethanol and prior rapidly cold shocked cells growing in 1% ethanol.

In most cases the thermograms show the cold shocked cells and the healthy cells to have similar heat outputs. In Figure 5-16 the two curves rest almost on top of one another. However in Figure 5-18 and Figure 5-19 the peak in heat output for the rapid cold shock cells appears slightly later than that of the healthy cells, as expected given the results of Section 5.1.2 which showed that a rapid cold shock significantly affects cell vitality. While all the cells growing in ethanol were characterized by a slower heat output, there is no clear visual trend distinguishing the healthy cells from cells exposed to rapid cold shock when grown in the presence of 1% ethanol.

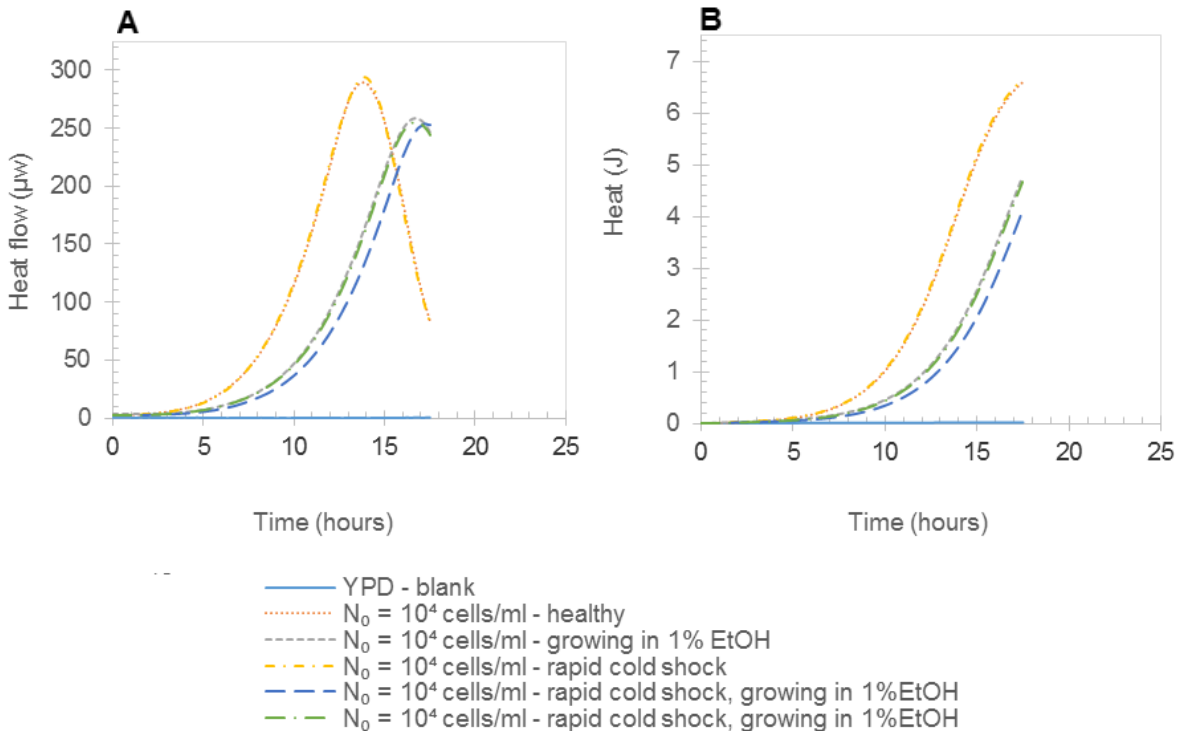

Figure 5-16: Heat flow (A) and heat curves (B) for experiment 13/08/2015, investigating the effects of a combined rapid cold shock and growth in ethanol in the presence of ethanol on yeast cells.

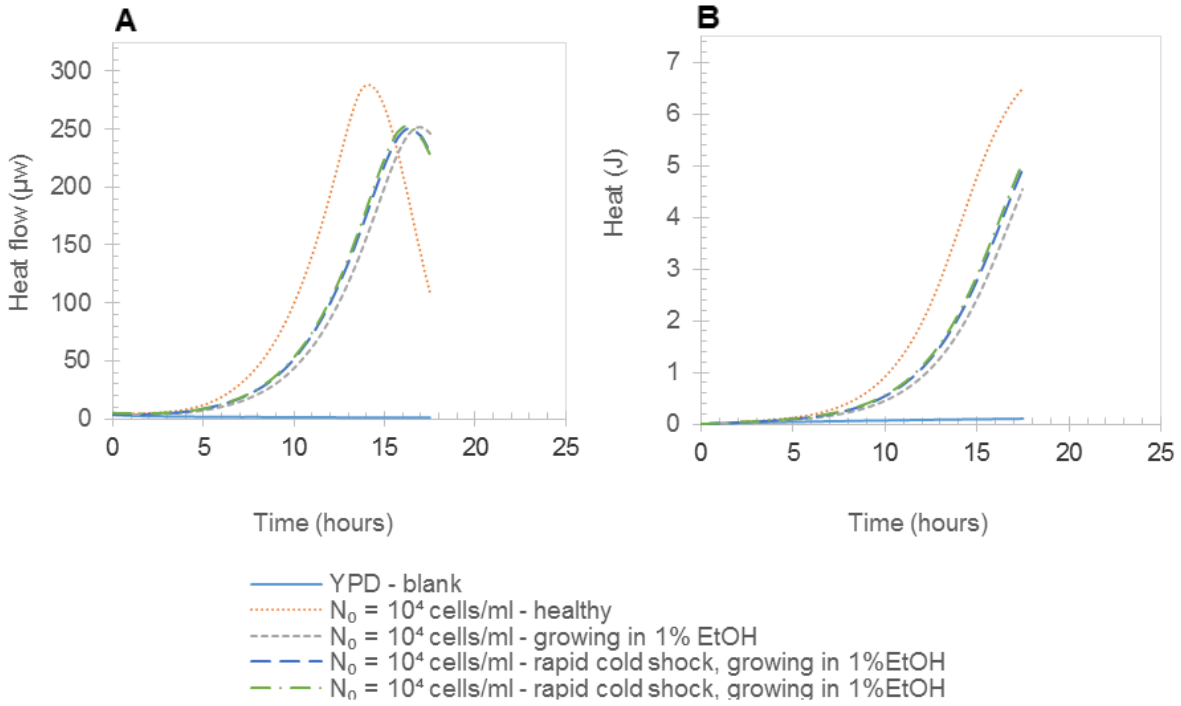

Figure 5-17: Heat flow (A) and heat curves (B) for experiment 20/08/2015, investigating the effects of a combined rapid cold shock and growth in ethanol in the presence of ethanol on yeast cells.

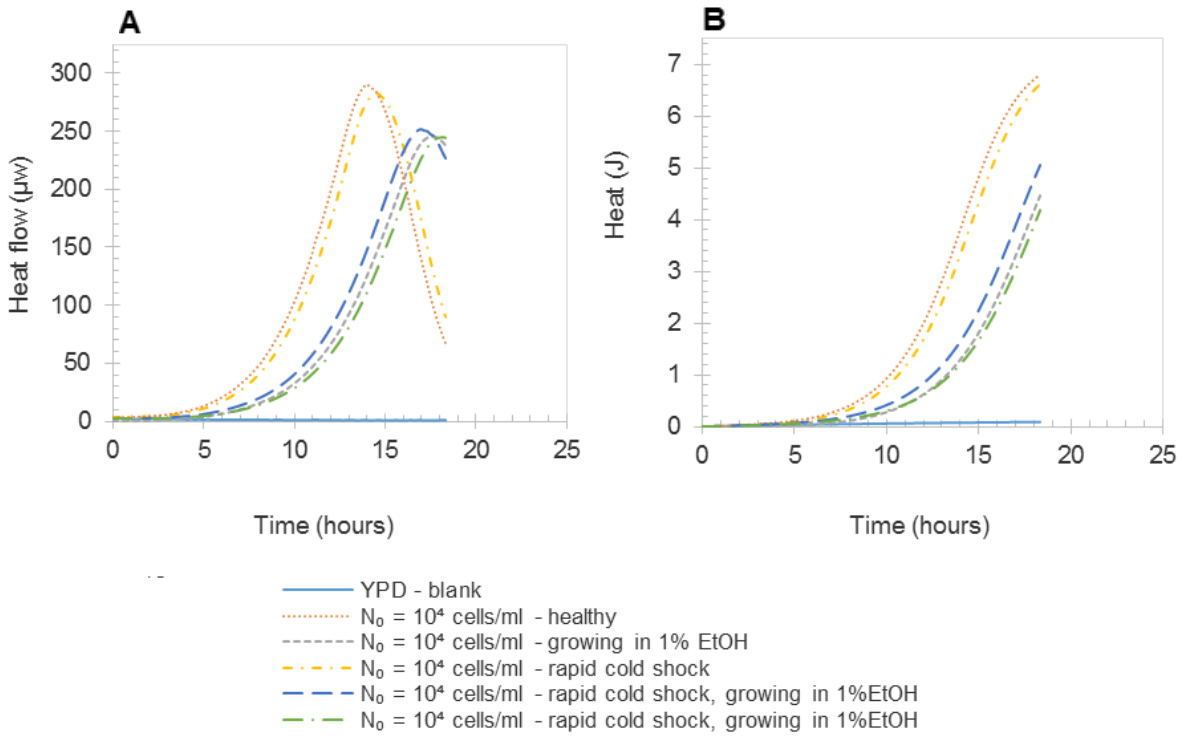

Figure 5-18: Heat flow (A) and heat curves (B) for experiment 21/08/2015, investigating the effects of a combined rapid cold shock and growth in ethanol in the presence of ethanol on yeast cells.

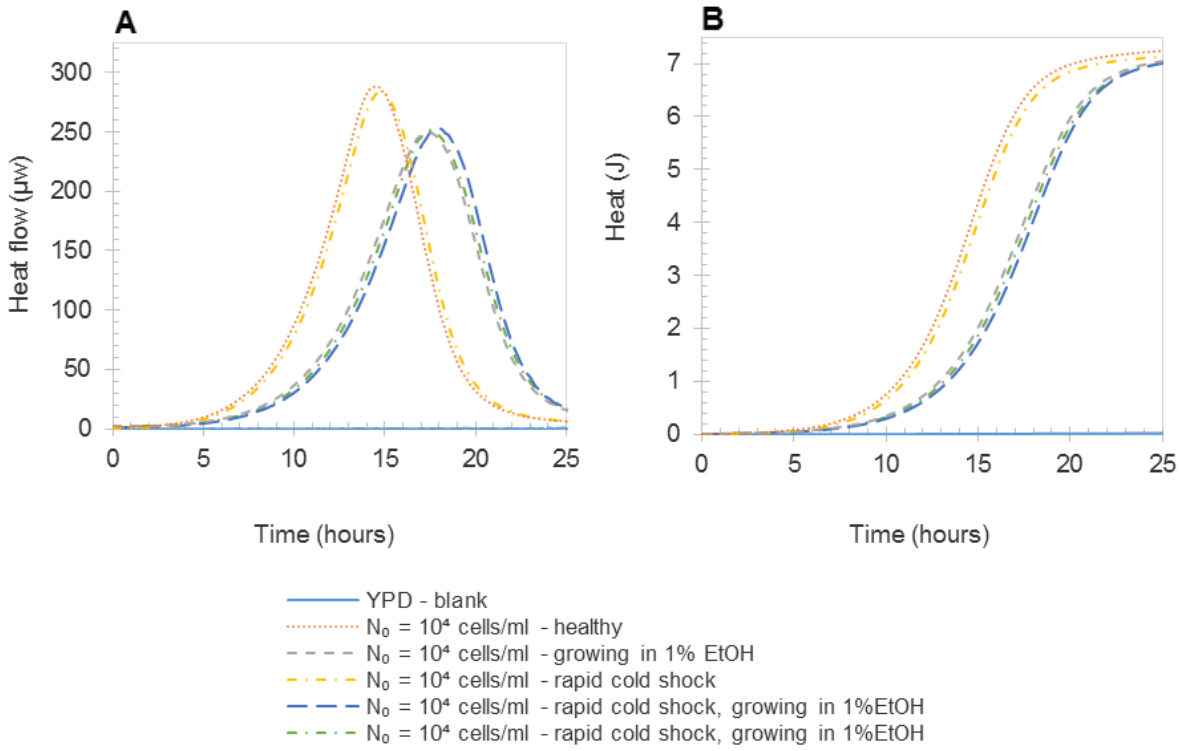

Figure 5-19: Heat flow (A) and heat curves (B) for experiment 22/08/2015, investigating the effects of a combined rapid cold shock and growth in ethanol in the presence of ethanol on yeast cells.

5.3.2 Quantitative results of the thermograms

Analysing the thermogram results quantitatively, the values of the absolute and normalised fitting parameters are given in Appendix C.3. As shown with the previous experiments, the equation fits to determine the specific growth rate and 'A' values were highly correlated to the data. An analysis of the average values of the cold shocked cells growing in 1% ethanol is presented in Table 5-13. As expected from the results of ethanol shock experiments (Section 5.2), in all cases there is a significant difference between the values determined for the healthy cells and the rapid cold shocked cells growing in 1% ethanol.

Table 5-13: Comparison between the average values of the normalized parameters determined for the healthy cells and cells exposed to rapid cold shocked growing in 1% ethanol

Parameter	**Average for healthy cells**		**Average for cold shocked cells growing in 1% EtOH**		**P value: t-Test comparing healthy cells and cold shocked cells growing in 1% EtOH***
	Value	Standard deviation	Value	Standard deviation	
μ_i/μ_m	1.00	0.00	0.88	0.01	7.14E-11
$t_{max,i}/t_{max,m}$	1.00	0.00	1.21	0.05	7.77E-06
A_i/A_m	1.00	0.00	0.71	0.16	1.34E-03

*Two-tailed test assuming unequal variances

A comparison of the average values determined for the cold shocked cells growing in 1% ethanol to that of the healthy cells growing in 1% ethanol is given in Table 5-14. Table 5-14 shows there to be no significant difference (P > 0.05) between the average values determined for the un-stressed cells growing in 1% ethanol to that of the cold shocked cells growing in 1% ethanol. Thus the thermal data implies that the prior rapid cold shock does not affect the performance of the cells. This, in turn, infers that the cells do not experience a cumulative stress under these conditions.

Table 5-14: Comparison between the average values of the normalized parameters determined for cells growing in 1% ethanol and rapid cold shocked cells growing in 1% ethanol

Parameter	**Average for cells growing in 1% EtOH**		**Average for cold shocked cells growing in 1% EtOH**		**P value: t-Test comparing cells growing in 1% EtOH and cold shocked cells growing in 1% EtOH***
	Value	Standard deviation	Value	Standard deviation	
μ_i/μ_m	0.89	0.01	0.88	0.01	0.2
$t_{max,i}/t_{max,m}$	1.22	0.02	1.21	0.05	1.0
A_i/A_m	0.69	0.11	0.71	0.16	1.0

*Two-tailed test assuming unequal variances

As discussed in Section 2.1.4, both a rapid cold shock and ethanol stress induce the production of HSP-12. It is possible that the cell is only capable of expressing a set amount of the protein thereby causing any further non-lethal stress not to have any additive effect (once maximum protein expression occurs). This also suggests that only a certain amount of the protein is needed to intercalate into the membrane to protect it.

5.3.3 Summary and discussion of key findings

A rapid cold shock has a small but noticeable effect on yeast metabolism as determined by heat generation, as shown in Section 5.1.2. Growth of yeast in the presence of 1% ethanol has a greater effect on yeast metabolism, as shown in Section 5.2. Yeast is reported to respond to both these stresses by the induction of key HSPs. On combining these stresses (the occurrence of a cold shock prior to placing yeast cells in ethanol), no cumulative stress effect was observed under the conditions of exposure. In all cases, the ethanol effect and analysis of metabolism followed the cold shock by a period of 2.5 hours, allowing sufficient time for the induction and expression of HSPs prior to the ethanol stress has no significant effect on the growth thermogram the cells produce. The similar viabilities between the healthy cells and the rapid cold shocked cells in Section 5.1.2 (Quantitative analysis of thermograms) rule out differences in initial population viability being the cause of any differences observed in the growth thermograms.

While cumulative stress response is not observed here, it has been observed under some stress conditions for yeast cultivation, particularly when analysis follows directly on exposure to the stress. Hence it is recommended that further work is done on the magnitude of combined stresses as well as the time courses in which the yeast are most vulnerable.

6 Conclusions and Recommendations

The aim of this work was to develop a method to measure yeast viability and vitality using isothermal microcalorimetry. This method was then applied to determine the effects of different stresses on yeast populations. In this chapter, the main conclusions arising from the method development and stress test results are first presented. The chapter ends with recommendations regarding further method development and recommendations regarding better understanding yeast stress.

6.1 Conclusions

The primary purpose of this work was to develop a method to assess yeast health using isothermal microcalorimetry. As part of this, one of the objectives of this work was to be able to determine cell viability calorimetrically. By changing the size of the initial viable cell population, it was confirmed that differences in the viable cell numbers present can be distinguished by comparing the different growth thermograms generated using the TAMIII microcalorimeter. By comparison with the initial cell number placed into the IMC, these data can be converted to cell viability. Differences in the order of magnitude of initial healthy cell populations are easily observed through visual inspection of the growth thermograms generated. Furthermore, these outcomes could be presented quantitatively (see below). The presence of dead cells had no effect on the growth thermograms produced, affirming that dead cells do not evolve any heat.

An initial healthy yeast cell population of approximately 10^4 cells/ml was found to be a good population size for the collection of IMC data under the conditions used. A larger initial cell population does not allow the heat generated by the insertion of a sample into the IMC to dissipate before significant metabolic heat generated from the cells is detected, implying that a clear base line is not observed. A population size smaller than 10^4 cells/ml has a protracted lag time. Where this may arise in the experiment, it is not desirable in the control.

A further objective of this work was to demonstrate the repeatability of the method developed. Throughout all the experiments, the microcalorimetric technique developed generated repeatable results. It was demonstrated that exponential growth and thus heat generation was observed. The exponential equation fit to the data:

$$heat = A * exp(\mu * t) + B \qquad \textit{Equation 4-3}$$

correlated well to the data points (R^2 > 0.9999 for each fit). In all cases, the calorimetric parameters (time to peak, the '*A*' value and specific growth rate, μ) produced across experiments in which cells were exposed to the same conditions (biological repeats) were consistent and statistically the same. The use of the '*A*' value, the exponential term coefficient, proved to be a more sensitive way to measure differences in viability and vitality, as compared to the t_{max}, the time taken for the heat flow/power of a sample to reach its maximum or peak heat flow value.

By fitting an exponential equation to the calorimetric data to yield the 'A' value and specific growth rate and recording the time taken for the heat flow of a sample to reach its maximum heat flow value, a number of key parameters are determined that enable yeast health to be accurately quantified in a repeatable manner. In terms of addressing the key questions:

- Can the analysis of the calorimetric thermograms produce the required parameters to determine cell viability and vitality from heat flow data?
- Can the thermometric data from the microcalorimetry be used to differentiate yeast viability and vitality?

it is affirmed that parameters can be derived from the thermograms that can be used to help determine and distinguish cell viability and vitality. The specific growth rate is a measured of cell vitality while the time to peak heat flow and the 'A' value represent a combination of viability and vitality.

The wet chemistry methods of methylene violet stain, used to confirm independently cell viability, and the acidification power test (modified for use in this work), used to confirm independently cell vitality, were shown to be repeatable (standard deviations routinely below 2% for both assays). The use of plate counts of CFU were shown to have much higher variability, with large standard deviations.

The last key question of this work:

- Do the stresses imposed on the yeast cells cause distinguishable differences in cell viability and vitality?

was addressed by the cold shock, ethanol shock and ethanol exposure experiments. A slow cold shock (cooling from 22 °C to 4 °C over a two hour period – yielding an average rate of cooling of 0.13 °C/minute) had no calorimetrically observable effect on the cells and no effect on cell viability. The slow cold shock did, however, produce differences in cell vitality as measured by the APT. It is possible that a change in the cell vitality was not observed calorimetrically due firstly to the delay in reading the cellular heat output and secondly to the much longer period over which the calorimetric signal is read. This is in contrast to the APT that measures the cell vitality as a brief 'snapshot' shortly after the stress occurred. This suggests that IMC data in the way it has been analysed in this work is not able to detect minor short-term changes in yeast health from which recovery is achieved in the first growth cycle.

The rapid cold shock (sudden cooling from 22 °C to 4 °C – yielding an average approximate rate of cooling of 18 °C/minute) produced both visually and quantitatively different calorimetric data as compared to healthy cells. The cells exposed to a rapid cold shock had significantly longer lag times, causing the peak in heat flow to occur later. The specific growth rate of the cells exposed to the rapid cold shock was calculated to be the same as that of the healthy yeast. The APT showed the rapid cold shock to reduce cell vitality significantly. In this case, the rapid cold shock caused a greater stress response with the more significant effects on cell metabolism being in effect over a longer period. The cells respond to stress because the cold changes the structure of the membrane and its ductility and permeability owing to the transition

temperature of the phospholipid membrane. This implies that the yeast metabolism changes and becomes depressed (the effect observed). The cells then respond to this stress genetically to try to overcome it – e.g. they produce HSP, change the lipid composition in membrane etc. As observed for the slow cold shock, no significant effect on cell viability was measured following rapid heat shock.

The exposure of the yeast cells to an ethanol shock (suspension of yeast cells in YPD containing different concentrations of ethanol at 22 °C for 1 hour) caused no significant calorimetrically observable difference in cell performance as compared to healthy cells. The ethanol shock also caused no difference in cell viability, as measured by CFU counts and methylene violet staining. A 4% ethanol shock caused a significant difference in cell vitality, according to the APT. Counter-intuitively, the 8% ethanol shock caused no significant difference in cell vitality, according to the APT. This suggests that the difference observed for the 4% ethanol shock may have been anomalous. Given the lack of an observable difference in the cell growth parameters ('*A*' value, specific growth rate μ, and t_{max},), an ethanol shock can be concluded to be a transient stress that the cell can recover from quickly.

On exposing cells to ethanol while growing, the presence of ethanol had a significant effect on the observable growth thermograms. The presence of ethanol severely retarded the cellular growth rate. Cells exposed to 8% ethanol showed no discernible signs of growth over a 40 hour period. Cells exposed to concentrations as low as 1% ethanol displayed growth thermograms that, through simple visual inspection, can be seen to be lagging as compared to healthy cell populations. The quantitative growth parameters also indicated significantly retarded growth as compared to the healthy cells. This observation and the calculated quantitative differences in cell growth in terms of both lag time and the specific growth rate is consistent with multiple sources in the literature.

Cells that were exposed to a rapid cold shock prior to being grown in ethanol showed no statistical difference in their performance measured by IMC to cells that had not been exposed to a rapid cold shock prior to being grown in ethanol. The two stresses are thus non-commutative over the time scale of the measurement. This was observed despite the fact that a rapid cold shock alone was seen to affect vitality and result in a longer lag time. It is postulated that once the cells are exposed to the rapid cold shock, expression of heat shock proteins such as HSP12 occurred allowing the cells to be protected on subsequent exposure to ethanol (sub-lethal). Alternatively, the magnitude of the effect of ethanol exposure exceeds that of the cold shock sufficiently for the cold shock effect to be masked by the ethanol exposure.

The calculated specific growth rate for the healthy cells, cold shocked cells and ethanol shocked cells varied insignificantly throughout all the experiments. This consistent specific growth rate of cells under the same conditions can be expected since any daughter cells produced have not experienced the stress or shock and are effectively growing in the same environment, yielding the same specific growth rate across experiments. The primary response to the stress was observed through a change in the lag time. This gave a measure of the time taken for the stressed cells to start dividing, producing un-stressed daughter cells

which acted to dilute the effect of the stress. In general, the yeast recovered relatively rapidly upon removal of the stress, even from what are widely considered harsh growth conditions (rapid temperature drop and ethanol exposure).

This work has shown that the microcalorimetric signal evolved is a function of the initial population viability and vitality. Differences in yeast population health can in some cases be determined visually relative to the performance of healthy cells by inspection of the relevant heat or power thermograms. The growth parameters determined quantitatively ('*A*', μ, and t_{max},) can be used to statistically compare the health of yeast populations relative to that of healthy cells. Certain stresses do cause distinguishable and quantifiable differences in cell viability and vitality. Therefore, there is potential for isothermal microcalorimetry to be further developed as a tool to measure yeast quality.

6.2 Recommendations

Given below is a list of recommendations and suggestions for future work to be carried out to better develop the IMC method used to quantify microbial viability and vitality and to evaluate stress response. This focusses particularly on the analysis of thermograms of stressed yeast populations:

- The data obtained in this work could be re-analysed to include data points going back to the early lag phase – e.g. between 5% (in this work 10% was used) and 70% of the total heat output. This would aid in detecting changes in growth parameters that may only be present early on in the growth phase, before large numbers of daughter cells are formed, thereby diluting out the prior stressed cells. This 'earlier' analysis of data may enable short-term minor changes in yeast health, such as the type of stress induced by the slow cold shock, to be detected using the IMC data.
- While the equation fits presented in this work were proven to be accurate, a more robust curve fitting technique (algorithm) could be developed by determining the fit region rigorously through gradient analysis. This may entail basing the region of the fit on the gradient (derivative curve) of the natural logarithm of the heat flow data, i.e. fitting the data strictly over the entire region where exponential growth is occurring. This would be instead of using arbitrary fitting regions e.g. between 10% and 70% of the total heat output, as used in this work.

Given below is a list of recommendations and suggestions for future work to be carried out in terms of better understanding yeast stress:

- HPLC analysis could be used to help determine what substrates or metabolites (if any) become limiting when growing the yeast in sealed ampoules.
- Analysis of expression of stress proteinsExpression of stress protein genes through transcriptomics or proteonomics could be utilised to determine a more direct link between the cellular response to stress, intracellular processes and the calorimetric signal.

- Further work to de-convolute changes in cell viability and vitality using the microcalorimetric data could make use of an extra measure of cell viability or vitality to do such.
- Cyclic exposure of yeast populations to stress could also be tested. Cyclic stress could help determine whether repetitive exposure of yeast to different stresses in a cyclic nature, such as the conditions yeast is exposed to under brewery conditions, has an adverse effect on yeast viability and vitality, or whether it enables resilience to be built into the strain through adaptation.
- The 'slide count' method used by Basson et al. (1997) or the 'Tadpoling' technique developed by Welch & Koshland (2013) should be investigated as an alternative independent measure of cell viability due to their large dynamic range and increased sensitivity over the traditional colony forming unit (petri-dish count) technique.
- IMC could be used for brewing yeast strain selection and analysis. Different strains could be subjected to varying degrees of stress and only the best performing strains selected. This could entail comparing full scale or small-scale fermentation tests with microcalorimetric data. Similarly, this approach could be applied to numerous other industrially or environmentally important micro-organisms, where only the best performing strains with respect to process or environmental stresses are selected quantitatively.

References

Abramova, N., Sertil, O., Mehta, S., Lowry, C. V., 2001. Reciprocal regulation of anaerobic and aerobic cell wall mannoprotein gene expression in *Saccharomyces cerevisiae*. J. Bacteriol. 183, 2881–2887.

Alklint, C., Wadsö, L., Sjöholm, I., 2005. Accelerated storage and isothermal microcalorimetry as methods of predicting carrot juice shelf-life. J. Sci. Food Agric. 85, 281–285.

Anderson, R.K.I., Jayaraman, K., Voisard, D., Marison, I.W., Stockar, U. Von, 2002. Heat flux as an on-line indicator of metabolic activity in pilot scale bioreactor during the production of *Bacillus thuringiensis* var. galleriae-based biopesticides. Thermochim. Acta 386, 127–138.

Antoce, O.-A., Antoce, V., Fukada, H., Takahashi, K., Kawasaki, H., Amano, N., Pomohaci, N., Machi, T., 1996a. Application of calorimetry to the study of ethanol tolerance of some yeast strains. Biocontrol Sci. 1, 3–10.

Antoce, O.-A., Antoce, V., Takahashi, K., 1997a. Calorimetric study of yeast growth and its inhibition by added ethanol at various pHs and temperatures. Netsu Sokutei 24, 206–213.

Antoce, O.-A., Antoce, V., Takahashi, K., Pomohaci, N., Namolosanu, I., 1977. Calorimetric determination of the inhibitory effect of C1 - C4 n-alcohols on growth of some yeast species. Thermochim. Acta 297, 33–42.

Antoce, O.-A., Antoce, V., Takahashi, K., Yoshizako, F., 1997b. Quantitative study of yeast growth in the presence of added ethanol and methanol using a calorimetric approach. Biosci. Biotechnol. Biochem. 61, 664–669.

Antoce, O.-A., Nămoloşanu, I.C., 2011. A rapid method for testing yeast resistance to ethanol for the selection of strains suitable for winemaking. Rom. Biotechnol. Lett. 16, 5953–5962.

Antoce, O.-A., Takahashi, K., Nămoloşanu, I., 1996b. Characterization of ethanol tolerance of yeasts using a calorimetric technique. Vitis 35, 105–106.

Arao, T., Asakura, M., Suzuki, Y., Tamura, K., Okamoto, A., Inubushi, H., Miki, M., 2004. Bioassay of various pesticides by microcalorimetry measuring the metabolic heat of yeast. Environ. Sci. 11, 303–12.

Arao, T., Hara, Y., Suzuki, Y., Tamura, K., 2005. Effect of high-pressure gas on yeast growth. Biosci. Biotechnol. Biochem. 69, 1365–1371.

Atri, M.S., Saboury, A.A., Ahmad, F., 2015. Biological applications of isothermal titration calorimetry. Phys. Chem. Res. 3, 319–330.

Austin, G.D., Watson, R.W.J., D'Amore, T., 1994. Studies of on-line viable yeast biomass with a capacitance biomass monitor. Biotechnol. Bioeng. 43, 337–341.

Axcell, B.C., O'Connor-Cox, E.S.C., 1996. The concept of yeast vitality – an alternative approach. Proc. 24th Conv. Inst. Brew. (Asia Pacific Sect. 64–71.

Bäckman, P., Breidenbach, R.W., Johansson, P., Wadsö, I., 1995. A gas perfusion microcalorimeter for studies of plant tissue. Thermochim. Acta 251, 323–333.

Baldoni, D., Hermann, H., Frei, R., Trampuz, A., Steinhuber, A., 2009. Performance of microcalorimetry for early detection of methicillin resistance in clinical isolates of *Staphylococcus aureus*. J. Clin. Microbiol. 47, 774–776.

Baranyi, J., 2010. Modelling and parameter estimation of bacterial growth with distributed lag time by József Baranyi. University of Szeged , Hungary.

Barros, N., Feijoó, S., Simoni, J.A., Prado, A.G.., Barboza, F.D., Airoldi, C., 1999. Microcalorimetric study of some Amazonian soils. Thermochim. Acta 328, 99–103.

Basson, L., 1996. Loss of Yeast quality during mechanical handling in a brewery: an investigation of cropping. University of Cape Town.

Beezer, A.E., Newell, R.D., Tyrrell, J. V, Tyrrell, H.J. V, 1977. Bioassay of nystatin bulk material by flow microcalorimetry. Anal. Chem. 49, 34–37.

Belaich, a., Belaich, J.P., 1976. Microcalorimetric study of the anaerobic growth of *Escherichia coli*:

growth thermograms in a synthetic medium. J. Bacteriol. 125, 14–18.

Belaich, J.P., Senez, J.C., Murgier, M., 1968. Microcalorimetric study of glucose permeation in microbial cells. J. Bacteriol. 95, 1750–1757.

Bendiak, D., 2000. Review of metabolic activity tests and their ability to predict fermentation performance. In: Smart, K.A. (Ed.), Brewing Yeast Fermentation Performance. Blackwell Science, Oxford, UK, pp. 34–45.

Bergman, L.W., 2001. Growth and maintenance of yeast. Methods Mol. Biol. 177, 9–14.

Birch, R.M., Walker, G.M., 2000. Influence of magnesium ions on heat shock and ethanol stress responses of *Saccharomyces cerevisiae*. Enzyme Microb. Technol. 26, 678–687.

Bonkat, G., Braissant, O., Widmer, A.F., Frei, R., Rieken, M., Wyler, S., Gasser, T.C., Wirz, D., Daniels, A.U., Bachmann, A., 2012. Rapid detection of urinary tract pathogens using microcalorimetry: Principle, technique and first results. BJU Int. 110, 892–897.

Braissant, O., Bachmann, A., Bonkat, G., 2015. Microcalorimetric assays for measuring cell growth and metabolic activity: Methodology and applications. Methods 76, 27–34.

Braissant, O., Bonkat, G., Wirz, D., Bachmann, a., 2013. Microbial growth and isothermal microcalorimetry: Growth models and their application to microcalorimetric data. Thermochim. Acta 555, 64–71.

Braissant, O., Wirz, D., Göpfert, B., Daniels, A.U., 2010. Use of isothermal microcalorimetry to monitor microbial activities. FEMS Microbiol. Lett. 303, 1–8.

Brettel, R., Lamprecht, I., Schaarschmidt, B., 1980. Microcalorimetric investigations of the metabolism of yeasts VII. Flow-calorimetry of aerobic batch cultures. Radiat. Environ. Biophys. 18, 301–309.

Briggs, D.E., Boulton, C.A., Brookes, P.A., Stevens, R., 2004. Brewing: Science and Practice. Woodhead Publishing Limited, Cambridge, England.

Cahill, J., Nixon, R., 2005. Allergic contact dermatitis to quaternium 15 in a moisturizing lotion. Australas. J. Dermatol. 46, 284–285.

CBS Databse, 2014. CBS8803 [WWW Document]. CBS-KNAW. URL http://www.cbs.knaw.nl/collections/BioloMICS.aspx?Table=CBS strain database&Name=CBS+8803&Fields=All&ExactMatch=T (accessed 4.9.15).

Chandler, M., Stanley, G. a, Rogers, P., Chambers, P., 2004. A genomic approach to defining the ethanol stress response in the yeast *Saccharomyces cerevisiae*. Ann Microbiol 54, 427–454.

Chang-Li, X., Hou-Kuhan, T., Zhau-Hua, S., Song-Sheng, Q., Yao-Ting, L., Hai-Shui, L., 1988. Microcalorimetric study of bacterial growth. Thermochim. Acta 123, 33–41.

Chen, H., Zhuang, R., Yao, J., Wang, F., Qian, Y., Masakorala, K., Cai, M., Liu, H., 2014. Short-term effect of aniline on soil microbial activity: a combined study by isothermal microcalorimetry, glucose analysis, and enzyme assay techniques. Environ. Sci. Pollut. Res. 21, 674–683.

Deere, D., Shen, J., Vesey, G., Bell, P., Bissinger, P., Veal, D., 1998. Flow cytometry and cell sorting for yeast viability assessment and cell selection. Yeast 14, 147–160.

Douglas, P., Meneses, F.J., Jiranek, V., 2006. Filtration, haze and foam characteristics of fermented wort mediated by yeast strain. J. Appl. Microbiol. 100, 58–64.

Fernández, S., Gonzalez, G., Sierra, J.A., 1991. The Acidification Power Test and the Behaviour of Yeast in Brewery Fermentations.pdf. Tech. quaterly - Master Brew. Assoc. Am. 28, 89–95.

Fujita, T., Nunomura, K., 1977. Calorimetric studies of yeast metabolism under nongrowing conditions. In: Lamprecht, I., Schaarschmidt, B. (Eds.), Application of Calorimetry in Life Sciences. Walter de Gruyter, Berlin, pp. 119–127.

Gabriel, P., Dienstbier, M., Matoulková, D., Kosař, K., Sigler, K., 2008. Optimised acidification power test of yeast vitality and its use in brewing practice. J. Inst. Brew. 114, 270–276.

Gibson, B.R., Lawrence, S.J., Leclaire, J.P.R., Powell, C.D., Smart, K.A., 2007. Yeast responses to stresses associated with industrial brewery handling, FEMS Microbiology Reviews.

Gómez, F., Toledo, R.T., Wadsö, L., Gekas, V., Sjöholm, I., 2004. Isothermal calorimetry approach to evaluate tissue damage in carrot slices upon thermal processing. J. Food Eng. 65, 165–173.

González, M., Canales, A.P., 1979. Spectrophotometric determination of vicinal diketones and their precursors in beer. J. Am. Soc. Brew. Chem. 37.

Grijspeerdt, K., Vanrolleghem, P., 1999. Estimating the parameters of the Baranyi-model for bacterial growth. Food Microbiol. 32, 31.

Hashimoto, M., Takahashi, K., 1982. Calorimetric studies of microbial growth: Quantitative relation between growth thermograms and inoculum size. Agric. Biol. Chem. 46, 1559–1564.

Heggart, H.M., Margaritis, A., Pilkington, H., Stewart, R.J., Dowhanick, T.M., Russel, I., 1999. Factors affecting yeast viability and vitality characterisitics: A review. Tech. quaterly - Master Brew. Assoc. Am. 36, 383–406.

Heggart, H.M., Margaritis, A., Stewart, R.J., Pilkington, H., Sobezak, J., Russel, I., 2000. Measurement of brewing yeast viability and vitality: A review of methods.pdf. Tech. quaterly - Master Brew. Assoc. Am. 37, 408–430.

Hoogerheide, J.C., 1975. Studies on the energy metabolism during anaerobic fermentation of glucose by baker's yeast. Radiat. Environ. Biophys. 11, 295–307.

Itoh, S., Takahashi, K., 1984. Calorimetric studies of microbial growth: Kinetic analysis of growth thermograms observed for bakery yeast at various temperatures. Agric. Biol. Chem. 48, 271–275.

Johansson, P., Wadsö, I., 1999. An isothermal microcalorimetric titration/perfusion vessel equipped with electrodes and spectrophotometer. Thermochim. Acta 342, 19–29.

Kandror, O., Bretschneider, N., Kreydin, E., Cavalieri, D., Goldberg, A.L., 2004. Yeast adapt to near-freezing temperatures by STRE/Msn2,4-dependent induction of Trehalose synthesis and certain molecular chaperones. Mol. Cell 13, 771–781.

Kaprelyants, a. S., Kell, D.B., 1992. Rapid assessment of bacterial viability and vitality by rhodamine 123 and flow cytometry. J. Appl. Bacteriol. 72, 410–422.

Kara, B. V, Simpson, W.J., Hammond, J.R.M., 1988. Prediction of the fermentation performance of brewing yeast with the acidification power test. J. Inst. Brew. 94, 153–158.

Kawachi, S., Arao, T., Hara, Y., Suzuki, Y., Tamura, K., 2010. Effects of compression with ethane, ethylene and their fluorinated derivatives on yeast growth. J. Phys. Conf. Ser. 215, 12168.

Kawachi, S., Hara, Y., Arao, T., Suzuki, Y., Tamura, K., 2010. Effects of compressed hydrocarbon gases on the growth activity of *Saccharomyces cerevisiae*. Biosci. Biotechnol. Biochem. 74, 1991–1996.

Kgari, G.L., 2008. Understanding the effect of cold stress on Brewers' Yeast quality. University of Cape Town.

Klingberg, T.D., Lesnik, U., Arneborg, N., Raspor, P., Jespersen, L., 2008. Comparison of *Saccharomyces cerevisiae* strains of clinical and nonclinical origin by molecular typing and determination of putative virulence traits. FEMS Yeast Res. 8, 631–640.

Kondo, K., Kowalski, L.R., Inouye, M., 1992. Cold shock induction of yeast NSR1 protein and its role in pre-rRNA processing. J. Biol. Chem. 267, 16259–65.

Kwolek-Mirek, M., Zadrag-Tecza, R., 2014. Comparison of methods used for assessing the viability and vitality of yeast cells. FEMS Yeast Res. 14, 1068–1079.

Ladbury, J.E., 2004. Application of isothermal titration calorimetry in the biological sciences: things are heating up! Biotechniques 37, 885–887.

Lamprecht, I., 1980. Growth and Metabolism in Yeasts. In: Beezer, A.E. (Ed.), Biological Microcalorimetry. Academic Press, London, pp. 43–112.

Lamprecht, I., Schaarschmidt, B., Welge, G., 1976. Microcalorimetric investigation of the metabolism of yeasts - V. Influence of ploidy on growth and metabolism. Radiat. Environ. Biophys. 13, 57–61.

Larsson, C., Nilsson, A., Blomberg, A., Gustafsson, L., 1997. Glycolytic flux is conditionally correlated with ATP concentration in *Saccharomyces cerevisiae*: a chemostat study under carbon- or nitrogen-limiting conditions. J Bacteriol 179, 7243–7250.

Lau, A., 2009. What Are Repeatability and Reproducibility? [WWW Document]. ASTM Stand. News.

URL http://www.astm.org/SNEWS/MA_2009/datapoints_ma09.html (accessed 6.2.15).

Lineweaver, H., Burk, D., 1934. The determination of enzyme dissociation constants. J. Am. Chem. Soc. 56, 658–666.

Lodolo, E.J., Kock, J.L.F., Axcell, B.C., Brooks, M., 2008. The yeast *Saccharomyces cerevisiae* - The main character in beer brewing. FEMS Yeast Res. 8, 1018–1036.

Madigan, M.T., Martinko, J.M., Stahl, D., Clark, D.P., 2010. Brock: Biology of Microorganisms, 13th Editi. ed. Prentice-Hall London.

Mager, W.H., Varela, J.C.S., 1993. Osmostress response of the yeast *Saccharomyces. Mol*. Microbiol. 10, 253–258.

Maskell, D.L., Kennedy, A.I., Hodgson, J.A., Smart, K.A., 2003. Chronological and replicative lifespan in Lager Brewing Yeast. In: Smart, K.A. (Ed.), Brewing Yeast Fermentation Performance. Blackwell Science, Oxford, UK, pp. 281–292.

Maskow, T., Harms, H., 2006. Real time insights into bioprocesses using calorimetry: State of the art and potential. Eng. Life Sci. 6, 266–277.

Meier-Schneiders, M., Schäfer, F., 1996. Quantification of small enthalpic differences in anaerobic microbial metabolism—a calorimetry-supported approach. Thermochim. Acta 275, 1–16.

Mirisola, M.G., Braun, R.J., Petranovic, D., 2013. Approaches to study yeast cell aging and death. FEMS Yeast Res. 14, 109–118.

Mochaba, F.M., O'Connor-Cox, E.S.C., Axcell, B.C., 1997. A novel and practical yeast vitality method based on Magnesium ion release. J. Inst. Brew. 103, 99–102.

Molecular Probes™, 2005. LIVE / DEAD ® Funga Light ™ Yeast viability kit quick facts.

Moonsamy, N., Mochaba, F., Majara, M., O'Connor-Cox, E.S.C., Axcell, B.C., 1995. Rapid yeast Trehalose measurement using near infrared reflectance spectrometry. J. Inst. Brew. 101, 203–206.

Morris, R.J., 1972. Lavoisier and the caloric theory. Br. J. Hist. Sci. 6, 1–38.

Murgier, M., Belaich, J.P., 1971. Microcalorimetric determination of the affinity of *Saccharomyces cerevisiae* for some carbohydrate growth substrates. J. Bacteriol. 105, 573–579.

Nagel, J.E., Fuscaldo, J.T., Fireman, P., 1977. Paraben Allergy. JAMA J. Am. Med. Assoc. 237, 1594.

Nkosi, J.C., 2001. The effect of cooling on Brewers' Yeast quality. University of Cape Town.

Okada, F., Kobayashi, A., Fujiwara, N., Takahashi, K., 1999. Bacteriostatic and bactericidal actions of antimicrobial drugs studied by microbial calorimetry. Biocontrol Sci. 4, 35–39.

Okuda, S., Takahashi, K., Nitta, Y., Fukada, H., Nakao, H., Kirihata, M., 1996. Theoretical aspects of the calorimetric analysis of antibacterial and antifungal actions (Japanese). J. Antibact. Antifung. Agents 24, 397–406.

Opekarová, M., Sigler, K., 1982a. Acidification power: indicator of metabolic activity and autolytic changes in *Saccharomyces cerevisiae*. Folia Microbiol. (Praha). 395–403.

Opekarová, M., Sigler, K., 1982b. Acidification power: Indicator of metabolic activity and autolytic changes in *Saccharomyces cerevisiae*. Folia Microbiol. (Praha). 27, 395–403.

Palhano, F.L., Orlando, M.T.D., Fernandes, P.M.B., 2004. Induction of baroresistance by hydrogen peroxide, ethanol and cold-shock in *Saccharomyces cerevisiae*. FEMS Microbiol. Lett. 233, 139–145.

Pankey, G. a, Sabath, L.D., 2004. Clinical relevance of bacteriostatic versus bactericidal mechanisms of action in the treatment of Gram-positive bacterial infections. Clin. Infect. Dis. 38, 864–870.

Peddie, F.L., Simpson, W.J., Kara, B. V., Robertson, S.C., Hammond, J.R.M., 1991. Measurement of endogenous Oxygen uptake rates of Brewers' Yeasts. J. Inst. Brew. 97, 21–25.

Pina, C., Santos, C., Couto, J.A., Hogg, T., 2004. Ethanol tolerance of five non-*Saccharomyces* wine yeasts in comparison with a strain of Saccharomyces cerevisiae—influence of different culture conditions. Food Microbiol. 21, 439–447.

Piper, P.W., Talreja, K., Panaretou, B., B, K., Praekelt, U.M., M, P., 1994. Induction of major heat-shock proteins of *Saccharomyces cerevisiae*, including plasma membrane Hsp30, by ethanol

levels above a critical threshold. Microbiology 140, 3031–3038.

Qian, Y., Yao, J., Russel, M., Wang, X., Sandy, E.H., 2015. Exploring medium-term impact of oxide nanoparticles on soil microbial activity by isothermal microcalorimetry and urease assay. Environ. Prog. Sustain. Energy n/a-n/a.

Rencken, I., Fleming, V., Meijering, I., Axcell, B., 1995. Determination of selected sterols and fatty acids in Yeast. J. Chromatogr. Sci. 33, 525–530.

Riis, S.B., Pedersen, H.M., Sorensen, N.K., Jakobsen, M., 1995. Flow cytometry and acidification power test as rapid techniques for determination of the activity of starter cultures of *Lactobacillus delbrueckii ssp. bulgaricus*. Food Microbiol. 12, 245–250.

Rong, X.-M., Huang, Q.-Y., Jiang, D.-H., Cai, P., Liang, W., 2007. Isothermal microcalorimetry: A review of applications in soil and environmental sciences. Pedosphere 17, 137–145.

Roy, D., Samson, R., 1988. Investigation of growth and metabolism of *Saccharomyces cerevisiae* (baker's yeast) using microcalorimetry and bioluminometry. J. Biotechnol. 8, 193–205.

Sahara, T., Goda, T., Ohgiya, S., 2002. Comprehensive expression analysis of time-dependent genetic responses in yeast cells to low temperature. J. Biol. Chem. 277, 50015–50021.

Šajbidor, J., Grego, J., 1992. Fatty acid alterations in *Saccharomyces cerevisiae* exposed to ethanol stress. FEMS Microbiol. Lett. 93, 13–16.

Sales, K., Brandt, W., Rumbak, E., Lindsey, G., 2000. The LEA-like protein HSP 12 in *Saccharomyces cerevisiae* has a plasma membrane location and protects membranes against desiccation and ethanol-induced stress. Biochim. Biophys. Acta - Biomembr. 1463, 267–278.

Schaarschmidt, B., Lamprecht, I., 1977. Microcalorimetric investigations of the metabolism of yeasts - VI. Diauxy during anaerobic growth on different saccharides. Radiat. Environ. Biophys. 14, 153–160.

Schaarschmidt, B., Lamprecht, I., 1978. Microcalorimetric study of yeast growth, utilization of different carbohydrates. Thermochim. Acta 22, 333–338.

Schaarschmidt, B., Zotin, A.I., Lamprecht, I., 1977. Quantitative relationship between heat production and weight during growth of microbial cultures. In: Lamprecht, I., Schaarschmidt, B. (Eds.), Application of Calorimetry in Life Sciences. Walter de Gruyter, Berlin, pp. 139–148.

Schade, B., Jansen, G., Whiteway, M., Entian, K.D., Thomas, D.Y., 2004. Cold adaptation in budding yeast. Mol. Biol. Cell 15, 5492–5502.

Schneiter, R., 2004. Genetics, Molecular and Cell Biology of Yeast. University of Fribourg, Fribourg, Switzerland.

Sherman, F., 2002. Getting Started with Yeast. Methods Enzymol. 350, 3–41.

Siebert, K.J., 2006. Haze formation in beverages. LWT - Food Sci. Technol. 39, 987–994.

Sigler, K., 2013a. Acidification power (AP) test and similar methods for assessment and prediction of fermentation activity of industrial microorganisms 2013, 204–208.

Sigler, K., 2013b. Acidification power (AP) test and similar methods for assessment and prediction of fermentation activity of industrial microorganisms. Kvasný průmysl 59, 204–208.

Sigler, K., Hofer, M., 1991. Mechanisms of acid extrusion in yeast. Biochim. Biophys. Acta - Rev. Biomembr. 1071, 375–391.

Sigler, K., Kotyk, A., Knotková, A., Opekarová, M., 1981. Processes involved in the creation of buffering capacity and in substrate-induced proton extrusion in the yeast *Saccharomyces cerevisiae*. Biochim. Biophys. Acta 643, 583–592.

Siro, M.-R., Romar, H., Lövgren, T., 1982. Continuous flow method for extraction and bioluminescence assay of ATP in baker's yeast. Eur. J. Appl. Microbiol. Biotechnol. 15, 258–264.

Smart, K.A., Chambers, K.M., Lambert, I., Jenkins, C., 1999. Use of Methylene Violet Staining Procedures to Determine Yeast Viability and Vitality. J. Am. Soc. Brew. Chem. 57, 18–23.

Stafford, R.A., 2003. Yeast Physical (Shear) Stress: The Engineering Perspective. In: Smart, K.A. (Ed.), Brewing Yeast Fermentation Performance. Wiley-Blackwell, Oxford, UK, pp. 39–45.

Stannard, C.J., Gibbs, P.A., 1986. Rapid microbiology: Applications of bioluminescence in the food industry a review. J. Biolumin. Chemilumin. 1, 3–10.

Stewart, G.G., 2001. Yeast management – the balance between fermentation efficiency and beer quality. Tech. quaterly - Master Brew. Assoc. Am. 38, 74–53.

TA Instruments, 2011. General Performance Test (GPT) for the TAM III. TA Instruments, New Castle, DE 19720, USA.

TA Instruments/TAMIII Brochure, 2012. Microcalorimetry. TA 25–47.

Takahashi, K., 2000. Calorimetric characterization of the inhibitory action of antimicrobial drugs and a proposal of bacteriostatic/bactericidal index. Netsu Sokutei 27, 170–178.

Theerarattananoon, K., Lin, Y.H., Peng, D.Y., 2008. Metabolic heat evolution of *Saccharomyces cerevisiae* grown under very-high-gravity conditions. Process Biochem. 43, 1253–1258.

Thonart, P., Custinne, M., Paquot, M., 1982. Zeta potential of yeast cells: application in cell immobilization. Enzyme Microb. Technol. 4, 191–194.

Trampuz, A., Salzmann, S., Antheaume, J., Daniels, A.U., 2007a. Microcalorimetry: A novel method for detection of microbial contamination in platelet products. Transfusion 47, 1643–1650.

Trampuz, A., Steinhuber, A., Wittwer, M., Leib, S.L., 2007b. Rapid diagnosis of experimental meningitis by bacterial heat production in cerebrospinal fluid. BMC Infect. Dis. 7, 116.

Tsukamoto, I., Constantinoiu, E., Furuta, M., Nishimura, R., Maeda, Y., 2004. Inactivation effect of sonication and chlorination on *Saccharomyces cerevisiae*. Calorimetric Analysis. Ultrason. Sonochem. 11, 167–172.

Van Uden, N., 1983. Effects of ethanol on the temperature relations of viability and growth in Yeast. Crit. Rev. Biotechnol. 1, 263–272.

van Zandycke, S.M., Simal, O., Gualdoni, S., Smart, K.A., 2010a. Yeast Quality and Fluorophore Technologies. In: Smart, K.A. (Ed.), Brewing Yeast Fermentation Performance. Wiley-Blackwell, Oxford, UK, pp. 149–161.

van Zandycke, S.M., Simal, O., Smart, K.A., 2010b. Vitality assessment using the fluorescent stain FUN1. In: Smart, K.A. (Ed.), Brewing Yeast Fermentation Performance. Blackwell Science, Oxford, UK, pp. 162–168.

Villadsen, J., Nielsen, J., Liden, G., 2011. Bioreaction Engineering Principles, Third Edit. ed. Springer, London.

von Ah, U., Wirz, D., Daniels, A.U., 2009. Isothermal micro calorimetry--a new method for MIC determinations: results for 12 antibiotics and reference strains of E. coli and S. aureus. BMC Microbiol. 9, 106.

von Stockar, U., Birou, B., 1989. The heat generated by yeast cultures with a mixed metabolism in the transition between respiration and fermentation. Biotechnol. Bioeng. 34, 86–101.

Wadsö, I., 1997. Trends in isothermal microcalorimetry. Chem. Soc. Rev. 26, 79.

Wadsö, I., 2009. Characterization of microbial activity in soil by use of isothermal microcalorimetry. J. Therm. Anal. Calorim. 95, 843–850.

Wadsö, I., Goldberg, R.N., 2001. Standards in isothermal microcalorimetry (IUPAC Technical Report). Pure Appl. Chem. 73, 1625–1639.

Wadsö, I., Wadsö, L., 2005. Systematic errors in isothermal micro- and nanocalorimetry. J. Therm. Anal. Calorim. 82, 553–558.

Wadsö, L., 2010. Operational issues in isothermal calorimetry. Cem. Concr. Res. 40, 1129–1137.

Wadsö, L., Gómez Galindo, F., 2009. Isothermal calorimetry for biological applications in food science and technology. Food Control 20, 956–961.

Walker, G.M., 1998. Yeast Physiology and Biotechnology. John Wiley & Sons, New York.

Welch, A.Z., Koshland, D.E., 2013. A simple colony-formation assay in liquid medium, termed “tadpoling”, provides a sensitive measure of *Saccharomyces cerevisiae* culture viability. Yeast 30, 501–9.

White, C., Zainasheff, J., 2010. Yeast: The Practical Guide to Beer Fermentation. Brewers

Publications, A Division ofthe Brewers Association, Colorado.

White, L.R., Richardson, K.E., Schiewe, A.J., White, C.E., 2003. Comparison of Yeast Viability/Vitality Methods and Their Relationship to Fermentation Performance. In: Smart, K.A. (Ed.), Brewing Yeast Fermentation Performance. Wiley-Blackwell, Oxford, UK, pp. 138–148.

White Labs, 2014. Cell Counting/Viability Testing [WWW Document]. URL http://www.whitelabs.com/beer/cell-counting-viability-testing-0 (accessed 6.17.15).

Wirkner, S., Takahashi, K., 2000. Some Theoretical Considerations on Calorimetrically Determined Bactericidality of Antimicrobial Drugs and Its Concentration Dependence. Netsu Sokutei 27, 179–185.

Wirkner, S., Takahashi, K., Furuta, M., Hayashi, T., 2001. Calorimetric Analysis of the Effect of Co-60 y-rays on the Growth of *Saccharomyces cerevisiae*. Netsu Sokutei 28, 106–113.

Wirkner, S., Takahashi, K., Furuta, M., Hayashi, T., 2002. Calorimetric study on the effect of Co-60 gamma-rays on the growth of microorganisms. Radiat. Phys. Chem. 63, 327–330.

Xie, W., 2008. Determination of NAD+ and NADH level in a single cell under H2O2 stress by capillary electrophoresis. Iowa State University.

Yang, L.N., Sun, L.X., Xu, F., Zhang, J., Zhao, J.N., Zhao, Z.B., Song, C.G., Wu, R.H., Ozao, R., 2010. Inhibitory study of two cephalosporins on *E. coli* by microcalorimetry. J. Therm. Anal. Calorim. 100, 589–592.

Yonsel, S., Bulbül-Çaliskan, G., Köni, M., Dagasan, L., Bülbül-Çaliskan, G., Köni, M., Dagasan, L., 2007. Monitoring of yeast metabolism with calorimetry. Chem. Biochem. Eng. Q. 21, 395–408.

Zabriskie, D.W., Humphrey, A.E., 1978. Estimation of fermentation biomass concentration by measuring culture fluorescence. Appl. Environ. Microbiol. 35, 337–343.

Zhang, Q., Liu, X., Ma, X., Fang, J., Fan, T., Wu, F., An, L., Feng, H., 2014. Microcalorimetric study of the effects of long-term fertilization on soil microbial activity in a wheat field on the Loess Plateau. Ecotoxicology 23, 2035–2040.

APPENDIX A. Analytical Methods

A.1 Methylene violet (alkaline) staining procedure

Reagents:

Methylene Violet 3RAX (Sigma-Aldrich), deionized water, glycine, NaOH.

Procedure:

1. Prepare methylene violet stock solution by dissolving methylene violet 3RAX in deionized water to a final concentration of 0.1% (w/v).
2. Prepare 0.1 *M* glycine buffer solution via the addition of glycine to deionized water. Adjust pH of 0.1 *M* glycine buffer to a pH of 10.6 using concentrated NaOH.
3. Dilute methylene violet stock solution 10-fold using 0.1 *M* glycine buffer (pH =10.6) – this constitutes the 'ready to use' stain.
4. Add 0.5 ml of ready to use stain with 0.5 ml of yeast cells in suspension*. Yeast suspension should contain ca. 10^7 cells/ml.
5. Vortex solution and allow to stand for ca. 10 minutes at room temperature (22 °C).
6. Pipette 1.3 µl onto a Helber (Hawksley) counting chamber.
7. Perform a cell count noting the cells that are stained violet (dead) and those that appear colourless (viable – living cells) using and Olympus (Olympus Optical co. Ltd, Japan) BX40F light microscope (100x magnification objective lens, with oil immersion) under phase 2 brightfields optics. See Section cell counting Appendix A.3 for further information.

Results:

In Figure A-1 and Figure A-2, examples of unstained (viable) and methylene violet stained (dead) cells can be observed, respectively. In the original procedure formulated by Smart et al. (1999), the yeast was washed and centrifuged three times using deionized water. In this work, washing of the yeast was found to be detrimental to the staining procedure as it resulted in all the cells being stained (0% viability). A possible cause for these erroneous viabilities could be due to the cells experiencing extreme osmotic shock during the washing procedure as they adapt from having grown on solid media to adjusting to growth in a liquid culture. This method was shown to be reproducible throughout Chapters 4 and 5.

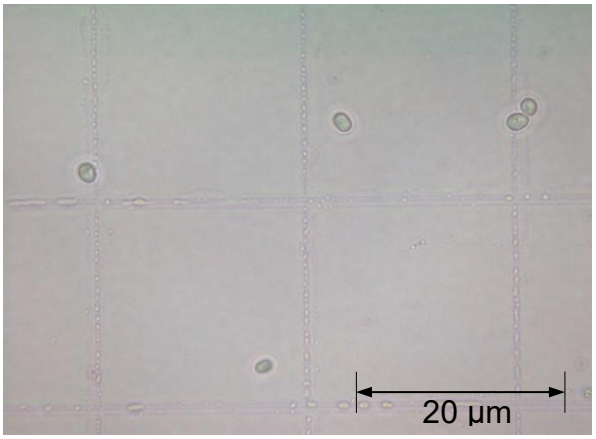

Figure A-1: Healthy yeast cells under 1000x magnification. Since these cells are healthy and able to metabolize the staining agent they remain colourless – unstained.

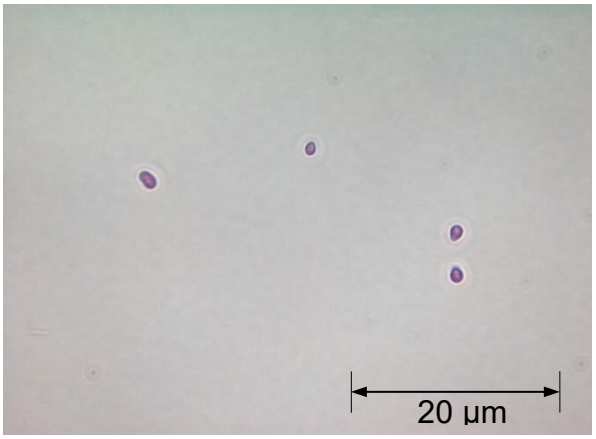

Figure A-2: Heat-killed, violet stained, yeast cells under 1000x magnification.

Table A-1: Reproducibility of methylene violet staining procedure

	Viability determined using methylene violet stain (%)				Average (%)	Standard deviation (%)
	Sample 1	Sample 2	Sample 3	Sample 4		
Healthy cells from YPD petri-dish	100	100	100	99	99.8	0.5
Heat-killed cells (10 min in a 80 °C heating block)	0	0	0	0	0	-
50/50 mix (by volume) of heat-killed cells to healthy cells from YPD petri-dish	50	53.3	50	38.9	48.1	6.3

A.2 Acidification power test

Reagents:

Distilled water, NaOH, glucose

Procedure:

Since the original APT was developed with brewery application in mind the amount of yeast required for the optimized APT as described by Gabriel et al. (2008) requires significantly more yeast than can be easily be grown on solid media. The test was thus adapted to work using lower volumes but the same concentrations.

Table A-2: Comparison of procedures literature procedure of the APT and the adapted procedure used in this study

Step	Adapted procedure applied in this study.	Procedure as described by Gabriel et al. (2008).
1	Yeast was grown on a YPD agar petri-dish at 30 °C for 72 hours.	Yeast samples from brewery were stored for up to 10 days at 2 °C, kept under beer.
2	Place approximately 330mg of wet yeast from an agar petri-dish into a 2 ml Eppendorf tube in the form of a yeast slurry in suspension[a].	Pour ~5 ml of thick yeast slurry into a centrifugation vessel and leave to stand for 15 minutes at room temperature.
3	Centrifuge the slurry at 600 rcf for 3 minutes.	Centrifuge slurry at 145 rcf for 1 minute.
4	Discard the supernatant.	
5	Re-suspend the yeast pellet using 1 ml deionized water (pH 6.3) by gently using a pipette to suck the water up and down until no more yeast clumps remain	Re-suspend the yeast pellet using 15 ml deionized water by mixing thoroughly
6	Centrifuge the slurry at 600 rcf for 3 minutes.	Centrifuge slurry at 145 rcf for 1 minute.
7	Repeat steps 4,5,6.	
8	Discard the supernatant.	
	Re-suspend the yeast pellet using 1 ml deionized water (pH 6.3) by gently using a pipette to suck the water up and down until no more yeast clumps remain.	Re-suspend the yeast pellet using 15 ml deionized water by mixing thoroughly.
9	Centrifuge the slurry at 1000 rcf for 10 minutes[a].	Centrifuge slurry at 1400 rcf for 10 minutes[a].
10	Discard the supernatant.	
11	Ensure that there is between 270mg – 360mg (9-12 g/100 ml) in the Eppendorf tube (this is usually achieved by the removal of a small portion of the wet yeast).	Weigh out between 1.5 g – 2 g of yeast into a measuring vessel.
12	Add 1 ml of deionised water (pH =6.3) is added to the yeast pellet (pH_0). Ensure that the yeast pellet is fully suspended (by using a pipette to suck up and down) before transferring the 1 ml of slurry into a 5 ml glass Bijoux bottle with stirrer bar. Use a further 1 ml of deionised water (pH6.3) to wash the remaining yeast slurry out of the Eppendorf tube into the Bijoux bottle. Lastly, add 1 ml of deionised water to the bijoux bottle (pH6.3). This gives a total volume of 3 ml of yeast slurry in the Bijoux bottle. Start the test timing upon the first addition of water (pH_0).	Add 15 ml of Aqual (reverse osmosis) water to the measuring vessel, and vortex 15 s to achieve a homogeneous cell suspension. Start the test timing upon the first addition of water (pH_0).
13	Place the Bijoux bottle on a magnetic stirrer set to ~250 rpm. Keep temperature between 22±1.5 °C (laboratory ambient temperature).	Set the stirring rate at >200 rpm. Keep temperature between 25±0.5 °C.

Step	Adapted procedure applied in this study.	Procedure as described by Gabriel et al. (2008).
14	Place a micro-pH probe (CyberScan 2500 pH)[b] into the liquid slurry. Record the initial pH	Thermostat the measuring vessel at 25 °C, while continuously recording the pH using a YATA pH instrument.
15	After 10 minutes record the pH (pH_{10}) and then add 1 ml of 20% glucose (yields an overall glucose concentration of 5%).	After 10 minutes add the required amount of glucose solution to achieve a glucose concentration of 5%.
16	Record the pH after 20 minutes (pH_{20}).	[pH is automatically logged throughout by the YATA pH instrument]

[a]Gabriel et al. (2008) report that the yeast pellet can be left for up to 6 hours kept under deionized water at room temperature.
[b]Calibrate the pH probe using the two standard buffer (pH 7 and pH 4) method.

The acidification power value is equal to 6.3 – pH_{20}. The typical APT value for healthy cells was 3, with the overall standard deviation being less than 2% - see Appendix D for further analysis.

A.3 Cell counting procedure

The use of cell counts using a light microscope is common in the brewing industry in order to determine the pitching rate (the amount of yeast added to a fresh batch of wort to start a brew). Cells are usually counted using a counting chamber/haemocytometer. Cells are easiest to count when they are in the 10^7 – 10^8 cells/ml range. In most instances, a number of serial dilutions are required to achieve this cell concentration. The cell numbers present in the original yeast slurry/suspension can easily be determined by taking into account the volume of the counting chamber and the number of serial dilutions.

Reagents:

Cell suspension to be counted, microscope oil, microscope lens tissue, Olympus BX40 Microscope and Haemocytometer (Helber counting chamber, Hawskey product).

Procedure:

1. Mix the cell suspension to be counted by vortexing for a few seconds to ensure a homogenous cell suspension.
2. Pipette 1.3 µl of the cell suspension onto a Haemocytometer (Helber counting chamber, Hawskey product).
3. Place a glass coverslip on top of the counting chamber. Ensure that there are no bubbles present.
4. Place a drop of oil on top of the cover slip
5. Place the counting chamber under the 100x (objective lens) oil immersion lens of the Olympus BX40 Microscope (10 x eyepiece). Either phase 2 or phase 3 brightfield light can be used.
6. Focus the microscope.

7. Count one large block, consisting of 16 (4x4) smaller squares. If the number of cells present in each large block exceeds ~60 cells then further dilution is required.
8. Count a further 3 large blocks, separated by one large block.
9. Record the number of cells observed (and note their colour if performing the methylene violet assay).
10. Calculate the cell concentration as follows:

$$(sum\ of\ cells\ counted\ in\ each\ large\ block) * 312500 * dilution\ factor = cell\ concetration/ml$$

The constant 312500 is calculated based on the counting chamber volume – counting chamber depth = 0.02mm and area = 1/400 mm^2.

A.4 Yeast streaking procedure

Due to the yeast used for all experiments originating from yeast grown on solid YPD agar media the manner in which the streaking was carried out was important.

Procedure:

1. Sterilize a streaking loop using a flame until the loop appears red hot.
2. Cool the loop on a clear patch of agar on the petri-dish that contains the colony to be picked to streak a new petri-dish.
3. Using the loop, pick a single colony of yeast and spread this colony on a fresh, sterile, YPD agar petri-dish. Spread the yeast in such a manner so as to cover one quarter to one fifth of the edge of an agar petri-dish.
4. Re-heat the streaking loop until red hot.
5. Touch the loop to a clear patch of agar, to cool the loop. Rotate the petri-dish 30 degrees and streak approximately 8 times from the cells deposited in step 3.
6. Re-heat the streaking loop until red hot.
7. Touch the loop to a clear patch of agar, to cool the loop. Rotate the petri-dish 30 degrees and streak approximately 5 times from the cells deposited from the streak lines of step 5.
8. Re-heat the streaking loop until red hot.
9. Touch the loop to a clear patch of agar, to cool the loop. Rotate the petri-dish 30 degrees and streak approximately 3 times from the cells deposited from the streak lines of step 7. See Figure A-3 for an illustration of the streaking procedure.

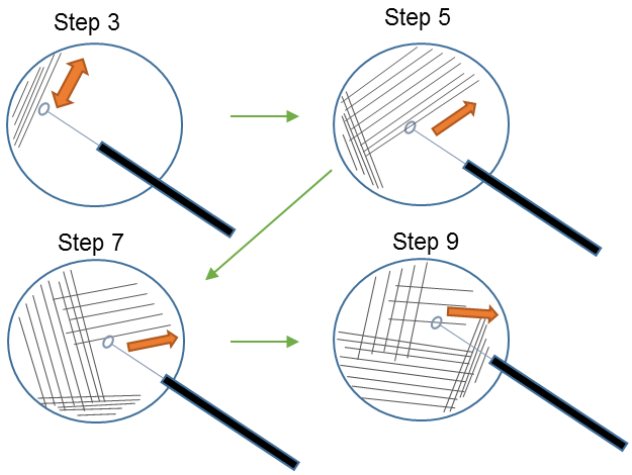

Figure A-3: Illustration of the streaking procedure employed. Step numbers refer to the procedure stated above.

A.5 Excel macro developed using VBA code to process raw data

Below is the VBA code that was developed to somewhat automate the processing of the raw heat data in Excel to improve the data analysis efficiency and reproducibility. The macro relies on relative cell referencing and a relative time scale (starting at t = 0) to be first set up. The macro further requires there to be 21 rows between the start of the data set and the top of the Excel sheet. Once the data has been extracted from the TAMIII assistant software (excluding any form of normalized data) the Macro should be run by clicking in the cell at the top of the heat data for each channel.

The code is shown in 2 column format to reduce its overall page length.

```
Sub Macro7_plus()
'
' Macro7_plus Macro
'
' Keyboard Shortcut: Ctrl+q
'


' turns off screen update + autocalculate

   Application.ScreenUpdating = False

   Application.Calculation = xlCalculationManual

' adds columns
    ActiveCell.Offset(0,
1).Columns("A:A").EntireColumn.Select
    Selection.Insert                Shift:=xlToRight,
CopyOrigin:=xlFormatFromLeftOrAbove

ActiveCell.Columns("A:A").EntireColumn.Select
    Selection.Insert                Shift:=xlToRight,
CopyOrigin:=xlFormatFromLeftOrAbove

ActiveCell.Columns("A:A").EntireColumn.Select
    Selection.Insert                Shift:=xlToRight,
CopyOrigin:=xlFormatFromLeftOrAbove

ActiveCell.Columns("A:A").EntireColumn.Select
    Selection.Insert                Shift:=xlToRight,
CopyOrigin:=xlFormatFromLeftOrAbove
    ActiveCell.Offset(20, -1).Range("A1").Select

    ActiveCell.Offset(-4, 0).Range("A1").Select
    ActiveCell.FormulaR1C1 = "A"
    ActiveCell.Offset(1, 0).Range("A1").Select
    ActiveCell.FormulaR1C1 = "B"
    ActiveCell.Offset(1, 0).Range("A1").Select
    ActiveCell.FormulaR1C1 = "u"
    ActiveCell.Offset(-2, 1).Range("A1").Select
    ActiveCell.FormulaR1C1 = "0.01"
    ActiveCell.Offset(1, 0).Range("A1").Select
    ActiveCell.FormulaR1C1 = "-0.04"
    ActiveCell.Offset(1, 0).Range("A1").Select
    ActiveCell.FormulaR1C1 = "0.369"
    ActiveCell.Offset(2, 0).Range("A1").Select
    ActiveCell.FormulaR1C1 = "heat-heatCh1"

    ActiveCell.Offset(1, 0).Range("A1").Select
    ActiveCell.FormulaR1C1 = "=RC[-1]-RC4"
    ActiveCell.Select


    Selection.Copy
    ActiveCell.Offset(0, -1).Range("A1").Select
    Selection.End(xlDown).Select
    ActiveCell.Offset(0, 1).Range("A1").Select
    Range(Selection, Selection.End(xlUp)).Select
    ActiveSheet.Paste
    ActiveCell.Offset(0, 0).Range("A1").Select
    Selection.End(xlUp).Select
    ActiveCell.Offset(0, 1).Range("A1").Select

    ActiveCell.Offset(-12, 0).Range("A1").Select
    ActiveCell.FormulaR1C1    =    "=COLUMN(R[-
5]C[-1])"
    ActiveCell.Offset(1, 0).Range("A1").Select
    ActiveCell.FormulaR1C1 = "=ROW(R[7]C[-1])"
    ActiveCell.Offset(1, 0).Range("A1").Select
    ActiveCell.FormulaR1C1    =    "=ADDRESS(R[-
1]C,R[-2]C,1,1)"
    ActiveCell.Offset(1, 0).Range("A1").Select
    ActiveCell.FormulaR1C1    =    "=ADDRESS(R[-
2]C+1,R[-3]C,1,1)"
    ActiveCell.Offset(1, 0).Range("A1").Select
    ActiveCell.FormulaR1C1    =    "=ADDRESS(R[-
3]C+2,R[-4]C,1,1)"
    ActiveCell.Offset(8, 0).Range("A1").Select
    ActiveCell.FormulaR1C1 = "f(t)"
    ActiveCell.Offset(1, 0).Range("A1").Select
    ActiveCell.FormulaR1C1 = _

"=INDIRECT(R11C)*EXP(INDIRECT(R13C)*RC
2)+INDIRECT(R12C)"


  ' new section

    Selection.Copy
    ActiveCell.Offset(0, -1).Range("A1").Select
    Selection.End(xlDown).Select
    ActiveCell.Offset(0, 1).Range("A1").Select
    Range(Selection, Selection.End(xlUp)).Select
    ActiveSheet.Paste
    ActiveCell.Offset(0, 1).Range("A1").Select

    ActiveCell.Offset(-1, 0).Range("A1").Select
    ActiveCell.FormulaR1C1 = "Error^2"
    ActiveCell.Offset(1, 0).Range("A1").Select

     ActiveCell.FormulaR1C1    =    "=(RC[-1]-RC[-
2])^2"
    ActiveCell.Select
    Selection.Copy
    ActiveCell.Offset(0, -1).Range("A1").Select
    Selection.End(xlDown).Select
    ActiveCell.Offset(0, 1).Range("A1").Select
    Range(Selection, Selection.End(xlUp)).Select
    ActiveSheet.Paste
    ActiveCell.Offset(0, 0).Range("A1").Select


'turns auto calc back on

    Application.Calculation                    =
xlCalculationAutomatic

     ActiveCell.Offset(-20, 0).Range("A1").Select
```

```
    'Application.CutCopyMode = False
    ActiveCell.FormulaR1C1 = "=COLUMN(R[1]C[-
4])"
    ActiveCell.Offset(1, 0).Range("A1").Select
    ActiveCell.FormulaR1C1 = "=ADDRESS(1,R[-
1]C,1,1)"
    ActiveCell.Offset(1, 0).Range("A1").Select
    ActiveCell.FormulaR1C1 = "=ADDRESS(3,R[-
2]C,1,1)"
    ActiveCell.Offset(1, 0).Range("A1").Select
    ActiveCell.FormulaR1C1 =
"=ADDRESS(10000,R[-3]C,1,1)"
    ActiveCell.Offset(1, 0).Range("A1").Select
    ActiveCell.FormulaR1C1 =
"=MAX(INDIRECT(R[-3]C):INDIRECT(R[-1]C))"
    ActiveCell.Offset(1, 0).Range("A1").Select
    Selection.FormulaArray = _
        "=MATCH(MAX(INDIRECT(R[-
4]C):INDIRECT(R[-2]C)),(INDIRECT(R[-
4]C):INDIRECT(R[-2]C)),0)"
    ActiveCell.Offset(1, 0).Range("A1").Select
    ActiveCell.FormulaR1C1 = "=ADDRESS(R[-
1]C,R[-6]C,1,1)"
    ActiveCell.Offset(1, 0).Range("A1").Select
    Selection.FormulaArray = _
        "=(MATCH(MIN(ABS(INDIRECT(R[-
5]C):INDIRECT(R[-1]C)-0.7*R[-
3]C)),(ABS(INDIRECT(R[-5]C):INDIRECT(R[-
1]C)-0.7*R[-3]C)),0))+2"
    ActiveCell.Offset(1, 0).Range("A1").Select
    ActiveCell.FormulaR1C1 = "=ADDRESS(R[-
1]C,R[-8]C,1,1)"
    ActiveCell.Offset(1, 0).Range("A1").Select
    Selection.FormulaArray = _
        "=(MATCH(MIN(ABS(INDIRECT(R[-
7]C):INDIRECT(R[-3]C)-0.1*R[-
5]C)),(ABS(INDIRECT(R[-7]C):INDIRECT(R[-
3]C)-0.1*R[-5]C)),0))+2"
    ActiveCell.Offset(1, 0).Range("A1").Select
    ActiveCell.FormulaR1C1 = "=ADDRESS(R[-
1]C,R[-10]C,1,1)"
    ActiveCell.Offset(1, 0).Range("A1").Select
    ActiveCell.FormulaR1C1 = "=R[-11]C+4"
    ActiveCell.Offset(1, 0).Range("A1").Select
    ActiveCell.FormulaR1C1 = "=ADDRESS(R[-
5]C,R[-1]C,1,1)"
    ActiveCell.Offset(1, 0).Range("A1").Select
    ActiveCell.FormulaR1C1 = "=ADDRESS(R[-
4]C,R[-2]C,1,1)"
    ActiveCell.Offset(1, 0).Range("A1").Select
    ActiveCell.FormulaR1C1 =
"=SUM(INDIRECT(R[-1]C):INDIRECT(R[-2]C))"
    ActiveCell.Offset(1, 0).Range("A1").Select
    ActiveCell.FormulaR1C1 = "=ADDRESS(R[-
6]C,R[-15]C+2,1,1)"
    ActiveCell.Offset(1, 0).Range("A1").Select
    ActiveCell.FormulaR1C1 = "=ADDRESS(R[-
9]C,R[-16]C+2,1,1)"
    ActiveCell.Offset(1, 0).Range("A1").Select
    ActiveCell.FormulaR1C1 = "=ADDRESS(R[-
8]C,R[-17]C+3,1,1)"
    ActiveCell.Offset(1, 0).Range("A1").Select
    ActiveCell.FormulaR1C1 = "=ADDRESS(R[-
11]C,R[-18]C+3,1,1)"

    ActiveCell.Range("A1").Select

    ActiveCell.Offset(-4, 0).Range("A1").Select
    SolverReset
    SolverOk SetCell:=ActiveCell, MaxMinVal:=2,
ValueOf:=0,
ByChange:=Range(ActiveCell.Offset(1, -2),
ActiveCell.Offset(3, -2)), Engine:=1,
EngineDesc:="GRG Nonlinear"
        SolverOptions Assumenonneg:=False
    SolverSolve True

   SolverOk SetCell:=ActiveCell, MaxMinVal:=2,
ValueOf:=0,
ByChange:=Range(ActiveCell.Offset(1, -2),
ActiveCell.Offset(3, -2)), Engine:=1,
EngineDesc:="GRG Nonlinear"
        SolverOptions Assumenonneg:=False
    SolverSolve True

   SolverOk SetCell:=ActiveCell, MaxMinVal:=2,
ValueOf:=0,
ByChange:=Range(ActiveCell.Offset(1, -2),
ActiveCell.Offset(3, -2)), Engine:=1,
EngineDesc:="GRG Nonlinear"
        SolverOptions Assumenonneg:=False
    SolverSolve True


    Application.Calculation = xlCalculationManual

    ActiveCell.Offset(-2, -3).Range("A1").Select
    ActiveCell.FormulaR1C1 = "R^2"
    ActiveCell.Offset(0, 1).Range("A1").Select
    ActiveCell.FormulaR1C1 = _

"=RSQ(INDIRECT(R[5]C[2]):INDIRECT(R[6]C[2])
,INDIRECT(R[3]C[2]):INDIRECT(R[4]C[2]))"
    ActiveCell.Offset(1, 0).Range("A1").Select

    ActiveCell.Offset(0, -1).Range("A1").Select
    ActiveCell.FormulaR1C1 = "t_max"
    ActiveCell.Offset(1, 0).Range("A1").Select
    ActiveCell.FormulaR1C1 = "t_50"
    ActiveCell.Offset(-1, 1).Range("A1").Select
    ActiveCell.FormulaR1C1 =
"=INDIRECT(ADDRESS(R[-8]C[2],2,1,1))"
    ActiveCell.Offset(1, 0).Range("A1").Select
    Selection.FormulaArray = _

"=INDIRECT(ADDRESS(((MATCH(MIN(ABS(IN
DIRECT(R[-12]C[2]):INDIRECT(R[-8]C[2])-
0.5*R[-10]C[2])),(ABS(INDIRECT(R[-
```

```
12]C[2]):INDIRECT(R[-8]C[2])-0.5*R[-
10]C[2])),0))+2),2,1,1))"

    ActiveCell.Offset(-14,
2).Range("A1:A18").Select
    'ActiveCell.Offset(4, 2).Range("A1").Activate
    With Selection.Font
        .ThemeColor = xlThemeColorDark1
        .TintAndShade = 0
    End With
     ActiveCell.Offset(18, 0).Range("A1").Select
    With Selection.Font
        .ThemeColor = xlThemeColorDark1
        .TintAndShade = 0
    End With
    ActiveCell.Offset(-7, -3).Range("A1").Select

    ActiveCell.Offset(-4, 2).Range("A1:A5").Select
    With Selection.Font
        .ThemeColor = xlThemeColorDark1
        .TintAndShade = 0
    End With
    ActiveCell.Offset(4, -2).Range("A1").Select

' turns on screen update + autocalculate


    Application.Calculation                         =
xlCalculationAutomatic
    Application.ScreenUpdating = True


End Sub
```

APPENDIX B. TAM III operational matters

There were a number of issues encountered throughout the execution of the experimental programme. These issues help further inform minor details regarding the 'best practice' experimental method to be employed. A number of these issues, and how they were corrected, for are outlined below:

1. Observing a slight rise in the heat flow after the main heat flow peak. This 'residual heat flow output can be observed in Figure A-4 from t = 17 hours onwards. This 'late rise' in heat output is considered significant and has a magnitude of approximately 10% of the maximum heat flow. The most likely cause for this late rise in heat output is due to the growth of yeast on the sides and in the cap of the ampule (i.e. yeast not growing in the liquid). It was consistently observed that if the sealed ampoules were tilted before being loaded into the IMC the late rise in heat flow would occur without fail. Whenever the ampoules were kept upright, this same phenomenon would not occur. It is hypothesized that the occurrence of this late peak in heat flow is due to the growth of yeast colonies on the ampoule walls and in the ampoule cap. The occurrence of such growth was confirmed upon visual inspection of the ampoules. These yeast colonies are not exposed to the same conditions as the yeast in the liquid. These yeast colonies are not exposed to the same toxic build-up of metabolic waste products in the liquid.
2. It was found that flaming the necks of the glass IMC ampoules prior to crimping also helped reduce the occurrence of any potential growth of yeast in the neck of the ampoule or in the metal cap, while also reducing the chance of contamination. The flaming of the neck of the ampoule with the un-crimped metal cap also helped make the crimping process easier and resulted in less deformation of the metal caps by the crimping tool.
3. The pressure in the ampoules cannot exceed more than approximately 2.5 bar without the metal cap potentially swelling or being dislodged. Therefore in the case of yeast, that has the ability to grow anaerobically and produce carbon dioxide, a pressure build-up can occur. In order to ensure that the pressure in the ampoule did not exceed 2.5 bar it was calculated (see Appendix B.3) that no more than 1 ml of YPD broth should be loaded into the ampoule.

B.1 Record of discarded channel data

Table A-3: Record of discarded experimental channel and run data

Date of run	Run name	Run type	Discarded data	Reason
12/04/2015	Yeast crude method – rep1	N_0 = 10^4	All channels	The ampoule were not kept upright causing yeast growth on the sides and in the caps of the ampoules. Additionally the cap of ampoule in Ch4 did not seal properly.
15/04/2015	Crude method rep2	N_0 = 10^4	Ch4, Ch6	Ch4 – ampoule became logged in TAMIII. Technician was called to remove the ampoule at a later stage. Ch6 – Clear outlier. This ampoule was knocked over during the loading procedure resulting on yeast growth on the walls of the ampoule.
02/06/2015	Full run – heat-killed cells	Heat-killed cells mixed with healthy cells	Ch5	Ch5 – ampoule broke and was re-loaded non-sterile.
25/06/2015	Slow cold shock 25_06	Slow cold shocked cells	All channels	The final baseline for each channel was taken incorrectly.
06/07/2015	Fast cold shock 06_07	Rapid cold shock	All channels	Widespread contamination in all channels that could be observed visually (turbidity in control sample – and presence of bacteria when examined under the microscope) and by the calorimetric signal.
06/08/2015	EtOH shock 06_08	Ethanol shock	Ch3	Ampoule was not properly sealed/crimped
20/08/2015	Combined EtOH and cold shock 20_08	Rapid cold shock cells	Ch4	Ampoule was re-crimped and fell on its side

B.2 Errors resulting due to improper procedural protocol

In the figures below, screen shots were taken of the thermograms recorded for experiments where the runs where the experimental data was discarded due to the occurrence of an immediately observable error. The source of the error is briefly discussed in the Caption of each Figure below.

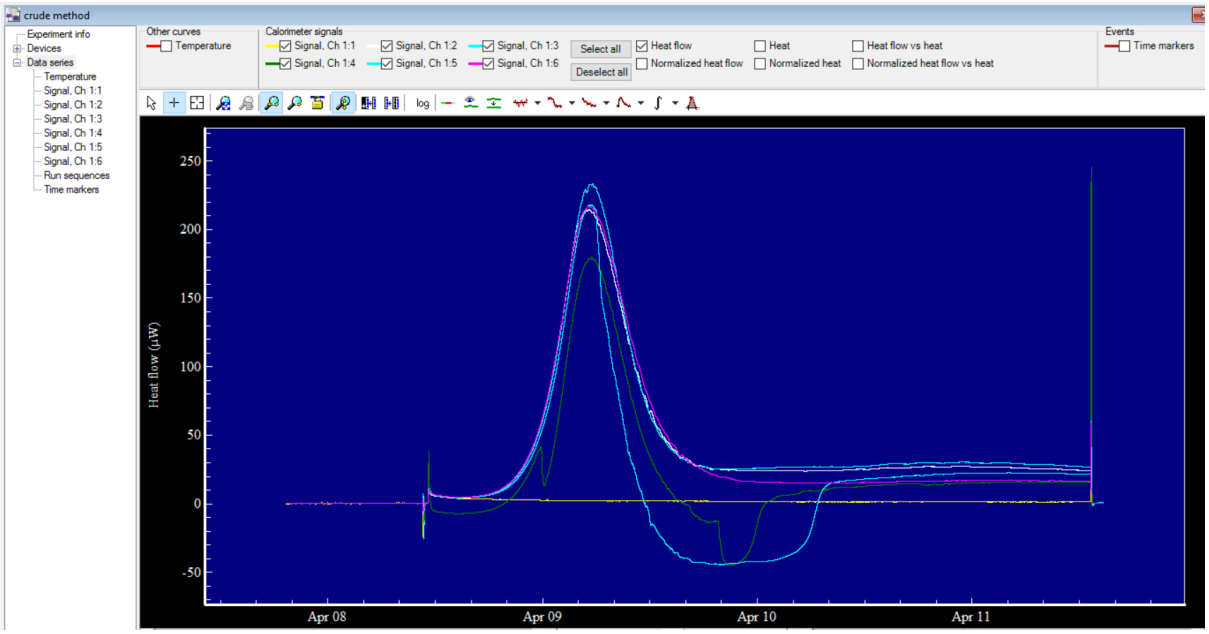

Figure A-4: Thermogram from experiments performed on 08/04/2015.
Run data was disregarded due to improperly sealed ampoules which is apparent from the heat flow curves that are negative, and the fact that the ampoules were not help upright therefore there was growth on the ampoule sides causing significant heat to be produced even after the main heat flow had occurred.

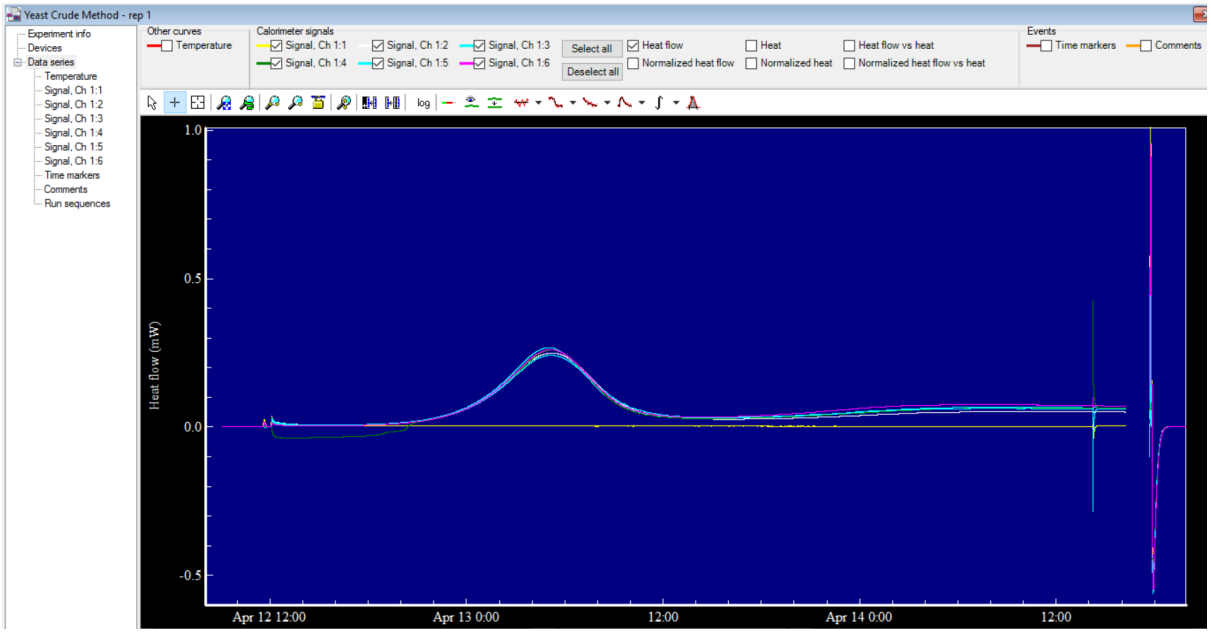

Figure A-5: Thermogram from experiments performed on 12/04/2015.
Run data was disregarded due to a power outage that occurred towards the end of the experiment which caused the disturbances seen in the heat flow curve. The ampoules in this run were also not help upright, causing significant heat to be produced even after the main heat flow had occurred.

The most likely cause of the elevated heat output long after the peak in heat flow was observed is that due to the ampoules being turned side-ways, there was yeast growing on the sides of the ampoule. This yeast was thus not exposed to any toxic buildup of nutrients and also had

more oxygen readily available. Thus the yeast growing on the side of the ampoule could continue to grow and respire for longer – causing the long heat flow 'tail observed in the figures above.

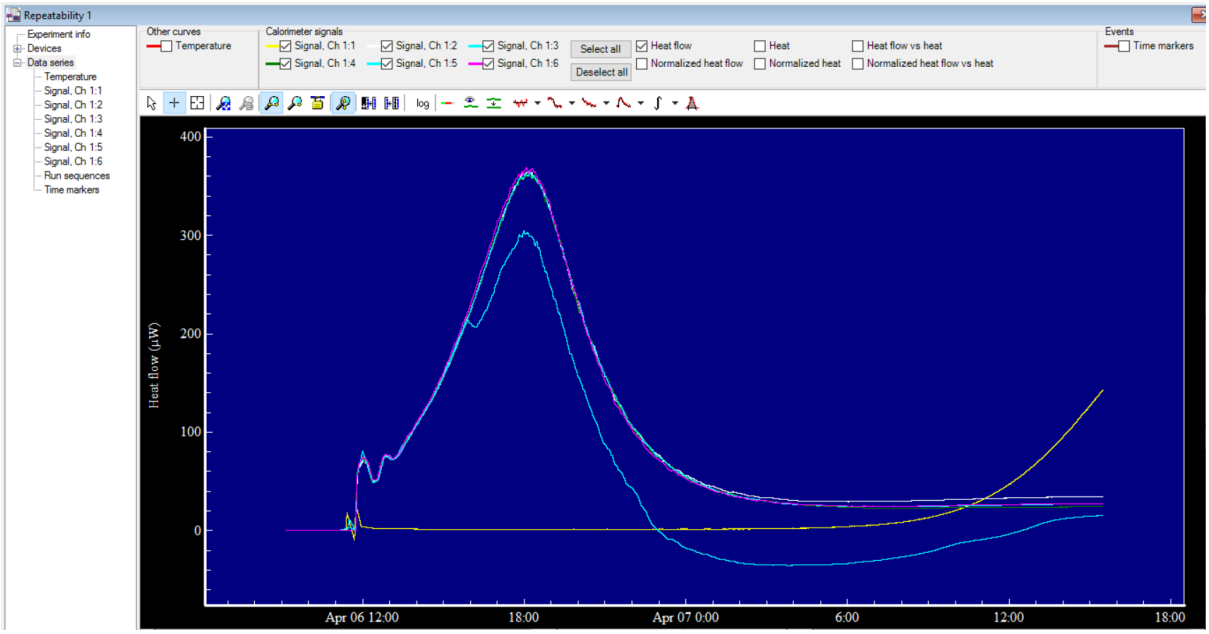

Figure A-6: Thermogram from experiments performed on 06/04/2015.
Run data was disregarded due to widespread contamination, confirmed by the rising heat flow produced by the yellow curve –the YPD blank. When the sample was examined under light microscope the presence of large numbers of bacteria was confirmed.

B.3 Maximum ampoule filling volume

It is important to note that since the microcalorimetric ampoules are airtight, the oxygen in the ampoule headspace (~3 ml of air) is expected to be rapidly be depleted by the yeast. When the yeast shifts to an anaerobic metabolism it will begin to produce CO_2 causing the pressure in the ampoule headspace to build. Since the ampoule can withstand a maximum pressure of approximately 2 barg, the ampoule was filled with only 1 ml YPD (see paragraph and calculations below). Using 1 ml of YPD also resulted in a volume easy to pipette into the ampoules.

The following calculations are based on the assumption that the glucose in the media is the limiting substrate and that the glucose is initially all consumed aerobically. After all the oxygen is depleted it is assumed that the yeast switch over to a completely anaerobic metabolism. The growth equation for aerobic growth under non-growing conditions (i.e. no biomass is produced) is given by Equation B-1:

$$C_6H_{12}O_6 + 6O_2 \rightarrow 6CO_2 + 6H_2O + 38\ ATP + 2874\ kJ \qquad \textit{Equation B-1}$$

Using the ideal gas law, given by Equation B-2,

$$\mathrm{n} = \frac{PV}{RT} \qquad \textit{Equation B-2}$$

Where P is the pressure in Pascal, V is the volume in m^3, R is the ideal gas constant (8.314 J/mol.K), n is the number of mols and T is the temperature in Kelvin.

In the case of the initial aerobic growth where the ampoule (4 ml total volume) is filled with 1 ml of cell suspension, at 30 °C (303 K), the number of mols of oxygen present in the 3 ml headspace is:

$$\mathrm{n} = \frac{101300 * 3 * 10^{-6}}{8.314 * 303}$$
$$\mathrm{n} = 1.69 * 10^{-5}\ mols \qquad \textit{Equation B-3}$$

Using Equation B-1, it is seen that the number of mols of glucose consumed is:

$$\mathrm{n} = \frac{1.69 * 10^{-5}}{6}$$
$$\mathrm{n} = 2.82 * 10^{-6}\ mols\ glucose \qquad \textit{Equation B-4}$$

The total amount of glucose present in 1 ml of solution is calculated using the concentration of glucose in the YPD and the molar mass of glucose (180 g/ml);

$$\mathrm{n} = \frac{20\ \mathrm{g/l}}{0.001l}\ 20\frac{g}{l} * 0.001\ l * 180\ g/mol$$
$$\mathrm{n} = 1.11 * 10^{-4}\ mols\ glucose \qquad \textit{Equation B-5}$$

Therefor the amount of glucose left for anaerobic consumption is;

$$\mathrm{n} = 1.11 * 10^{-4} - 2.82 * 10^{-6}$$
$$\mathrm{n} = 1.08 * 10^{-4}\ mols\ glucose \qquad \textit{Equation B-6}$$

The anaerobic metabolism of yeast (under-non growing conditions – constitutes the maximum amount of CO_2 that could be produced) is given as:

$$C_6H_{12}O_6 \rightarrow 2C_2H_5OH + 2CO_2 + 2\ ATP + 92\ kJ \qquad \textit{Equation B-7}$$

Therefore the amount of carbon dioxide produced is;

$$\mathrm{n} = 1.08 * 10^{-4} * 2$$
$$\mathrm{n} = 2.16 * 10^{-4}\ mols\ CO_2 \qquad \textit{Equation B-8}$$

The pressure exerted by that amount of CO_2 is calculated as;

$$\mathrm{P} = \frac{nRT}{V} \qquad \textit{Equation B-9}$$
$$\mathrm{P} = \frac{2.16 * 10^{-4} * 3.14 * 303}{3 * 10^{-6}}$$
$$\mathrm{P} = 1.8\ \mathrm{bar}$$

If the same calculation is performed using 2 ml volume of cells the final pressure comes to 5.6 bar – much more than the recommended maximum of ~2.5bar. Therefore only 1 ml of cell suspension was loaded into each ampoule.

B.4 TAMIII calibration

The TAMIII was re-calibrated frequently. A General Performance Test (GPT) was run via the TAMIII Assistant Software each time the machine was re-started. The GPT is an electric calibration procedure executed by the TAMIII software to calibrate the TAMIII as well as a performance verification, which checks that post-calibration each channel is performing within the manufacturer's specifications.

The TAMIII assistant software, as a part of the GPT protocol, performs a gain calibration, re-calculates time constants based on heat pulses and collects a baseline for 24 hours. The final results of the GPT include a verification of the short-term noise, long term stability and the time constants for each of the channels (TA Instruments, 2011).

APPENDIX C. Stress test results – calculated fitting parameters

C.1 Cold shock experiments

Slow cold shock

Analysing the slow cold shock results quantitatively, the absolute values of the fitting parameters are given in Table A-4 below and the normalised values are given in Table A-5. The equation fits to determine the specific growth rate and 'A' values, were highly correlated to the data, as seen by the R^2 values.

Table A-4: Calculated parameters for equation fits of all slow cold shock experiments

Date of experiment	N_0 – total (cells/ml)	R^2	μ (hr^{-1})	A (J)	t_{max} (hr)
29/06/2015	10^4 - Healthy	0.99995	0.370	2.45E-02	14.6
	10^4 - Healthy	0.99994	0.364	2.69E-02	14.0
	10^4 - Slow cold shock	0.99994	0.368	2.18E-02	14.5
	10^4 - Slow cold shock	0.99993	0.374	1.95E-02	14.6
	10^4 - Slow cold shock	0.99993	0.364	2.30E-02	14.6
01/07/2015	10^4 - Healthy	0.99993	0.372	2.36E-02	14.0
	10^4 - Healthy	0.99993	0.372	2.43E-02	14.0
	10^4 - Slow cold shock	0.99993	0.373	2.29E-02	14.2
	10^4 - Slow cold shock	0.99993	0.374	2.41E-02	14.1
	10^4 - Slow cold shock	0.99992	0.372	2.35E-02	14.1
02/07/2015	10^4 - Healthy	0.99992	0.372	2.51E-02	14.0
	10^4 - Healthy	0.99993	0.372	2.52E-02	13.9
	10^4 - Slow cold shock	0.99993	0.367	2.61E-02	14.0
	10^4 - Slow cold shock	0.99993	0.372	2.44E-02	14.0
	10^4 - Slow cold shock	0.99993	0.369	2.54E-02	14.1
03/07/2015	10^4 - Healthy	0.99993	0.372	2.05E-02	14.4
	10^4 - Healthy	0.99993	0.372	2.11E-02	14.4
	10^4 - Slow cold shock	0.99993	0.372	2.24E-02	14.2
	10^4 - Slow cold shock	0.99994	0.370	2.26E-02	14.2
	10^4 - Slow cold shock	0.99993	0.370	2.29E-02	14.1

Table A-5: Calculated normalized parameters for equation fits of the slow cold shock experiments

Date of experiment	N_0 (cells/ml)	μ_i/μ_m	$t_{max,i}/t_{max,m}$	A_i/A_m
29/06/2015	10^4 - Healthy	1.008	1.019	0.954
	10^4 - Healthy	0.992	0.981	1.046
	10^4 - Slow cold shock	1.002	1.018	0.848
	10^4 - Slow cold shock	1.019	1.021	0.759
	10^4 - Slow cold shock	0.991	1.024	0.896
01/07/2015	10^4 - Healthy	1.001	1.000	0.986
	10^4 - Healthy	0.999	1.000	1.014
	10^4 - Slow cold shock	1.002	1.011	0.957
	10^4 - Slow cold shock	1.005	1.001	1.006
	10^4 - Slow cold shock	1.000	1.002	0.979
02/07/2015	10^4 - Healthy	0.999	1.004	0.998
	10^4 - Healthy	1.001	0.996	1.002
	10^4 - Slow cold shock	0.988	1.007	1.035
	10^4 - Slow cold shock	1.000	1.008	0.969
	10^4 - Slow cold shock	0.991	1.009	1.007
03/07/2015	10^4 - Healthy	1.000	1.001	0.987
	10^4 - Healthy	1.000	0.999	1.013
	10^4 - Slow cold shock	1.002	0.984	1.076
	10^4 - Slow cold shock	0.995	0.984	1.085
	10^4 - Slow cold shock	0.995	0.983	1.099

Rapid cold shock

Analysing the results quantitatively, the absolute values of the fitting parameters are given in Table A-6 and the normalised values are given in Table A-7. Table A-6 shows that the equation fits, to determine the specific growth rate and 'A' values, were highly correlated to the data – as seen by the R^2 values.

Table A-6: Calculated parameters for equation fits of all rapid cold shock experiments

Date of experiment	N_0 – total (cells/ml)	R^2	μ (hr^{-1})	A (J)	t_{max} (hr)
05/07/2015	10^4 - Healthy	0.99994	0.367	2.58E-02	14.0
	10^4 - Healthy	0.99993	0.369	2.59E-02	14.1
	10^4 - Fast cold shock	0.99992	0.371	1.77E-02	14.9
	10^4 - Fast cold shock	0.99992	0.363	2.01E-02	15.2
	10^4 - Fast cold shock	0.99994	0.370	1.87E-02	14.9
07/07/2015	10^4 - Healthy	0.99993	0.367	2.25E-02	14.6
	10^4 - Healthy	0.99993	0.370	2.14E-02	14.5
	10^4 - Fast cold shock	0.99991	0.371	1.73E-02	15.2
	10^4 - Fast cold shock	0.99992	0.368	1.88E-02	14.9
	10^4 - Fast cold shock	0.99993	0.371	1.73E-02	15.0

Date of experiment	N_0 – total (cells/ml)	R^2	μ (hr^{-1})	A (J)	t_{max} (hr)
08/07/2015	10^4 - Fast cold shock	0.99992	0.371	1.72E-02	14.9
	10^4 - Fast cold shock	0.99992	0.372	1.75E-02	15.1
	10^4 - Healthy	0.99992	0.372	2.16E-02	14.3
	10^4 - Healthy	0.99993	0.369	2.23E-02	14.5
	10^4 - Healthy	0.99992	0.373	2.10E-02	14.5
09/07/2015	10^4 - Healthy	0.99993	0.369	8.75E-03	16.9
	10^4 - Healthy	0.99992	0.370	9.10E-03	16.6
	10^4 - Fast cold shock	0.99992	0.368	7.46E-03	17.3
	10^4 - Fast cold shock	0.99992	0.369	6.76E-03	17.8
	10^4 - Fast cold shock	0.99992	0.370	7.06E-03	17.3

Table A-7: Calculated normalized parameters for equation fits of the rapid cold shock experiments

Date of experiment	N_0 – total (cells/ml)	μ_i/μ_m	$t_{max,i}/t_{max,m}$	A_i/A_m
05/07/2015	10^4 - Healthy	0.998	0.997	1.00
	10^4 - Healthy	1.002	1.003	1.00
	10^4 - Fast cold shock	1.010	1.058	0.69
	10^4 - Fast cold shock	0.987	1.080	0.78
	10^4 - Fast cold shock	1.006	1.058	0.73
07/07/2015	10^4 - Healthy	0.997	1.003	1.03
	10^4 - Healthy	1.003	0.997	0.97
	10^4 - Fast cold shock	1.008	1.045	0.79
	10^4 - Fast cold shock	1.000	1.027	0.86
	10^4 - Fast cold shock	1.008	1.035	0.79
08/07/2015	10^4 - Fast cold shock	1.001	1.035	0.79
	10^4 - Fast cold shock	1.002	1.044	0.81
	10^4 - Healthy	1.001	0.990	1.00
	10^4 - Healthy	0.994	1.004	1.03
	10^4 - Healthy	1.005	1.006	0.97
09/07/2015	10^4 - Healthy	0.999	1.009	0.98
	10^4 - Healthy	1.001	0.991	1.02
	10^4 - Fast cold shock	0.996	1.035	0.84
	10^4 - Fast cold shock	0.999	1.064	0.76
	10^4 - Fast cold shock	1.002	1.033	0.79

C.2 Ethanol shock

Analysing the results quantitatively, the absolute values of the fitting parameters are given in Table A-8 below and the normalised values are given in Table A-9. As shown with the previous experiments, Table A-8 shows that the equation fits to determine the specific growth rate and '*A*' values were highly correlated to the data, as seen by the R^2 values. Table A-8 highlights

the inconsistent performance, in terms of the *A* and t_{max} values, of the 4% ethanol shocked cells in the 28/07/2015 experiment and the 8% ethanol shocked cells in the 02/08/2015 experiment. There were no issues encountered or anomalies observed when preparing these two samples, thus the channel data was not discarded.

Table A-8: Calculated parameters for equation fits of all ethanol shock experiments

Date of experiment	**N_0 - total**	**R^2**	**μ (hr^{-1})**	**A (J)**	**t_{max} (hr)**
28/07/2015	10^4 - Healthy	0.99992	0.370	1.89E-02	14.8
	10^4 – 4% EtOH shock	0.99993	0.364	3.41E-02	13.4
	10^4 – 8% EtOH shock	0.99991	0.375	1.69E-02	14.8
	10^4 – growing in 4% EtOH	0.99991	0.191	1.51E-02	30.7
	10^4 – growing in 8% EtOH	-	-	-	-
30/07/2015	10^4 - Healthy	0.99993	0.372	2.98E-02	13.6
	10^4 – 4% EtOH shock	0.99993	0.368	3.09E-02	13.5
	10^4 – 8% EtOH shock	0.99992	0.363	3.24E-02	13.7
	10^4 – growing in 1% EtOH	0.99993	0.328	2.27E-02	16.6
	10^4 – growing in 2% EtOH	0.99992	0.283	1.86E-02	19.4
02/08/2015	10^4 - Healthy	0.99994	0.366	3.92E-02	13.3
	10^4 – 4% EtOH shock	0.99994	0.366	3.70E-02	13.3
	10^4 – 8% EtOH shock	0.99993	0.364	2.47E-02	14.4
	10^4 – growing in 1% EtOH	0.99995	0.331	2.83E-02	15.7
	10^4 – growing in 2% EtOH	0.99994	0.284	2.15E-02	19.3
04/08/2015	10^4 - Healthy	0.99993	0.369	2.64E-02	13.9
	10^4 – 4% EtOH shock	0.99993	0.367	2.96E-02	13.9
	10^4 – 4% EtOH shock	0.99993	0.372	2.91E-02	13.7
	10^4 – 8% EtOH shock	0.99992	0.363	3.33E-02	13.7
	10^4 – 8% EtOH shock	0.99992	0.365	3.32E-02	13.6
06/08/2015	10^4 - Healthy	0.99992	0.376	3.68E-02	12.8
	10^4 – 8% EtOH shock	0.99992	0.373	2.84E-02	13.5
	10^4 – 12% EtOH shock	0.99993	0.373	3.24E-02	13.1
	10^4 – 12% EtOH shock	0.99993	0.372	3.20E-02	13.3

Table A-9: Calculated normalized parameters for equation fits of the ethanol shock experiments

Date of experiment	N_0 - total	μ_i/μ_m	$t_{max,i}/t_{max,m}$	A_i/A_m
28/07/2015	10^4 - Healthy	1.000	1.000	1.00
	10^4 – 4% EtOH shock	0.985	0.908	1.80
	10^4 – 8% EtOH shock	1.015	1.002	0.89
	10^4 – growing in 4% EtOH	0.517	2.075	0.80
	10^4 – growing in 8% EtOH	0.000	0.000	0.00
30/07/2015	10^4 - Healthy	1.000	1.000	1.00
	10^4 – 4% EtOH shock	0.990	0.992	1.04
	10^4 – 8% EtOH shock	0.977	1.005	1.09
	10^4 – growing in 1% EtOH	0.881	1.225	0.76
	10^4 – growing in 2% EtOH	0.762	1.431	0.62
02/08/2015	10^4 - Healthy	1.000	1.000	1.00
	10^4 – 4% EtOH shock	1.001	1.002	0.94
	10^4 – 8% EtOH shock	0.996	1.080	0.63
	10^4 – growing in 1% EtOH	0.906	1.178	0.72
	10^4 – growing in 2% EtOH	0.777	1.452	0.55
04/08/2015	10^4 - Healthy	1.000	1.000	1.00
	10^4 – 4% EtOH shock	0.994	0.997	1.12
	10^4 – 4% EtOH shock	1.008	0.982	1.10
	10^4 – 8% EtOH shock	0.985	0.981	1.26
	10^4 – 8% EtOH shock	0.988	0.978	1.26
06/08/2015	10^4 - Healthy	1.000	1.000	1.00
	10^4 – 8% EtOH shock	0.992	1.053	0.77
	10^4 – 12% EtOH shock	0.994	1.023	0.88
	10^4 – 12% EtOH shock	0.989	1.033	0.87

C.3 Combined ethanol and cold shock

Analysing the results quantitatively, the values of the absolute value of the fitting parameters are given in Table A-10 below and the normalised values are given in Table A-11. As shown with the previous experiments, Table A-10 shows that the equation fits to determine the specific growth rate and ‘A’ values were highly correlated to the data. The data in Table A-10 pertaining to the purely cold shocked cells and the cells growing in 1% ethanol has already been analysed as part of the rapid cold shock experiments (Section 5.1.2) and the ethanol shock experiments (Section 5.2).

Table A-10: Calculated parameters for equation fits of all combined ethanol and cold shock experiments

Date of experiment	N_0 - total	R^2	μ (hr^{-1})	t_{max} (hr)	A (J)
13/08/2015	10^4 - Healthy	0.99993	0.371	14.0	2.68E-02
	10^4 - growing in 1% EtOH	0.99993	0.330	16.8	1.88E-02
	10^4 - Rapid cold shock	0.99994	0.372	13.9	2.58E-02
	10^4 - Rapid cold shock + growing in 1% EtOH	0.9999	0.327	17.2	1.54E-02
	10^4 - Rapid cold shock + growing in 1% EtOH	0.99994	0.329	16.8	1.84E-02
20/08/2015	10^4 - Healthy	0.99993	0.372	14.2	2.24E-02
	10^4 - growing in 1% EtOH	0.99993	0.330	17.0	1.73E-02
	10^4 - Rapid cold shock + growing in 1% EtOH	0.99993	0.327	16.3	2.09E-02
	10^4 - Rapid cold shock + growing in 1% EtOH	0.9999	0.328	16.2	2.13E-02
21/08/2015	10^4 - Healthy	0.99994	0.369	14.1	2.36E-02
	10^4 - growing in 1% EtOH	0.99992	0.332	17.6	1.26E-02
	10^4 - Rapid cold shock	0.99993	0.370	14.7	1.98E-02
	10^4 - Rapid cold shock + growing in 1% EtOH	0.99994	0.325	17.0	1.71E-02
	10^4 - Rapid cold shock + growing in 1% EtOH	0.99993	0.329	18.3	1.16E-02
22/08/2015	10^4 - Healthy	0.99994	0.367	14.5	2.07E-02
	10^4 - growing in 1% EtOH	0.99994	0.325	17.6	1.55E-02
	10^4 - Rapid cold shock	0.99993	0.369	14.9	1.81E-02
	10^4 - Rapid cold shock + growing in 1% EtOH	0.9999	0.327	17.6	1.38E-02
	10^4 - Rapid cold shock + growing in 1% EtOH	0.99994	0.323	18.0	1.37E-02

Table A-11: Calculated normalized parameters for equation fits of the combined ethanol and cold shock experiments

Date of experiment	**N_0 (cells/ml)**	**μ_i/μ_m**	**$t_{max,i}/t_{max,m}$**	**A_i/A_m**
13/08/2015	10^4 - Healthy	1.00	1.00	1.00
	10^4 - growing in 1% EtOH	0.89	1.20	0.70
	10^4 - Rapid cold shock	1.00	0.99	0.96
	10^4 - Rapid cold shock + growing in 1% EtOH	0.88	1.24	0.57
	10^4 - Rapid cold shock + growing in 1% EtOH	0.89	1.20	0.69
20/08/2015	10^4 - Healthy	1.00	1.00	1.00
	10^4 - growing in 1% EtOH	0.89	1.20	0.77
	10^4 - Rapid cold shock + growing in 1% EtOH	0.88	1.15	0.93
	10^4 - Rapid cold shock + growing in 1% EtOH	0.88	1.14	0.95
21/08/2015	10^4 - Healthy	1.00	1.00	1.00
	10^4 - growing in 1% EtOH	0.90	1.25	0.54
	10^4 - Rapid cold shock	1.00	1.04	0.84
	10^4 - Rapid cold shock + growing in 1% EtOH	0.88	1.21	0.73
	10^4 - Rapid cold shock + growing in 1% EtOH	0.89	1.30	0.49
22/08/2015	10^4 - Healthy	1.00	1.00	1.00
	10^4 - growing in 1% EtOH	0.89	1.22	0.75
	10^4 - Rapid cold shock	1.01	1.03	0.87
	10^4 - Rapid cold shock + growing in 1% EtOH	0.89	1.21	0.66
	10^4 - Rapid cold shock + growing in 1% EtOH	0.88	1.24	0.66

APPENDIX D. APT data

This sections contains the absolute Acidification Power Test (APT) values for each experiment. The values in grey are from experimental runs where the corresponding calorimetric data was discarded.

D.1 Method validation across varied metabolic activity using heat killing experiments

Table A-12: APT data for heat killing experiments

	Healthy cells					Heat Killed cells		
Date of experiment	Technical repeat			Avg.	Std. dev	Technical repeat	Avg.	Std. dev
	1	2	3			1		
02_06	2.95	2.90		2.93	0.04	-0.81	-0.81	
04_06	3.02			3.02		-0.81	-0.81	
07_06	3.08	2.98	2.97	3.01	0.06	-0.84	-0.84	
10_06	2.99	2.91		2.95	0.06			
21_06	2.93	2.87		2.90	0.04	-0.79	-0.79	
23_06	3.02			3.02		-0.69	-0.69	
Total average				2.97	0.05		-0.79	0.06

D.2 Cold shock experiments

Table A-13: APT data for slow cold shock experiments

	Healthy cells				Cold shocked cells			
Date of experiment	Technical repeat		Avg.	Std. dev	Technical repeat		Avg.	Std. dev
	1	2			1	2		
25_06	2.88		2.88		2.89		2.89	
29_06	3.19		3.19		3.07		3.07	
01_07	3.19	3.07	3.13	0.08	3.08		3.08	
02_07	3.20		3.20		3.07		3.07	
03_07	3.21	3.11	3.16	0.07	3.05	3.14	3.10	1.75
Total average			3.11	0.13			3.04	0.09

Table A-14: APT data for fast cold shock experiments – APT data from the combined ethanol and cold shock experiments

	Healthy cells				Cold shocked cells			
Date of experiment	Technical repeat 1	2	Avg.	Std dev.	Technical repeat 1	2	Avg.	Std dev.
05_07	3.14		3.14		2.90	2.96	2.93	0.04
07_07	3.16		3.16		2.97	2.96	2.97	0.01
08_07	3.13	3.08	3.11	0.04	3.08	3.04	3.06	0.03
09_07	3.09	2.94	3.02	0.11	2.89	2.91	2.90	0.01
13_08	2.79		2.79		2.75	2.78	2.77	0.02
20_08	3.05		3.05		2.91	2.92	2.92	0.01
21_08	3.13		3.13		3.01	3.14	3.08	0.09
22_08	3.04		3.04		2.93	2.92	2.93	0.01
Total average			3.05	0.12			2.94	0.10

D.3 Ethanol shock experiments

Table A-15: APT data for the ethanol shock experiments

	Healthy cells			4% ethnaol shocked			8% ethnaol shocked			12% ethnaol shocked		
Date of exp	Tech rep 1	Avg	Std dev.	Tech rep 1	Avg	Std dev.	Tech rep 1	Avg	Std dev.	Tech rep 1	Avg	Std dev.
28_07	3.15			3.02			3.06					
30_07	3.07			3.01			3.07					
02_08	3.11			3.03			3.02					
04_08	3.06			2.93			2.99					
06_08	2.96						3.01			3.01		
Total average		3.07	0.07		3.00	0.05					3.01	

APPENDIX E. Risk Assessment and project ethics

Because the project will include an experimental component, it is necessary to consider the potential risks that may be encountered in addition to those associated with the paper based study component. It is important to acknowledge the risks associated with the project and try actively to minimise and manage them accordingly.

In terms of live cultures, the lab strain of yeast to be used is non-pathogenic and ultimately ranked as a very low biohazard risk (CBS Databse, 2014) to humans and the environment. Brewing yeast is also non-harmful, as is apparent by its use in the food industry. When working with yeast in an anaerobic state the biggest safety concern relates to pressure build-up. Although not scientifically verified, some home brewers have reported pressure build-ups in excess of 7 bar. High pressure can cause vessels to rupture, potentially causing harm especially if the vessel is made from glass. If the glass ampoules used rupture inside the calorimeter it can cause significant damage to the machine. If such an incident were to occur, the calorimeter would most likely be unusable until a technician repairs it at great cost.

Other significant risks associated with the work to be undertaken are due to the stresses to be tested – ethanol toxicity, pH stress and temperature shocks. In concentrated form, ethanol is flammable and toxic. Acid can cause chemical burns. In order to help minimize the risk of the two aforementioned chemicals, the appropriate PPE will be worn at all times. When temperature shocking the yeast, the necessary precautions should be taken; either the correct insulating clothing must be worn or the exposure time should be short enough that no harmful effects (e.g. hypothermia) occur to the experimenter. All acid and ethanol waste will need to be disposed of in the correct reciprocals and sent for treatment.

Because the work will be carried out in an active laboratory with numerous other experiments taking place, each with their own associated risks, general good laboratory practice should be adhered to. Workspaces should be as kept clean as possible and all waste should be disposed of in the correct bin. Any unidentified chemicals should be treated as hazardous. If the building fire alarm sounds, the laboratory should be evacuated calmly and quickly. In terms of working in an environmentally conscious manner; where appropriate, waste should be recycled as well as the use of water and electricity minimised wherever possible.

An Anglo Risk Matrix evaluating a number of the risks mentioned above can be found in Appendix F. The average risk rating was low, the highest risk was 7 (medium).

In terms of ethical issues surrounding the nature of the work to be undertaken, an ethics form has been competed, signed by all necessary parties and submitted to faculty (found on the following page). As indicated on the completed form (next page), there are no apparent ethical issues arising from the work to be undertaken.

EBE Faculty: Assessment of Ethics in Research Projects

Any person planning to undertake research in the Faculty of Engineering and the Built Environment at the University of Cape Town is required to complete this form before collecting or analysing data. When completed it should be submitted to the supervisor (where applicable) and from there to the Head of Department. If any of the questions below have been answered YES, and the applicant is NOT a fourth year student, the Head should forward this form for approval by the Faculty EIR committee: submit to Ms Zulpha Geyer (Zulpha.Geyer@uct.ac.za; Chem Eng Building, Ph 021 650 4791). Students must include a copy of the completed form with the thesis when it is submitted for examination.

Name of Principal Researcher/Student: Matthew Myers Department: Chem. Eng.

If a Student: Degree: MSc Supervisor: Prof Sue Harrison

If a Research Contract indicate source of funding/sponsorship:

Research Project Title: Determining the vitality and viability of yeast cells using isothermal microcalorimetry

Overview of ethics issues in your research project:

Question 1: Is there a possibility that your research could cause harm to a third party (i.e. a person not involved in your project)?	YES	NO X
Question 2: Is your research making use of human subjects as sources of data? If your answer is YES, please complete Addendum 2.	YES	NO X
Question 3: Does your research involve the participation of or provision of services to communities? If your answer is YES, please complete Addendum 3.	YES	NO X
Question 4: If your research is sponsored, is there any potential for conflicts of interest? If your answer is YES, please complete Addendum 4.	YES	NO X

If you have answered YES to any of the above questions, please append a copy of your research proposal, as well as any interview schedules or questionnaires (Addendum 1) and please complete further addenda as appropriate.

I hereby undertake to carry out my research in such a way that

- there is no apparent legal objection to the nature or the method of research; and
- the research will not compromise staff or students or the other responsibilities of the University;
- the stated objective will be achieved, and the findings will have a high degree of validity;
- limitations and alternative interpretations will be considered;
- the findings could be subject to peer review and publicly available; and
- I will comply with the conventions of copyright and avoid any practice that would constitute plagiarism.

Signed by:

	Full name and signature	Date
Principal Researcher/Student: Matthew Myers	Matthew Dean Myers Signed	12/02/2015

This application is approved by:

Supervisor (if applicable):	Signed SIL HARRISON	13/2/2015
HOD (or delegated nominee): Final authority for all assessments with NO to all questions and for all undergraduate research.	Signed	13/2/15
Chair : Faculty EIR Committee For applicants other than undergraduate students who have answered YES to any of the above questions.		

APPENDIX F. Risk Assessment Matrix

Standard Anglo Risk Matrix **Loss Type** (Additional 'Loss Types' may exist for an event; identify & rate accordingly)	Hazard Effect / Consequence (Where an event has more than one 'Loss Type', choose the 'Consequence' with the highest rating) **1 Insignificant**	**2 Minor**	**3 Moderate**	**4 Major**	**5 Catastrophic**
(S/H) Harm to People (Safety / Health)	First aid case / Exposure to minor health risk	Medical treatment / Exposure to major health risk	Loss time injury / Reversible impact on health	Single fatality or loss of quality of life / Irreversible impact on health	Multiple fatalities / Impact on health ultimately fatal
(EI) Environmental Impact	Minimal environmental harm - L1 incident	Material environmental harm - L2 incident remediable short term	Serious environmental harm - L2 incident remediable within LOM	Major environmental harm - L2 incident remediable post LOM	Extreme environmental harm - L3 incident irreversible
(BI/MD) Business Disruption / Material Damage & Other Consequential Losses	No disruption to operation / R500k to less than R5m	Brief disruption to operation / R5m to less than R50m	Partial shutdown / R50m to less than R500m	Partial loss of operation R500m to less than R5bn	Substantial or total loss of R5bn and more
(L&R) Legal & Regulatory	Low level legal issue	Minor legal issue; non compliance and breaches of the law	Serious breech of law; investigation/report to authority, prosecution and/or moderate penalty possible	Major breech of the law; considerable prosecution and penalties	Very considerable penalties & prosecutions. Multiple law suits & jail terms
(R/S/C) Impact on Reputation/Social/Community	Slight impact - public awareness may exist but no public concern	Limited impact - local public concern	Considerable impact - regional public concern	National impact - national public concern	International impact - international public attention

Likelihood	**Examples** (Consider near-hits as well as actual events)	**Risk Rating**				
5 Almost Certain	The unwanted event has occurred frequently; occurs in order of one or more times per year & is likely to reoccur within 1 year	11 (M)	16 (H)	20 (H)	23 (Ex)	25 (Ex)
4 Likely	The unwanted event has occurred infrequently; occurs in order of less than once per year & is likely to re-occur within 5 years	7 (M)	12 (M)	17 (H)	21 (Ex)	24 (Ex)
3 Possible	The unwanted event could well have occurred in the business at some point within 10 years	4 (L)	8 (M)	13 (H)	18 (H)	22 (Ex)
2 Unlikely	The unwanted event has happened in the business at some time; or could happen within 20 years	2 (L)	5 (L)	9 (M)	14 (H)	19 (H)
1 Rare	The unwanted event has never been known to occur in the business; or is highly unlikely that it could ever occur beyond 20 years	1 (L)	3 (L)	6 (M)	10 (M)	15 (H)

Interpretation of Risk Level

Risk Rating	**Risk Level**	**Guidelines for Risk Matrix**
21 to 25	**(Ex) – Extreme**	Eliminate, avoid, implement specific action plans / procedures to manage & monitor
13 to 20	**(H) – High**	Proactively manage
6 to 12	**(M) – Medium**	Actively manage
1 to 5	**(L) – Low**	Monitor & manage as appropriate

Figure A-7: Anglo Risk Matrix evaluated in the context of the research undertaken

Table A-16: Basic risk assessment report based on the Anglo Risk Matrix

No.	Sub System	Hazard - "what if"	Risk	Current Controls	Loss Type	C	L	R	Recomm. Additional Controls	C	L	R
1	General preparation and disposal of yeast into and out of glass ampoules	Mechanical - Glass ampoule breaks/shatters either due to excessive pressure build-up or being dropped	Injury to hand, body or limbs	Wear necessary PPE (shoes, lab coat, safety glasses, gloves) Correct crimping tool to be used. Maximum of 1 ml YPD to be used in glass ampoules.	S/H	1	4	7(M)				
		Biohazzard - Improper disposal of yeast solution (e.g. throw down drain by mistake)	Minor environmental impact	Dispose of yeast culture either via the use of biocide or by autoclaving before disposal.	EI and L&R	1	4	EI 7(M); L&R 1(L)				
		Chemical – acid spills when testing pH stress, or ethanol spills when performing ethanol stress tests	Skin or eye burns/contact	Wear necessary PPE (shoes, lab coat, safety glasses, gloves)	S/H	1	4	7(M)				
		Electrical – electrical machinery use such as vortex machine	Electric shock	Do not expose electrical machinery to liquid. Do not touch exposed wires	S/H	1	3	4(L)				
2	TAMIII microcaloirmeter	Mechanical - Incorrect loading, unloading or power trips of machine causes a malfunction	Experimental loss time, extreme cost of repair	Only trained users of the TAMIII may load or unload samples. Any minor faluts should be reported immediately to prevent further issues developing. TAM III runs on an uninterrupted power supply. Maximum of 1 ml YPD to be used in glass ampoules.	BI/MD	3	1	6(M)				
		Mechanical - Glass ampoule breaks/shatters inside machine due to excessive pressure build-up										

3	Experimental programme and project topic	Ethical - The experimental programme is viewed as detrimental to society and impacts on reputation/social/ community due to cultural/religious or social factors of other individuals	Negative impact on CeBER's reputation/abilit y to carry out research	All research requires ethics clearance	R/S/C	1	1	1(L)				

APPENDIX G. Plagiarism Declaration

DEPARTMENT OF CHEMICAL ENGINEERING

UNIVERSITY OF CAPE TOWN

MSc thesis

Determining the viability and vitality of yeast using isothermal microcalorimetry

2015			
Name (Student number)	**Matthew Myers (MYRMAT002)**		
Date Completed: 12-11-2016		**Date Handed-In: 14-11-2016**	

DECLARATION

1. I know that plagiarism is wrong. Plagiarism is to use another's work and to pretend that it is one's own.
2. This report is my own work.
3. I have not allowed, and will not allow, anyone to copy this work with the intention of passing it off as his or her own work.
4. Where idea that are not my own have been reported they have been correctly cited
5. I know the meaning of plagiarism and declare that all the work in the document, save for that which is properly acknowledged, is my own. This thesis/dissertation has been submitted to the Turnitin module (or equivalent similarity and originality checking software) and I confirm that my supervisor has seen my report and any concerns revealed by such have been resolved with my supervisor.

Signature	Signed by candidate

APPENDIX – DATA

Please refer to the electronically attached MS Excel data files. Contact the Centre for Bioprocess Engineering Research (CeBER) (Chemical Engineering Department, University of Cape Town) for further information rearding the data.